# Development of a platform technology for enhanced endo/lysosomal escape of targeted toxins by structurally specific oleanane saponins

Inaugural-Dissertation to obtain the academic degree

Doctor rerum naturalium (Dr. rer. nat.)

Conducted at the

Institute of Laboratory Medicine, Clinical Chemistry and Pathobiochemistry

Charité – Universitätsmedizin Berlin

and the

Institute of Pharmacy

Freie Universität Berlin

Submitted at the

Department of Biology, Chemistry, Pharmacy

Freie Universität Berlin

by

Roger Gilabert-Oriol

Berlin, May 2014

First supervisor: Prof. Dr. Matthias F. Melzig

Second supervisor: Prof. Dr. Hendrik Fuchs


Disputation: 18th of July 2014

# Index

# Abbreviations

| | |
|---|---|
| ADCC | Antibody-dependent cell-mediated cytotoxicity |
| $^{Alexa}$Saporin | Saporin-Alexa Fluor 488 |
| $^{Alexa}$ST | Saporin-Trastuzumab-Alexa Fluor 488 |
| ATP | Adenosine triphosphate |
| BCA | Bicinchoninic acid |
| BSA | Bovine serum albumin |
| CHCA | $\alpha$-Cyano-4-hydroxycinnamic acid |
| DE | Dianthin-30-epidermal growth factor |
| DMEM | Dulbecco's modified Eagle's medium |
| $DT_{390}$-EGF | Diphtheria toxin$_{390}$-epidermal growth factor |
| DTT | Dithiothreitol |
| EDC | 1-Ethyl-3-(3-dimethylaminopropyl)carbodiimide |
| EDTA | Ethylenediaminetetraacetic acid |
| EGF | Epidermal growth factor |
| EGFR | Epidermal growth factor receptor |
| ERAD | Endoplasmic reticulum-associated degradation |
| FBS | Fetal bovine serum |
| $GI_{50}$ | 50% Growth inhibition |
| HER2 | Epidermal growth factor receptor 2 |
| HPLC | High-performance liquid chromatography |
| HRP | Horseradish peroxidase |
| IDCC | Immunotoxin-dependent cell-mediated cytotoxicity |
| IPTG | Isopropyl $\beta$-D-1-thiogalactopyranoside |
| LB | Lysogeny broth |
| $M_a$ | Absolute molecular mass |
| MALDI-TOF-MS | Matrix-assisted laser desorption/ionization time-of-flight mass spectrometry |
| MTT | 3-(4,5-Dimethylthiazol-2-yl)-2,5-diphenyltetrazolium bromide |
| MWCO | Molecular weight cut off (defined by Millipore and Carl Roth) |

| | |
|---|---|
| NAG | β-*N*-Acetylglucosaminidase |
| NCI | Normalized cell index |
| NK | Natural killer cell |
| NHS | *N*-Hydroxysuccinimide |
| NMWL | Nominal molecular weight limit (defined by Merck Millipore) |
| NTA | Nitrilotriacetic acid |
| PBMC | Peripheral blood mononuclear cell |
| PBS | Phosphate buffered saline |
| pI | Isoelectric point |
| PI | Propidium iodide |
| PMS | Phenazine-methosulfate |
| PS | Penicillin/Streptomycin |
| RBC | Red blood cell |
| RD | Response difference |
| RIP | Ribosome-inactivating protein |
| RPMI | Roswell Park Memorial Institute medium |
| RTA | Ricin A-chain |
| SDS-PAGE | Sodium dodecyl sulfate-polyacrylamide gel electrophoresis |
| SA | Saponinum album |
| SC | Saporin-Cetuximab |
| SE | Saporin-epidermal growth factor |
| SH | Saporin-horseradish peroxidase |
| SPDP | *N*-succinimidyl-3-(2-pyridyldithio)propionate |
| SR | Saporin-Rituximab |
| ST | Saporin-Trastuzumab |
| TMB | 3,3′,5,5′-Tetramethylbenzidine |
| XTT | 2,3-Bis-(2-methoxy-4-nitro-5-sulfophenyl)-2*H*-tetrazolium-5-carboxanilide |

# 1. Introduction

## 1.1. Ribosome-inactivating proteins

### 1.1.1. Definition

Ribosome-inactivating proteins (RIPs) are a specific class of toxins that act on the ribosomal machinery *via* their *N*-glycosidase activity [1]. Mostly of plant origin, RIPs have been described as *N*-glycosidases that specifically remove adenine residues from the ribosomal RNA (rRNA) and thus de-purinate the conserved alpha-sarcin loop of the 28S rRNA. As a result of their enzymatic activity, the binding of the eukaryotic elongation factor is prevented [2] and this leads to an irreversible inhibition of protein synthesis that finally results in cell death [3].

There are basically two main subclasses of plant RIPs, namely type 1 and type 2. Type 1 RIPs consist of a single toxic domain. Examples of type I RIPs are saporin from *Saponaria officinalis* L., dianthin-30 from *Dianthus caryophyllus* L., gelonin from *Gelonium multiflorum* A. Juss., pokeweed antiviral protein from *Phytolacca americana* L. and bouganin from *Bougainvillea spectabilis* Willd. [4]. In contrast, type 2 RIPs comprise of two domains, a toxic domain (A-chain) and a cell binding domain (B-chain of lectin type), which are mostly linked *via* a disulfide bond. Toxins such as ricin from *Ricinus communis* L., abrin from *Abrus precatorius* L. and volkensin from *Adenia volkensii* Harms. belong to the group of type 2 RIPs [5].

In general, type I RIPs are considered to have lower cytotoxicity. This is not because of a lower enzymatic activity but due to the lack of a B-chain, which makes the process of cellular internalization inefficient [6]. Since type I RIPs lack the cell binding domain, this kind of plant toxins have been extensively used as fusion proteins by coupling the toxins either chemically or recombinantly to components that are able to facilitate their cellular internalization [7]. In addition, in the recent decade, increasing data has appeared indicating that the use of endosomal escape enhancers may result in significant augmentation of the efficacy of RIPs. These approaches providing higher efficacy have promisingly improved the therapeutic utility of RIPs as targeted toxins or immunotoxins [6].

### 1.1.2. Endocytosis, cytosolic delivery and enzymatic activity

The toxic potential of RIPs is determined by their ability to reach the ribosomes, which are located in the cytosol. Thus, RIPs that are able to overcome cellular barriers end up exhibiting

tremendous toxic potential. Passing cellular barriers includes the internalization which is generally facilitated by their B-chain present in type 2 RIPs. The B-chain serves as a galactose/*N*-acetylgalactosamine binding domain (lectin) and is linked to the A-chain *via* disulfide bonds. Past binding with glycoproteins or glycolipids that have numerous galactose residues on their surface, ricin is endocytosed *via* clathrin-dependent as well as clathrin-independent endocytosis and is thereafter delivered into early endosomes. From there it is transported to the Golgi-apparatus by retrograde transport and finally reaches the endoplasmic reticulum, where the disulfide bond is cleaved [8, 9] and the enzymatically active A-chain is partially unfolded [10]. To facilitate its entry into the cytosol, the A-chain exploits a mechanism that is known as endoplasmic reticulum-associated degradation (ERAD). The partially unfolded A-chain is transported to the cytosol [11, 12] where it is fully refolded to regain the conformational integrity as an enzymatically active form and is able to inactivate the ribosomes by de-purinating the rRNA [13].

The exact mechanism of the internalization of type 1 RIPs is not deciphered so far. Previous studies indicated a receptor-mediated endocytosis of type I RIPs by low density lipoprotein (LDL) receptors [14-17]. Contrastingly, some other results confirmed a receptor independent endocytosis [18]. However, the exertion of toxic effects appears to be independent of the internalization mechanism. The toxicity determining factor is the ability of type 1 RIPs to cross the endo/lysosomal membrane. Since type 1 RIPs do not contain any transduction domains facilitating the endo/lysosomal escape into the cytosol, they are less cytotoxic. Upon endocytosis, type 1 RIPs are delivered into cellular compartments that are positive for lysobisphosphatidic acid (LBPA) (a specific eukaryotic phospholipid marker for late endosomes) and the lysosomal-associated membrane proteins LAMP1 and LAMP2 [18, 19]. Nearly all type I RIPs are thereafter degraded within the lysosomes [20].

## 1.2. Saponins

### 1.2.1. Structure and properties

Saponins are a highly diverse group of plant and marine glycosides that are composed of a steroidal or triterpenoidal aglycone (sapogenin) and one or more sugar chains [21]. Depending on the number of sugar chains attached, they are classified as monodesmosidic (one sugar chain), bisdesmosidic (two sugar chains) and in rare cases trisdesmosidic (three sugar chains) [22]. Sugar chains mostly comprise of glucose, galactose, xylose, rhamnose and glucuronic acid along

with numerous others, and each of these chains can independently either be linear or branched. Both the number and type of sugar moieties is variable [23]. All these different possibilities, together with the variations observed in the nature of the aglycone, confer a great variability to the saponins (Table 1).

A number of biological effects are attributed to saponins, including membrane permeabilizing characteristics [24] and hemolytic activity [25], being the most common. Pharmacologically, saponins are known to have anti-viral, anti-fungal, anti-inflammatory and anti-allergic properties [26]. Furthermore, they have promising applications in cancer therapy, based on their ability to inhibit angiogenesis, reduction of invasiveness, cell cycle arrest and induction of apoptosis [27]. Saponins have been applied together with other anti-tumor drugs to enhance their cytotoxicity in tumor therapy [28, 29]. In addition, saponins can modulate the immune system of mammals and their usage as vaccine adjuvants has acquired significant interest [30, 31].
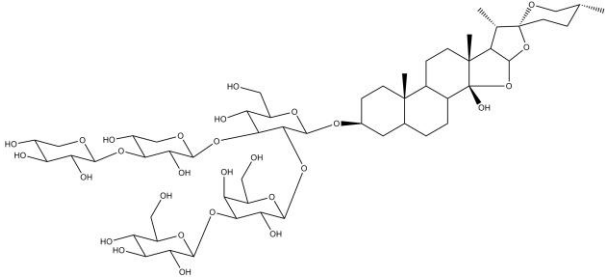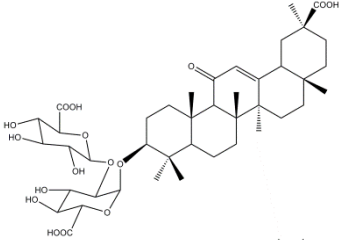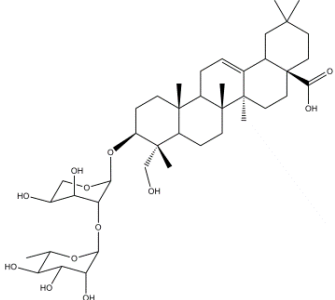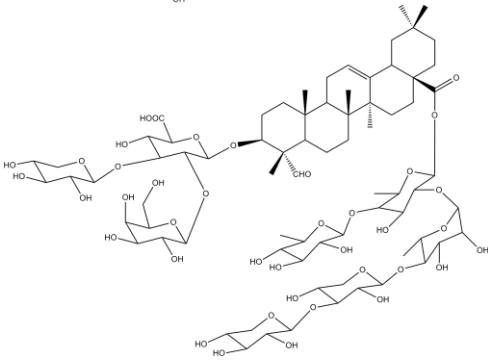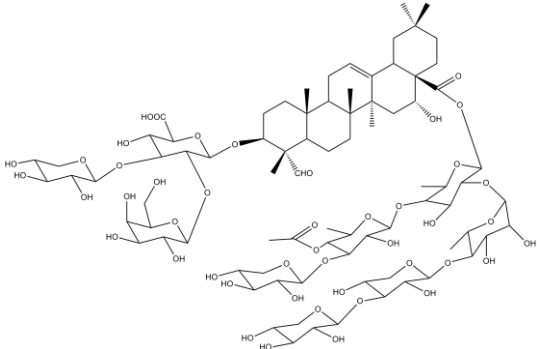
Although several studies have been conducted to date, the mechanism of interaction between saponins and cellular membranes remains to be unclear. The attempts to correlate membrane permeabilizing effects and hemolysis of saponins have not succeeded in giving a clear representation [32]. While in certain cases cholesterol content in cellular membrane was set into relation with membrane permeabilizing effects and pore formation of saponins [25], other studies indicated that this is not the case [33]. Parameters such as the number of sugar chains attached to the aglycone have been also correlated with hemolytic activity and membrane permeability [34]. Further studies on membrane permeabilizing effects of saponins would provide better understanding of the *modus operandi* of saponins in their interaction with membranes [35].

### 1.2.2.   Synergism between saponins and type I ribosome-inactivating proteins

A relevant characteristic of certain oleanane saponins (a subclass of triterpenoidal saponins) is their ability to specifically augment the cytotoxicity of particular ribosome-inactivating proteins (RIPs) [36]. The synergistic potentiation occurs at non-permeabilizing and non-toxic concentrations of the saponin. The synergistic principle has been reported for a definite subset of isolated triterpenoidal saponins from the Caryophyllaceae family [37].

**Table 1.** Name, plant source and chemical structure of some saponins of interest. Digitonin is a strong permeabilizing monodesmosidic steroidal saponin. Glycyrrhizinic acid and α-hederin are monodesmosidic oleanane saponins (a subclass of triterpenoidal saponins) [38]. Certain *Gypsophila* saponins (SA1641) and *Saponaria* saponins (SO1861) are bisdesmosidic oleanane saponins with variable membrane permeabilizing effects.

| Saponin | Plant source | Structure |
|---|---|---|
| Digitonin | *Digitalis purpurea* L. | |
| Glycyrrhizinic acid | *Glycyrrhiza glabra* L. | |
| α-Hederin | *Hedera helix* L. | |
| *Gypsophila* saponins (SA1641) | *Gypsophila arrostii* Guss. | |
| *Saponaria* saponins (SO1861) | *Saponaria officinalis* L. | |

## 1. Introduction

The structural features of saponins that are highly recommendable for their enhancing effects have been studied extensively [39]. It is now established that bisdesmosidic triterpenoidal saponins that have a gypsogenin or quillaic acid backbone with a glucuronic acid at C-3 position are most effective, moreover there are further specific structural and sugar chain requirements that lead to a relatively small number of saponins that are able to act as synergistic enhancers. The following saponins have been reported for this effect: *Agrostemma* saponins [40] from *Agrostemma githago* L.; Saponinum album (SA) [27], which is a saponin mixture isolated from *Gypsophila paniculata* L. and *Gypsophila arrostii* Guss.; SA1641 [41], isolated from SA; SO1861 [42] from *Saponaria officinalis* L. and *Quillaja* saponins [43] from *Quillaja saponaria* Mol.
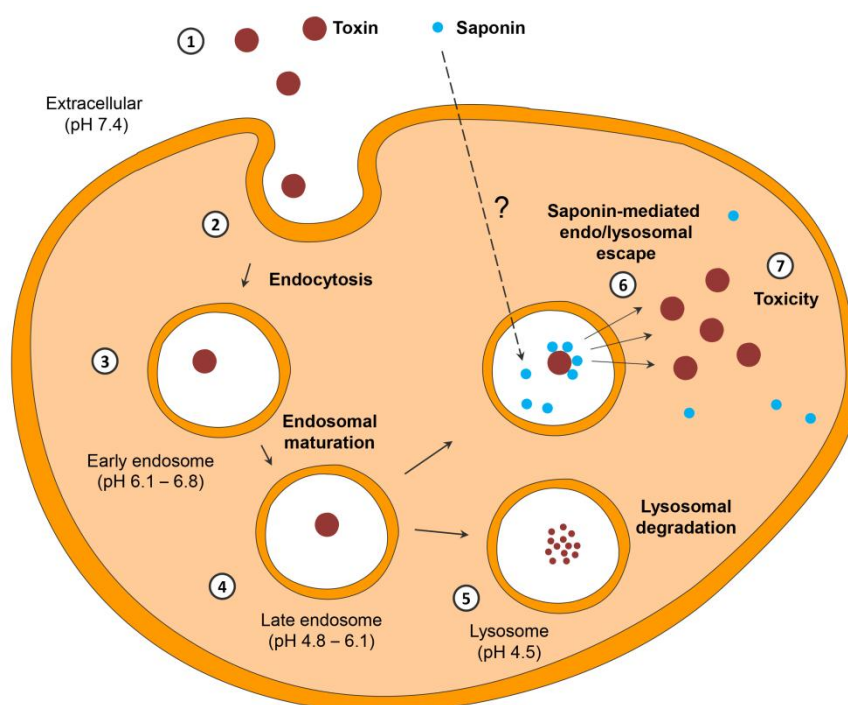


**Figure 1.** A schematic description for the efficacy enhancement of certain plant type I RIPs using triterpenoidal saponins. 1. The toxin reaches the cell. 2. Internalization and formation of endosomal vesicles. 3. Maturation of the endosomal vesicles along with the entrapped toxin. 4. Late endosome formation. 5. The toxin undergoes lysosomal degradation and thus the toxic effect is not elicited. 6. Particular saponins accumulate inside the endo/lysosomes by unknown mechanisms. The presence of saponins facilitates the endo/lysosomal release of the toxin in a pH dependent manner. 7. The toxin induces cell death inside the cytosol *via* apoptosis.

As already detailed, for exerting cytotoxicity the toxin moieties have to be released into the cytosol. However, the cytosolic transfer of toxin molecules into the cytosol is mostly an inefficient process. The synergistic cytotoxicity enhancement by triterpenoidal saponins was first observed in the case of the type 1 RIP agrostin [40, 44]. Thereafter, the synergistic enhancement was investigated for the toxin saporin [36]. Even cell types that are normally less sensible to the effect of saporin, such as macrophage-like U937 cells, were efficiently killed by saporin + SA

[45]. Weng et al. studied the mechanistic aspects of the synergistic effect of saporin and triterpenoidal saponins. The investigations showed that the saponin-mediated augmentation of the cytotoxicity was not based on stimulation of endocytosis neither of phagocytosis, but on the potentiation of the endosomal escape of the toxin [46, 47]. The hypothesis has been confirmed in recent studies for saporin and SO1861, both compounds being biosynthesized in the seeds of *Saponaria officinalis* L. [42]. It has been demonstrated that triterpenoidal saponins specifically mediate the release of saporin out of the intracellular compartments into the cytosol without affecting the integrity of the plasma membrane. The relevant cellular compartments were identified as late endosomes and lysosomes. Further studies revealed that endosomal acidification is a prerequisite for the saponin-mediated release of saporin. Binding analysis demonstrated an association of the triterpenoidal saponins with saporin in a pH-dependent manner [6]. A schematic description for the efficacy enhancement of type I RIPs by triterpenoidal saponins is presented in Figure 1.

## 1.3. Targeted toxins and immunotoxins

### 1.3.1. Construction of targeted toxins and immunotoxins

Targeted toxins are a group of therapeutics used in targeted tumor therapies, a strategy that is based on the specific killing of cancer cells and the concomitant decrease of side effects in comparison to non-targeted cancer therapies. Targeted toxins are composed of two functional moieties: a toxic enzyme that induces cytotoxicity generally by inactivating protein synthesis and triggering apoptosis, and a targeting ligand that directs the conjugate to the target cell [48]. Typical targeting domains used as ligands are growth factors, cytokines, antibodies or antibody fragments (in the latter two cases the conjugate is designated as immunotoxin) that recognize their respective receptors on cell surfaces [7].

The toxic moiety, either the complete type 1 or 2 RIP or the A-chain of a type 2 RIP, is typically coupled to the ligand by a chemical cross-linker, resulting in a protein conjugate [7]. Coupling of an antibody or its fragment to the isolated toxin *via* disulfide linkage appears to be the most effective strategy. In general, the RIPs lack thiol groups for a disulfide linkage and therefore it needs to be synthetically introduced. Alternatively, toxin and ligand can be recombinantly fused at the DNA level by molecular cloning and expressed as a fusion protein [49].

### 1.3.2. Monoclonal antibodies

Monoclonal antibodies are commonly used in cancer therapy. In this approach, therapeutic antibodies are directed to cancer cells by targeting proteins that are specifically expressed on the cellular surface of tumor cells. Examples of Food and Drug Administration (FDA)-approved therapeutic monoclonal antibodies include Cetuximab (anti-epidermal growth factor receptor, anti-EGFR, Erbitux®), Panitumumab (anti-EGFR, Vectibix®), Trastuzumab (anti-epidermal growth factor receptor 2, anti-HER2, Herceptin®), Rituximab (anti-CD20, Rituxan®) and Ofatumumab (anti-CD20, Arzerra®) [50].

Various modes of action of monoclonal antibodies have been characterized *in vitro*. Binding of the antibody to a target receptor expressed on the cellular surface blocks the interaction of the receptor with a native ligand, interferes with a multimerization process and triggers the internalization of the receptor, thus inhibiting signal transduction pathways and cell cycle progression or causing apoptosis of the target cells [51]. In addition, monoclonal antibodies may also interact in several ways with the innate immune system of the recipient. One of the most important modality of therapeutic antibodies *in vivo* is the antibody-dependent cell-mediated cytotoxicity (ADCC), mainly effectuated by natural killer (NK) cells [52]. Unfortunately monoclonal antibody-based therapy encompasses certain limitations and may result in the failure of the treatment due to certain mechanisms, which include dysfunctions in triggering the ADCC [53] or other factors such as the compensatory activation of parallel signaling pathways [54, 55].

Because targeted toxins (referred to as immunotoxins in case of an antibody serving as the targeting ligand) carry a toxin capable to cause cell death, the application of these toxins is a promising strategy to circumvent some of their limitations. Two main aspects should be considered in the designing of immunotoxins. Firstly, some studies pointed to a contribution of the antibody-dependent cellular cytotoxicity to the *in vivo* therapeutic efficacy of an immunotoxin [56, 57]. However, it is still generally believed that the ability of triggering ADCC by the immunotoxin is lost when monoclonal antibodies are conjugated to a toxin [58]. It is therefore important to verify this conjecture. Secondly, despite numerous successful preclinical data, immunotoxins are still causing immunogenic responses and may therefore be rapidly blocked and neutralized by the immune system of recipients, thus leading to a failure of the therapy [59]. For this reason, an ideal immunotoxin should combine the functionality of the monoclonal antibody (antagonistic binding to targeted receptors and interaction with the innate immune system) with the cell-killing activity of the toxic moiety. In addition, the usage of

efficacy enhancers is of great importance in order to decrease the dosage in patients and thus reduce the side effects as well as possible adverse immune reactions.

### 1.3.3. Internalization, cytosolic release and lysosomal degradation

When the toxins are transformed into targeted toxins, there are numerous critical situations specifying their fate. First of all, the receptor that is being addressed by the targeted toxin should be over-expressed on the tumor cells but only less expressed on normal cells. Besides, it is important to select antigens that undergo enhanced endocytosis after ligand binding because this facilitates a rapid delivery of the toxin into the cancer cells [60]. A considerable number of different receptors have been addressed to date [61], amongst them are cytokine receptors [62], tumor necrosis factor receptor, growth factor receptors [63, 64] and cluster of differentiation CD22 [65], CD25 [66] and CD30 [67].

The next important step after binding of the targeted toxins to the receptor is their internalization into the cell. This process is mediated by clathrin-dependent or clathrin-independent endocytosis. Once internalized, the targeted toxin is delivered into early endosomes. Early endosomes are part of the endosomal transport system, which is an intracellular vesicular and tubular compartment surrounded by cytosol. Within early endosomes, endocytosed ligands (targeted toxins) are either designated for recycling or they are further transported into late endosomes and finally lysosomes for degradation [68, 69].

Since targeted toxins exert their anti-tumoral efficacy only in the cytosol, it is a vital prerequisite for their efficacy that they are able to escape from the endosomal network into the cytosol. Targeted toxins fused to truncated variants of bacterial toxins such as diphtheria toxin (DT) from *Corynebacterium diphtheriae* utilize the native translocation domain (T domain) of DT to escape from early endosomes into the cytosol [70-72] while other targeted toxins such as *Pseudomonas* exotoxin A employ a KDEL-related motive of their toxin moieties to be retrogradely delivered into the endoplasmic reticulum and then transported into the cytosol [73]. However, plant-derived toxins such as the type 1 RIPs saporin and gelonin or the A-chain of the type 2 RIP ricin do not comprise such translocation domains.

As mentioned above, lysosomal degradation is one of the main issues in targeted tumor therapies [74]. Although it may be compensated by increasing the dosage of the targeted toxins, this approach promotes undesirable side effects. The generation of modified targeted toxins that are

resistant against lysosomal degradation is an attractive strategy to increase the efficacy of targeted toxins [75]. Furthermore, lysosomal degradation can be outweighed by combination strategies that mediate the endo/lysosomal escape of targeted toxins.

### 1.3.4. Targeted toxins based on ribosome-inactivating proteins

Plant ribosome-inactivating proteins (RIPs) constitute the toxic part of a major portion of targeted toxins. Amongst various RIPs used for the construction of targeted toxins (see Table 2), the leading toxin components are ricin A-chain (RTA), saporin and gelonin. A lot of different targeting ligands have been successfully coupled to these toxins and have shown high specificity in *in vitro* and preclinical evaluations.

Initially, targeted toxins were constructed with native ricin and were tested *in vitro* in the presence of high concentrations of lactose which prevented the non-specific binding of ricin B-chain [76]. Blocking of the oligosaccharide binding sites was used to prevent off-target ricin uptake and provided the possibility of applying the immunotoxins *in vivo* [77]. The separation of RTA and ricin B-chain by chemical reduction allowed conjugation of the antibody to the catalytic subunit, mainly through cross-linkers containing a disulfide bond. Despite the high yield and good stability of these targeted toxins, one of the main disadvantages for them was a heterogeneous composition [78]. Furthermore, it is well known that the glycosylated residues of RTA also facilitate non-specific uptake by macrophages. Therefore, in order to prevent the non-specific uptake, RTA was submitted to a process of deglycosylation before conjugation to the antibody and formation of the immunotoxin [79].

The advancement of recombinant tools led to a common utilization of these techniques for the production of the toxins. These targeted toxins are obtained by linking the gene portion encoding the antigen-binding fragments of an antibody (e.g. scFv) to the gene encoding the native catalytic domain or a mutated version of the toxin. Once the DNA-construct is available, it can be multiplied in bacteria, yeast or algae [80, 81]. Expression of fusion proteins comprising of a type I RIP is also very well reported. An epidermal growth factor receptor (EGFR)-targeted, dianthin-30-based fusion protein has been successfully expressed in bacteria [82] and saporin has been expressed as an EGFR-targeted fusion protein as well [6, 83]. Furthermore, saporin has been fused to the basic fibroblast growth factor (FGF-2) [84], to the placental growth factor-2 (PlGF-2) [85] and to the amino-terminal fragment of human urokinase (ATF) [86].

**Table 2.** RIPs used for the construction of targeted toxins. Species, type and absolute molecular mass (Ma) is indicated for each of the toxins.

| Species | RIP | Type | Ma (kDa) | Ref. |
|---|---|---|---|---|
| *Abrus precatorius* L. | abrin | 2 | 63 | [87] |
| *Bougainvillea spectabilis* Willd. | bouganin (*Bougainvillea spectabilis* RIP) | 1 | 26.2 | [88] |
| *Bryonia dioica* Jacq. | bryodin-1 (BD-1) | 1 | 30 | [89] |
| *Bryonia dioica* Jacq. | bryodin-2 (BD-2) | 1 | 27 | [90] |
| *Citrullus colocynthis* Schrad. | colocin 1 | 1 | 26.3 | [91] |
| *Cucurbita moschata* Duchesne ex Poir. | moschatin | 1 | 29 | [92] |
| *Dianthus caryophyllus* L. | dianthin-30 | 1 | 29.5 | [93] |
| *Dianthus caryophyllus* L. | dianthin-32 | 1 | 31.7 | [94] |
| *Gelonium multiflorum* A. Juss. | gelonin (GAP31) | 1 | 31 | [95] |
| *Hordeum vulgare* L. | barley translation inhibitor (barley toxin I, BRIP) | 1 | 31 | [96] |
| *Hordeum vulgare* L. | barley toxin II | 1 | 30 | [97] |
| *Jatropha curcas* L. | curcin | 1 | 28.2 | [98] |
| *Luffa aegyptiaca* Mill. | *Luffa* ribosomal inhibitory protein (LRIP) | 1 | 30 | [99] |
| *Luffa cylindrica* Mill. | luffin-A (alpha-luffin) | 1 | 27 | [100] |
| *Luffa cylindrica* Mill. | luffin-B (beta-luffin) | 1 | 28 | [101] |
| *Luffa cylindrica* Mill. | luffin-P1 | 1 | 5.2 | [102] |
| *Momordica charantia* L. | momordin (*Momordica charantia* inhibitor) | 1 | 23 | [103] |
| *Momordica cochinchinensis* Spreng | momorcochin | 1 | 32 | [91] |
| *Phytolacca americana* L. | PAP (Pokeweed antiviral protein, *Phytolacca* antiviral protein) | 1 | 29 | [104] |
| *Phytolacca americana* L. | PAP II (Pokeweed antiviral protein II) | 1 | 30 | [105] |
| *Phytolacca dioica* L. | PD-S2 (*Phytolacca dioica* RIP 2) | 1 | 29.6 | [106] |
| *Ricinus communis* L. | ricin | 2 | 62 | [107] |
| *Sambucus ebulus* L. | ebulin I (ebulin 1) | 2 | 56 | [108] |
| *Sambucus nigra* L. | nigrin b | 2 | 58 | [109] |
| *Saponaria ocymoides* L. | ocymoidine | 1 | 30.2 | [110] |
| *Saponaria officinalis* L. | saporin | 1 | 29.5 | [111] |
| *Trichosanthes kirilowii* Maxim. | trichosanthin (TCS) | 1 | 26 | [112] |
| *Trichosanthes kirilowii* Maxim. | trichokirin | 1 | 27 | [113] |
| *Vaccaria pyramidata* Medik. | pyramidatine | 1 | 28 | [110] |
| *Viscum album* L. | viscumin (mistletoe lectin I) | 2 | 60 | [114] |

### 1.3.5. Efficacy enhancers

In the past, a number of strategies have been attempted to circumvent the problems associated with immunogenicity, vascular leak syndrome and other off-target effects that are associated with targeted toxin therapy (Table 3). Conventionally, the use of certain chemicals like chloroquine (lysosomotropic agents) has been employed [115]. Such compounds lead to an elevation of the endosomal pH, thereby protecting the toxin from lysosomal enzyme degradation. Other strategies involve the use of osmotic regulators such as calcium channel antagonists (verapamil) [116] or pore forming agents such as listeriolysin O from *Listeria monocytogenes* [63]. The usage of efficacy enhancers certainly helped in improving the efficacy of immunotoxins but their proof in preclinical and clinical studies is still limited.

Further approaches have been under scrutiny for their ability to prevent the lysosomal degradation of targeted toxins by mediating their endosomal escape into the cytosol. Some examples include, photochemical internalization [117], cell penetration by protein transduction domains [118], and the use of triterpenoidal saponins [6, 42].

### 1.3.6. Synergistic enhancement by saponins and their role in targeted tumor therapy

The cytotoxicity enhancing properties of triterpenoidal saponins were first observed for the type I RIP agrostin from *Agrostemma githago* L. and the cognate triterpenoidal saponins from *Agrostemma githago* L. [40]. After the finding of this phenomenon, the augmentation effects by saponins were investigated for targeted toxins. The first recombinant toxin that was studied consisted of saporin as toxin moiety and epidermal growth factor (EGF) as the ligand [119]. The fact that the target cell-specific cytotoxicity of the targeted toxin was enhanced by up to a 385,000-fold encouraged further studies. Several saponins were tested in the presence of the targeted toxin but only SA (a saponin mixture from *Gypsophila paniculata* L. and *Gypsophila arrostii* Guss.) and *Quillaja* saponins exhibited this effect [43]. The principle was validated in cell culture models but in addition fresh cells directly prepared after surgery of an oral squamous cell carcinoma (OSCC) were successfully treated with the combination [120]. In a study where the effect of saporin-epidermal growth factor (SE) in combination with SA was investigated on a panel of cell lines with different expression patterns of EGFR, enhancement factors ranging from 9,000- to 2,500,000-fold were observed [121].

**Table 3.** List of efficacy enhancers employed in the improvement of immunotoxin efficacy.

| Efficacy enhancers | Compounds | Characteristics | Ref. |
|---|---|---|---|
| Lysosomotropic amines | ammonium chloride, methylamine, dimethylamine, trimethylamine, amantadine, chloroquine, lipopolyamines, β-glycylphenyl-naphthylamide (GPN), quinacrine | inorganic and organic compounds; effect in endosomes; immunotoxin enhancement (RTA, Gel, Sap, PE); factor 10–13,300 | [122-127] |
| Carboxylic ionophores | monensin, grisorixin, lasalocid, nigericin | organic compounds; effect in lysosomes; immunotoxin enhancement (RTA, Gel); factor 6,700–50,000 | [122, 125, 128] |
| Calcium channel antagonists | verapamil, diltiazem, methoxyverapamil (D-600), varapamil analogues, perhexiline, SR 33557, SR 33287 | organic compounds; effect in lysosomes or other vesicles; immunotoxin enhancement (RTA, Gel, PE); factor 2–2,000 | [116, 125, 127, 129, 130] |
| Organic polymers | poly(amidoamine)s (PAAs) | organic polymers; effect in endosomes and lysosomes; immunotoxin enhancement (RTA, Sap, Gel); factor 100 | [131, 132] |
| Other organic compounds | retinoic acid, cyclosporin A, brefeldin-A, bryostatin 1, wortmannin | organic compounds; effect in endosomes and lysosomes, Golgi apparatus or cell signaling; immunotoxin enhancement (RTA, Sap, Gel, PE); significant increase to factor 1,000 | [133-138] |
| Viruses and viral peptides | adenovirus, penton base protein (adenovirus capsid protein), KFT25, hemagglutinin HA2, HA23, preS2-domain of hepatitis-B virus surface antigen | viruses and viral particles; effect in endosomes, lysosomes and other vesicles; immunotoxin enhancement (RTA, Sap, Gel, Dia, PE, Ang); factor 2–10,000 | [93, 118, 139-147] |
| Bacterial peptides | listeriolysin O, *Pneumococcal* pneumolysin (PLO), *Streptococcal* streptolysin O (SLO), T domain of diphtheria toxin, domain II of *Pseudomonas* exotoxin A, REDLK | peptides; effect in endosomes, endoplasmic reticulum or *trans*-Golgi network; immunotoxin enhancement (PE, DT, GzmB); from no-effect to effect | [148-152] |
| Human peptides | KDEL | peptides; effect in endoplasmic reticulum; immunotoxin enhancement (RTA, PE); factor 100–1,000 | [153, 154] |
| Animal and human proteins | α-interferon (INF), perforin, Rituximab | proteins; effect in early endosomes or cell signaling; immunotoxin enhancement (RTA, Sap, GzmB); significant increase to factor 80 | [155-157] |

| Efficacy enhancers | Compounds | Characteristics | Ref. |
|---|---|---|---|
| Plant saponins | Saponinum album (SA), SA1641, *Saponaria* saponins, SO1861, *Agrostemma* saponins, *Quillaja* saponins | triterpenoidal saponins; effect in late endosomes and lysosomes; immunotoxin enhancement (Sap, Dia); significant increase to factor 2,500,000 | [27, 40-43] |
| Plant proteins | ricin B-chain | proteins; effect in internalization and cell signaling; immunotoxin enhancement (RTA); significant increase to factor 6 | [158-160] |
| Synthetic peptides | pJVE | peptides; effect in endosomes; immunotoxin enhancement (Dia); factor 2 | [93] |
| Physicochemical techniques | photochemical internalization | technique; effect in endosomes; immunotoxin enhancement (Sap, Gel); factor 1,000 | [117, 161, 162] |

Mechanistic studies were performed to understand the endocytic pathways of SE in combination with SA [35]. After binding to EGFR, small amounts of SE entered the cytosol *via* clathrin-independent pathways. However, most of the targeted toxin was internalized *via* clathrin-dependent endocytosis and was unable to cross the membrane of acidic endosomes, thus being degraded in the lysosomes. Only in the presence of triterpenoidal saponins, SE achieved the endo/lysosomal escape and reached the cytosol where it exerted its cytotoxicity.

SE has been tested in the presence of purified saponins from SA (SA1641), achieving a significant augmentation of cytotoxicity in EGFR expressing NIH3T3 cells [41]. Similar potentiation factors were acquired by a targeted toxin consisting of EGF and dianthin-30, a type I RIP with high homology to saporin. SE has been also applied in combination with purified saponins from *Saponaria officinalis* L. (SO1861) [42]. The efficacy of SO1861 in combination with targeted toxins was confirmed in a real time cytotoxicity evaluation [163]. Further *Saponaria* saponins purified after agarose gel electrophoresis were tested in combination with SE [42]. In this case, the targeted toxin alone required a 10,000-fold higher concentration compared to the combination with saponins to induce cell death after a period of nearly 48 h of incubation.

To demonstrate the applicability of the combination therapy, *in vivo* experimentation in mice was first conducted with a targeted toxin consisting of saporin, EGF and a molecular adapter in

combination with SA [164]. The therapy resulted in a 94% tumor volume reduction even when using a 50-fold lower targeted toxin concentration. Further experiments were carried out to study *in vivo* the synergistic anti-tumor effect of SE and SO1861 [83]. In the evaluation of acute toxicity, SO1861 did not present any toxicity in mice up to a dose of 100 μg/treatment. The combined therapy of SE and SO1861 resulted in a reduction of more than 90% in the average tumor volume. No statistically significant liver or kidney damage was observed during the therapy.

## 1.4. Objectives

Targeted toxins are a group of therapeutics that has been intensively studied and hold promising potential for their use in tumor-specific therapies. The effectiveness of targeted toxins is exhibited only when they are target-specifically internalized and able to escape from the endo/lysosomal vesicles. Although there is scientific evidence generated, which indicates that the use of oleanane saponins (a subclass of triterpenoidal saponins) as endo/lysosomal escape enhancers may result in augmentation of the efficacy of targeted toxins, this synergistic cytotoxicity enhancement has only been investigated in the case of two targeted toxin, namely saporin-epidermal growth factor (SE) and dianthin-30-epidermal growth factor (DE), containing the same ligand.

Therefore, the main objective of this thesis was to develop strategies for a platform technology to enhance the endo/lysosomal escape of targeted toxins. In such a system, the ligand of targeted toxins will be exchanged depending on the target cell type, and the synergistic principle between saporin and triterpenoidal saponins will be simultaneously exploited to achieve an enhanced cytotoxicity. In this way, different kinds of cancer cells with specific receptors will be targeted and treated with higher specificity and efficacy. To achieve all this, the following subgoals were defined.

Firstly, despite the fact that certain oleanane saponins possess the ability to synergistically enhance the cytotoxicity of type I RIPs at non-toxic concentrations, such saponins are also known for presenting membrane permeabilizing effects at higher concentrations. In order to differentiate between the two aspects, permeabilizing effects of oleanane saponins will be evaluated on different biological membranes.

Secondly, saporin will be characterized *in vitro* and its cytotoxicity will be compared to other RIPs such as gelonin and ricin A-chain (RTA). A panel of immunotoxins comprising of saporin and different monoclonal antibodies will be chemically constructed and their binding capacity, payload delivery and capacity to trigger antibody-dependent cell-mediated cytotoxicity (ADCC) will be evaluated. Most importantly, the cytotoxicity enhancement of immunotoxins by triterpenoidal saponins will be determined.

Thirdly, an expression system for an inactive variant of saporin that has been described in the literature (saporin-KQ) will be established in order to open the possibility to generate a platform for enhanced non-toxic intracellular drug delivery. In this platform, the inactive saporin will enhance the endo/lysosomal escape of its cargo but will not cause any associated cytotoxicity.

Fourthly, a reporter assay for the endo/lysosomal escape will be developed to allow the study of the intracellular distribution of toxins in the presence of endo/lysosomal escape enhancers such as triterpenoidal saponins. Furthermore, the expression yield and cytotoxicity of the targeted toxins SE and DE will be compared in order to find, which of the two fusion proteins is more suitable for further development. Finally, the cytotoxicity enhancement of the targeted toxins SE, DE and diphtheria toxin$_{390}$-epidermal growth factor (DT$_{390}$-EGF) by triterpenoidal saponins will be measured to facilitate the understanding about the toxin specificity of this phenomenon.

# 2. Materials and methods

## 2.1. Materials

### 2.1.1. Instruments and devices

#### 2.1.1.1. Electrophoresis

- Dual Vertical Mini-Gel Unit MGV-202-U (CBS Scientific Company, San Diego, CA, USA)
- E835 power supply (Consort, Turnhout, Belgium)
- Mini Sub Cell GT System (Bio-Rad, Hercules, CA, USA)
- UV Transilluminator 312/254 nm (Intas, Göttingen, Germany).

#### 2.1.1.2. Western blot

- Optimax X-Ray Film Processor (Protec Medizintechnik, Oberstenfeld, Germany)
- Siemens $13 \times 18$ Cassette (Siemens, München, Germany)
- Trans-Blot Cell (Bio-Rad, Hercules, CA, USA)

#### 2.1.1.3. Spectrophotometers

- Nanodrop ND-1000 Spectrophotometer (Peqlab, Erlangen, Germany)
- Photometer 1101 M (Eppendorf, Hamburg, Germany)
- SpectraMax 340PC Absorbance Microplate Reader (Molecular Devices, Sunnyvale, CA, USA)

#### 2.1.1.4. Cell culture

- $CO_2$-Incubator Modell 311 (Forma Scientific/Thermo Scientific, Waltham, MA, USA)
- Dounce tissue grinder pestle, small clearance, working volume 2 ml (Sigma-Aldrich, Steinheim, Germany)
- Dounce tissue grinder pestle, small clearance, working volume 7 ml (Sigma-Aldrich, Steinheim, Germany)
- Heraeus HERAsafe Safety Cabinet (Heraeus/Thermo Scientific, Waltham, MA, USA)
- Neubauer chamber (Labor Optik, Bad Homburg, Germany)
- xCELLigence System RTCA (Roche Applied Science, Mannheim, Germany)

### 2.1.1.5. Centrifuges

- Cell centrifuge Megafuge 2.0 R (Heraeus/Thermo Scientific, Waltham, MA, USA)
- Microcentrifuge 5415 R (Eppendorf, Hamburg, Germany)
- Microcentrifuge PicoFuge (Stratagene, La Jolla, CA, USA)
- Optima L-90K Ultracentrifuge (Beckman Coulter, Krefeld, Germany)

### 2.1.1.6. Microscopy

- Axiovert 25 Microscope (Carl Zeiss, Jena, Germany)
- Focus stabilizer (Definite Focus, Carl Zeiss, Jena, Germany)
- Laser scanning microscope (LSM780, Axio Observer Z1, MicroImaging, Carl Zeiss, Jena, Germany) equipped with a Plan-Apochromat 63×/1.40 oil objective.

### 2.1.1.7. Other devices

- ABI PRISM 310 Genetic Analyser (Advanced Biolab Service, München, Germany)
- Branson Sonifier 250 (G. Heinemann, Schwäbisch Gmünd, Germany)
- ELx508V Microplate Strip Washer (BioTek Instruments, Winooski, VT, USA)
- FACScalibur (Becton Dickinson, Heidelberg, Germany)
- Incubated shaker Unitron (Infrors HT, Bottmingen, Switzerland)
- MALDI-TOF-MS instrument (Ultraflex-II TOF/TOF, Bruker Daltonics, Bremen, Germany) equipped with a 200 Hz solid-state Smart beam laser
- Thermoblock QBT (Grant Instruments, Cambridgeshire, UK)
- Vacuum concentration system Heto Holten A/S CT 110 (Leybold Heraeus, Hanau, Germany)

### 2.1.2. Consumables

### 2.1.2.1. Western blot

- Nitrocellulose membrane Hybond-C Extra (GE Healthcare, Uppsala, Sweden)
- Photographic paper Amersham Hyperfilm ECL (GE Healthcare, Uppsala, Sweden)

### 2.1.2.2. Chromatography

- Bio-Gel P-30 Medium (Bio-Rad, Hercules, CA, USA)
- Econo-Pac chromatography columns (Bio-Rad, Hercules, CA, USA)
- Ni-nitrilotriacetic acid (NTA) agarose (Protino Ni-NTA agarose, Macherey-Nagel, Düren, Germany)
- NucleoSEQ chromatography columns (Macherey-Nagel, Düren, Germany)
- PD-10 desalting column (GE Healthcare, Uppsala, Sweden)

### 2.1.2.3. Cell culture

- 96-well E-plate (Roche Applied Science, Mannheim, Germany)
- CellTrics 30 μm filter device (Partec, Görlitz, Germany)
- Falcon Cell Scraper, Handle: 25 cm; Blade: 1.8 cm (Fisher Scientific/Thermo Scientific, Waltham, MA, USA)
- μ-Dish 35 mm, low (Ibidi, Martiensried, Germany)

### 2.1.2.4. Other consumables

- Amicon Ultra-15 10,000 nominal molecular weight limit (NMWL) (Merck Millipore, Carrigtwohill, Ireland)
- Carboxymethylated C1 sensor chip (GE Healthcare, Uppsala, Sweden)
- Maxi Sorb U16 module (Nalgene Nunc, Panfield, NY, USA)
- Microcon Centrifugal Filter, Ultracel YM-3, regenerated cellulose 3,000 molecular weight cut off (MWCO) (Millipore, Billerica, MA, USA)
- ZelluTrans/Roth dialysis membrane T4, 12,000-14,000 MWCO (Carl Roth, Karlsruhe, Germany)

### 2.1.3. Chemicals

### 2.1.3.1. Plasmids

- 6× his-tagged-dianthin-30-epidermal growth factor (DE)-pET11d [82]
- 6× his-tagged-diphtheria toxin$_{390}$-epidermal growth factor (DT$_{390}$-EGF)-pET11d [165]
- 6× his-tagged-saporin-epidermal growth factor (SE)-pET11d [166]
- 6× his-tagged-saporin-KQ-pEN08H (Entelechon, Regensburg, Germany)

- 6× his-tagged-saporin-pET11d [166]

### 2.1.3.2. Primers

- Forward primer binding at the T7 promoter (5'-TAATACGACTCACTATAG-3')
- Reverse primer of the pET11d vector (5'-CCTGACGTCTAAGAAACC-3')

### 2.1.3.3. Antibodies

- Cetuximab (Erbitux®) (Merck, Darmstadt, Germany)
- Polyclonal goat anti-rabbit immunoglobulins/horseradish peroxidase (HRP) (Dako Cytomation, Hamburg, Germany)
- Rabbit polyclonal antibody against saporin (self-raised)
- Rituximab (Rituxan®) (Hoffmann-La Roche, Basel, Switzerland)
- Trastuzumab (Herceptin®) (Hoffmann-La Roche, Basel, Switzerland)

### 2.1.3.4. Other proteins

- Bovine serum albumin (BSA) (Albumin Standard, Thermo Scientific, Waltham, MA, USA)
- *Eco*RI-HF (Fermentas/Thermo Scientific, Waltham, MA, USA)
- Epidermal growth factor receptor (EGFR) Human Sf9 (ProSpec-Tany Technogene, East Brunswick, NJ, USA)
- Epidermal growth factor receptor 2 (HER2) Protein His Tag (Sino Biological, Beijing, P. R. China)
- Gelonin from *Gelonium multiflorum* A. Juss. (Enzo Life Sciences, Farmingdale, NY, USA)
- Horseradish peroxidase (HRP) (Serva Electrophoresis, Heidelberg, Germany)
- Ligase T4 (Fermentas/Thermo Scientific, Waltham, MA, USA)
- *Nco*I-HF (Fermentas/Thermo Scientific, Waltham, MA, USA)
- Ricin A-chain (RTA) from *Ricinus communis* L. (Sigma-Aldrich, Steinheim, Germany)
- Saporin-anti-CD22 (Advanced Targeting Systems, San Diego, CA, USA)
- Saporin-anti-CD25 (Advanced Targeting Systems, San Diego, CA, USA)
- Trypsin Gold, Mass Spectrometry Grade (Promega, Fitchburg, WI, USA)

### 2.1.3.5. Saponins

- Digitonin from *Digitalis purpurea* L. (Ysat, Wernigerode, Germany)
- Glycyrrhizinic acid from *Glycyrrhiza glabra* L. (Carl Roth, Karlsruhe, Germany)
- *Quillaja* saponin 1 from *Quillaja saponaria* Mol., Saponin from quillaja bark, sapogenin content 20–35%, product number S4521 - 10G (Sigma-Aldrich, Steinheim, Germany)
- *Quillaja* saponin 2 from *Quillaja saponaria* Mol., Saponin, sapogenin content 10–11%, product number 6857.1 (Carl Roth, Karlsruhe, Germany)
- SA1641 was purified from SA by high-performance liquid chromatography (HPLC) by Dr. Alexander Weng [41]
- SA1657 was purified from SA by HPLC by Dr. Stefan Böttger [6]
- Saponinum album (SA), saponin mixture isolated from *Gypsophila paniculata* L. and *Gypsophila arrostii* Guss. (Merck, Darmstadt, Germany)
- SO1861 from *Saponaria officinalis* L. was isolated from the roots of the plant (Galke, Gittelde, Germany) by HPLC by Dr. Mayank Thakur [83]
- α-Hederin from *Hedera helix* L. (Sigma-Aldrich, Steinheim, Germany)

### 2.1.3.6. Cell culture

- 0.25% Trypsin-ethylenediaminetetraacetic acid (EDTA) (Gibco/Invitrogen, Karlsruhe, Germany)
- Dulbecco's modified Eagle's medium (DMEM) (PAA Laboratories, Pasching, Austria)
- Dulbecco's phosphate buffered saline (PBS) without $Ca^{2+}$ and $Mg^{2+}$ (PAA Laboratories, Pasching, Austria)
- Fetal bovine serum (FBS) (BioChrom KG, Berlin, Germany)
- Lymphocyte Separation Media (PromoCell, Heidelberg, Germany)
- Mononuclear Cell Medium (PromoCell, Heidelberg, Germany)
- Penicillin/Streptomycin (PS) (Gibco/Invitrogen, Karlsruhe, Germany)
- Roswell Park Memorial Institute (RPMI)-1640 medium (PAA Laboratories, Pasching, Austria)
- RPMI-1640 medium without phenol red (PAA Laboratories, Pasching, Austria)

### 2.1.3.7. Fluorescent dies

- Propidium iodide (PI), ≥94% (HPLC) (Sigma-Aldrich, Steinheim, Germany)
- Hoechst 33342 (Life Technologies, Carlsbad, CA, USA)

- CellMask Deep Red (Invitrogen, Darmstadt, Germany)
- pHrodo Red Dextran, 10 kDa (Invitrogen, Darmstadt, Germany)
- Alexa Fluor 488 Carboxylic Acid, 2,3,5,6-Tetrafluorophenyl Ester (Alexa Fluor 488 5-TFP) (Molecular Probes, Eugene, USA)

### 2.1.3.8. Electrophoresis reagents

- Acrylamide 4K - Solution (30%) - Mix 37.5:1 Acrylamide : Bisacrylamide (AppliChem, Darmstadt, Germany)
- Agarose NEEO Ultra (Carl Roth, Karlsruhe, Germany)
- Bromophenol blue Na-salt (Serva Electrophoresis, Heidelberg, Germany)
- Coomassie Brillant blue R-250 (AppliChem, Darmstadt, Germany)
- PageRuler Prestained Protein Marker (Fermentas/Thermo Scientific, Waltham, MA, USA)
- Quick-Load 1 kb DNA Ladder (New England Biolabs, Ipswich, MA, USA)
- Unstained Protein Molecular Weight Marker (Fermentas/Thermo Scientific, Waltham, MA, USA)

### 2.1.3.9. Sequencing reagents

- BigDye Terminator 5× Sequencing Buffer (Applied Biosystems, Carlsbad, CA, USA)
- BigDye Terminator Mix (Applied Biosystems, Carlsbad, CA, USA)
- Hi-Di formamide (Applied Biosystems, Carlsbad, CA, USA)

### 2.1.3.10. Kits

- Human NK Cell Isolation Kit (Miltenyi Biotec, Bergisch Gladbach, Germany)
- Pierce BCA Protein Assay (Pierce/Thermo Scientific, Waltham, MA, USA)
- Zymoclean Gel DNA Recovery Kit (Zymo Research, Irvine, CA, USA)
- Zyppy Plasmid Miniprep Kit (Zymo Research, Irvine, CA, USA)

### 2.1.3.11. Other chemicals

- α-Cyano-4-hydroxycinnamic acid (CHCA) (Sigma-Aldrich, Steinheim, Germany)
- 2,3-Bis-(2-methoxy-4-nitro-5-sulfophenyl)-2$H$-tetrazolium-5-carboxanilide (XTT) (Serva Electrophoresis, Heidelberg, Germany)

- 3-(4,5-Dimethylthiazol-2-yl)-2,5-diphenyltetrazolium bromide (MTT) (Calbiochem, Darmstadt, Germany)

- 3,3′,5,5′-Tetramethylbenzidine (TMB) (Merck, Darmstadt, Germany)

- 4-nitrophenyl *N*-acetyl-β-D-glucosaminide (Sigma-Aldrich, Steinheim, Germany)

- Adenosine triphosphate (ATP), > 98 %, 100 mM solution (Carl Roth, Karlsruhe, Germany)

- Ampicillin sodium salt (Carl Roth, Karlsruhe, Germany)

- Doxorubicin hydrochloride (Sigma-Aldrich, Steinheim, Germany)

- HBS-EP running buffer (GE Healthcare, Uppsala, Sweden)

- Live cell imaging solution (Invitrogen, Darmstadt, Germany)

- *N*-succinimidyl-3-(2-pyridyldithio)propionate (SPDP) (Pierce/Thermo Scientific, Waltham, MA, USA)

- Phenazine-methosulfate (PMS) (Serva Electrophoresis, Heidelberg, Germany)

- Protease inhibitor Complete (Roche Applied Science, Mannheim, Germany)

- Triton X-100 (Sigma-Aldrich, Steinheim, Germany)

- UltraPure Herring Sperm DNA Solution (Invitrogen, Darmstadt, Germany)

- Isopropyl β-D-1-thiogalactopyranoside (IPTG) (AppliChem, Darmstadt, Germany)

### 2.1.4. Bacterial strains

- *Escherichia coli* Library Efficiency DH5α Competent Cells (Life Technologies, Carlsbad, CA, USA)

- *Escherichia coli* Rosetta 2(DE3) pLysS Competent Cells (Novagen, San Diego, CA, USA)

### 2.1.5. Cell lines

- BT-474 cells (ACC-64, human breast ductal carcinoma, obtained from the Department of Tumor Biology, Universitätsklinikum Hamburg-Eppendorf, Germany)

- ECV-304 cells (ACC-310, human urinary bladder carcinoma) (Deutsche Sammlung von Mikroorganismen und Zellkulturen, Braunschweig, Germany)

- HER14 cells (Swiss mouse embryo NIH-3T3 cells transfected with human EGFR, obtained from E.J. Zoelen, Department of Cell Biology, University of Nijmegen, The Netherlands)

- Ramos cells (ACC-603, human B-lymphocyte Burkitt lymphoma) (Deutsche Sammlung von Mikroorganismen und Zellkulturen, Braunschweig, Germany)

- TSA-EGFR (BALB/C mouse mammary adenocarcinoma cells transfected with human EGFR, TSA cells obtained from S. Bulfone-Paus, Institut für Immunologie, Freie Universität Berlin, transfection performed in Institut für Laboratoriumsmedizin, Klinische Chemie und Pathobiochemie, Charité – Universitätsmedizin Berlin)

### 2.1.6. Computer software

- BIAevaluation software 4.1.1. (GE Healthcare, Uppsala, Sweden)
- BLASTP 2.2.27+ (NCBI, USA)
- Cn3D (version 4.3) (NCBI, USA)
- Compute pI/Mw (http://web.expasy.org/compute_pi/, ExPASy, Swiss Institute of Bioinformatics, Lausanne, Switzerland)
- EnzymeX (Makentosj, Amsterdam, The Netherlands)
- GraphPad Prism 5 (GraphPad Software, La Jolla, CA, USA)
- IBM SPSS Statistics Version 21 (IBM Corporation, Armonk, NY, USA)
- Jmol 11.9.7 (http://www.jmol.org)
- Mascot (Matrix Science, London, UK)
- Mfold (http://mfold.rna.albany.edu/?q=mfold, [167])
- PlasmaDNA (University of Helsinki, Helsinki, Finland)
- Protein Structure Comparison Tool V 1.2 (RCSB PDB, USA)
- Rare Codon Search (http://www.bioline.com/calculator/01_11.html)
- RTCA Software 1.2.1.1002 (Roche Applied Science, Mannheim, Germany)
- T-COFFEE (Version_9.03.r1318) (http://tcoffee.vital-it.ch/apps/tcoffee/index.html, ExPASy, Swiss Institute of Bioinformatics, Lausanne, Switzerland)
- ZEN 2010 (Carl Zeiss, Jena, Germany)

## 2.2.  Molecular biology methods

### 2.2.1.   Transformation

Plasmids were transformed either into *Escherichia coli* Library Efficiency DH5α Competent Cells (Life Technologies) for replication or into *Escherichia coli* Rosetta 2(DE3) pLysS Competent Cells (Novagen) to recombinantly express the encoded protein. To do so, 100 ng of the plasmid was added to 20 µl bacteria from the stock solution of the supplier. Transformation was facilitated by a heat-shock (30 min on ice, 90 s at 42 °C and 1 min on ice). Further, 300 µl Lysogeny broth (LB) (10 g/l pepton, 5 g/l yeast extract, 10 g/l NaCl, pH 7.0) medium without antibiotic was added to the bacteria and the suspension was incubated for 1 h at 37 °C under continuous shaking at 200 rpm. A preheated LB medium-agar plate with 50 µg/ml ampicillin was inoculated with 100 µl bacteria suspension and the plate was incubated overnight at 37 °C.

### 2.2.2.   Molecular cloning of saporin-KQ

The DNA for saporin-KQ previously reported in the literature [168] was synthesized and cloned into a pEN08H vector (6× his-tagged-saporin-KQ-pEN08H) by Entelechon. A simulation of the cloning assay was firstly performed with the computer software PlasmaDNA (University of Helsinki). Thereafter, the digestion of the commercial plasmid was done by *Nco*I-HF (C^CATGG) and *Eco*RI-HF (G^AATTC). 6× his-tagged-DE-pET11d was digested with the same restriction enzymes. The reaction mixture was prepared by adding 0.1 µl *Nco*I-HF (10 U/µl) and 0.1 µl *Eco*RI-HF (10 U/µl) to either 500 ng 6× his-tagged-saporin-KQ-pEN08H or 6× his-tagged-DE-pET11d, 1 µl 10× Ne Buffer 4 and $H_2O$ up to 10 µl. Thereafter the digestion mixture was incubated overnight at 37 °C. To separate the digested DNA for saporin-KQ and the digested vector pET11d from the other digestion products, an agarose gel electrophoresis was performed (see section 2.2.3). The bands that contained the digestion products of interest were cut and DNA was extracted with the Zymoclean Gel DNA Recovery Kit (Zymo Research). The concentration of the extracted digestion products was determined by the Nanodrop ND-1000 Spectrophotometer (Peqlab).

The calculations for the ligation between digested DNA for saporin-KQ and digested vector pET11d were performed using the computer software EnzymeX (Makentosj). The optimal volumes of insert and vector were determined for an insert/vector molar ratio of 3:1. The reaction mixture was prepared by adding 0.2 µl ligase T4 (5 U/µl) to the corresponding amounts

of insert and vector (50 ng), 2 µl 10× ligase buffer, 1 µl adenosine triphosphate (ATP) (10 mM) and H$_2$O up to 20 µl. The ligation mixture was incubated overnight at 16 °C. The following day, the temperature was raised to 22 °C for 10 min, to 37 °C for 10 min and finally to 65 °C for 10 min. The ligation product was immediately used or stored at −20 °C.

### 2.2.3. Agarose gel electrophoresis

Agarose gel electrophoresis was used as a technique to separate DNA. Agarose gel electrophoresis was performed with a 1% (w/v) agarose gel in Tris acetate EDTA (TAE) buffer (40 mM Tris, 5 mM sodium acetate and 1 mM EDTA, pH 7.2) in the presence of ethidium bromide at a final concentration of 0.4 µg/ml. DNA solution was added to the well of the agarose gel and electrophoresis was carried out at 120 V and 100 mA (E835 power supply from Consort) for 30 min without any gradient in a Mini Sub Cell GT System (Bio-Rad). Quick-Load 1 kb DNA Ladder (0.5–10.0 kb) (New England Biolabs) was simultaneously analyzed to estimate the molecular mass of the DNA samples. Separated DNA was visualized under UV light at 254 nm (UV Transilluminator 312/254 nm, Intas).

### 2.2.4. Replication of plasmids

To replicate a plasmid, a transformation was done into *Escherichia coli* Library Efficiency DH5α Competent Cells as described before. A colony of the bacteria transformed by the plasmid was picked and added to 5 ml LB with 50 µg/ml ampicillin. It was incubated overnight at 37 °C while shaking at 200 rpm. On the next day, 4 ml of the 5 ml culture was centrifuged at 5,000$g$ for 5 min. The supernatant was discarded and the pellet was re-suspended in 600 µl H$_2$O. Then, the plasmid was extracted with the Zyppy Plasmid Miniprep Kit (Zymo Research). After following the protocol indicated by the manufacturer (Zymo Research), the DNA concentration was determined by the Nanodrop ND-1000 Spectrophotometer and the plasmid was stored at −20 °C.

### 2.2.5. DNA sequencing

The DNA sequence for saporin-KQ in pET11d was sequenced by the method of BigDye Terminator Sequencing (Applied Biosystems). This step was performed in order to check whether the DNA for saporin-KQ was inserted properly into the vector pET11d. The forward

primer binding at the T7 promoter, at the 5'-end of the insert (5'-TAATACGACTCACTATAG-3') or the reverse primer of the pET11d vector binding at the 3'-end of the insert (5'-CCTGACGTCTAAGAAACC-3') were used to prepare the two PCR master mixes: 1 µl of either forward or reverse primer (10 pmol/µl), 100 ng plasmid, 2 µl BigDye Terminator $5\times$ Sequencing Buffer (Applied Biosystems), 1.5 µl BigDye Terminator Mix (Applied Biosystems) and $H_2O$ up to 10 µl. After the PCR reactions for sequencing were conducted, the dye-terminators were removed from the PCR products by the NucleoSEQ chromatography columns (Macherey-Nagel). After clean-up of the sequencing PCR products, 10 µl of purified PCR product was obtained for each PCR reaction. It was centrifuged under vacuum (Vacuum concentration system Heto Holten A/S CT 110, Leybold Heraeus) for 7 min at room temperature, thereafter 25 µl Hi-Di formamide (Applied Biosystems) was added and the mixture was incubated at 95 °C for 3 min. The samples were finally sequenced with the ABI PRISM 310 Genetic Analyser (Advanced Biolab Service).

## 2.3.  Protein chemistry methods

### 2.3.1.  Protein expression in *Escherichia coli*

The plasmids coding for saporin ($6\times$ his-tagged-saporin-pET11d [166]), saporin-KQ ($6\times$ his-tagged-saporin-KQ-pET11d), saporin-epidermal growth factor (SE) ($6\times$ his-tagged-SE-pET11d [166]), dianthin-30-epidermal growth factor (DE) ($6\times$ his-tagged-DE-pET11d [82]) or diphtheria toxin$_{390}$-epidermal growth factor ($DT_{390}$-EGF) ($6\times$ his-tagged-$DT_{390}$-EGF-pET11d [165]) were transformed into *Escherichia coli* Rosetta 2(DE3) pLysS Competent Cells. A small amount (3 ml) of LB medium with 50 µg/ml ampicillin was inoculated with a colony from the plate and the bacteria were incubated for 8 h at 37 °C and 200 rpm. An amount of 50 µl of this bacterial suspension was added to 500 ml of LB medium with 50 µg/ml ampicillin and the culture was allowed to proliferate overnight at 37 °C and 200 rpm. Subsequently, the volume of bacterial suspension was scaled-up to a culture of 2 l and bacteria grew under the same conditions until an optical density ($A_{600nm}$) of 0.9 was reached (Photometer 1101 M, Eppendorf). Thereafter, protein expression was induced by the addition of isopropyl β-D-1-thiogalactopyranoside (IPTG) at a final concentration of 1 mM. Protein expression lasted for 3 h at 37 °C and 200 rpm. Finally, the bacterial suspension was centrifuged at 5,000$g$ and 4 °C for 5 min, re-suspended in 20 ml phosphate buffered saline (PBS) (137 mM NaCl, 2.7 mM KCl, 8.1 mM $Na_2HPO_4$, 1.47 mM $KH_2PO_4$ according to Dulbecco [169]) and stored at –20 °C until use.

### 2.3.2.  Toxicity of targeted toxins in *Escherichia coli*

In order to determine the toxicity of the targeted toxins SE and DE in *Escherichia coli* Rosetta 2(DE3) pLysS, 3 ml of LB medium supplemented with 50 µg/ml ampicillin was inoculated with a colony from the plate (efficiently transformed bacteria) and the bacteria were incubated for 8 h at 37 °C and 200 rpm. Subsequently, 1 ml of this bacterial suspension was added to 100 ml LB medium supplemented with 50 µg/ml ampicillin and the culture was allowed to grow until an approximate optical density of 0.27. Protein expression was induced by adding IPTG at the final concentration of 1 mM and cell growth was monitored for the following 3 h. Optical density was read every 30 min with a SpectraMax 340PC Absorbance Microplate Reader (Molecular Devices).

### 2.3.3.  Protein purification by Ni-NTA affinity chromatography

After expression bacterial suspension was thawed and lysed with an ultrasound device (Branson Sonifier 250, G. Heinemann). Lysates were centrifuged at 15,800$g$ and 4 °C for 30 min and imidazole added to a final concentration of 20 mM. The supernatant containing the expressed protein was purified by Ni-nitrilotriacetic acid (NTA) agarose affinity chromatography (Protino Ni-NTA agarose). The supernatant was incubated with 2 ml of Ni-NTA agarose under continuous shaking for 30 min at 4 °C. Subsequently, the material was poured into a 20-ml-column (Econo-Pac chromatography columns, Bio-Rad). The column was washed three times with 10 ml wash buffer (50 mM $NaH_2PO_4$, 300 mM NaCl, 20 mM imidazole, pH 8.0) and the protein was eluted by increasing concentrations of imidazole in wash buffer (31, 65, 125 and 250 mM). Elution was performed by 10 ml of each imidazole concentration and fractions of 2 ml were collected. Eluates were analyzed by sodium dodecyl sulfate-polyacrylamide gel electrophoresis (SDS-PAGE) [7.5 % or 12% (w/v) gel depending on the molecular mass of the protein], pooled afterwards and dialyzed overnight at 4 °C against 2 l PBS (see section 2.3.5). The desalted protein was concentrated by an Amicon Ultra-15 10,000 NMWL (Merck Millipore). The protein concentration was determined by a bicinchoninic acid (BCA) (Pierce BCA Protein Assay) assay (see section 2.3.6) and the protein stored at −20 °C.

In case of $DT_{390}$-EGF, protein got accumulated in inclusion bodies during expression. Therefore, the supernatant was discarded after centrifugation of lysates at 15,800$g$ and 4 °C for 30 min.

Pellet was briefly washed with $H_2O$ and re-suspended in buffer B (100 mM $NaH_2PO_4$, 10 mM Tris HCl, 8 M urea, pH 8.0). The re-suspended pellet was incubated in buffer B under continuous shaking for 1 h and thereafter pellets were centrifuged at 15,800$g$ and 4 °C for 30 min. On this occasion, supernatant was collected and imidazole was added to a final concentration of 20 mM. Ni-NTA agarose affinity chromatography was performed as described above, with the only difference that buffer B was used instead of wash buffer to maintain the protein in its denatured state during the purification. After analysis by SDS-PAGE [12% (w/v)], eluates were pooled and $DT_{390}$-EGF was dialyzed in several steps with decreasing concentrations of urea (see section 2.3.5). Protein concentration was determined by a BCA assay and protein was stored at –20 °C.

### 2.3.4. SDS-PAGE

Proteins were analyzed by sodium dodecyl sulfate-polyacrylamide gel electrophoresis (SDS-PAGE) in 7.5 % (w/v) gels in the case of saporin-Trastuzumab (ST), saporin-Cetuximab (SC), saporin-Rituximab (SR) and saporin-horseradish peroxidase (SH), or in 12% (w/v) gels in the case of saporin, saporin-KQ, SE, DE and $DT_{390}$-EGF. Electrophoresis was performed at 200 V and 60 mA for each gel (E835 power supply from Consort) for 40 min in a Dual Vertical Mini-Gel Unit MGV-202-U (CBS Scientific Company).

Unstained Protein Molecular Weight Marker (14.4–116 kDa) (Fermentas/Thermo Scientific) was used in the analysis of low molecular mass proteins while PageRuler Prestained Protein Marker (10–170 kDa) (Fermentas/Thermo Scientific) was used in the analysis of higher molecular mass proteins and for those proteins that were further characterized by Western blot. Furthermore, SDS-PAGE was performed under non-reducing conditions and under reducing conditions. In the latter case, 2-mercaptoethanol [8% (v/v)] was added in the loading buffer.

After the SDS-PAGE, gels were stained with a solution of 0.1% (w/v) Coomassie Blue R-250 (AppliChem) in 40% (v/v) methanol and 10% (v/v) acetic acid, destained in a solution of 20% (v/v) ethanol and 10% (v/v) acetic acid and the gels were finally fixed in a solution of 25% (v/v) methanol and 4% (v/v) glycerol.

### 2.3.5. Dialysis and concentration of protein solutions

The fractions that contained the protein of interest (previously purified by Ni-NTA affinity chromatography and analyzed by SDS-PAGE) were pooled and dialyzed overnight at 4 °C against 2 l PBS. To achieve a concentrated protein solution, the desalted protein was concentrated by repeated centrifugation steps of 5 min at 4,000$g$ with the Amicon Ultra-15 10,000 NMWL until a volume of approximately 2 ml was achieved.

In the case of $DT_{390}$-EGF, the fractions that contained the protein (previously purified by Ni-NTA affinity chromatography in buffer B and analyzed by SDS-PAGE) were pooled and $DT_{390}$-EGF was allowed to refold by dialysis in several steps with decreasing concentrations of urea. First, protein solution was dialyzed overnight at 4 °C against 2 l of 2 M urea in buffer B. Then, protein solution was dialyzed overnight against 1 M urea in buffer B. Protein was again dialyzed overnight at 4 °C against buffer B without urea and thereafter for 3 h against PBS. Finally, $DT_{390}$-EGF was concentrated as described above.

### 2.3.6. Determination of protein concentration by BCA assay

Protein concentration was determined by the BCA assay (Pierce BCA Protein Assay, Pierce/Thermo Scientific). To determine the protein concentration of unknown samples, a standard curve was prepared with bovine serum albumin (BSA) (Albumin Standard, Thermo Scientific) by measuring the mean absorbance at 562 nm after the experiment (following the indications of the manufacturer, Pierce/Thermo Scientific) for the concentrations of 0.05, 0.10, 0.15, 0.25, 0.50, 0.75, 1.00, 1.50 and 2.00 mg/ml BSA and deducting it from the blank. The absorbance was measured by the SpectraMax 340PC Absorbance Microplate Reader.

### 2.3.7. Chemical conjugation of saporin to monoclonal antibodies

Chemical cross-linking of antibodies to saporin was performed *via* *N*-succinimidyl-3-(2-pyridyldithio)propionate (SPDP, Pierce/Thermo Scientific). Trastuzumab (5 mg) (Herceptin®, Hoffmann-La Roche), Cetuximab (5 mg) (Erbitux®, Merck), Rituximab (5 mg) (Rituxan®, Hoffmann-La Roche) and saporin (1 mg) (molar ratio of 1:1 for Trastuzumab : saporin, for Cetuximab : saporin and for Rituximab : saporin) were separately dialyzed overnight against PBS supplemented with 1 mM EDTA, 0.02% (w/v) sodium azide, pH 7.5 (PBS-EDTA). All

proteins were modified with 20 mM SPDP for 1 h at 25 °C and were dialyzed overnight against PBS-EDTA again. The modified saporin was chemically reduced by 150 mM dithiothreitol (DTT) for 30 min at 25 °C and thereafter DTT was removed using a PD-10 desalting column (GE Healthcare). SPDP-modified Trastuzumab, Cetuximab and Rituximab were separately mixed with the modified saporin and incubated for 18 h at 25 °C. The resulting products ST, SC and SR were purified in a first step by size-exclusion chromatography. The immunotoxins were purified in a second step by Ni-NTA affinity chromatography. Finally, the purified immunotoxins were analyzed by SDS-PAGE [7.5% (w/v) gel] under reducing and non-reducing conditions.

### 2.3.8. Protein purification by size-exclusion chromatography

ST, SC and SR were purified by size-exclusion chromatography with Bio-Gel P-30 Medium (Bio-Rad) directly after the chemical conjugation. Bio-Gel P-30 Medium (3.2 g) was allowed to hydrate for 12 h at 20 °C with 75 ml PBS. Gel was stored in 30% (v/v) ethanol solution at 4 °C until use.

Hydrated Bio-Gel P-30 Medium was centrifuging at $4,000g$ and 25 °C for 5 min and re-suspended in PBS. This washing step was repeated twice. Then, 10 ml of the gel was added to the 20-ml-column (Econo-Pac chromatography columns, Bio-Rad) and allowed to settle down. The column was washed with 20 ml PBS and 1 ml of protein solution containing the conjugate of saporin to monoclonal antibody (conjugate was previously concentrated with an Amicon Ultra-15 10,000 NMWL until a volume of 1 ml was achieved) was applied to the column. Conjugates were eluted with 10 ml PBS and 20 fractions of 0.5 ml were collected. In the case of ST, the conjugate was eluted with additional 10 ml PBS and 10 further fractions of 1 ml were collected. The protein concentration in each of the eluted fractions was determined by the BCA assay and fractions containing protein were further analyzed by SDS-PAGE [7.5% (w/v) gel] and Western blot.

### 2.3.9. Chemical conjugation of saporin to HRP

Chemical conjugation of saporin to horseradish peroxidase (HRP) was performed *via* modification of the *N*-glycans of HRP by sodium periodate ($NaIO_4$) oxidation and sodium borohydride ($NaBH_4$) reduction.

Freshly prepared 0.1 M $NaIO_4$ (185.05 µl) was added to 7.30 mg HRP (previously dissolved in 2 ml water) and the solution was stirred for 20 min at room temperature protecting it from light. The modified HRP was dialyzed overnight at 4 °C against 8 l of 1 mM sodium acetate buffer (pH 4.4). In parallel, 2 ml saporin (1.235 mg/ml) was buffered with 200 µl sodium hydrogen carbonate buffer (0.2 M, pH 9.5). The pH value of the dialyzed modified HRP was adjusted to 9.0–9.5 by adding 80 µl sodium hydrogen carbonate buffer and it was immediately mixed with the saporin solution (molar ratio of 2:1 for HRP : saporin). The mixture was stirred for 2 h at room temperature. After the incubation time, 100 µl of freshly prepared $NaBH_4$ (4 mg/ml) was added to the mixture and it was further stirred for 2 h at 4 °C. The protein solution was dialyzed overnight against 2 l PBS. Saporin-horseradish peroxidase (SH) solution was further purified by Ni-NTA affinity chromatography.

### 2.3.10. Western blot

Proteins (ST, SC, SR, saporin-KQ and SH) were separated by SDS-PAGE [7.5% or 12% (w/v) gel] and then blotted at 50 V and 15 °C for 1 h to a nitrocellulose membrane (Hybond-C Extra). The membrane was blocked for 30 min with blocking solution [PBS with 5% (w/v) skim milk powder] and incubated with a self-raised rabbit polyclonal antibody against saporin (1:300 diluted) for further 30 min. The membrane was washed 4 times with $PBSB_{0.2}$ [PBS with 0.2% (w/v) Brij58, pH 7.4] for 10 min each time and thereafter it was treated with polyclonal goat anti-rabbit immunoglobulins/HRP (1:10,000 diluted) (Dako Cytomation) for 30 min. The membrane was washed again for 4 times with $PBSB_{0.2}$. The binding of the secondary antibody was detected by enhanced chemiluminescence reaction. After exposure, the photographic paper (Amersham Hyperfilm ECL, GE Healthcare) was developed by an Optimax X-Ray Film Processor (Protec Medizintechnik).

For a stability analysis, ST, SC and saporin were incubated at 37 °C for 6 or 24 h with conditioned medium [RPMI-1640 medium (PAA Laboratories) supplemented with 10% fetal bovine serum (FBS) (BioChrom KG) and 1% Penicillin/Streptomycin (PS) (Gibco/Invitrogen) which was consumed for one week by BT-474 cells at 37 °C and 5% $CO_2$ and centrifuged at 800$g$ for 5 min before addition to the proteins]. After the incubation period, proteins in the medium were separated by SDS-PAGE [7.5% (w/v) gel] and further analyzed by Western blot as described above.

### 2.3.11.  Determination of *N*-glycosidase activity

*N*-glycosidase activity of proteins was determined by the cleavage and release of adenine residues from herring sperm DNA [82, 170]. First, a standard curve was prepared with adenine by measuring the absorbance at 260 nm (reference at 300 nm) for the concentrations of 10, 20, 40, 80, 160 and 320 pmol/µl adenine. Absorbance was measured by the Nanodrop ND-1000 Spectrophotometer (Peqlab).

To determinate the *N*-glycosidase activity of a toxin, 10 µl herring sperm DNA (100 µg) (Invitrogen) was added to 30 pmol toxin and acetate buffer (50 mM $CH_3COONa$, 100 mM KCl, pH 5.0) up to 50 µl. The mixture was incubated under continuous shaking at 50 °C for 1 h. After the incubation period, the mixture was transferred to a filtration device (3,000 MWCO) (Millipore) and centrifuged at 4 °C and 5,000*g* for 45 min. Absorbance of the filtrate was measured at 260 nm (reference at 300 nm).

For the investigation of the influence of triterpenoidal saponins on the *N*-glycosidase activity of saporin and ricin A-chain (RTA), SA1641 [final concentration of 5 µg/ml (3.05 µM)] was added to the reaction mixture.

### 2.3.12.  Determination of peroxidase activity

Peroxidase activity of SH was measured by adding 100 µl of the conjugate (concentrations from 0.00001 to 100 nM) to 100 µl of reagent [80 mM citric acid, 0.4 mg/ml 3,3′,5,5′-tetramethylbenzidine (TMB), 0.2 µg/ml $H_2O_2$, pH 3.95]. The mixture was incubated for 15 min at room temperature. The reaction was stopped by addition of 50 µl $H_2SO_4$ (3.3 M) and absorbance of the mixture was measured at 450 nm (reference at 490 nm) by a SpectraMax 340PC Absorbance Microplate Reader.

The procedure for determination of peroxidase activity was modified to measure the activity of SH released from isolated lysosomes. The protein solution (20 µl of supernatant after last centrifugation step, see section 2.4.8) was mixed first with 30 µl translocation buffer (T buffer) (20 mM HEPES, 10 mM $MgSO_4$ and 0.1 M KCl, pH 7.0). Thereafter, 50 µl of reagent was added and the mixture was incubated for 1 h at room temperature. The reaction was stopped by adding 25 µl $H_2SO_4$ (3.3 M). Absorbance was measured at 450 nm (reference at 490 nm).

To determine the peroxidase activity of SH in cellular fractions (see section 2.4.9), either 50 µl of (a) cytosolic fraction or (b) lysosomal fraction was added to 20 µl citrate buffer (80 mM citric acid, pH 3.95). After incubation of the fractions for 5 min, precipitate was discarded by centrifugation at 16,100$g$ for 2 min. Then, 50 µl of the reagent was added to the supernatant. The mixture was incubated for 5 min at room temperature and the reaction was stopped by adding 50 µl $H_2SO_4$ (3.3 M). Absorbance was measured at 450 nm (reference at 490 nm).

### 2.3.13. Surface plasmon resonance spectroscopy

Binding of ST and SC to their cellular receptors was characterized by surface plasmon resonance spectroscopy. Carboxymethylated C1 sensor chips (GE Healthcare) were activated by 1-ethyl-3-(3-dimethylaminopropyl)carbodiimide (EDC) / $N$-hydroxysuccinimide (NHS) chemistry following the instructions of the manufacturer (GE Healthcare). ST or SC was immobilized in acetate buffer (10 mM $CH_3COONa$, pH 5.0) at 5 µl/min using HBS-EP running buffer (GE Healthcare). ST was immobilized to a level of 270 response units (RU) and SC to 355 RU. To delineate specific from unspecific binding, a control surface treated chemically with EDC/NHS but without immobilized protein was used. Running buffer in this experiment was Dulbecco's PBS without $Ca^{2+}$ and $Mg^{2+}$ (PAA Laboratories). The flow rate was adjusted to 30 µl/min and 100 µl of the soluble extracellular domain of each receptor was injected for a potential interaction with the immobilized immunotoxins. Soluble recombinant HER2 (amino acid 1 to 652) (Sino Biological) was diluted with the running buffer and injected at the final concentrations of 1, 2 and 4 µg/ml to test binding to ST. Soluble recombinant EGFR (amino acid 25 to 647) (ProSpec-Tany Technogene) was also diluted with running buffer and injected at the final concentrations of 1.3, 2.6 and 5.2 µg/ml to investigate binding to SC. Both association and dissociation phases lasted for 200 s. Sensorgrams were referred to the control surface and analyzed by BIAevaluation software 4.1.1. (GE Healthcare). $K_D$ values were calculated by a non-linear regression (one site – specific binding, binding – saturation) by the software GraphPad Prism 5 (GraphPad Software, La Jolla, CA, USA).

### 2.3.14. Fluorescence labeling

ST was conjugated to Alexa Fluor 488 Carboxylic Acid, 2,3,5,6-Tetrafluorophenyl Ester (Alexa Fluor 488 5-TFP) (Molecular Probes) by adding 100 µl carbonate buffer (1 M $Na_2CO_3$, pH 9.0)

and 108 µl of the fluorescent dye (5 mg/ml in DMSO) to a solution of 1 ml of ST (0.186 mg/ml in PBS). Labeling reaction was allowed for 1 h at room temperature and thereafter ST-Alexa Fluor 488 ([Alexa]ST) was purified from the unconjugated fluorophore by dialysis overnight at 4 °C against 2 l PBS. Saporin was conjugated to Alexa Fluor 488 5-TFP following the same procedure and after the dialysis against PBS, purified saporin-Alexa Fluor 488 ([Alexa]saporin) was obtained.

### 2.3.15. MALDI-TOF-MS

The targeted toxins SE and DE were analyzed by matrix-assisted laser desorption/ionization time-of-flight mass spectrometry (MALDI-TOF-MS) after recombinant expression in *Escherichia coli* and purification by Ni-NTA affinity chromatography. Peptides were obtained by trypsin in-gel digestion as described previously [171]. In concrete, 2 µg SE or DE were analyzed by SDS-PAGE. After staining with a solution of 0.1% (w/v) Coomassie Blue R-250 and destaining as explained in section 2.3.4, the respective bands were separately cut into small sized gel pieces and incubated with 20 µl acetonitril : 100 mM $NH_4HCO_3$ [1:1 (v/v)] for 15 min at room temperature. Bands were further washed 4 times with 30 µl acetonitril and subsequently lyophilized by a Vacuum concentration system Heto Holten A/S CT 110 (Leybold Heraeus). Then, bands were incubated with 20 µl DTT (100 mM in 100 mM $NH_4HCO_3$) for 30 min at 56 °C and washed 2 times with 30 µl acetonitril. Bands were treated with 20 µl iodoacetamide (55 mM in 100 mM $NH_4HCO_3$) for 30 min at room temperature protecting it from light and thereafter incubated with 20 µl $NH_4HCO_3$ (100 mM) for 15 min, washed 2 times with 30 µl acetonitril and lyophilized. Subsequently, bands were incubated with Trypsin Gold, Mass Spectrometry Grade (Promega) at a concentration of 12.5 µg/ml in 25 mM $NH_4HCO_3$ firstly for 30 min on ice and secondly overnight at 37 °C. Finally, digested peptides were extracted from each band by addition of a solution (10 µl) of 40% (v/v) acetonitril and 0.1% (v/v) trifluoroacetic acid, and incubation under continuous shaking overnight at room temperature.

Peptide masses were analyzed by MALDI-TOF-MS using an Ultraflex-II TOF/TOF instrument (Bruker Daltonics) equipped with a 200 Hz solid-state Smart beam laser. The mass spectrometer was operated in the positive reflector mode. Mass spectra were acquired over an *m/z* range of 600–4,000. α-Cyano-4-hydroxycinnamic acid (CHCA) was used as the matrix and protein digest samples were spotted using the dried droplet technique. MS/MS spectra of selected peptides

were acquired in the LIFT mode [172]. Database searches were performed using Mascot (Matrix Science). One missed cleavage was allowed and mass tolerance was usually set at $\pm$ 75 ppm.

## 2.4. Cell biology methods

### 2.4.1. Cell culture

ECV-304 cells (human urinary bladder carcinoma cell line) were cultured in Dulbecco's modified Eagle's medium (DMEM) (PAA Laboratories) supplemented with 10% fetal bovine serum (FBS) (BioChrom KG) and 1% Penicillin/Streptomycin (PS) (Gibco/Invitrogen). HER14 cells (Swiss mouse embryo NIH-3T3 cells transfected with human EGFR) and TSA-EGFR cells (BALB/C mouse mammary adenocarcinoma cells transfected with human EGFR) were grown in DMEM supplemented with 10% FBS and 1% PS. In the case of HER14 and TSA-EGFR cells, cell culture plates were pre-incubated with 0.1% (w/v) gelatin solution (100 µl/well). BT-474 cells (human breast ductal carcinoma) were cultured in RPMI-1640 medium (PAA Laboratories) supplemented with 10% FBS and 1% PS. Ramos cells (human B-lymphocyte Burkitt lymphoma) were grown in RPMI-1640 medium without phenol red (PAA Laboratories) supplemented with 20% FBS and 1% PS. Cells were allowed to proliferate in a humidified 5% $CO_2$ incubator at 37 °C. Dulbecco's PBS without $Ca^{2+}$ and $Mg^{2+}$ (PAA Laboratories) was used in the washing steps and 0.25% Trypsin-EDTA (Gibco/Invitrogen) for cell detachment.

### 2.4.2. End-point determination of the cytotoxicity by MTT assay

A cell number optimization for ECV-304 and HER14 cells was first performed to find the optimal initial cell number per well for the cytotoxicity assay. An initial amount of 100 µl/well of DMEM supplemented with 10% FBS and 1% PS containing different amount of cells (1,000; 2,000; 4,000; 6,000; 8,000; 10,000; 12,000; 14,000; 16,000; 18,000 and 20,000) of either ECV-304 or HER14 cells was pipetted in a 96-well plate. The cell number count was calculated with a Neubauer chamber (Labor Optik) and use of an Axiovert 25 Microscope (Carl Zeiss). In the case of HER14 cells, the 96-well plate was pre-incubated with 0.1% (w/v) gelatin solution (100 µl/well). Cells were allowed to proliferate at 37 °C and 5% $CO_2$ for 24 h. Then, medium was removed and 180 µl/well fresh medium plus 20 µl/well PBS was added to the wells. Cells were allowed to proliferate further 48 h under the same conditions as before.

## 2. Materials and methods

To determine the degree of cell proliferation, the final viable cell number was determined by the 3-(4,5-dimethylthiazol-2-yl)-2,5-diphenyltetrazolium bromide (MTT) assay. A solution of MTT (5 mg/ml, 30 µl/well) was pipetted directly to the media. The plate was incubated at 37 $^{\circ}$C for 2 h and thereafter media containing MTT was removed. Formazan solubilizer (50 µl/well) consisting of 82% (v/v) isopropanol (pure), 10% (v/v) of SDS solution [10% (w/v)] and 8% (v/v) of HCl solution (1 M) was added to the plate and after shaking it for 5 min, the absorbance was measured at 570 nm (reference at 630 nm) by the SpectraMax 340PC Absorbance Microplate Reader.

For analysis of the cytotoxicity of SA1641, 100 µl/well of DMEM supplemented with 10% FBS and 1% PS containing either 8,000 ECV-304 cells or 4,000 HER14 cells was pipetted in the 96-well plate. After 24 h of cell proliferation, medium was removed and 180 µl/well medium (untreated control cells) or medium containing SA1641 (final concentrations of 1, 2, 3, 5, 10, 20 and 40 µg/ml) was added to the wells. In addition, 20 µl/well PBS was added. Cells were allowed to proliferate further 48 h in the presence of saponin and cell viability was calculated at the end of the experiment by the MTT assay. Percentages of cell survival were calculated referring to the untreated cells.

To evaluate the cytotoxicity of saporin + SA1641, 100 µl/well of DMEM supplemented with 10% FBS and 1% PS containing either 4,000 ECV-304 cells or 2,000 HER14 cells was added. After 24 h of cell incubation, medium was removed and 180 µl/well medium containing SA1641 [final concentration of 5 µg/ml (3.05 µM)] and 20 µl/well PBS containing saporin (final concentrations from 0.000001 to 1,000 nM) was added. Then, 48 h after addition of compounds, cell viability was determined by the MTT assay. In the case of the cytotoxicity evaluation of saporin, gelonin or RTA + SO1861, cell viability was calculated by the MTT assay at the end point of the real-time cytotoxicity assay (see section 2.4.4.).

To determine the cytotoxicity of saporin or saporin-KQ + SO1861, 100 µl/well of DMEM supplemented with 10% FBS and 1% PS containing 4,000 ECV-304 cells was added. Cells were allowed to grow for 24 h and thereafter the medium was removed. Then, 180 µl/well medium containing SO1861 [final concentration of 2 µg/ml (1.07 µM)] and 20 µl/well PBS containing either saporin or saporin-KQ (final concentrations from 0.1 to 1,000 nM) was added. For the cytotoxicity evaluation of saporin or SH + SA1641, 180 µl/well medium containing SA1641 (final concentration of 5 µg/ml) and 20 µl/well PBS containing either saporin or SH (final concentrations from 0.01 to 100 nM) was added. To determine the cytotoxicity of saporin or DT$_{390}$-EGF + Saponinum album (SA), 180 µl/well medium containing SA [final concentration of

2 µg/ml (1.33 µM)] and 20 µl/well PBS containing either saporin or $DT_{390}$-EGF (final concentrations from 0.1 to 1,000 nM) was added. The experiments were continued as described previously.

### 2.4.3.   End-point determination of the cytotoxicity by XTT assay

A cell number optimization for Ramos cells was first conducted to find the optimal initial cell number per well for the cytotoxicity assay. An initial amount of 100 µl/well of RPMI-1640 medium without phenol red supplemented with 20% FBS and 1% PS containing different numbers of Ramos cells (800; 1,600; 3,100; 6,200; 12,500; 25,000; 50,000 and 100,000) was pipetted in a 96-well plate. Directly after seeding the cells, 50 µl/well medium was added to the wells and cell viability was measured by the 2,3-bis-(2-methoxy-4-nitro-5-sulfophenyl)-2*H*-tetrazolium-5-carboxanilide (XTT) assay.

To perform the XTT assay, 50 µl of a solution of XTT (1 mg/ml) and phenazine-methosulfate (PMS) (8 µg/ml) was added directly to the media. The plate was incubated at 37 ºC for 2 h and thereafter the absorbance was measured at 450 nm by the SpectraMax 340PC Absorbance Microplate Reader.

To analyze the cytotoxicity of SA1641, SA1657 and SO1861, 100 µl/well of RPMI-1640 medium without phenol red supplemented with 20% FBS and 1% PS containing 20,000 Ramos cells was added. Cells were allowed to proliferate for 24 h. Thereafter, 25 µl/well medium was added. In addition, 25 µl/well medium (untreated control cells) or medium containing SA1641, SA1657 or SO1861 (final concentrations of 0.13, 0.25, 0.5, 1 and 2 µg/ml) was added to the wells. When analyzing the cytotoxicity of SR, saporin-anti-CD22 (Advanced Targeting Systems) or saporin-anti-CD25 (Advanced Targeting Systems) + SO1861, 25 µl/well medium containing SO1861 [final concentration of 1 µg/ml (0.54 µM)] and 25 µl/well medium containing SR, saporin-anti-CD22 or saporin-anti-CD25 (final concentrations from 0.000001 to 10 nM) was added. Cells were allowed to grow for further 72 h in the presence of the compounds and cell proliferation was measured at the end of the experiment by the XTT assay. Percentages of cell viability were calculated referring to the untreated cells.

### 2.4.4. Real-time monitoring of membrane permeabilizing effects and cytotoxicity

Membrane permeabilizing effects of oleanane saponins were studied by the impedance-based xCELLigence System (Roche Applied Science). Firstly, 50 µl DMEM supplemented with 10% FBS and 1% PS was pipetted in each well of an E-plate (Roche Applied Science). E-plates incorporate a sensor electrode array at the well bottom in order to measure the impedance in real time. The impedance was set to zero for medium alone. Thereafter 5,000 ECV-304 cells were added (50 µl/well) and cells were allowed to settle on the plate surface for 20 min. Following this, the plate was clamped onto the plate station and the impedance measurement was started. Cells were allowed to proliferate for approximately 19 h as indicated by an increase of impedance. Then, 50 µl/well medium (untreated control cells) or 50 µl/well medium supplemented with digitonin, glycyrrhizinic acid, Saponinum album (SA), SA1641, SO1861, *Quillaja* saponin 1 or *Quillaja* saponin 2 was added to the wells, achieving the final concentrations of 3, 6, 12 and 24 µM. Furthermore, a group of wells were treated with 50 µl medium in the presence of a highly lytic concentration of Triton X-100 (5% v/v in medium) as a positive control. After the addition of the compounds, cells were monitored for the following 3 h. Data collected during the experiment was analyzed with the RTCA Software 1.2.1.1002 (Roche Applied Science).

The cytotoxicity of saporin, gelonin or RTA + SO1861 was evaluated in real time by the same impedance-based system. DMEM supplemented with 10% FBS and 1% PS (50 µl/well) was added to the 96-well E-plate. Then, 50 µl/well medium containing 5,000 ECV-304 cells was added. Cells were incubated for 24 h and thereafter 100 µl/well medium (untreated) or 100 µl/well medium containing SO1861 [final concentration of 1 µg/ml (0.54 µM)] was added in the case of control cells. For the evaluation of the other compounds, 50 µl/well medium containing saporin, gelonin or RTA (final concentrations from 0.1 to 100 nM) plus 50 µl/well medium or medium containing SO1861 was added to the wells. Cells were monitored in real time for 66 h. In addition, at the end of the experiment (total time of 90 h) cell viability was evaluated by the MTT assay (see section 2.4.2).

For the cytotoxicity analysis of ST + SO1861, 50 µl/well RPMI-1640 medium supplemented with 10% FBS and 1% PS was pipetted in the E-plate. Thereafter 10,000 BT-474 cells were added (50 µl/well) and cells were allowed to grow for 18 h. Then, 100 µl/well medium (untreated) or 100 µl/well medium containing SO1861 [final concentration of 2.5 µg/ml (1.34 µM)] was added in the case of control cells. For the evaluation of ST, 50 µl/well medium containing the immunotoxin (final concentrations from 0.1 to 100 nM) plus 50 µl/well medium

or medium containing SO1861 was added to the wells. Cells were monitored in real time until the end of the experiment (total time of 70 h).

For the cytotoxicity analysis of SC + SO1861, the 96-well E-plate was pre-coated with 0.1% (w/v) gelatin solution (100 µl/well) to facilitate the subsequent adhesion of cells. Gelatin solution was removed and then 50 µl/well DMEM supplemented with 10% FBS and 1% PS medium was pipetted in the E-plate. Thereafter 5,000 TSA-EGFR cells were added (50 µl/well) and cells were allowed to grow for 22 h. Then, 100 µl/well medium (untreated) or 100 µl/well medium containing SO1861 [final concentration of 2 µg/ml (1.07 µM)] was added in the case of control cells. For the evaluation of SC, 50 µl/well medium containing the immunotoxin (final concentrations from 1 to 100 nM) plus 50 µl/well medium or medium containing SO1861 was added to the wells. Cells were monitored in real time until the end of the experiment (total time of 67 h).

For the characterization of ST and SC regarding their binding properties, antibody-dependent cell-mediated cytotoxicity (ADCC) and cytotoxicity augmentation by SO1861 after ADCC, 50 µl/well RPMI-1640 medium supplemented with 10% FBS and 1% PS was pipetted in the 96-well E-plate. After setting the impedance to zero, 10,000 BT-474 cells were seeded (50 µl/well) and allowed to proliferate. For competitive assays of Trastuzumab/ST and Cetuximab/SC either of the following compounds were added after 13 h: (1) 100 µl medium without any further compounds or (2–6) 100 µl medium supplemented with (2) 2.5 µg/ml SO1861; (3) ST (final concentration of 1 nM) and SO1861; (4) SC (final concentration of 0.001 nM) and SO1861; (5) ST, SO1861 and 1,000 nM Trastuzumab; or (6) SC, SO1861 and 1,000 nM Cetuximab. After addition of the compounds, cells were monitored for further 57 h.

For non-competitive assays in the presence and absence of natural killer (NK) cells the following compounds were added after 23 h: (1) 100 µl medium without any further compounds or (2–6) 100 µl medium supplemented with (2) 10 nM Trastuzumab; (3) 10 nM ST; (4) 1:2 NK cells (ratio between BT-474 and NK cells); (5) 10 nM Trastuzumab and 1:2 NK cells or (6) 10 nM ST and 1:2 NK cells. Cetuximab and SC were tested analogously. Both NK cells from donor I and donor II (see section 2.5.1) were tested for each of the conditions. Cell viability was continuously monitored for further 48 h and then medium supplemented with SO1861 (50 µl/well) was added reaching a final concentration of 2.5 µg/ml. Cells were again monitored until the end of the experiment (total time of 110 h).

To evaluate the cytotoxicity of SE and DE, the 96-well E-plate was pre-coated with 0.1% (w/v) gelatin solution (100 µl/well) to facilitate the subsequent adhesion of cells. Gelatin solution was removed and 50 µl/well DMEM supplemented with 10% FBS and 1% PS was pipetted. Thereafter 8,000 HER14 cells were added (50 µl/well) and cells were allowed to proliferate for 25 h. The following compounds were added: 100 µl medium (untreated), 100 µl medium supplemented with SE or DE (final concentrations of 1 and 10 nM) or 100 µl medium supplemented with doxorubicin hydrochloride (Sigma-Aldrich) as positive control at the final concentrations of 1 and 1,000 nM. Cells were monitored in real time until the end of the experiment (total time of 67 h).

For the cytotoxicity evaluation of SE, DE or $DT_{390}$-EGF + SO1861, 50 µl/well DMEM supplemented with 10% FBS and 1% PS was pipetted in the E-plate. Thereafter 2,000 ECV-304 cells were added (50 µl/well) and cells were allowed to grow for 20 h. Then, 100 µl/well medium (untreated) or 100 µl/well medium containing SO1861 (final concentration of 2 µg/ml) was added in the case of control cells. For the evaluation of SE, DE or $DT_{390}$-EGF, 50 µl/well medium containing the targeted toxins (final concentrations from 0.1 to 100 nM) plus 50 µl/well medium or medium containing SO1861 was added to the wells. Cells were monitored in real time until the end of the experiment (total time of 50 h).

### 2.4.5. Evaluation of cell membrane permeabilization by flow cytometry

Short term cell membrane permeabilizing effects of oleanane saponins (incubation time of 1 h) was measured by a propidium iodide (PI) uptake assay. ECV-304 cells were seeded in 24-well plates and were allowed to grow up to 90% confluence. Cell culture medium was aspirated and 300 µl medium per well containing 4 µg/ml PI and oleanane saponin (at the final concentrations of 3, 6, 12, 24 and 48 µM) was added. Cells treated only with medium containing PI served as controls. Cells were incubated for 1 h and thereafter medium containing PI and oleanane saponin was removed. Cells were re-suspended in 200 µl 0.25% Trypsin-EDTA and afterwards 200 µl PBS supplemented with 10% FBS was added. Cell suspensions were stored at room temperature. Subsequently, fluorescence was measured by a FACScalibur (Becton Dickinson).

### 2.4.6. Isolation of lysosomes

For the isolation of lysosomes in order to evaluate the lysosomal membrane permeabilizing effects of oleanane saponins, ECV-304 cells were seeded in 75 cm$^2$ dishes and grown to confluence in DMEM supplemented with 10% FBS and 1% PS. Cells of 8 dishes ($3 \times 10^7$ cells) were washed with 2 ml Dulbecco's PBS without Ca$^{2+}$ and Mg$^{2+}$ and subsequently detached using 2 ml of 0.25% Trypsin-EDTA. Detachment was stopped by adding 3 ml cell culture medium and re-suspended cells were centrifuged for 5 min at 800$g$ and 4 °C. Cells were washed with 10 ml ice-cold PBS and centrifuged again for 5 min. The washing step was repeated once and cells were re-suspended with 6 ml ice-cold PBS. The cell suspension was loaded into a 7-ml-cell homogenizer with a small clearance pestle (Sigma-Aldrich) and homogenized for 28 cycles. The homogenate was centrifuged at 1,000$g$ for 10 min at 4 °C. The pellet was discarded and the supernatant further centrifuged at 20,000$g$ for 20 min at 4 °C. Then the supernatant was discarded and the 20,000$g$ pellet containing lysosomes was re-suspended in 400 µl ice-cold translocation buffer (T buffer) (20 mM HEPES, 10 mM MgSO$_4$ and 0.1 M KCl, pH 7.0) supplemented with 2 mM ATP. The crude lysosomal fraction was stored at 4 °C.

For the evaluation of the lysosomal escape of SH in isolated lysosomes from cells previously treated with the same conjugate, ECV-304 cells were incubated with medium containing SH (100 nM). After 6 h of addition of the compound, cells were washed with 2 ml PBS and detachment of cells was initiated by addition of 2 ml 0.25% Trypsin-EDTA. The procedure to isolate the lysosomes was carried out as described previously.

### 2.4.7. Evaluation of lysosomal membrane permeabilizing effects

Permeabilizing effect of oleanane saponins was measured on lysosomal membranes. The crude lysosomal fraction (see section 2.4.6) was shortly centrifuged at 1,000$g$ for 2 min at 4 °C to discard the aggregated organelles. The crude lysosomal fraction (5 µl) was incubated at 37 °C for 1 h only with 45 µl T buffer (control) or with 45 µl T buffer in the presence of oleanane saponins at the final concentrations from 0.05 to 50 µM. After incubation, lysosome suspensions were centrifuged at 20,000$g$ for 20 min and the amount of the lysosomal enzyme β-$N$-acetylglucosaminidase (NAG) present in the supernatant (released from the lysosomes) was determined by adding 10 µl supernatant to 90 µl of a substrate solution (0.09 M citrate buffer, 1 mg/ml 4-nitrophenyl $N$-acetyl-β-D-glucosaminide, pH 4.7) previously equilibrated at 37 °C. After incubation for 10 min at 37 °C, the reaction was stopped by adding 200 µl Na$_2$CO$_3$ (0.4 M).

The absorbance was measured at 405 nm with a SpectraMax 340PC Absorbance Microplate Reader.

### 2.4.8. Endo/lysosomal release of SH from isolated organelles

The specific lysosomal escape of saporin-horseradish peroxidase (SH) in the presence of saponins was determined in lysosomes isolated from cells pre-treated with SH (see section 2.4.6). The crude lysosomal fraction of cells previously treated with SH was shortly centrifuged at 1,000$g$ for 2 min at 4 °C to discard the aggregated organelles.

The crude lysosomal fraction (15 µl) was incubated at 37 °C for 1 h only with 55 µl T buffer (control) or with 55 µl T buffer in the presence of digitonin, α-hederin or SA1641 at the final concentrations of 0.5, 5, 10, 20, 30, 40 and 50 µM. After incubation, lysosomal suspensions were centrifuged at 20,000$g$ for 20 min. The amount of the SH present in the supernatant (released from the lysosomes) was determined by measuring the peroxidase activity (see section 2.3.12).

### 2.4.9. Endo/lysosomal release of SH measured by cell fractionation

For the evaluation of the lysosomal escape of SH *via* cellular fractionation of cells previously treated with the same conjugate in the presence of SA1641, ECV-304 cells were seeded in 75 cm$^2$ dishes and grown to confluence in DMEM supplemented with 10% FBS and 1% PS. Cells of 4 dishes ($1.5 \times 10^7$ cells) were treated with 2 ml SH (100 nM in medium) ± SA1641 [final concentration of 5 µg/ml (3.05 µM)] at 37 °C for 6 h. Cells were washed 3 times with 2 ml ice-cold Dulbecco's PBS without Ca$^{2+}$ and Mg$^{2+}$. Subsequently, 1 ml ice-cold PBS was added and cells were scraped (Falcon Cell Scraper, Fisher Scientific/Thermo Scientific) from the cell culture dishes. Furthermore, 1 ml ice-cold PBS supplemented with protease inhibitor Complete (Roche Applied Science) was added to re-suspended cells. The cell suspension was loaded into a 2-ml-cell homogenizer with a small clearance pestle (Sigma-Aldrich) and homogenized for 28 cycles. The homogenate was centrifuged at 1,000$g$ for 10 min at 4 °C. The pellet was discarded and supernatant was further centrifuged at 100,000$g$ and 4 °C for 1 h with the Optima L-90K Ultracentrifuge (Beckman Coulter). After ultracentrifugation, the supernatant corresponded to the (a) cytosolic fraction while the pellet contained all cellular organelles, including the lysosomes. Pellet was re-suspended, frozen and thawed 5 times in order to disrupt the lysosomal membranes and centrifuged again at 100,000$g$ and 4 °C for 1 h. After this second

ultracentrifugation step, the supernatant corresponded to the (b) lysosomal fraction. The presence of SH in both (a) cytosolic fraction and (b) lysosomal fraction was analyzed by the determination of peroxidase activity (see section 2.3.12).

### 2.4.10.  Confocal fluorescence microscopy

To visualize the internalization of ST, BT-474 cells (50,000 cells/dish) were seeded in a cell culture µ-Dish 35 mm, low (Ibidi) and grown in RPMI-1640 medium supplemented with 10% FBS and 1% PS for 24 h. Medium was removed and 800 µl medium supplemented with 100 nM saporin-Trastuzumab-Alexa Fluor 488 ([Alexa]ST) was added to the cells, which contained in the case of the competitive assay with unconjugated antibody in addition 1,000 nM Trastuzumab. Cells were incubated further 24 h. Then, cells were treated with 8 µl (1 mg/ml) Hoechst 33342 (Life Technologies) for 2 h. Five minutes before finishing the incubation time, 1 µl CellMask Deep Red (Invitrogen) was added to the cells. In the case of colocalization studies, 8 µg pHrodo Red Dextran, 10 kDa (Invitrogen) and Hoechst 33342 were added 2 h before the end of the incubation time without the addition of CellMask Deep Red. Cells were washed three times with live cell imaging solution (Invitrogen) supplemented with 5 mM D(+)glucose and thereafter covered with 800 µl of the same solution. Cell culture dishes were fixed in a heating chamber and maintained at 37 °C during the microscopy process. Finally, cells were observed by a laser scanning microscope (LSM780, Axio Observer Z1, Carl Zeiss) equipped with a Plan-Apochromat 63×/1.40 oil objective. Focus stability was insured by Definite Focus (Carl Zeiss). Acquisition of images was done *via* the software ZEN 2010 (Carl Zeiss).

### 2.4.11.  Live cell imaging

Endo/lysosomal release of internalized saporin was visualized by live cell imaging in the presence of red dextran. For this experiment, ECV-304 cells (50,000 cells/dish) were seeded in a cell culture µ-Dish 35 mm, low (Ibidi) and grown in DMEM medium supplemented with 10% FBS and 1% PS for 24 h. Medium was removed and 800 µl medium supplemented with 1,000 nM [Alexa]saporin was added to the cells. Cells were incubated for 6 h and two hours before finishing this incubation time, 8 µg pHrodo Red Dextran (10 kDa) was added. Cells were washed three times with live cell imaging solution supplemented with 5 mM D(+)glucose and covered with 800 µl of the same solution. Similarly to the already described set up in the

previous section (2.4.10), cell culture dishes were fixed in a heating chamber and maintained at 37 °C during the microscopy process. For the visualization of the endo/lysosomal escape of $^{Alexa}$saporin, a final concentration of 10 µg/ml (6.09 µM) SA1641 was added at the start of the microscopy process and images were captured every 30 s for a period of 2 h.

For the visualization of the endo/lysosomal escape of $^{Alexa}$ST, a final concentration of 2.5 µg/ml (1.34 µM) SO1861 was added to BT-474 cells 140 s after the start of the microscopy process and images were taken every 20 s during 12 min. In both cases, cells were observed by laser scanning microscopy with the same equipment described in the previous section.

## 2.5. *Ex vivo* methods

### 2.5.1. Isolation of natural killer cells

In order to isolate human natural killer (NK) cells, blood (60 ml) was collected from two male human donors (donor I and II). Blood was diluted (1:1) with PBS and peripheral blood mononuclear cell (PBMC) fraction was isolated using Lymphocyte Separation Media (PromoCell). After separation of PBMCs, the cell fraction was washed with PBS containing 0.1% BSA and centrifuged at 400$g$ and 25 °C for 20 min. The washing step was repeated twice. PBMCs were filtered through a CellTrics 30 µm filter device (Partec) to remove cell clusters and were washed again under the same conditions as before.

NK cells were isolated from the PBMC fraction using a negative selection by magnetic-activated cell sorting (MACS). For this purpose, Human NK Cell Isolation Kit (Miltenyi Biotec) was used. In this approach, non-NK cells (i.e. T-lymphocytes, B-lymphocytes, stem cells, dendritic cells, monocytes, granulocytes and erythroid cells) were indirectly magnetically labeled with a cocktail of biotin-conjugated antibodies against linage-specific antigens and a cocktail of magnetic beats. Thereafter, the magnetically labeled non-NK cells were retained on the separation column placed in a magnetic field while the unlabeled and untouched NK cells (CD56$^+$) passed through. After collection of purified NK cells, they were centrifuged at 500$g$ and 25 °C for 30 min. Cells were re-suspended in Mononuclear Cell Medium (PromoCell) and immediately used in the subsequent experiment of real-time monitoring of cell-mediated cytotoxicity (see section 2.4.4).

### 2.5.2. Hemolysis assay

For the evaluation of permeabilizing effects of oleanane saponins on red blood cells (RBCs), freshly collected human RBCs were washed and suspended (4% v/v) in a 0.9% (w/v) NaCl solution. In a 96-well plate, 150 µl per well of this RBCs solution was added. An amount of 50 µl 0.9% (w/v) NaCl solution (negative control), 0.9% (w/v) NaCl solution supplemented with 5% (v/v) Triton X-100 (positive control) or 50 µl 0.9% (w/v) NaCl solution containing oleanane saponin at the final concentrations of 1.5, 3, 6, 12, 24 and 48 µM was further added. RBCs were incubated at 37 °C for 30 min and afterwards centrifuged at 2,000 rpm for 10 min. The supernatant (100 µl) was transferred from each well into the respective well in a flat bottomed 96-well plate. Percentage of hemoglobin that was released from the RBCs was calculated by measuring the absorbance at 405 nm by the SpectraMax 340PC Absorbance Microplate Reader and referring to controls.

## 2.6. Bioinformatic methods

### 2.6.1. Structural alignment of proteins

The structural alignment of saporin, dianthin-30, gelonin and RTA was performed by MISTRAL (http://eole2.lsce.ipsl.fr/ipht/mistral/protein.php) [173]. Structural data from proteins were acquired from RCSB Protein Data Bank: saporin (PDB ID 1QI7) [174] , dianthin-30 (PDB ID 1RL0) [175], gelonin (PDB ID 3KTZ) [176] and RTA (PDB ID 1IFT) [177].

The structural alignment of saporin and dianthin-30 was performed by the Protein Structure Comparison Tool V 1.2 (RCSB PDB) using the same structural data as before: saporin (PDB ID 1QI7) and dianthin-30 (PDB ID 1RL0).

According to the literature, to get the required X-ray diffraction images of the toxins mentioned above, the authors of those studies conducted the following experiments. Saporin was crystallized to a resolution of 2.0 Å and the structure was solved by combined molecular replacement with the REPLACE package of programs [178] using the coordinates of pokeweed antiviral protein (PAP, PDB ID 1PAF) [179] as template. Dianthin-30 was crystallized to a resolution of 1.4 Å and the structure was solved by molecular replacement with the program AMoRe [180] using the coordinates of saporin (PDB ID 1QI7) as template. Gelonin was crystallized to a resolution of 2.0 Å and the structure was solved by molecular replacement with AMoRe using the RTA structure (PDB ID 1BR6) [181] as starting model. RTA was crystallized

to a resolution of 1.8 Å and the structure was solved by molecular replacement using a search-model derived from the coordinates of the ricin orthorhombic crystal structure in the Brookhaven National Laboratory Protein Data Bank (entry pdblaai) [177].

### 2.6.2. Visualization of protein structure

Structure alignments were visualized with Jmol 11.9.7 (http://www.jmol.org). The backbones of proteins are shown as traces. The secondary structure is presented as a cartoon for pictorial description. In the case of identification of specific amino acids within the structure of saporin (e.g. active site or relevant amino acids), the protein structure was visualized with Cn3D (version 4.3) (NCBI).

### 2.6.3. Amino-acid sequence alignment

The sequence alignment of the toxins saporin, dianthin-30, gelonin and RTA was performed using T-COFFEE (Version_9.03.r1318) (ExPASy, Swiss Institute of Bioinformatics). On the other side, the sequence alignment of fusion proteins (SE and DE) was carried out using BLASTP 2.2.27+ (NCBI).

### 2.6.4. Further bioinformatic analysis

Theoretical absolute molecular mass (Ma) and isoelectric point (pI) of proteins were calculated by the Compute pI/Mw (ExPASy, Swiss Institute of Bioinformatics). Rare codons at the mRNA level of SE and DE were identified by Rare Codon Search (http://www.bioline.com/calculator/ 01_11.html). Furthermore, the online software Mfold (http://mfold.rna.albany.edu/?q=mfold) was used to determine the mRNA structure of the same fusion proteins.

### 2.6.5. Statistical analysis

An independent two-sample Student's *t*-test was conducted to find out if the differences, either in the protein yield after recombinant expression and purification of SE and DE, or in the toxicity of SE and DE to the bacteria during the expression process, were significant. The test was two-tailed and the confidence interval percentage was set to 95%. Equal variances were assumed for

the two distributions. $p \leq 0.05$ was regarded as significant. The statistical analyses were performed with IBM SPSS Statistics Version 21 (IBM Corporation).

# 3. Results

## 3.1. Evaluation of membrane permeabilizing effects of oleanane saponins

### 3.1.1. Real-time analysis of saponin permeabilizing effects on cell membranes

Structurally specific oleanane saponins are responsible for the specific cytotoxicity enhancement of certain type I ribosome-inactivating protein (RIPs) when these are applied at low concentrations. Nevertheless, oleanane saponins also exhibit unspecific membrane permeabilizing effects at higher doses. As an initial work, permeabilizing effects of oleanane saponins were investigated on different biological membranes to distinguish specific toxin cytotoxicity enhancement from unspecific membrane disruption.

Permeabilizing effects of saponins on cell membranes of ECV-304 cells were monitored in real time with the xCELLigence System (Roche Applied Science). In this system, the electrical impedance across micro electrodes that are integrated on the bottom of 96-well plates is measured in real time. As impedance depends on the adhesion degree and morphology of cells, it can be used to study cell viability and proliferation of cells in the presence of compounds as well as membrane permeabilizing effects of saponins on cell membranes. Results are displayed as a cell index, i.e. a dimensionless parameter that is derived as a relative change in the measured electrical impedance to represent the cell status. For a better comparison between the different conditions tested in the experiment and to consider the real number of cells in wells with the same conditions, cell index values are normalized at the time point right before the addition of compounds. All original cell index values are divided by the corresponding cell index value at the normalization time, thus obtaining the normalized cell index (NCI).

The different saponins under study were added to cells and their short term effect (incubation time of 3 h) was continuously examined (Figure 2). As observed in the case of the untreated control (cells treated only with medium), there was an initial decrease in NCI due to the addition of medium. Thereafter past the incubation time, NCI recovered a value of 1. In the case of cells treated with Triton X-100 (5%), the rupture of the cell membrane was immediate and NCI was already zero in the first measurement after the addition of compounds.

Digitonin (monodesmosidic steroidal saponin) showed moderate effects on the cell membrane with a concentration of 3 µM (Figure 2a). However, with higher concentrations of saponin, NCI values decreased considerably leading to a minimum NCI value of 0.4 (6 µM) and below 0.2 (12

and 24 µM). Interestingly, NCI values started to increase rapidly after 1 h of incubation at 6 and 12 µM. Contrastingly, glycyrrhizinic acid (monodesmosidic oleanane saponin) had no permeabilizing effects on cell membranes in all the concentrations tested and NCI values revealed a pattern comparable to the untreated control (Figure 2b).
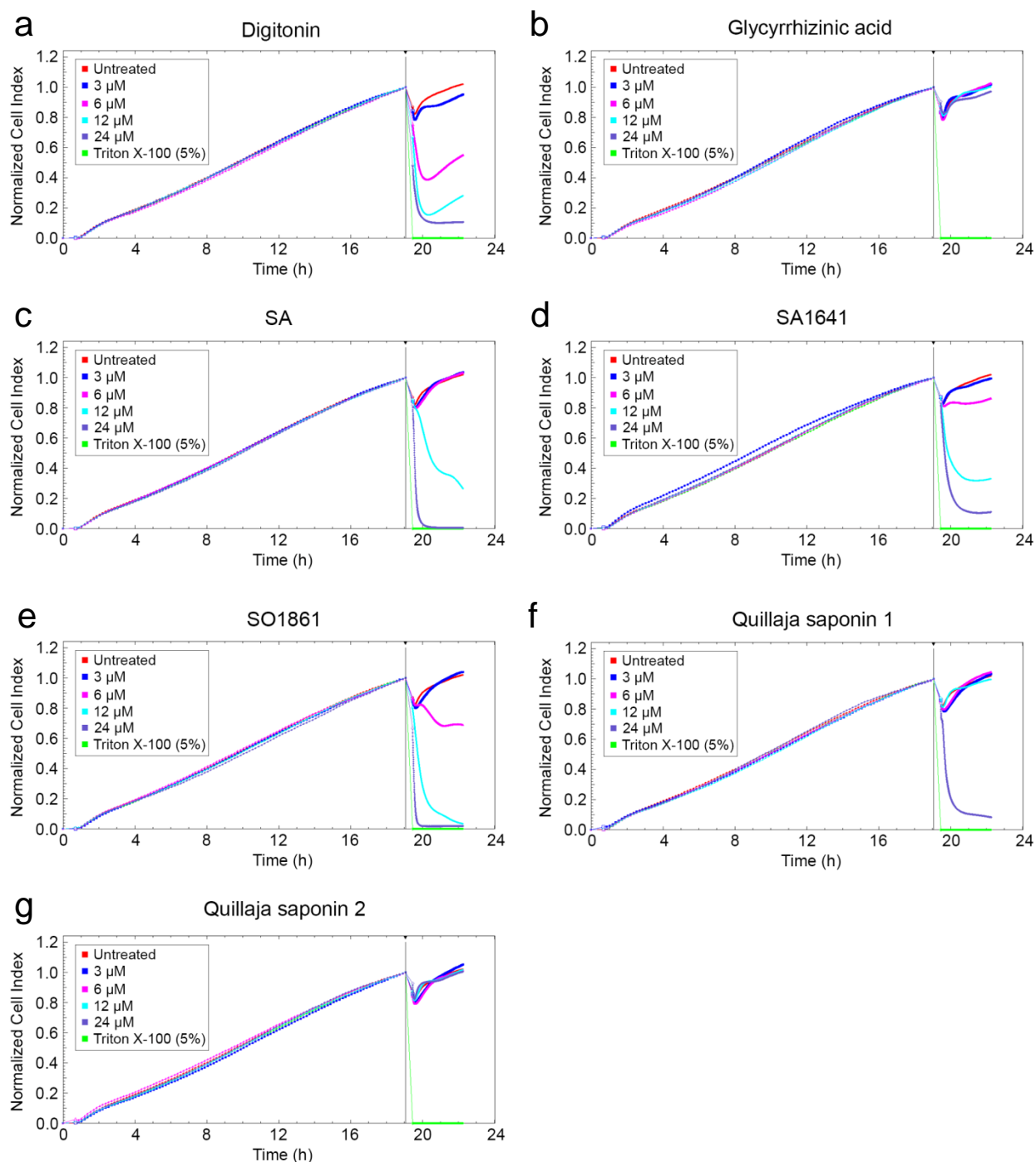


**Figure 2.** Real-time monitoring of permeabilizing effects of saponins on cell membranes. ECV-304 cells (5,000 cells/well) grew for 19 h and then saponins (3, 6, 12 and 24 µM) or Triton X-100 (5%) were added. Short term effects of compounds were analyzed for the following 3 h by an impedance-based real-time cell monitoring system. Cell indexes were normalized at the time of addition of compounds. Results are given separately for **(a)** digitonin, **(b)** glycyrrhizinic acid, **(c)** SA, **(d)** SA1641, **(e)** SO1861, **(f)** *Quillaja* saponin 1 and **(g)** *Quillaja* saponin 2. Data represents the mean, $n = 3$. Untreated control cells and cells treated with Triton X-100 are equally drawn in all panels for a better comparison.

Saponinum album (SA), SA1641, SO1861, *Quillaja* saponin 1 and 2 are bisdesmosidic oleanane saponins. SA (Figure 2c) had no permeabilizing effects at concentrations of 3 and 6 µM. However, the effects appeared at 12 µM, where the curve went down to an NCI of 0.4 and started to decrease again after 2 h of incubation. The effects at 24 µM were comparable to those caused by Triton X-100 (5%). SA1641 (Figure 2d) had similar permeabilizing effects as SA. On one hand, it was slightly more effective at a concentration of 6 µM. On the other hand, SA1641 showed less permeabilizing effects on cell membrane at higher concentrations (12 and 24 µM). SO1861 (Figure 2e) was the most lytic saponin at the high concentrations of 12 and 24 µM indicated by a drop down of the NCI to zero within the observed incubation time. Permeabilizing effects at 6 µM were moderate (NCI of 0.6) and there were no effects at 3 µM. *Quillaja* saponin 1 and 2 are crude extracts from the same plant but from different suppliers. *Quillaja* saponin 1 (Figure 2f) showed no membrane permeabilizing effects up to 12 µM, but its toxicity increased drastically at 24 µM, as the NCI curve achieved a minimum of 0.1 after 3h. *Quillaja* saponin 2 (Figure 2g) revealed a different pattern from *Quillaja* saponin 1, as it did not cause any membrane permeabilizing effects, even at the highest concentration tested.

### 3.1.2.  Effect of saponins on cell membrane permeability

A propidium iodide (PI) uptake assay was performed in order to analyze the membrane permeabilizing effects of triterpenoidal saponins on cell membranes of ECV-304 cells within a short term incubation time of 1 h (Figure 3). PI is a fluorescent stain for nucleic acids, is not permeant to the cell membranes and is only incorporated to cells in the case they lose cell membrane integrity. PI can be employed to assess cell membrane permeability induced by compounds such as triterpenoidal saponins.

Saponins displayed no membrane permeabilizing effects on cell membranes up to a concentration of 6 µM. Particularly, membrane permeabilizing effects of digitonin were observed with concentrations higher than 12 µM. PI uptake by cells incubated in the presence of digitonin was only measured up to 24 µM for technical reasons since cellular membranes were totally disrupted at the highest concentration of digitonin (48 µM), and the posterior analysis by flow cytometry was not possible. A similar effect was observed with high concentrations of other saponins, i.e. SA, SO1861 and *Quillaja* saponin 1.

Digitonin led to a moderate PI uptake at 24 µM (median fluorescence of 158) and was totally disruptive at 48 µM. Glycyrrhizinic acid showed no permeabilizing effects up to 48 µM. While

SA had a median fluorescence of 539 at 24 µM and lysed the cell membrane completely at 48 µM, the purified SA1641 had a median fluorescence of 220 and 398 at concentrations of 24 and 48 µM, respectively. SO1861 showed a median fluorescence of 551 at 12 µM and was totally lytic with higher concentrations. *Quillaja* saponin 1 and 2 showed different membrane permeabilizing effects on ECV-304 cell membranes. While *Quillaja* saponin 1 exhibited a median fluorescence of 328 at 24 µM and was completely disruptive at 48 µM, *Quillaja* saponin 2 did not show any membrane permeabilizing effects within the concentrations tested.
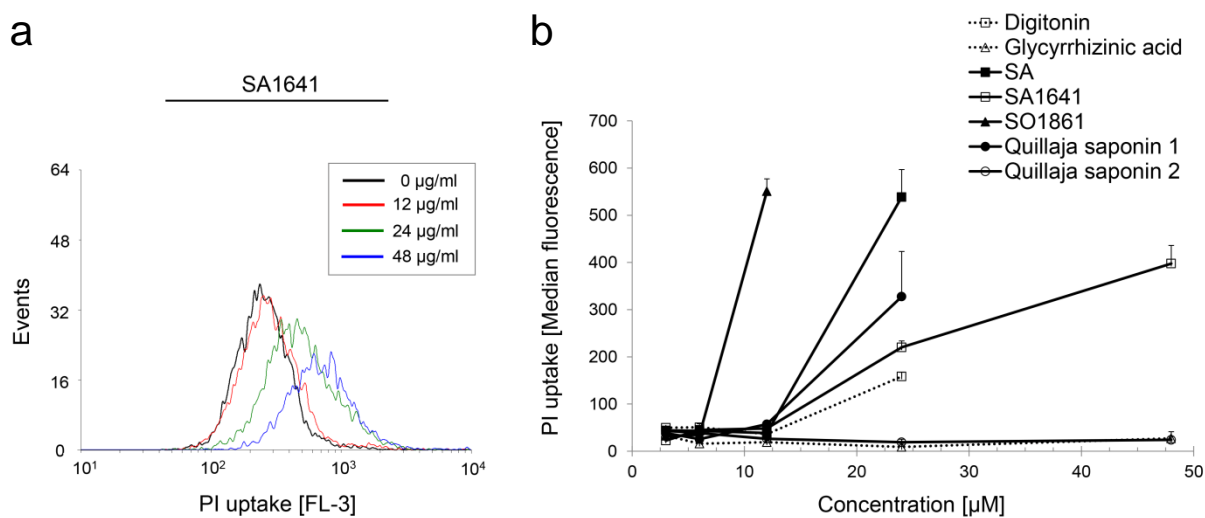


**Figure 3.** Membrane permeabilizing effects of saponins on cell membranes of ECV-304 cells. Membrane permeabilizing effects were measured by a PI uptake assay. **(a)** Flow cytometric histograms of cells after incubation (37 °C and 1 h) with SA1641 at the concentrations of 12, 24 and 48 µM in the presence of PI. **(b)** PI uptake (median fluorescence) was analyzed for digitonin, glycyrrhizinic acid, SA, SA1641, SO1861, *Quillaja* saponin 1 and 2 at the concentrations of 3, 6, 12, 24 and 48 µM and referred to the control. Each data point is the mean ± SD, $n = 3$.

### 3.1.3.    Effect of saponins on lysosomal membranes

Short term lysosomal membrane permeabilizing effects of saponins were determined by a β-*N*-acetylglucosaminidase (NAG) release assay (Figure 4) after an incubation period of 1 h at 37 °C. Digitonin had a substantial membrane permeabilizing effect on lysosomal membranes at concentrations higher than 6 µM. It showed a progressive increase in membrane permeabilization exhibiting the second most lytic effects of all examined substances at the highest concentration tested ($A_{405nm} = 0.329$ at 48 µM). Glycyrrhizinic acid had no membrane permeabilizing effects on lysosomal membranes up to 48 µM ($A_{405nm} = 0.002$), indicating a low lytic activity. While SA1641, purified from SA, showed low lytic properties at the highest concentration ($A_{405nm} = 0.075$), SA itself had high lytic effects on lysosomal membranes ($A_{405nm} = 0.288$ at 48 µM), comparable to those caused by digitonin. Although having no lytic effect up to 6 µM (common pattern observed amongst all saponins tested), at higher concentrations,

SO1861 exhibited the highest lysosomal membrane disrupting effects ($A_{405nm}$ = 0.261 at 24 µM and $A_{405nm}$ = 0.460 at 48 µM). Surprisingly, although being commercial saponin mixtures from the same plant, a notable difference between *Quillaja* saponin 1 and *Quillaja* saponin 2 was found by the NAG test. *Quillaja* saponin 2 showed no lytic properties in the concentration range tested (results comparable to those of glycyrrhizinic acid as $A_{405nm}$ = 0.006 at 48 µM) but *Quillaja* saponin 1 had moderate lytic effects on lysosomes at the highest concentration ($A_{405nm}$ = 0.137).
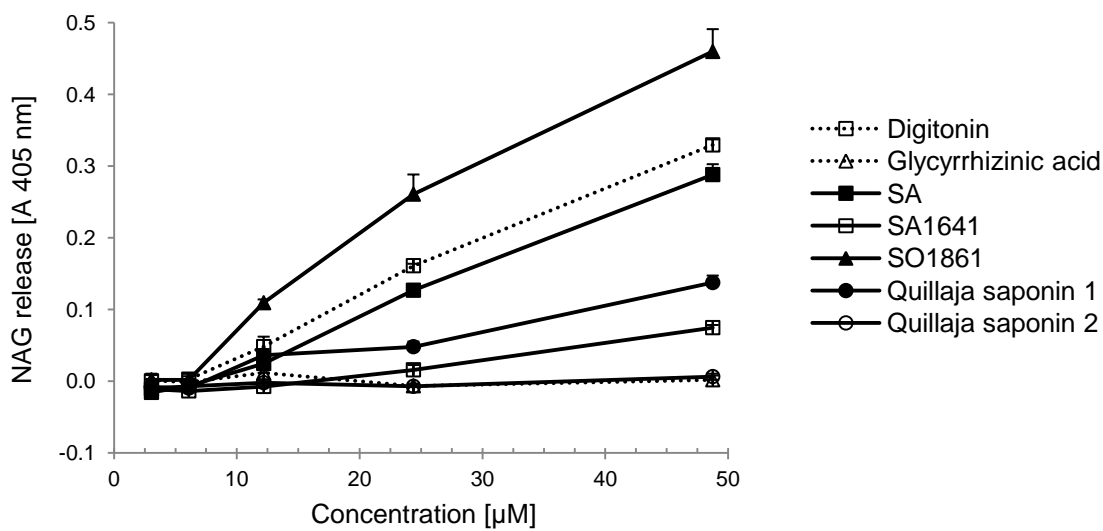


**Figure 4.** Membrane permeabilizing effects of saponins on lysosomal membranes. Isolated lysosomes from ECV-304 cells were incubated at different concentrations (3, 6, 12, 24 and 48 µM) of digitonin, glycyrrhizinic acid, SA, SA1641, SO1861, and *Quillaja* saponin 1 and 2 at 37 °C for 1 h. Release of NAG was determined by reading the absorbance at 405 nm after substrate conversion. Each data point represents the mean ± SD, *n* = 3.

### 3.1.4. Permeabilizing effects of saponins on red blood cells

The effect of saponins on cell membranes of human red blood cells (RBCs) was characterized by a hemolysis assay (Figure 5). Digitonin appeared to be the most lytic of the saponins tested on RBCs cell membranes as it was the only one presenting hemolytic activity at a low concentration of 3 µM (22%), had considerable effects at 6 µM (68%) and already achieved a maximal membrane permeabilizing effect at 12 µM (more than 80%). In contrast, glycyrrhizinic acid revealed the less hemolytic profile as it had no lytic activity in all the concentrations tested.

Different patterns were observed for the other saponins. Firstly, SA1641 and *Quillaja* saponin 2 had a low hemolysis profile, presenting no hemolysis up to 12 µM, moderate hemolysis of 30% for SA1641 and 61% for *Quillaja* saponin 2 at 24 µM and both only achieving a maximal hemolysis at 48 µM. Secondly, SA and *Quillaja* saponin 1 had a moderate hemolysis character. SA caused 10% at 6 µM, 71% at 12 µM and complete lysis at 24 µM. *Quillaja* saponin 1 showed

27% at 6 μM, 67% at 12 μM and also complete hemolysis at 24 μM. Thirdly, a single saponin had a high hemolytic profile comparable to that of digitonin. SO1861 presented 61% hemolysis at 6 μM and complete membrane permeabilizing effects at 12 μM.
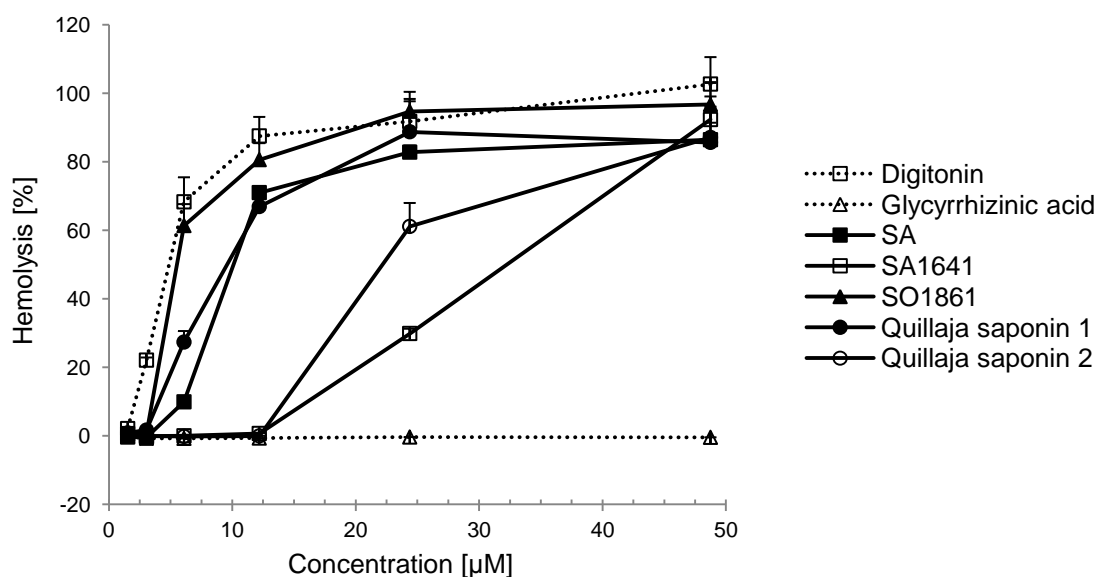


**Figure 5.** Membrane permeabilizing effects of saponins on cell membranes of human RBCs. Cells were incubated at the concentrations of 1.5, 3, 6, 12, 24 and 48 μM of digitonin, glycyrrhizinic acid, SA, SA1641, SO1861, *Quillaja* saponin 1 and 2 at 37 °C for 30 min. Hemoglobin release from permeabilized RBCs was determined by reading the absorbance at 405 nm. Each data point is the mean ± SD, $n = 3$.

## 3.2. Production and purification of proteins

### 3.2.1. Chemical cross-linking of saporin to monoclonal antibodies

For the development of a platform system for enhanced endo/lysosomal escape of targeted toxins, three saporin-based immunotoxins were constructed. Saporin was cross-linked to Trastuzumab (Herceptin[®]), Cetuximab (Erbitux[®]) or Rituximab (Rituxan[®]) *via* covalent linkage introduced by *N*-succinimidyl-3-(2-pyridyldithio)propionate (SPDP). After conjugation of proteins, the reaction mixture was directly analyzed by sodium dodecyl sulfate-polyacrylamide gel electrophoresis (SDS-PAGE) under non-reducing conditions (Figure 6). In the cases of the cross-linking reactions of saporin to either Trastuzumab or Rituximab, a considerable amount of protein precipitated, thus reducing the total yield of immunotoxin production. For this reason, the reaction mixtures of ST and SR were briefly centrifuged at 4,000*g* for 5 min before the electrophoretic analysis.
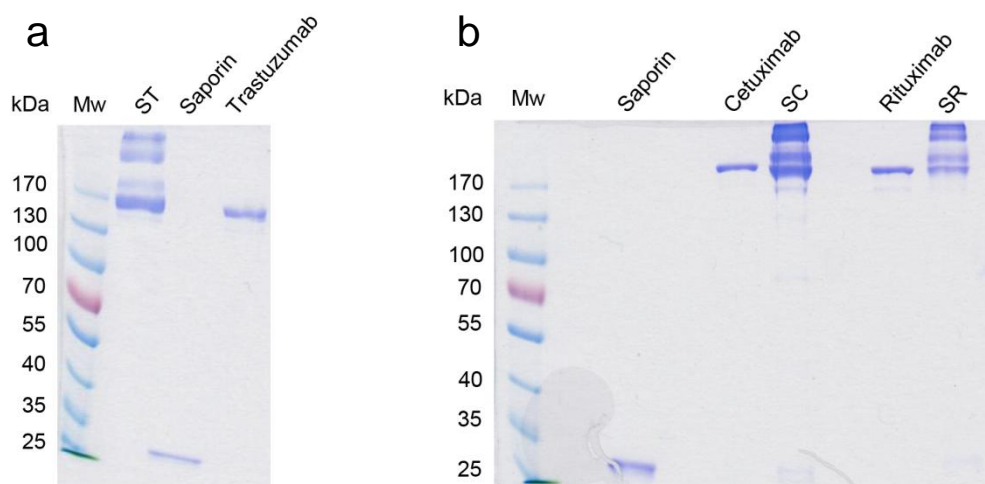
**Figure 6.** Chemical conjugation of saporin and monoclonal antibodies. Saporin was chemically cross-linked to **(a)** Trastuzumab, **(b)** Cetuximab and Rituximab *via* covalent linkage introduced by SPDP. After chemical conjugation, the reaction mixture was analyzed by SDS-PAGE under non-reducing conditions. Saporin and monoclonal antibodies were also analyzed as unconjugated controls.

Several bands were identified in the gel for saporin-Trastuzumab (ST) (Figure 6a), saporin-Cetuximab (SC) and saporin-Rituximab (SR) (Figure 6b). In each of the reaction mixtures, the band with the lowest molecular mass of approximately 170 kDa was the unconjugated therapeutic antibody, as it had exactly the same molecular mass as the corresponding control. Further bands with higher molecular mass represented conjugates of ST, SC or SR with different molecular ratios (e.g. 1 molecule of monoclonal antibody coupled to 1 molecule of saporin, 1 molecule of monoclonal antibody coupled to 2 molecules of saporin, etc.). Only minor amounts of saporin were detected in the gels, indicating that saporin was almost completely conjugated to the monoclonal antibodies.

### 3.2.2.   Size-exclusion chromatography of saporin-based immunotoxins

Purified ST, SC and SR were required for the establishment of the new platform technology. To separate unconjugated saporin from the rest of compounds (unconjugated monoclonal antibodies and immunotoxins), the reaction mixtures were firstly purified by size-exclusion chromatography (Figure 7). The protein concentration was determined in each of the eluted fractions by a BCA assay (Figure 7a, d and g).

**ST**

a



b



c



**SC**

d
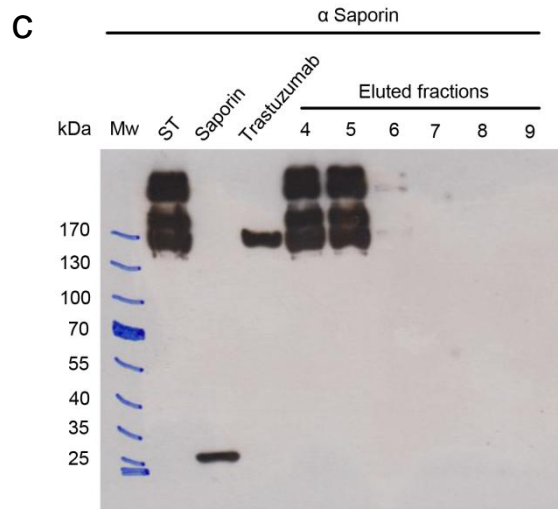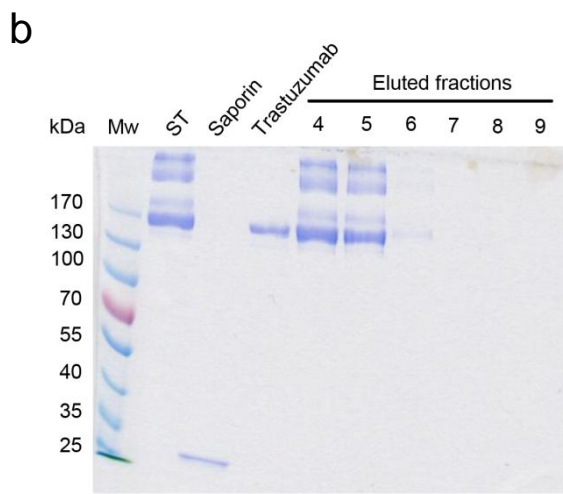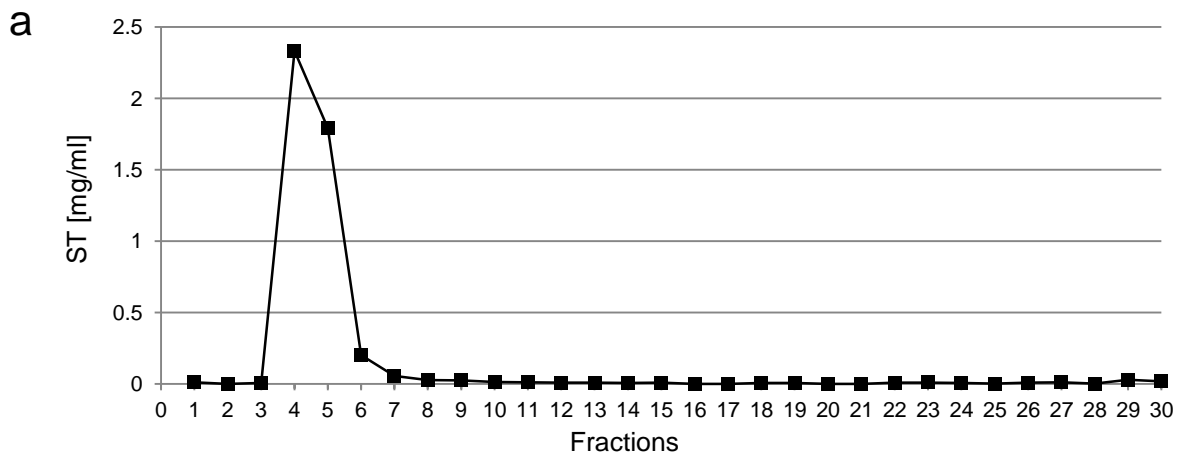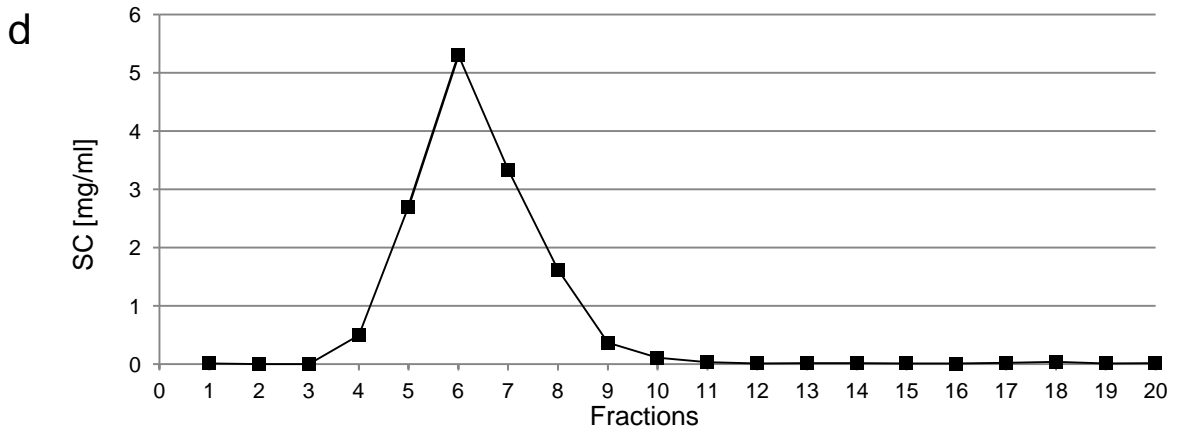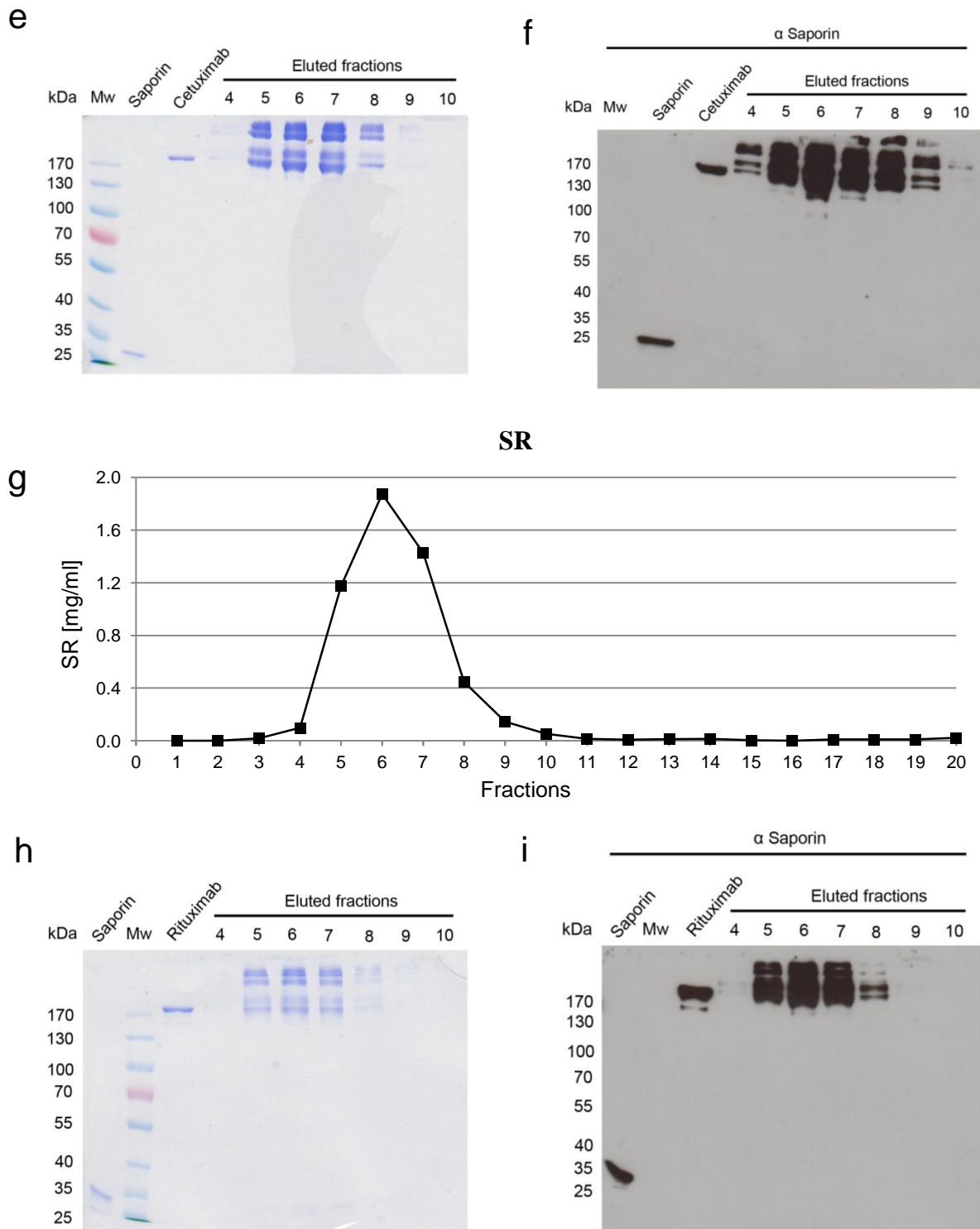
**Figure 7.** Size-exclusion chromatography of immunotoxins. **(a, d, g)** ST was eluted by 20 ml phosphate buffered saline (PBS) and 30 fractions (20 fractions of 0.5 ml plus 10 fractions of 1 ml) were collected. SC and SR were eluted by 10 ml PBS and 20 fractions of 0.5 ml were collected. Determination of the protein concentration was performed by a bicinchoninic acid (BCA) assay in each of the eluted fractions after size-exclusion chromatography. **(b, e, h)** Fractions that contained protein (4–9 for ST; 4–10 for SC and SR) were analyzed by SDS-PAGE under non-reducing conditions. Conjugates were visualized in these fractions. Unconjugated saporin and unconjugated monoclonal antibodies were included as controls. In the case of ST, the original conjugation mixture (already shown in Figure 6a) is presented again as a control for a better comprehension. **(c, f, i)** Furthermore, fractions 4–9 for ST and 4–10 for SC and SR were analyzed by Western blot with a primary polyclonal antibody against saporin. No saporin was observed in the fractions that contain the immunotoxins. Unconjugated Trastuzumab, Cetuximab and Rituximab were detected in the Western blot probably due to a cross-reaction of the polyclonal goat anti-rabbit immunoglobulins/HRP (secondary antibody) to the monoclonal antibodies.

Fractions 4–9 (for ST) and fractions 4–10 (for SC and SR) contained protein and were therefore analyzed by SDS-PAGE (Figure 7b, e and h). In the case of ST, fraction 4 and 5 contained a thicker band that was apparently the unconjugated Trastuzumab as it had the same molecular mass as the unconjugated monoclonal antibody. In addition, both fractions contained other bands with higher molecular mass that represented conjugates of ST with different molecular ratios. In fraction 6 and 7, only small amounts of conjugates or Trastuzumab were detected. In the case of SC, fractions 5–8 contained the unconjugated Cetuximab and conjugates of SC with different molecular ratios. Fraction 4, 9 and 10 contained only small amounts of conjugates or Cetuximab. In the case of SR, fractions 5–7 contained the unconjugated Rituximab and conjugates of SR with different molecular ratios, while only small amounts of these proteins were observed in fractions 4, 8 and 9. Unconjugated saporin was found in none of the analyzed fractions.

Furthermore, purity of the ST, SC and SR solutions was assessed by Western blot with a primary polyclonal antibody against saporin (Figure 7c, f and i). Fractions were evaluated and no saporin was detected. Therefore, purification of the immunotoxins and monoclonal antibodies from saporin was achieved.

### 3.2.3.   Chemical cross-linking of saporin to HRP

To develop a reporter assay for the endo/lysosomal escape of toxins in the presence of endo/lysosomal escape enhancers such as triterpenoidal saponins, saporin was chemically conjugated to horseradish peroxidase (HRP) *via* covalent linkage and the reaction mixture was analyzed by SDS-PAGE (Figure 8). A diffused band with high molecular mass was identified by the reaction mixture in the gel. This band in all probability contained conjugates of saporin-horseradish peroxidase (SH) with different molecular ratios of saporin conjugated to HRP. Furthermore, a band with the same molecular mass as HRP was observed while no unconjugated saporin was detected in the reaction mixture. Apparently, saporin was completely cross-linked to HRP but some HRP remained unconjugated after the chemical cross-linking reaction.
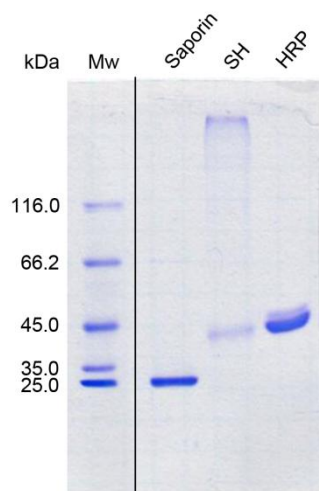
**Figure 8.** Chemical conjugation of saporin and HRP. Saporin and HRP were chemically cross-linked *via* covalent linkage introduced by modifying the *N*-glycans of HRP by sodium periodate (NaIO$_4$) oxidation and sodium borohydride (NaBH$_4$) reduction. The reaction mixture was directly analyzed by SDS-PAGE under non-reducing conditions. Saporin and HRP served as unconjugated controls. Contrast has been slightly modified for a better visualization of the bands.

### 3.2.4.   Purification of proteins by Ni-NTA affinity chromatography

In order to conduct the experiments in this work, the proteins saporin, ST, SC, SR, saporin-KQ, SH, SE, DE and DT$_{390}$-EGF were needed. For this reason, after heterologous expression in *Escherichia coli*, the recombinant proteins saporin, saporin-KQ, SE, DE and DT$_{390}$-EGF were purified by Ni-nitrilotriacetic acid (NTA) affinity chromatography and eluted fractions from the chromatography were analyzed by SDS-PAGE (Figure 9). The conjugates were also purified by Ni-NTA affinity chromatography after chemical conjugation and size-exclusion chromatography in the case of ST, SC and SR or directly after chemical conjugation in the case of SH.

Saporin was soluble and did not remain trapped in inclusion bodies during the expression as indicated by the lack of a thick band corresponding to the protein in the bacterial pellet (Figure 9a). Bacterial proteins lacking the 6× his-tag did not bind to the column and were found in the flow-through. The proteins that bound unspecifically to the column were eluted during the three wash steps. Saporin that contains a 6× his-tag at the N-terminus with affinity to the column (Ni-NTA agarose) was eluted with increasing concentrations of imidazole. The elution pattern of saporin, as well as of the other proteins purified by Ni-NTA affinity chromatography, is presented in Table 4. Fractions containing the purified protein (Pure fractions, see Table 4) of interest and no or only minor amounts of co-purified proteins were pooled together.
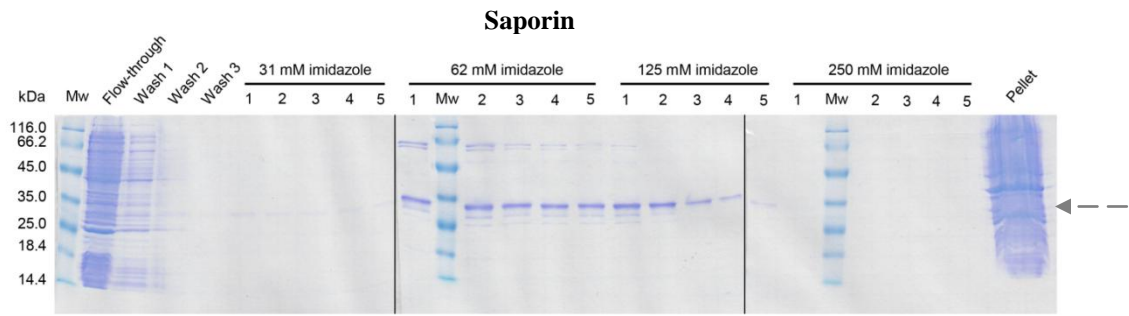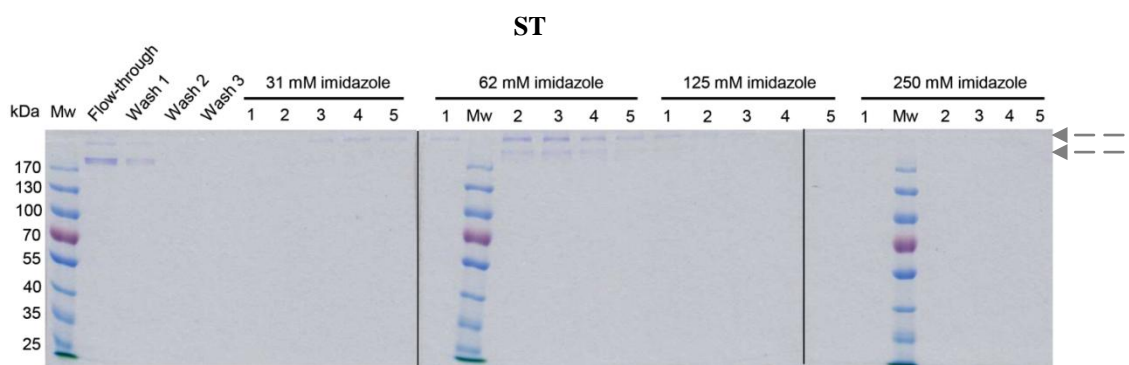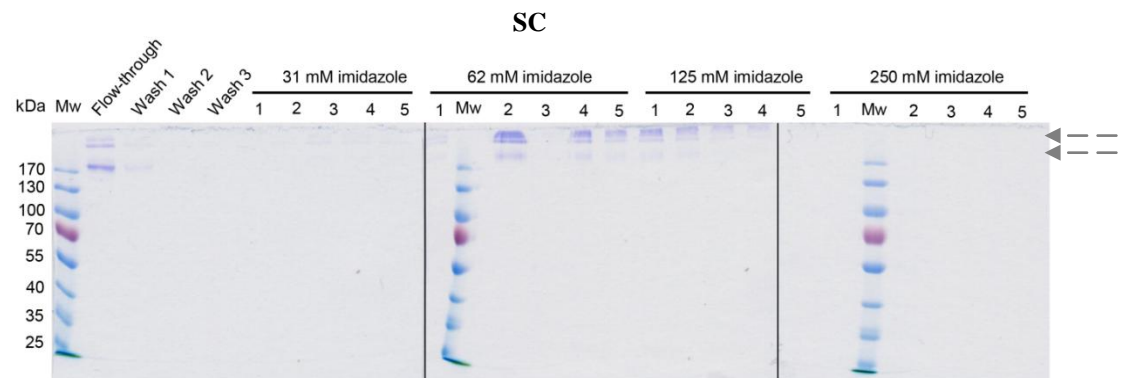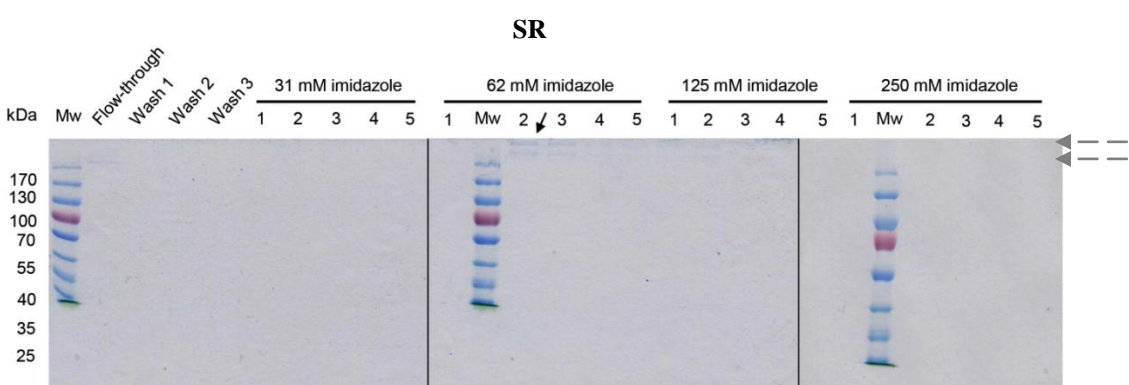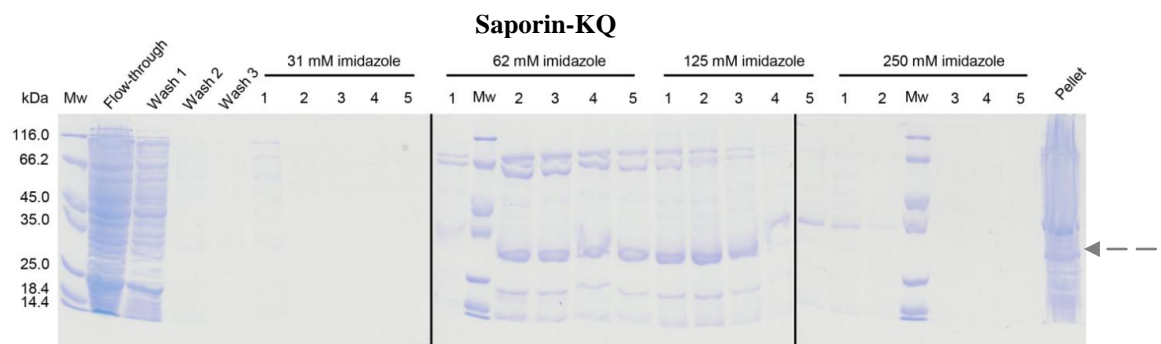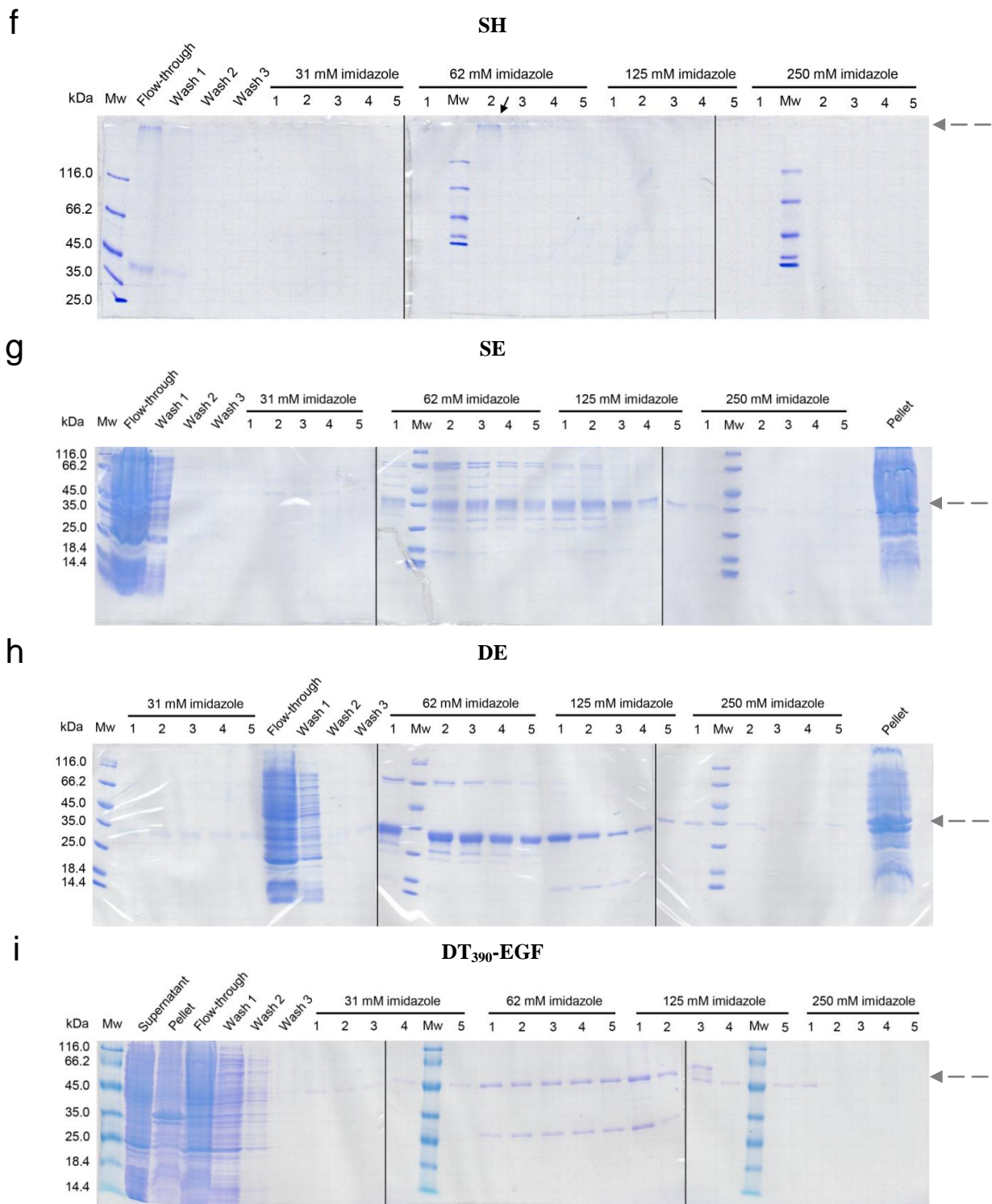
**Figure 9.** Purification of proteins by Ni-NTA affinity chromatography. (**a**) Saporin, (**b**) ST, (**c**) SC, (**d**) SR, (**e**) saporin-KQ, (**f**) SH, (**g**) SE, (**h**) DE and (**i**) $DT_{390}$-EGF were eluted by increasing concentrations of imidazole (31, 62, 125 and 250 mM). After the purification, SDS-PAGE analysis of the flow-through, wash fractions and eluted fractions at the four different concentrations was performed under non-reducing conditions. The approximate molecular mass of the purified proteins of interest is indicated with a grey discontinuous arrow in the right side of the images. Bacterial pellets were included in the electrophoretic analysis for those proteins that were heterologously expressed in *Escherichia coli* system. In the case of $DT_{390}$-EGF, the targeted toxin was purified under denaturing conditions and the supernatant discarded before the denaturation of the bacterial pellets was also analyzed. In the case of ST, SR and SH, the contrast has been slightly modified for a better visualization of the bands. Only in the two latter cases, the concrete bands containing the purified proteins are indicated with a black arrow on the top of the images.

Immunotoxin solutions were purified to remove unconjugated monoclonal antibodies (Figure 9b, c and d). Unconjugated monoclonal antibodies that did not contain the 6× his-tag were directly eluted in the flow-through and during the washing steps. A certain amount of immunotoxins was eluted in the flow-through and washing steps as well, apparently because the cross-linking reaction of saporin to the monoclonal antibodies resulted in the partial masking of the 6× his-tag and prevented the affinity binding of a subset of immunotoxins to the column. However, immunotoxins with accessible 6× his-tag bound strongly to the column and were eluted with increasing imidazole concentrations. The total yield of the processes after the chemical conjugation and the two-step purification was 1.5 mg of ST, 1.5 mg of SC and 0.5 mg of SR corresponding to 25% in the first two cases and 8% in the latter case of protein (monoclonal antibody plus toxin) input.

The elution pattern of the enzymatically inactive variant of saporin (saporin-KQ) (presenting a 6× his-tag at the N-terminus) previously reported in the literature [168] was comparable to that of saporin (Figure 9e). SH solution was purified to remove unconjugated HRP (Figure 9f). The elution pattern was similar to those observed for ST, SC and SR. In this case, the total yield of the process was around 1.4 mg of conjugate corresponding to 14% of protein (toxin plus HRP) input.

Saporin-epidermal growth factor (SE) and dianthin-30-epidermal growth factor (DE) consist of a 6× his-tag at the N-terminus, either saporin or dianthin-30 as a toxin moiety and epidermal growth factor (EGF) as a ligand at the C-terminus. The elution pattern of both fusion proteins was comparable to that of saporin (Figure 9g and h). Although all the expression and purification steps were conducted exactly under the same conditions, two main differences between SE and DE were observed. Firstly, the bands of DE showed higher intensity than those of SE. Therefore, a better yield for DE was expected after expression and purification. In fact, after determining the protein concentration of all fractions that contained protein, the total amount of protein was $2.36 \pm 0.22$ mg SE/l and $4.10 \pm 0.06$ mg DE/l of bacteria ($A_{600nm} = 0.9$). These results differ significantly (t-test, $p \leq 0.05$) and were reproduced three times. Secondly, less by-products and degradation fragments were observed in the SDS-PAGE of DE. Bands of DE were sharper while those of SE were more diffuse. For these reasons, it was concluded that DE was expressed in a higher quantity and better quality than SE by the same expression system under uniform conditions.

**Table 4.** Elution pattern of proteins purified by Ni-NTA affinity chromatography. Theoretical absolute molecular mass (Ma), fractions where proteins are eluted (Eluted fractions) and fractions where the proteins are eluted with no or only minor amounts of co-purified proteins (Pure fractions) are specified for each of the proteins.

| Protein | Theoretical Ma (Da) | Eluted fractions | Pure fractions |
|---|---|---|---|
| Saporin | 29,742 | F1 (62 mM) – F5 (125 mM) | F3 (62 mM) – F5 (125 mM) |
| ST | 175,272 205,014 | F3 (31 mM) – F2 (125 mM) | F3 (31 mM) – F2 (125 mM) |
| SC | 175,542 205,284 | F3 (31 mM) – F5 (125 mM) | F3 (31 mM) – F2 (125 mM) |
| SR | 173,602 203,344 | F2 (62 mM) – F2 (125 mM) | F2 (62 mM) – F2 (125 mM) |
| Saporin-KQ | 29,871 | F2 (62 mM) – F3 (125 mM) | F2 – F3 (125 mM) |
| SH | 69,742 High Ma | F1 – F3 (62 mM) | F1 – F3 (62 mM) |
| SE | 36,258 | F1 (62 mM) – F2 (250 mM) | F1 (125 mM) – F2 (250 mM) |
| DE | 36,182 | F1 (31 mM) – F5 (250 mM) | F1 – F5 (31 mM) F4 (62 mM) – F5 (250 mM) |
| DT$_{390}$-EGF | 50,018 | F1 (31 mM) – F1 (250 mM) | F1 – F5 (31 mM) F4 (125 mM) – F1 (250 mM) |

Diphtheria toxin$_{390}$-epidermal growth factor (DT$_{390}$-EGF) is composed of the 6× his-tagged (at the N-terminus) catalytic and translocation domains of DT fused to EGF (at the C-terminus). DT$_{390}$-EGF accumulated in inclusion bodies and was therefore purified under denaturing conditions (Figure 9i). The elution pattern of DT$_{390}$-EGF was similar to that of saporin.

### 3.2.5. Identity validation of proteins

The identity of saporin and the conjugates ST, SC and SR was validated by Western blot with a primary polyclonal antibody against saporin (see Figure 7c, f and i). In the case of saporin, a band with an approximate molecular mass of 30 kDa was specifically detected. In the case of ST, SC and SR, bands with high molecular mass representing the conjugates with different molecular ratios were specifically identified. Unconjugated Trastuzumab, Cetuximab and Rituximab were

also detected most probably due to a unspecific cross-reaction of the polyclonal goat anti-rabbit immunoglobulins/HRP (secondary antibody) to the monoclonal antibodies.

Saporin-KQ (a fraction containing some co-purified proteins, see section 3.2.4) was analyzed by SDS-PAGE (Figure 10a) and the identity of saporin-KQ was evaluated by Western blot with a primary polyclonal antibody against saporin (Figure 10b). Both saporin and saporin-KQ were specifically detected. Saporin-KQ was also detected in the pellet, indicating a proper heterologous expression of the protein in bacteria. Considering all the results described in this section, the identity of saporin-KQ was successfully validated.
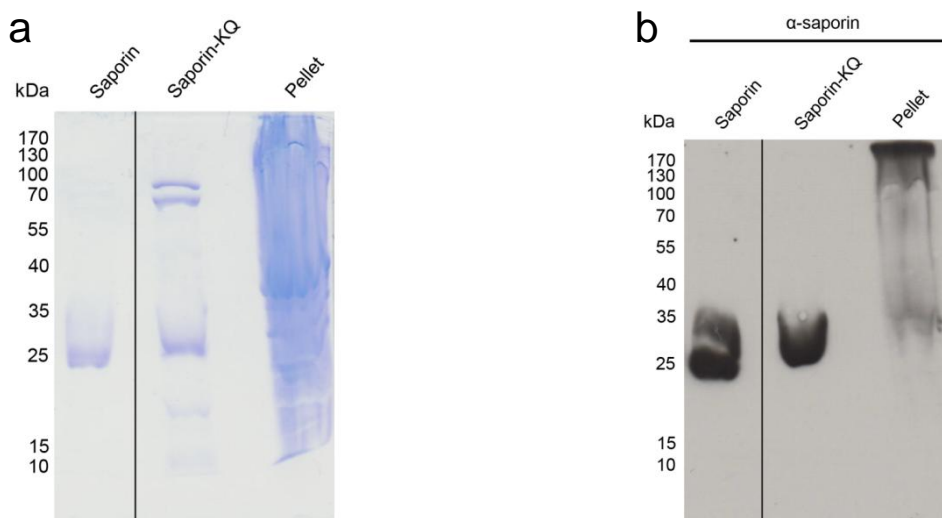


**Figure 10.** Identity validation of saporin-KQ. **(a)** Saporin-KQ was analyzed by SDS-PAGE under non-reducing conditions. Saporin and a pellet of the bacteria that had expressed saporin-KQ were simultaneously analyzed as controls. **(b)** Saporin-KQ was analyzed by Western blot with a primary polyclonal antibody against saporin.

Although chemical conjugation of SH was already validated by the specific binding of the conjugate (containing the $6\times$ his-tag in the saporin moiety) to the Ni-NTA agarose and detection of the high molecular mass conjugate after SDS-PAGE (see section 3.2.4), validation of the cross-linking reaction was confirmed again by Western blot with a primary polyclonal antibody against saporin (Figure 11). Both saporin (intense band in the unconjugated control) and SH (slight band) were specifically detected. Unconjugated saporin was not detected in the conjugate solution.
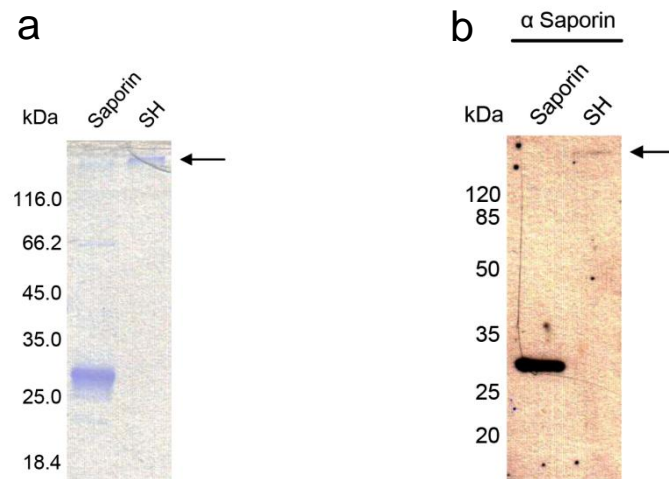
**Figure 11.** Validation of chemical conjugation of saporin and HRP. **(a)** SH was analyzed by SDS-PAGE under non-reducing conditions. The conjugate was visualized in the gel (see arrow). The unconjugated saporin was included as a control. **(b)** SH was analyzed by Western blot with a primary polyclonal antibody against saporin. Saporin (intense band in the unconjugated control) and conjugate (slight band, see arrow) were specifically detected in the membrane. No unconjugated saporin was detected in the SH solution. Contrast has been modified to facilitate the visualization of the bands.

In the case of SE and DE, the expected molecular masses were 36,258 Da and 36,182 Da, respectively. Since bands with molecular masses in this mass range were observed in each of the gels (see Figure 9g and h), the correct expression of SE and DE was anticipated. Nevertheless, identity of the targeted toxins was validated by mass spectrometric analyses (Figure 12). In the case of SE, 10 main peaks were obtained by matrix-assisted laser desorption/ionization time-of-flight mass spectrometry (MALDI-TOF-MS) (*m/z* of 789, 851, 1186, 1244, 1260, 1560, 1649, 2085, 2222 and 2585) (Figure 12a) and 5 of those peptides were further analyzed by MS/MS (*m/z* of 1244, 1260, 1649, 2222 and 2585). Peptides identified by mass spectrometry matched with the protein RIP2_SAPOF in SwissProt database (ribosome-inactivating protein saporin-2 from *Saponaria officinalis* L.) and covered 56% of the amino-acid sequence of SE.

In the case of DE, 10 main peaks were obtained by MALDI-TOF-MS (*m/z* of 789, 831, 1244, 1260, 1560, 1649, 1896, 2011, 2069 and 2225) (Figure 12b) and 3 of those peptides were further investigated by MS/MS (*m/z* of 1896, 2011 and 2225). This time, peptides matched with the protein RIP0_DIACA in SwissProt database (antiviral protein DAP-30 from *Dianthus caryophyllus* L.) and corresponded to 48% of the amino-acid sequence of DE. Two of the peptides found in the spectra of both fusion proteins (*m/z* of 789 and 1560) corresponded to the EGF domain at the C-terminus and three other peptides (*m/z* of 1244, 1260 and 1649) to an identical amino-acid sequence of saporin and dianthin-30 domains.
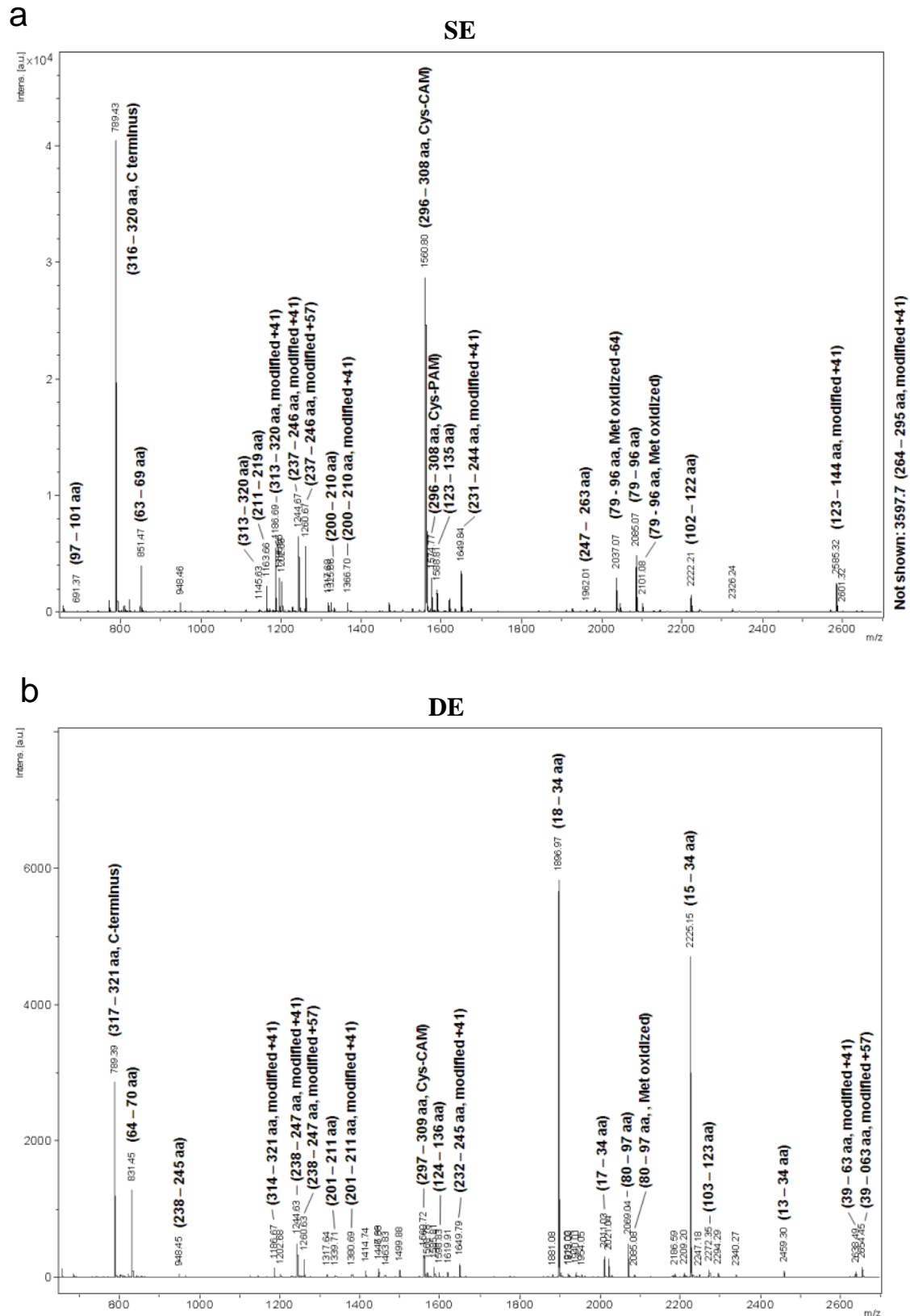
**Figure 12.** Identity validation of SE and DE by mass spectrometry. Targeted toxins were in-gel digested with trypsin and peptides were analyzed by MALDI-TOF-MS. **(a)** In the case of SE, identified peptides matched with the protein RIP2_SAPOF (ribosome-inactivating protein saporin-2 from *Saponaria officinalis* L. in SwissProt database). **(b)** In the case of DE, peptides matched with the protein RIP0_DIACA (antiviral protein DAP-30 from *Dianthus caryophyllus* L.). Furthermore, two peptides found in both spectra (*m/z* of 789 and 1560) corresponded to the EGF domain at the C-terminus.

DT$_{390}$-EGF was cloned, recombinantly expressed, purified and characterized *in vitro* in a previous publication [165]. For this reason, the identity of DT$_{390}$-EGF is not validated in the present work.

## 3.3. Characterization of saporin

### 3.3.1. Optimization of the cell number for MTT assays

Functional saporin was needed to construct the immunotoxins (monoclonal antibodies coupled to saporin) that will be used to develop a platform system for the enhanced endo/lysosomal escape. To evaluate the cytotoxicity of saporin, the initial cell number for 3-(4,5-dimethylthiazol-2-yl)-2,5-diphenyltetrazolium bromide (MTT) assays had to be optimized. The optimal initial cell number for ECV-304 and HER14 cells in the proliferation assay was estimated by measuring the viability of different initial amounts of cells (Figure 13).
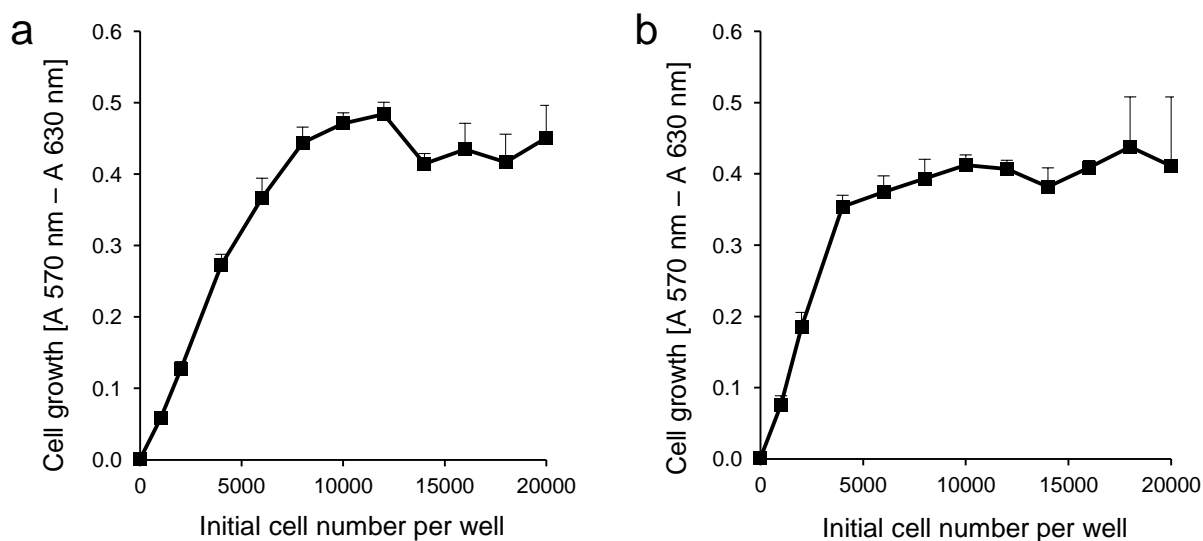


**Figure 13.** Optimization of the initial cell number in a proliferation assay (MTT assay). Different amounts of **(a)** ECV-304 cells and **(b)** HER14 cells were initially seeded in a 96-well plate. Cells were allowed to grow for 24 h. Then, medium was changed and cells proliferated further for 48 h. Finally, the cell viability was measured by an MTT assay. Each data point is the mean ± SD, $n = 4$.

In the case of ECV-304 cells (Figure 13a), a saturation of the absorbance signal was observed for an initial cell number of 8,000 (A$_{570\,nm}$ − A$_{630\,nm}$ = 0.44) and higher. In the case of HER14 cells (Figure 13b), the saturation of the absorbance signal was observed beginning with an initial cell number of 4,000 (A$_{570\,nm}$ − A$_{630\,nm}$ = 0.35). Therefore, the initial cell numbers of either 4,000 or 8,000 ECV-304 cells/well and either 2,000 or 4,000 HER14 cells/well were considered as optimal for testing the cytotoxicity of compounds in an MTT assay.

### 3.3.2. Cytotoxicity of saporin in combination with SA1641

In order to discover whether the heterologously expressed and purified saporin was active and synergistically enhanced by triterpenoidal saponins, the cytotoxicity of saporin and its combination with SA1641 was investigated in ECV-304 and HER14 cells (Figure 14).

Firstly, the cytotoxicity of SA1641 was evaluated in ECV-304 and HER14 cells as a control to find the highest non-cytotoxic concentration of triterpenoidal saponins. In the case of ECV-304 cells (Figure 14a), SA1641 was non-cytotoxic up to a concentration of 5 µg/ml (3.05 µM). With higher concentrations, cell viability was reduced progressively to 88% at 10 µg/ml, 51% at 20 µg/ml and 15% at 40 µg/ml. The concentration that causes 50% growth inhibition ($GI_{50}$) was estimated to be 20.6 µg/ml on ECV-304 cells. In the case of HER14 cells (Figure 14b), SA1641 was non-cytotoxic up to the same concentration as in ECV-304 cells (5 µg/ml). However, the cytotoxicity pattern at higher concentrations was slightly different. While cell viability was only reduced to approximately 80% at 10 and 20 µg/ml, a total cell death was observed by application of 40 µg/ml. SA1641 had a $GI_{50}$ of 27.8 µg/ml on HER14 cells. Based on these observations, the concentration of 5 µg/ml SA1641 was considered to have no cytotoxic effects on ECV-304 or HER14 cells in the following proliferation assays.

Then, saporin was tested in cytotoxicity assays in combination with triterpenoidal saponins. The administration of saporin to ECV-304 cells (Figure 14c) had a clear cytotoxic effect at higher concentrations (10–1,000 nM). The $GI_{50}$ value of saporin on ECV-304 cells was 186.8 nM. Nevertheless, the application of saporin in combination with SA1641 at the non-cytotoxic concentration of 5 µg/ml (3.05 µM) resulted in a complete inhibition of cell growth at high concentrations and further clear cytotoxicity at lower concentrations down to 0.1 nM. In fact, the $GI_{50}$ value of saporin in combination with SA1641 on ECV-304 cells was 0.23 nM. An enhancement factor of 800-fold was calculated as the ratio of the $GI_{50}$ of saporin and the $GI_{50}$ of saporin + SA1641.

Similar effects were observed when saporin was applied in combination with SA1641 on HER14 cells (Figure 14d). In this case, a $GI_{50}$ value of 680.7 nM was observed for saporin alone, while a $GI_{50}$ of 0.39 nM was measured for the combination. Therefore, an enhancement factor of 1,700-fold was calculated. Cytotoxic activity and synergistic cytotoxicity enhancement by SA1641 of saporin was confirmed in both cell lines.
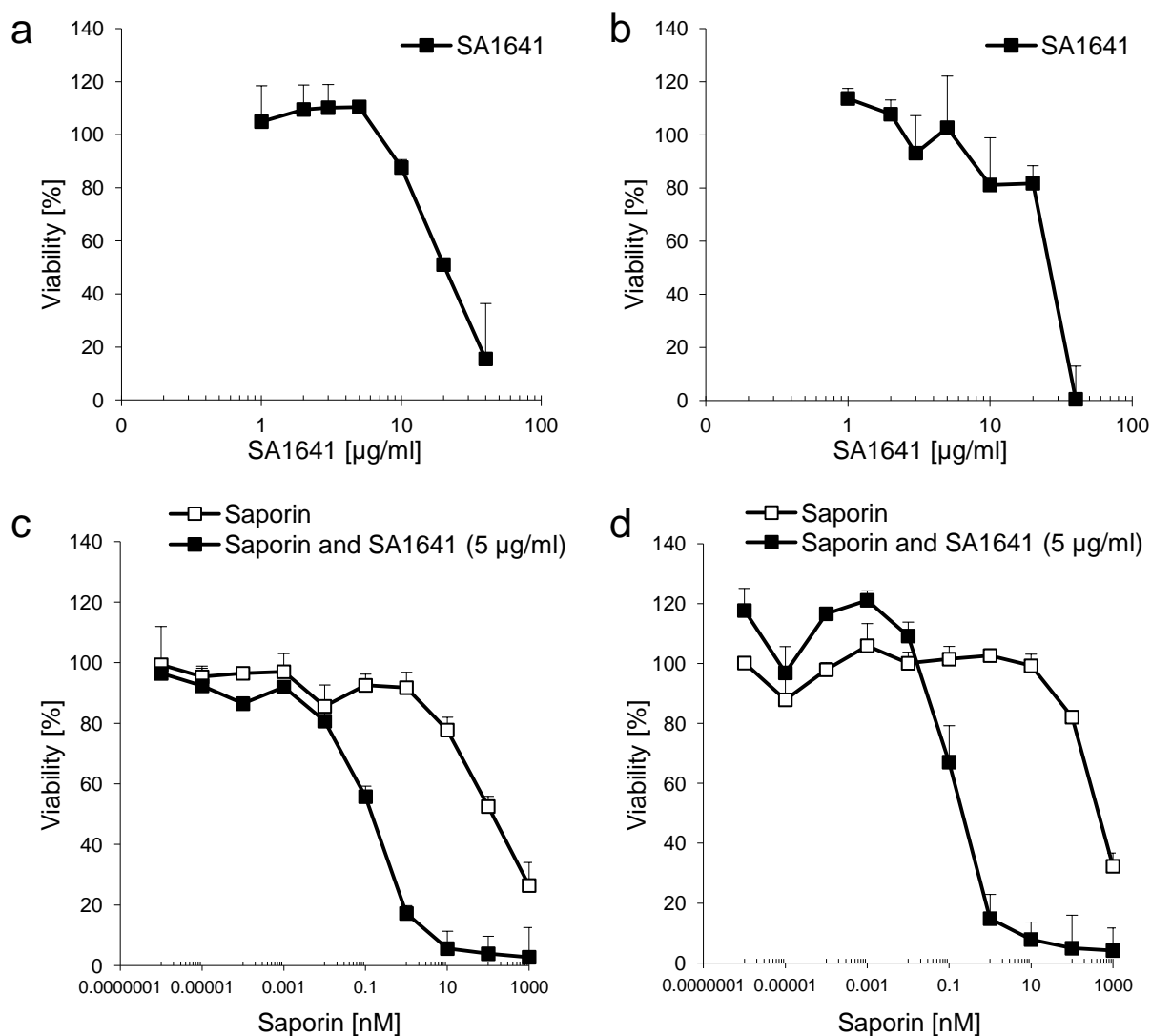
**Figure 14.** Cytotoxicity of saporin in combination with SA1641. **(a)** ECV-304 cells (8,000 cells/well) and **(b)** HER14 cells (4,000 cells/well) were treated with different concentrations of SA1641 (1–40 µg/ml). **(c)** ECV-304 cells (4,000 cells/well) and **(d)** HER14 cells (2,000 cells/well) were treated with saporin in a concentration range from 0.000001 to 1,000 nM ± SA1641 (5 µg/ml). After 48 h, cell viability was determined by an MTT assay and referred to untreated control cells. Data represents the mean ± SD, $n = 4$.

### 3.3.3. Effect of SA1641 on enzymatic activity of saporin

A standard curve with adenine was prepared to estimate the amount of cleaved adenine by *N*-glycosidases of unknown activity from herring sperm DNA. *N*-glycosidase activity of saporin was measured in the presence and absence of 5 µg/ml (3.05 µM) SA1641 to investigate whether there is an influence or possible binding of SA1641 to the active site of the protein, which can affect the enzymatic activity (Table 5). Such experiments provide additional information for the understanding of the interaction of saporin and triterpenoidal saponins, which finally leads to the augmentation of cytotoxicity. As ricin A-chain (RTA, catalytic domain of ricin) is not

synergistically enhanced by triterpenoidal saponins (see section 3.4.1), *N*-glycosidase activity of RTA was also evaluated in combination with SA1641 for comparison.

**Table 5.** *N*-glycosidase activity of saporin and RTA in the presence or absence of SA1641. *N*-glycosidase activity was identical in the case of saporin ± 5 µg/ml SA1641, indicating neither influence nor possible interactions of the triterpenoidal saponin to the active site of the toxin. Each value represents the mean ± SD, *n* = 3.

| | *N*-glycosidase activity | | | |
|---|---|---|---|---|
| | saporin | | RTA | |
| SA1641 | - | + | - | + |
| Adenine release [pmol/pmol toxin/h] | 227.7 ± 0.4 | 227.3 ± 0.8 | 24.6 ± 0.4 | 29.5 ± 0.0 |

Release of adenine from herring sperm DNA was identical after incubation of saporin or saporin + SA1641 with the substrate. Furthermore, similar adenine release was observed in the case of RTA and its combination with SA1641. Therefore, it was concluded that triterpenoidal saponins do neither influence the enzymatic activity nor bind to the active site of type I RIPs under acidic conditions.

### 3.3.4. Endo/lysosomal release of saporin in the presence of SA1641 and red dextran

Mechanistic studies were performed with saporin-Alexa Fluor 488 ([Alexa]saporin) to observe the endo/lysosomal escape of the toxin in the presence of SA1641 (Figure 15). Internalization of [Alexa]saporin was visualized by live cell imaging 6 h after addition of the compound to cells. [Alexa]saporin accumulated mostly in the organelles that colocalize with the pHrodo Red Dextran, 10 kDa (a compound incorporated in acidic vesicles), thus indicating that [Alexa]saporin accumulated in acidic vesicles e.g. late endosomes and lysosomes.

Release of [Alexa]saporin from the endo/lysosomes into the cytosol was only detected after the addition of triterpenoidal saponins. Around 100 min after addition of 10 µg/ml (6.09 µM) SA1641, a diffused fluorescence within the whole cell clearly indicated the release of the toxin (see fluorescence intensity from 6,000 s until the end of the experiment in the single cell analysis in Figure 15b). SA1641 specifically mediated the endo/lysosomal escape of saporin, but did not present any unspecific membrane permeabilizing effects on the biological membranes.

a



b
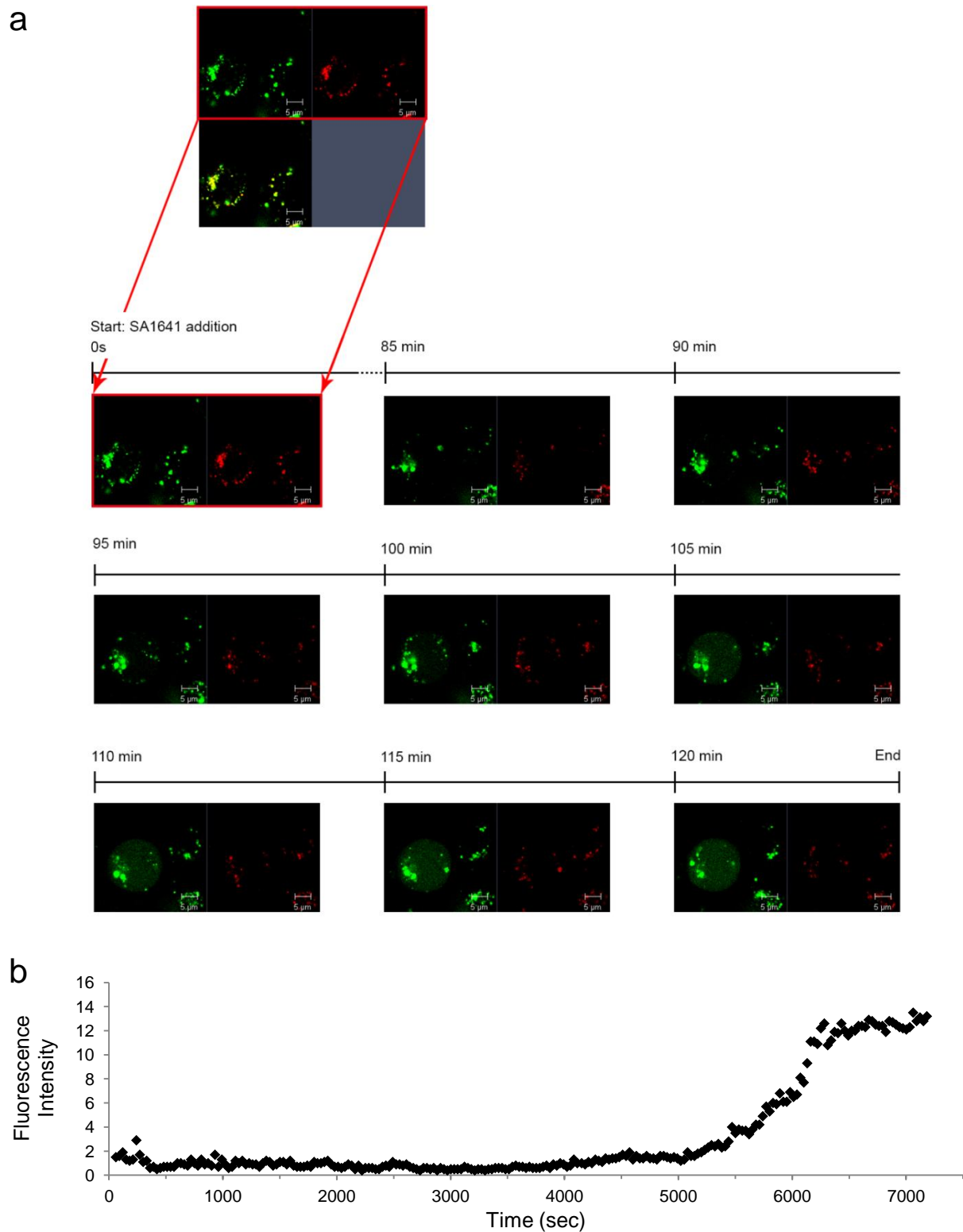


**Figure 15.** Internalization, colocalization and endo/lysosomal release of saporin. **(a)** ECV-304 cells were visualized by live cell imaging (confocal fluorescence microscopy) 6 h after addition of the toxin. [Alexa]Saporin is visualized in green fluorescence (upper left quarter). [Alexa]saporin colocalized with red dextran (visualized in red fluorescence, upper right quarter) as observed in the merger (lower left quarter). Endo/lysosomal escape of [Alexa]saporin was observed approximately 100 min after addition of 10 µg/ml SA1641 (diffusion of green fluorescence within the cell without any effects on cell membrane and endo/lysosomal membrane integrity). The LSM780 laser scanning microscope equipped with a Plan-Apochromat 63×/1.40 oil objective was utilized in this experiment. **(b)** Single cell analysis depicting the endo/lysosomal escape of saporin. Fluorescence intensity in the cytosol of the cell indicates the amount of [Alexa]saporin released from the endo/lysosomes.

Firstly, the cell membrane remained unaffected by SA1641 because no leakage of toxin out of the cell was observed. Secondly, endo/lysosomal membrane also remained unaffected by the triterpenoidal saponin since the pH-sensitive dye red dextran exhibited continuous fluorescence even after the toxin was released. Endo/lysosomes preserved their integrity and thus their internal acidic environment until the end of the experiment.

## 3.4. Specificity of the toxin in its enhancement by triterpenoidal saponins

### 3.4.1. Cytotoxicity of saporin, gelonin and RTA in combination with SO1861

The toxin specificity of the cytotoxicity enhancement mediated by triterpenoidal saponins was studied in order to identify which type I RIPs are subject to augmentation effects. For this reason, the cytotoxicity of saporin and its combination with SO1861 was investigated in ECV-304 cells and compared to the cytotoxicity of gelonin, RTA and their respective combinations with the same triterpenoidal saponin (Figure 16). In the case of saporin (Figure 16a), only the highest concentration was slightly toxic (76% viability) and the $GI_{50}$ was outside of the examined range (> 100 nM). However, there was a strong enhancement of cytotoxicity in combination with 1 µg/ml (0.54 µM) SO1861 since cytotoxicity was observed down to a concentration of 0.1 nM. The $GI_{50}$ of saporin in combination with SO1861 was 0.18 nM and the enhancement factor was > 550-fold.

In the case of gelonin (Figure 16b), a behavior similar to saporin was observed regarding its cytotoxicity. Gelonin alone only presented slight cytotoxicity at 100 nM (88% viability) and the $GI_{50}$ was outside the range (> 100 nM). Nevertheless, gelonin + SO1861 appeared to be much more toxic. The $GI_{50}$ of the combination was 0.38 nM and this represented an enhancement factor of > 270-fold. RTA was the most cytotoxic protein among the toxins tested in this experiment (Figure 16c). RTA presented cytotoxic effects down to a concentration of 0.1 nM (73% viability) and its $GI_{50}$ was 0.58 nM. But in this case, RTA + SO1861 did not result in the augmentation of cytotoxicity ($GI_{50}$ of 0.54 nM).
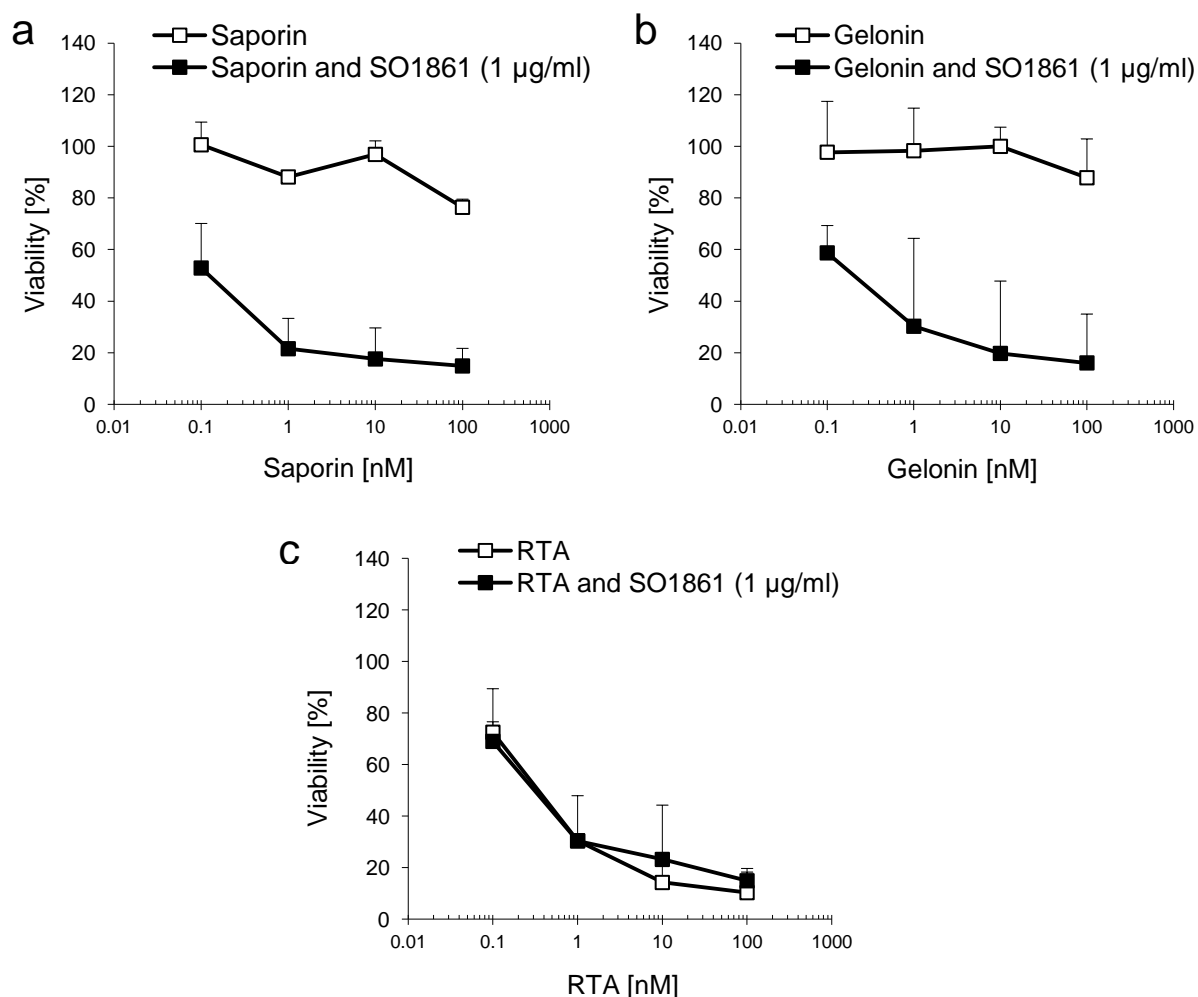
**Figure 16.** Cytotoxicity of saporin, gelonin and RTA in combination with SO1861. ECV-304 cells (5,000 cells/well) were treated with **(a)** saporin, **(b)** gelonin or **(c)** RTA in a concentration range from 0.1 to 100 nM ± SO1861 (1 µg/ml) for 66 h. Cell viability was measured by an MTT assay and referred to untreated control cells. Data represents the mean ± SD, $n$ = 2–8.

### 3.4.2. Cytotoxicity of saporin, gelonin and RTA in combination with SO1861 recorded in real time

To obtain additional information about the toxin specificity, the synergistic cytotoxicity augmentation of saporin, gelonin and RTA by SO1861 was evaluated in real time. ECV-304 cell growth increased linearly up to a normalized cell index (NCI) of 1.00 at the normalization time (Figure 17). At this moment, compounds were added to the cells. In the case of untreated control cells, only fresh medium was pipetted and the NCI increased continuously until reaching a maximum NCI of 1.69 at 65.0 h. Thereafter, untreated cells entered in a plateau phase and the NCI value was maintained until the end of the experiment (NCI = 1.61). In the case of cells treated with only 1 µg/ml (0.54 µM) SO1861, the growth curve was similar to the untreated cells and an NCI of 1.48 was reached at the end of the experiment.

a



b



c
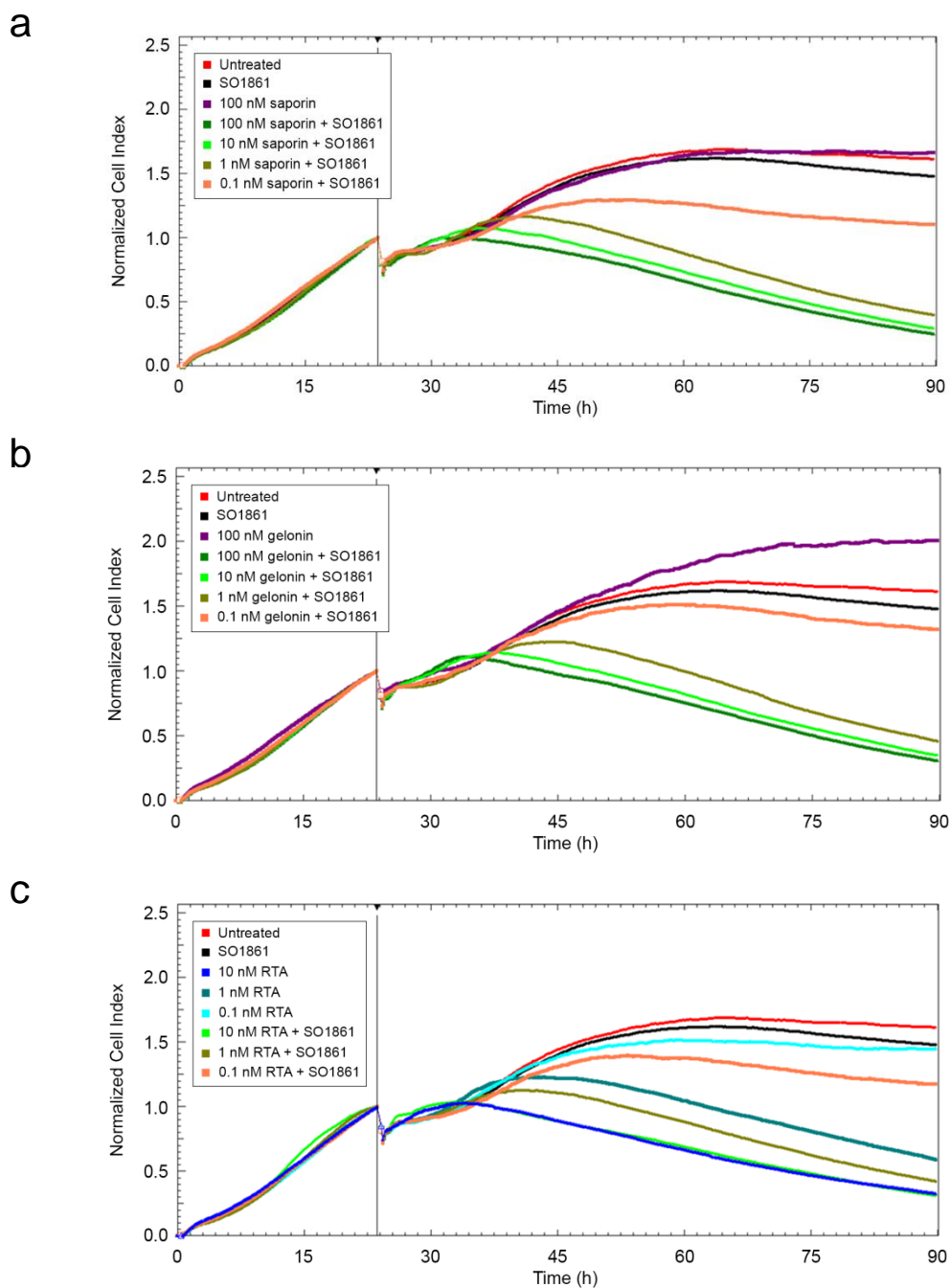


**Figure 17.** Real-time monitoring of the cytotoxicity of saporin, gelonin and RTA in combination with SO1861. ECV-304 cells (5,000 cells/well) were treated with **(a)** saporin, **(b)** gelonin or **(c)** RTA in a concentration range from 0.1 to 100 nM ± SO1861 (1 µg/ml) for 66 h. Cell viability was determined by an impedance-based real-time cytotoxicity assay. Cell indexes were normalized when compounds were added. Curves represent the mean, $n = 2$–8. The curves for untreated control cells and cells treated with only SO1861 are equally drawn in more than one panel for a better comparison.

Saporin was non-cytotoxic at a concentration of 100 nM (Figure 17a). However, saporin in combination with SO1861 exhibited potentiated cytotoxic effects. In the presence of SO1861, saporin was cytotoxic at the end of the experiment at the final concentrations of 1 nM (NCI =

0.40), 10 nM (NCI = 0.29) and 100 nM (NCI = 0.25). At the lowest concentration of saporin (0.1 nM), the combination treatment resulted in a cytotoxicity enhancement as well (NCI = 1.11).

In the case of gelonin (Figure 17b), the toxin alone did not cause any cytotoxic effects at a concentration of 100 nM. Similarly to the effects observed with saporin, an augmentation of the cytotoxicity was observed when gelonin was administered in combination with SO1861. In the presence of the triterpenoidal saponin, gelonin was cytotoxic at the final concentrations of 1 nM (NCI = 0.46), 10 nM (NCI = 0.35) and 100 nM (NCI = 0.31) at the end of the experiment. Cell viability was only slightly reduced to an NCI of 1.32 at the end of the experiment at a lower concentration of 0.1 nM gelonin. Gelonin was slightly less cytotoxic in combination with SO1861 than saporin. However, tremendous enhancement of cytotoxicity was observed for both toxins.

In the case of RTA (Figure 17c), the toxin alone was already cytotoxic at 1 and 10 nM (NCI = 0.59 and 0.33, respectively). RTA at a final concentration of 0.1 nM was not toxic any more (NCI = 1.45 at 90.0 h). When RTA was applied in combination with SO1861, cytotoxicity was only slightly increased at the concentrations of 0.1 nM (NCI = 1.17 at 90.0 h) and 1 nM (NCI = 0.42 at 90.0 h). In higher concentrations of RTA, the toxin presented very similar cytotoxic effects either alone or in combination with SO1861. The drastic cytotoxicity augmentation of saporin or gelonin in the presence of SO1861 was not observed for RTA.

### 3.4.3. Structural alignment of saporin, dianthin-30, gelonin and RTA

Structural alignment of the toxins that had been tested for cytotoxicity enhancement by triterpenoidal saponins was proposed as a methodology to find whether certain structural features of the toxins had a direct relation to the augmentation effects. Therefore, an alignment of protein structures was performed for the toxins, namely saporin (PDB 1QI7), dianthin-30 (PDB 1RL0), gelonin (PDB 3KTZ) and RTA (PDB 1IFT) (Figure 18). Saporin and gelonin are toxins that are subject to a synergistic augmentation of their cytotoxicity in combination with triterpenoidal saponins. Dianthin-30 also exhibits enhanced cytotoxicity in the presence of triterpenoidal saponins (see cytotoxicity of the targeted toxin DE in section 3.10.2). Agrostin, another toxin reported to be enhanced by triterpenoidal saponins, was not included in the alignment since neither its three-dimensional structure nor its amino-acid sequence have been described so far. In contrast, RTA is a toxin that does not get potentiated in the presence of triterpenoidal saponins.
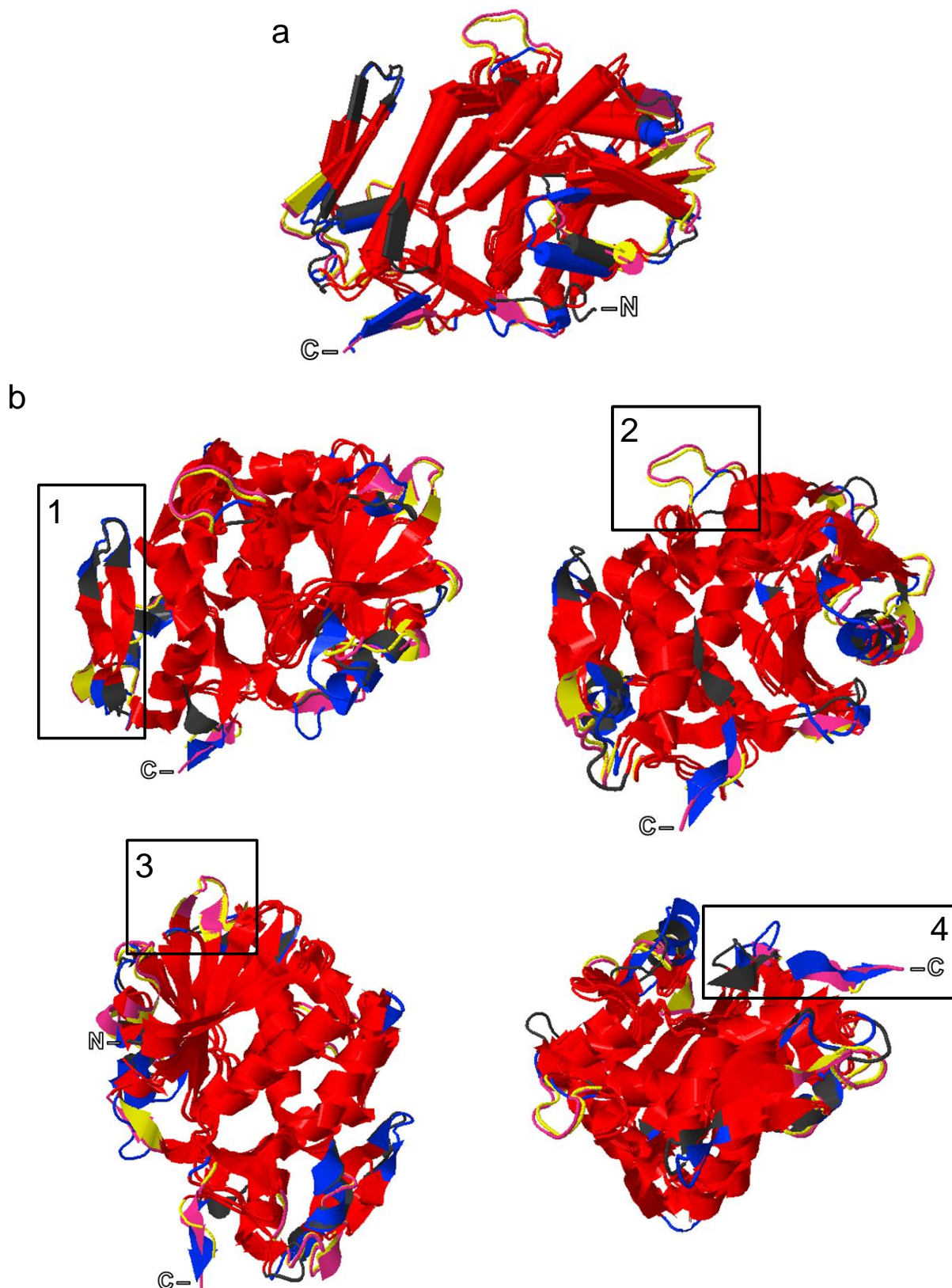
**Figure 18.** Structural alignment and differences between RTA compared to all other RIPs saporin, dianthin-30 and gelonin. **(a)** Annealing regions in the alignment of three-dimensional structures of saporin (PDB 1QI7, in yellow), dianthin-30 (PDB 1RL0, in pink), gelonin (PDB 3KTZ, in grey) and RTA (PDB 1IFT, in blue) are highlighted in red. **(b)** Four slight structural differences were identified (1–4). Three of the structural differences were located in loops (1–3) and one structural difference was found at the C-terminus (4). However, none of these differences can explain why three toxins (saporin, dianthin-30 and gelonin) were enhanced in their efficacy by triterpenoidal saponins and one (RTA) was not.

The four proteins showed a very similar three-dimensional structure (Figure 18a). Features that are in common among saporin, dianthin-30 and gelonin but differ from RTA were searched in the structural alignment. These features could be related to specific amino-acid sequences of the toxins that interact with triterpenoidal saponins and are required to exhibit the synergistic augmentation effects. However, only four slight structural variations were observed in certain loops (differences 1–3, see Figure 18b) or in the C-terminal sequence (difference 4), but in these cases RTA behaved similarly to gelonin (differences 1–3) or to saporin and dianthin-30 (difference 4).

The details of the four structural differences are presented in Table 6. Since none of these differences are common in the three toxins that exhibit synergistic cytotoxicity enhancement by triterpenoidal saponins (saporin, dianthin-30 and gelonin) but different in the toxin that does not present cytotoxicity enhancement (RTA), no relation can be established between the structural features of the toxins and their synergistic cytotoxicity enhancement mediated by triterpenoidal saponins.

**Table 6.** Structural differences between RTA compared to all other RIPs saporin, dianthin-30 and gelonin identified after structural alignment of these four proteins. For each structural difference (1–4, see Figure 18), its position in the amino-acid sequence of saporin, its amino acid and structural conformation, and similarities or differences between the structural conformation of saporin and the three other toxins are specified.

| Structural difference | Position (in saporin) | Amino-acid sequence (in saporin) | Structural conformation (in saporin) | Similar in | Different from |
|---|---|---|---|---|---|
| 1 | 230–233 | FGFG | short loop | short loop in dianthin-30 | long loop in gelonin and RTA |
| 2 | 128–135 | QITQGDKS | long loop | long loop in dianthin-30 | short loop in RTA and no loop in gelonin |
| 3 | 80–84 | DNTNV | short loop | short loop in dianthin-30 | no loop in gelonin and RTA |
| 4 | 248–253 | YLGKPK | C-terminal sequence towards a specific direction | C-terminal sequence towards same direction in dianthin-30 and RTA | C-terminal sequence towards opposite direction in gelonin |

### 3.4.4. Alignment of amino acid sequences of saporin, dianthin-30, gelonin and RTA

To determine if certain amino acids of the toxins were responsible for the augmentation effects by triterpenoidal saponins, an amino-acid sequence alignment was performed for the toxins saporin, dianthin-30, gelonin and RTA (Figure 19).

```
                                    5
Saporin       1 VTS-----ITLDLVNPTAGQYSSFVDKIRNNVKDPNLK-YGG   36
Dianthin-30   1 ATA-----YTLNLANPSASQYSSFLDQIRNNVRDTSLI-YGG   36
Gelonin       1 GLD----TVSFSTKGATYITYVNFLNELRVKLKPEGNS-HGI   37
RTA           1 MVPKQYPIINFTTAGATVQSYTNFIRAVRGRLTTGADVRHFI   42

cons          1          .:    ..:   * .*:  :* .:       :    42

                                  2
Saporin      37 TDI-AVIGPPSK-EKFLRINFQSSRG-TVSLGLKRDNLYVVA   75
Dianthin-30  37 TDV-AVIGAPSTTDKFLRLNFQGPRG-TVSLGLRRENLYVVA   76
Gelonin      38 PLLRKKCDDP-G-KCFVLVALSNDNGQLAEIAIDVTSVYVVG   77
RTA          43 PVLPNRVGLPIN-QRFILVELSNHAFLSVTLALDVTNAYVVG   83

cons         43 . :      . *   . *: : :..    . :.:   . ***.  84

                               3              4
Saporin      76 YLAMDNTNVNRAYYFKS--EITSAELTALFPEATTANQKALE  115
Dianthin-30  77 YLAMDNANVNRAYYFKN--QITSAELTALFPEVVVANQKQLE  116
Gelonin      78 YQVR-----NRSYFFKD--APD-AYEGLFKNT--I-KTRLH  108
RTA          84 YRAG-----NSAYFFHPDNQEDAEAITHLFTDV--QNRYTFA  118

cons         85 * .      * :*:*:         ** :.   : :       126

Saporin     116 YTEDYQSIEKNAQITQGDKSRKELGLGTDLLLTFMEA---VN  154
Dianthin-30 117 YGEDYQAIEKNAKITTGDQSRKELGLGTNLLITMIDG---VN  155
Gelonin     109 FGGSYPSLEGEKA------YRETTDLGTEPLRIGIKKLDENA  144
RTA         119 FGGNYDRLEQLAGN-----LRENIELGNGPLEEAISALYYS   155

cons        127 :  .*  :*             *:   **   *   :.     168

Saporin     155 KKARVVKNEARFLLIAIQMTAEVARFRYIQNLVTK--NFPNK  194
Dianthin-30 156 KKVRVVKDEARFLLIAIQMTAEAARFRYIQNLVTK--NFPNK  195
Gelonin     145 IDNYKPTEIASSLLVVIQMVSEAARFTFIENQIRN--NFQQR  184
RTA         156 TGGTQLPTLARSFIICIQMISEAARFQYIEGEMRTRIRYNRR  197

cons        169          *  ::: *** :*.*** :*:. :  .  .: .:  210

Saporin     195 FDSDNKVIQFEVSWRKISTAIYGDAKNGVFNKDYDFGF----  232
Dianthin-30 196 FDSENKVIQFQVSWSKISTAIFGDCKNGVFNKDYDFGF----  233
Gelonin     185 IRPANNTISLENKWGKLSFQIRTSGANGMFSEAVELERANGK  226
RTA         198 SAPDPSVITLENSWGRLSTAIQES-NQGAFASPIQLQRRNGS  238

cons        211   .  ..* :: .* ::*   *  .  :* * .  ::       252

                                              1
Saporin     233 ----GKVRQVKDLQMGLLMYLGK-PK-  253
Dianthin-30 234 ----GKVRQAKDLQMGLLKYLGR-PKS  255
Gelonin     227 KYYVTAVDQVKP-KIALLKFVDKDPR-  251
RTA         239 KFSVYDVSILLPP-IIALMVYRCAPPP-  263

cons        253         *       :.*: :     *    278
```

**Figure 19.** Amino-acid sequence alignment of saporin, dianthin-30, gelonin and RTA. In color, common amino acids between saporin, dianthin-30 and gelonin not identical to those of RTA. The different colors indicate the similarity of the different amino acids of RTA compared to the common amino acids in the other toxins: red, no similarity; yellow, similar size or evolutionary preserved hydrophobicity; green, same size and hydrophobicity. In grey, residues forming the active site. Common amino acids between saporin, dianthin-30 and gelonin not identical in RTA may be related with the toxin cytotoxicity enhancement by triterpenoidal saponins. Amino acids relevant for the amino-acid sequence alignment of SE and DE in section 3.9.4 are indicated with black squares.

Amino acids that are shared between saporin, dianthin-30 and gelonin but are different from RTA were searched in the sequence alignment. Amino acids accomplishing this condition may be responsible for the synergistic cytotoxicity enhancement of certain type I RIPs (saporin, dianthin-30 and gelonin) by triterpenoidal saponins.

There are 57 amino acids in common between saporin, dianthin-30 and gelonin. However, 38 of these amino acids are also in common with RTA and there is only a total of 19 amino acids in common with saporin, dianthin-30 and gelonin but different in RTA. Out of theses 19 amino acids, 8 amino acids have same size and hydrophobicity comparable to those of RTA, 2 amino acids have similar size or evolutionarily preserved hydrophobicity similar to those of RTA, and 9 amino acids do not share any similarities to those of RTA.

A detailed list of all the 19 amino acids in common between saporin, dianthin-30 and gelonin but different from RTA is shown in Table 7. Most probably, amino acids that have the same size and hydrophobicity (high similarity) may not have any influence on the capacity of the toxins to interact with triterpenoidal saponins. However, those amino acids that are only similar (medium similarity) and especially those that do not have any similarities to the amino acids of RTA (no similarity), can be relevant and related to the cytotoxicity augmentation of the toxins mediated by triterpenoidal saponins.
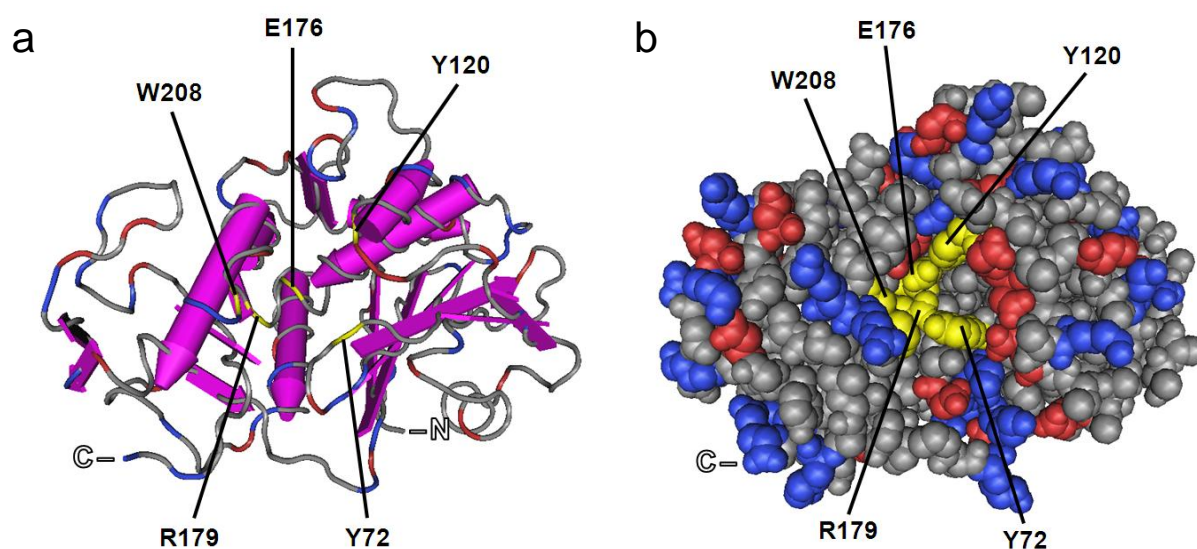


**Figure 20.** Active site of saporin in the three-dimensional structure. **(a)** Amino acids comprising of the active site of saporin are highlighted in yellow in the protein scheme. **(b)** The active site is highlighted in yellow in the molecular space fill picture of saporin. Since amino acids in the active site of saporin are in common with RTA and *N*-glycosidase activity of the toxins is not influenced in the presence of SA1641 (see section 3.3.3), these amino acids are not certainly related to the cytotoxicity enhancement properties of the toxin by triterpenoidal saponins.

Amino acids that do not certainly have any relevance in the cytotoxicity enhancement effects are those comprising of the active site (Figure 20). These amino acids are in common between saporin, dianthin-30, gelonin and RTA (see Figure 19, in grey).

**Table 7.** Amino acids that are identical in saporin, dianthin-30 and gelonin but different in RTA and selected properties.

| Position (in saporin) | Identical amino acids | Amino acid in RTA | Similarity | Changes in the amino-acid side chains of RTA | Presence on surface |
|---|---|---|---|---|---|
| 35 | G | E | no | neutral → negative | yes |
| 60 | G | E | no | neutral → negative | yes |
| 86 | R | S | no | positive → polar | yes |
| 91 | K | H | high | positive | yes |
| 97 | A | E | no | hydrophobic → negative | yes |
| 114 | L | F | high | hydrophobic | no |
| 143 | I | N | no | hydrophobic → polar | no |
| 167 | L | F | high | hydrophobic | no |
| 168 | L | I | high | hydrophobic | no |
| 185 | N | G | medium | polar → neutral | yes |
| 190 | N | R | medium | polar → positive | yes |
| 191 | F | Y | high | hydrophobic | yes |
| 199 | N | P | no | polar → cyclic | yes |
| 210 | K | R | high | positive | yes |
| 221 | N | Q | high | polar | yes |
| 237 | Q | I | no | polar → hydrophobic | yes |
| 239 | K | I | no | positive → hydrophobic | yes |
| 246 | L | M | high | hydrophobic | no |
| 253 | K | P | no | positive → cyclic | yes |

Another factor that must be considered in the case of the 19 amino acids that appear in the list of Table 7 is the presence on the surface of the toxins. Since relevant amino acids for the augmentation properties must be able to physically interact with the triterpenoidal saponins or the intracellular environment, only amino acids (1) in common between the three toxins but not with RTA, (2) with medium or no similarity to the corresponding amino acids in RTA, and

additionally (3) present on the surface of the toxins may have an important role in the cytotoxicity enhancement.

All amino acids accomplishing these three conditions (10 amino acids) were identified in the protein structure of saporin (Figure 21). The presumably relevant amino acids are the following: R86, A97, N199 and K253 (Figure 21a); G60 (Figure 21b); N185, N190, Q237 and K239 (Figure 21c); and G35 (Figure 21d). These amino acids may be responsible for triggering the enhanced cytotoxicity of type I RIPs.
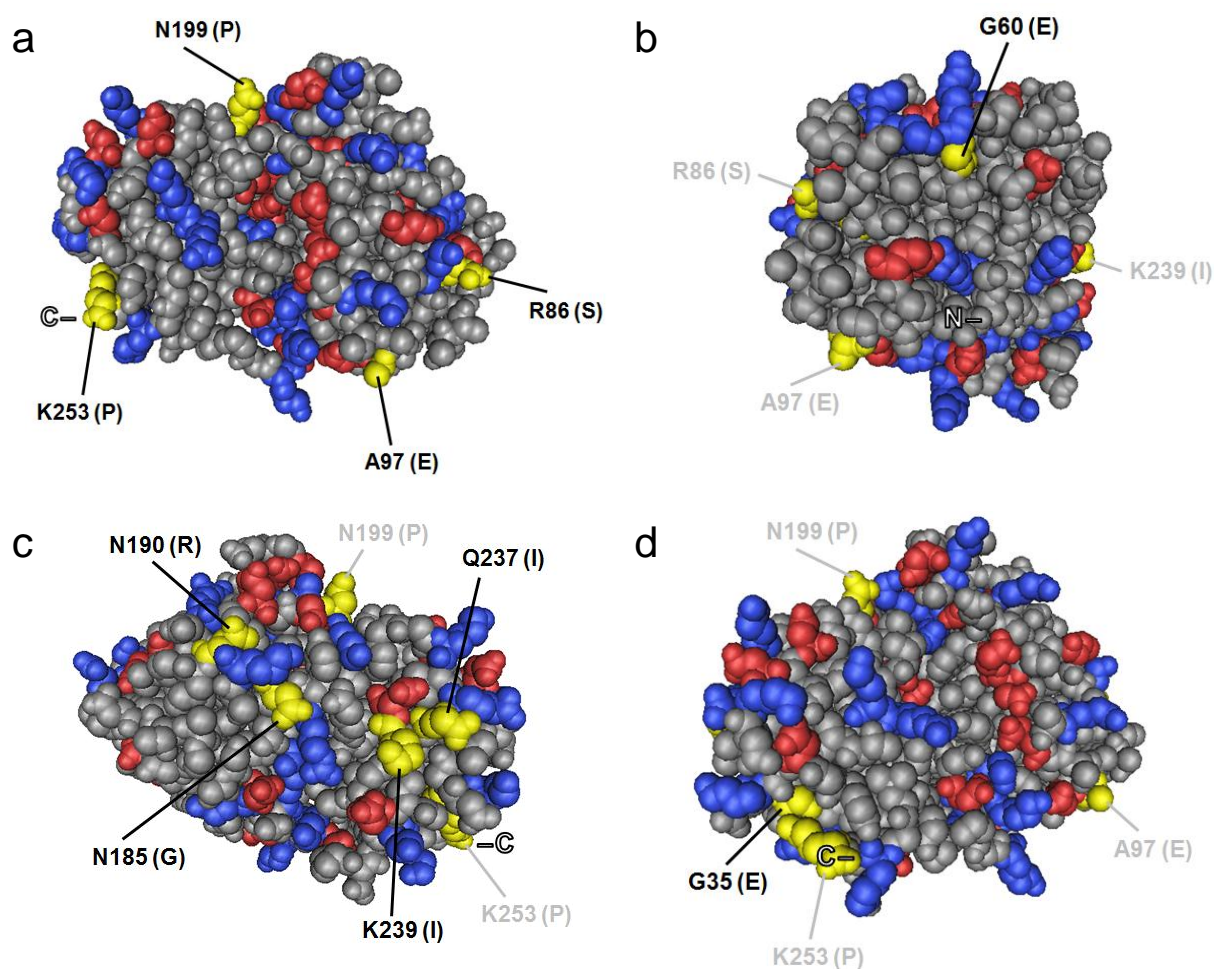


**Figure 21.** Identification of relevant amino acids after amino-acid sequence alignment of saporin, dianthin-30, gelonin and RTA. The presumably relevant amino acids are **(a)** R86, A97, N199 and K253; **(b)** G60; **(c)** N185, N190, Q237 and K239; and **(d)** G35. All relevant amino acids are highlighted in yellow and accomplish three conditions. Firstly, the amino acids are in common between saporin, dianthin-30 and gelonin (toxins that are synergistically enhanced by triterpenoidal saponins) but not with RTA (does not exhibit cytotoxicity augmentation). Secondly, the common amino acids have only medium or no similarity to the corresponding amino acids in RTA. Thirdly, the amino acids are present on the surface of the toxins. The highlighted amino acids are labeled by their position in the amino-acid sequence of saporin. Respective amino acids in RTA are written in parentheses. For a better comprehension, some relevant amino acids are repeated (in grey) in more than one molecular space fill model.

## 3.5. Characterization of the platform technology for enhanced endo/lysosomal escape with ST and SC

### 3.5.1. Reduction of immunotoxins

ST and SC were first used to develop a platform system for endo/lysosomal escape enhancement of targeted toxins by triterpenoidal saponins. In such a platform, the ligand of immunotoxins will be exchanged to target different cell types of interest, and the synergistic principle between saporin and triterpenoidal saponins will be simultaneously exploited to achieve potentiated cytotoxicity.

Further relevant aspects such as binding capacity, payload delivery and ability to trigger antibody-dependent cell-mediated cytotoxicity (ADCC) by immunotoxins also needed to be investigated. An ideal immunotoxin should combine the functionality of the therapeutic monoclonal antibody (antagonistic binding to targeted receptors and interaction with the innate immune system) with the cell-killing activity of the toxic moiety. In addition, it should definitely be sensitive for triterpenoidal saponins to achieve the tremendous augmentation of anti-tumoral efficacy, thus leading to a decrease of the dosage, side effects and possible adverse immune reactions in patients.

Firstly, in order to characterize the chemical cross-linkage introduced between saporin and the therapeutic antibodies, purified ST and SC were analyzed by SDS-PAGE under non-reducing conditions (Figure 22a). Both immunotoxins showed two bands corresponding to one molecule of antibody coupled to either one or two molecules of toxin. In the case of ST, a third weak band was identified, probably a modified ST due to a different glycosylation pattern of the antibody moiety (similarly to the modifications observed for single Trastuzumab). Neither free antibodies nor free saporin was observed in ST and SC solutions, displaying the purity of the immunotoxin solutions after purification.

Under reducing conditions (Figure 22b) the disulfide bonds introduced by the cross-linker in the case of the conjugates and the disulfide bonds of the antibodies were cleaved and the antibody heavy chains were separated from the antibody light chains and saporin. The bands that have approximately 25 kDa and are observed in case of Trastuzumab and Cetuximab represent the light chain of the respective monoclonal antibodies. Considering the information provided by the controls, it is concluded that the bands that have approximately 25 kDa and are observed for ST and SC correspond to both light chains of monoclonal antibodies and saporin. In addition, the

bands that have approximately 50 kDa are the antibody heavy chains from both antibodies and immunotoxins.
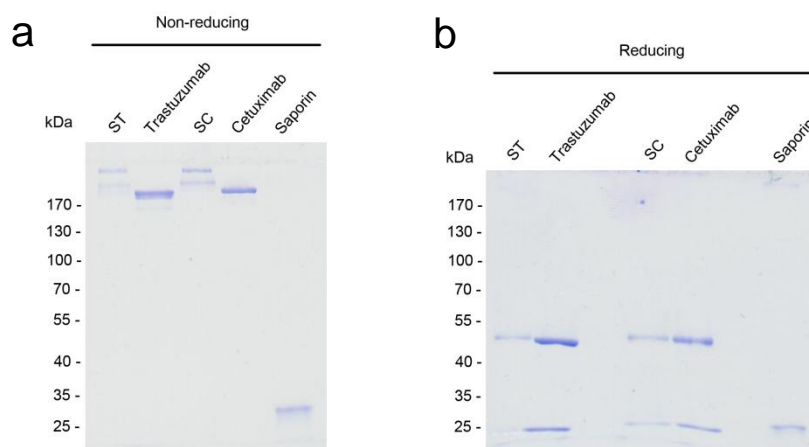


**Figure 22.** SDS-PAGE analysis of ST, Trastuzumab, SC, Cetuximab and saporin. Electrophoresis was performed (**a**) under non-reducing conditions and (**b**) under reducing conditions.

### 3.5.2. *N*-glycosidase activity of immunotoxins

*N*-glycosidase activity of ST and SC was measured and compared to that of unconjugated saporin to investigate whether there was an influence of the chemical conjugation process to the enzymatic activity of the toxin moiety (Table 8). *N*-glycosidase activity of saporin was evaluated as a positive control while Trastuzumab, Cetuximab and bovine serum albumin (BSA) were included in the experiment as negative controls.

**Table 8.** *N*-glycosidase activity of ST and SC. *N*-glycosidase activity of immunotoxins was measured by the cleavage of adenine residues from herring sperm DNA. *N*-glycosidase activity of saporin (positive control) and Trastuzumab, Cetuximab and BSA (negative controls) was determined as well for comparison. Each value represents the mean ± SD, $n = 3$.

| Protein | Adenine release [pmol adenine/pmol toxin/h] | Adenine release [%] |
|---|---|---|
| Saporin | 94.3 ± 1.1 | 100.0 ± 1.2 |
| ST | 59.4 ± 0.6 | 63.0 ± 0.6 |
| Trastuzumab | 4.1 ± 0.3 | 4.3 ± 0.4 |
| SC | 62.1 ± 1.2 | 65.8 ± 1.2 |
| Cetuximab | 0.6 ± 3.3 | 0.6 ± 3.5 |
| BSA | 1.5 ± 0.6 | 1.6 ± 0.6 |

Release of adenine after incubation of herring sperm DNA with ST and SC was of 59.4 and 62.1 pmol adenine/pmol toxin/h, respectively. Since the adenine release of saporin was evaluated as 94.3 pmol adenine/pmol toxin/h, *N*-glycosidase activity was reduced to 63.0% in the case of ST and to 65.8% in the case of SC. Although the *N*-glycosidase activity of the toxin moiety was reduced after the chemical conjugation, most importantly immunotoxins presented enzymatic activity and were therefore suitable for further studies. No adenine release was observed in the case of the negative controls.

### 3.5.3.   Binding of immunotoxins to cellular receptors

To determine the binding of ST and SC to their respective receptors by surface plasmon resonance spectroscopy, immunotoxins were immobilized on the carboxymethylated surface of a gold sensor chip and soluble truncated variants of either epidermal growth factor receptor 2 (HER2) (Figure 23a) or epidermal growth factor receptor (EGFR) (Figure 23b) were injected. During the association phase, HER2 (4 µg/ml) showed binding to the immunotoxin with a response difference (RD) of 48.9. During the dissociation phase, HER2 remained strongly bound to ST and only a minimal amount of receptor was dissociated from the immunotoxins. At the end of the dissociation phase an RD of 45.8 was measured, which was similar to the value at the end of the association phase. The binding profile of HER2 to ST was similar at the two other concentrations tested. At 1 and 2 µg/ml, HER2 bound strongly to the immobilized ST with an RD of 26.0 and 45.0 at the end of the association phase and an RD of 9.7 and 29.7 at the end of the dissociation phase, respectively.

Soluble EGFR bound to SC during the association phase at a concentration of 5.2 µg/ml (RD of 95.9 at the end of association). Most of the EGFR remained bound to SC during the dissociation phase (RD of 78.1 at the end of dissociation) indicating a very strong interaction between the receptor and the immunotoxins. A very similar pattern was observed at lower concentrations of EGFR (1.3 and 2.6 µg/ml). An RD of 62.9 was measured at a concentration of 1.3 µg/ml while an RD of 75.7 was determined at a concentration of 2.6 µg/ml at the end of the association phase. Almost all EGFR was still bound to the immunotoxin (RD = 49.2 at 1.3 µg/ml and RD = 57.1 at 2.6 µg/ml) at the end of the dissociation phase.
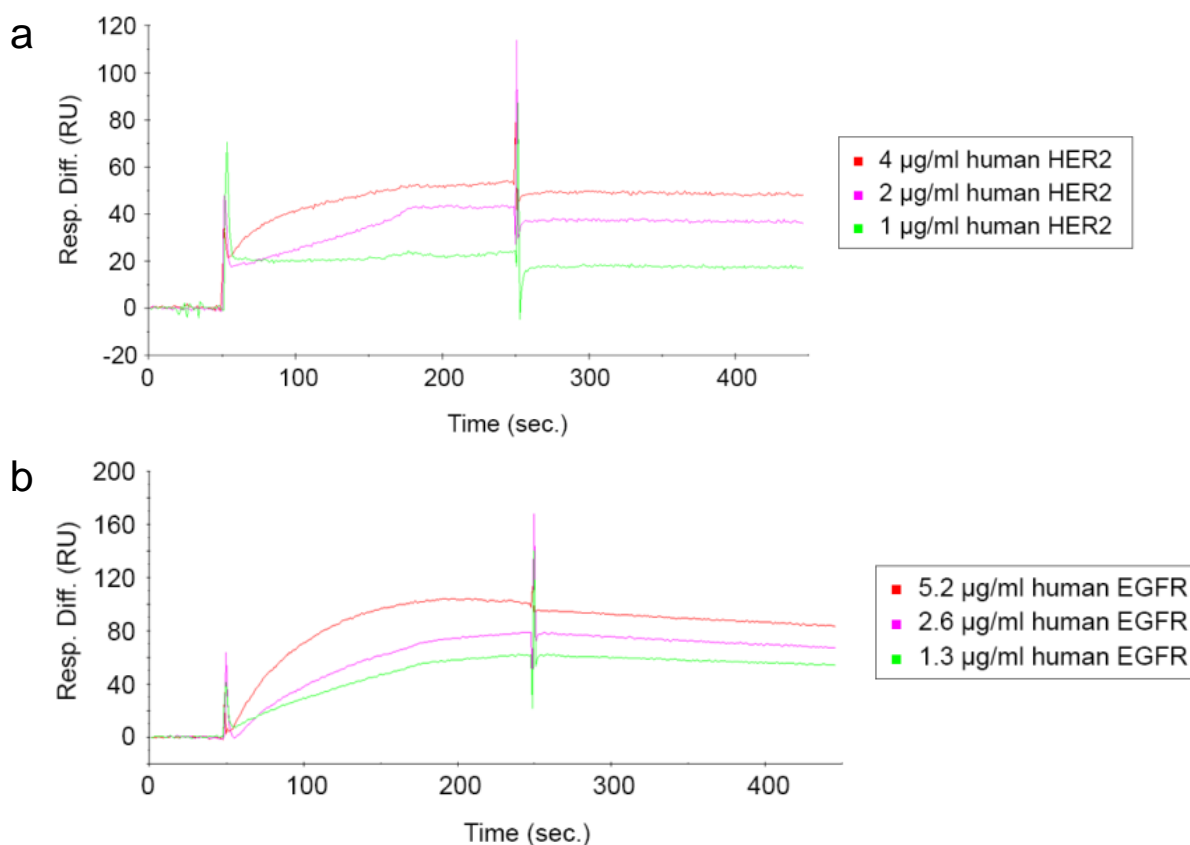
**Figure 23.** Binding of immunotoxins to soluble receptors by surface plasmon resonance spectroscopy. **(a)** ST was immobilized on a carboxymethylated C1 sensor chip and soluble human recombinant HER2 was injected at three different concentrations (1, 2 and 4 µg/ml) at a flow rate of 30 µl/min. **(b)** SC was immobilized on the same type of sensor chip and soluble human recombinant EGFR was injected at 1.3, 2.6 and 5.2 µg/ml. Both association and dissociation phases lasted for 200 s.

The objective of this experiment was to observe a specific concentration-dependent binding of the soluble receptors HER2 and EGFR to the corresponding immunotoxins. For this reason, the binding of the soluble receptors was evaluated at only three concentrations. Nevertheless, to get a hint of the binding affinities, $K_D$ values were calculated by a non-linear regression (one site – specific binding, binding – saturation) to 19.1 nM for HER2 and to 13.4 nM for EGFR. Interestingly, similar $K_D$ values for the binding of soluble HER2 to Trastuzumab (9.4 nM [182]) and of soluble EGFR to Cetuximab (5.2 nM [183]) are reported in the literature, indicating that the $K_D$ values calculated for ST and SC are in the same range that those for Trastuzumab and Cetuximab.

### 3.5.4. Real-time monitoring of the cytotoxicity of ST and SC

In order to investigate in real time the synergistic cytotoxicity enhancement of ST and SC by triterpenoidal saponins, cells were treated with the immunotoxins + SO1861 (Figure 24). Firstly,

cytotoxicity of ST in the presence of SO1861 was evaluated in BT-474 cells (Figure 24a). BT-474 cells grew quickly within the first 3 h but during the next 15 h the cell growth only increased slightly until the normalization time. Then, in the case of untreated control cells, only fresh medium was added and the NCI increased progressively until a value of 8.81 at the end of the experiment. In the case of cells treated with 2.5 µg/ml (1.34 µM) SO1861, only slight cytotoxicity was caused and an NCI of 7.47 was reached at the end of the experiment. ST was non-toxic at a concentration of 100 nM. However, a tremendous cytotoxicity enhancement was observed when ST was applied in combination with SO1861. ST + SO1861 resulted in a complete cell death at all the concentrations tested (0.1 to 100 nM).
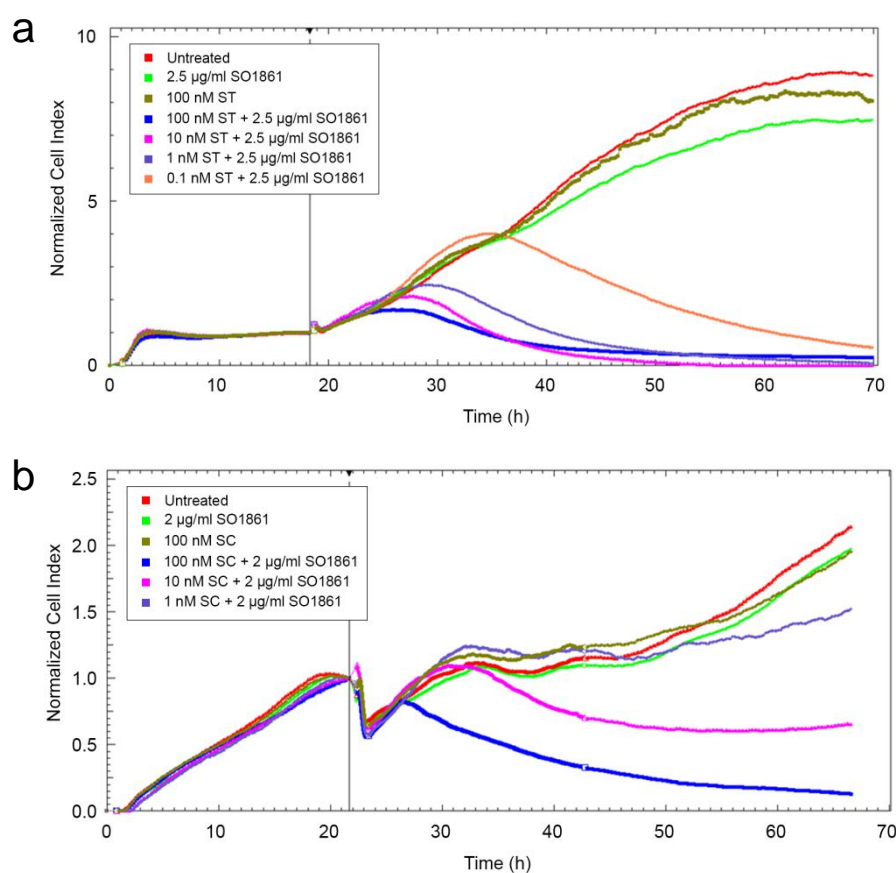


**Figure 24.** Real-time monitoring of the cytotoxicity of ST and SC in combination with SO1861. **(a)** BT-474 cells (10,000 cells/well) were treated with ST in a concentration range from 0.1 to 100 nM ± SO1861 (2.5 µg/ml) for 52 h. **(b)** SC was applied to TSA-EGFR cells (5,000 cells/well) in a concentration range from 1 to 100 nM ± SO1861 (2 µg/ml) for 45 h. Cell viability was monitored by an impedance-based real-time cytotoxicity assay and cell indexes were normalized at the time of addition of compounds. Curves show the mean, $n = 2$–8.

Secondly, cytotoxicity of SC in combination with SO1861 was investigated in TSA-EGFR cells (Figure 24b). TSA-EGFR cells grew linearly up to the normalization time. After addition of the compounds, the NCI of untreated control cells (only medium was added) progressively increased until a value of 2.14 at the end of the experiment. In the case of cells treated with 2 µg/ml (1.07

µM) SO1861, the growth curve behave in a similar way to the untreated control and an NCI of 1.97 was achieved at the end of the experiment. While SC was non-toxic at a concentration of 100 nM, a drastic cytotoxicity enhancement was observed when SC was applied in combination with SO1861. SC in the presence of SO1861 caused a total cell death at 100 nM. Cytotoxicity augmentation in combination with SO1861 was also observed at 10 nM (NCI = 0.66 at 66.5 h) and in a minor degree at 1 nM (NCI = 1.52 at 66.5 h).

In this experiment, cytotoxicity was used as the read-out to measure the relative amount of immunotoxin that was able to escape from the endo/lysosomal vesicles to the cytosol. In this way, the higher is the cytotoxicity, the higher is the amount of immunotoxin that crossed the endo/lysosomal membrane. Since the cytotoxicity of ST and SC drastically augmented in the presence of SO1861, the basis for a platform technology for enhanced endo/lysosomal escape of immunotoxins by triterpenoidal saponins was considered to be established for the first time.

### 3.5.5. Competitive binding between immunotoxins and free antibodies

Cells were treated with an excess of unconjugated antibodies to study their competitive effect on the binding of the immunotoxins to the respective cellular receptors and consequently to determine if immunotoxins are target-specifically internalized (Figure 25). Cells reached a plateau phase from 8 to 13.5 h, but as observed in the untreated control, after addition of fresh medium, cells started to grow again until reaching another stable phase which would be maintained with slightly loss of signal until the end of the experiment (NCI = 1.60). The impedance of the cells treated with 2.5 µg/ml (1.34 µM) SO1861 alone increased only slightly more than untreated cells and then gradually decreased to a similar impedance value to the untreated control (NCI = 1.51).

The NCI of cells treated with ST at 1 nM in combination with SO1861 (Figure 25a) increased tremendously to a maximum value of 4.01 after 23.5 h but then continuously decreased to very low values, representing almost a total cell death at the end of the experiment. The appearance of a peak directly after treatment can be attributed to cell swelling (probably indicating an initiation of the apoptotic process), which results in an increased impedance due to the larger area covered by the swollen cells. Repeating the same conditions (ST at 1 nM and SO1861 at 2.5 µg/ml) but with the addition of Trastuzumab in excess (1,000 nM), cells grew similarly to the untreated control and remained unaffected by the immunotoxin indicating target-specific competition.

Cells were also incubated in the presence of SC (0.001 nM) and SO1861 (Figure 25b). NCI increased to a maximum value of 3.54 at 24.5 h but decreased again rapidly to an NCI value of 0.95 (at 44.5 h). Cell viability further continuously decreased and at the end of the experiment almost all the cells were dead. However, cells treated with SC and SO1861 in the same concentrations as before but with the addition of Cetuximab in excess (1,000 nM) proliferated in a totally different way. The curve increased to an NCI of 3.04 at 34.0 h and decreased to impedance values similar to those of untreated cells at the end of the experiment (NCI = 1.29), confirming that the presence of the unconjugated Cetuximab also blocked the toxicity of SC.
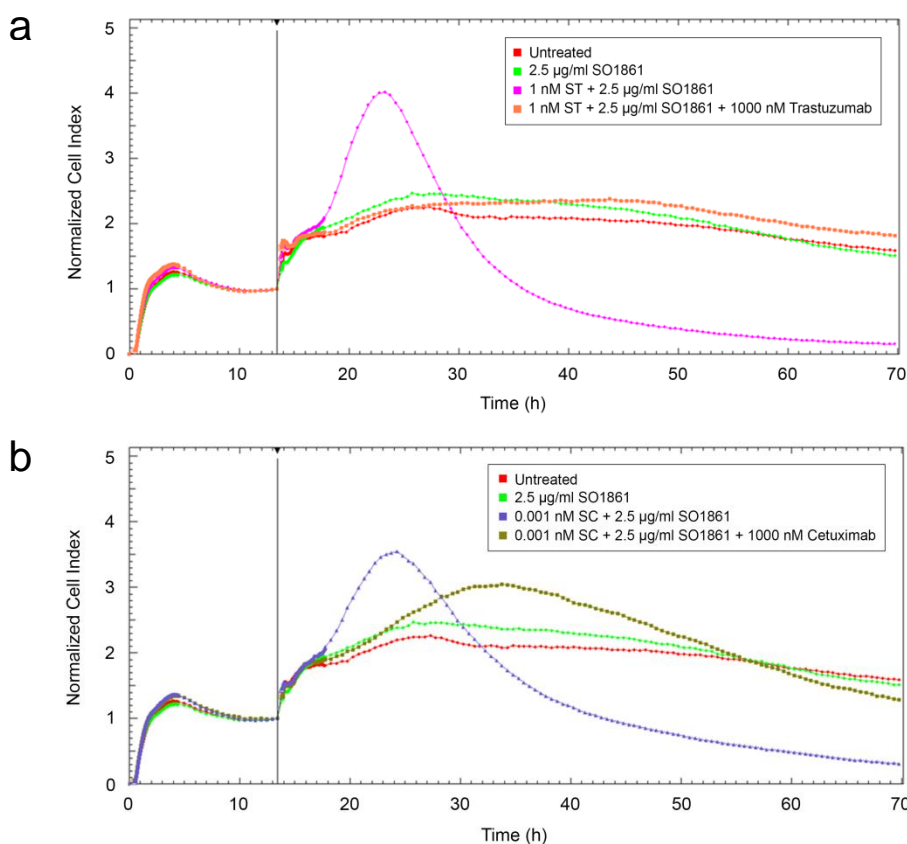


**Figure 25.** Competitive assay between immunotoxins and antibodies in excess. BT-474 cells (10,000 cells/well) were seeded and allowed to grow until the compounds were added at 13.5 h. **(a)** Cells were incubated with 1 nM ST and SO1861 (2.5 µg/ml) ± unconjugated Trastuzumab (1,000 nM) for 57 h. **(b)** SC was tested at a concentration of 0.001 nM in combination with SO1861 ± unconjugated Cetuximab (1,000 nM) also for 57 h. Cell viability was measured in real time by an impedance-based cytotoxicity assay and cell index normalization was performed at the time of addition of compounds. Curves are the mean, *n* = 2. The curves representing untreated control cells and cells treated with SO1861 alone are equally depicted in both panels for clarity.

### 3.5.6. Antibody-dependent cell-mediated cytotoxicity of immunotoxins

Cells were treated with unconjugated antibodies and immunotoxins in the presence of natural killer (NK) cells isolated from the blood of two human male donors in order to analyze the antibody-dependent cell-mediated cytotoxicity (ADCC) (Figure 26a and b). BT-474 cells grew quickly within the first 2 h but during the next 21 h the cell growth only increased up to an NCI of 1.00 at the normalization time (23 h). Thereafter, in the case of untreated control cells, only fresh medium was pipetted and the NCI increased almost linearly until a value of 7.38 at the end of the experiment.
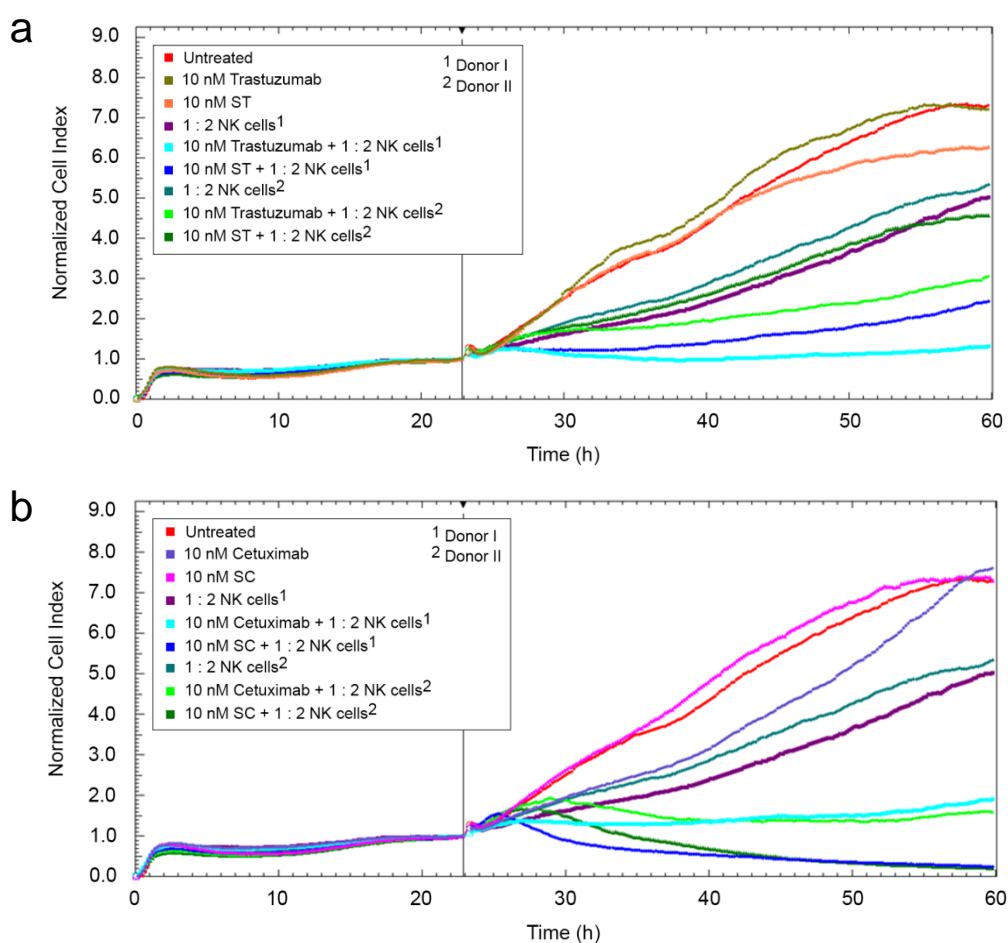


**Figure 26.** ADCC of immunotoxins. BT-474 cells (5,000 cells/well) were seeded and allowed to grow until the different compounds were added at 23.0 h. **(a)** To investigate ADCC, BT-474 cells were incubated with Trastuzumab and ST ± 1:2 NK cells (ratio between BT-474 and NK cells) from donor I and II. **(b)** BT-474 cells were treated in addition with Cetuximab and SC ± 1:2 NK cells from both donors. All unconjugated antibodies and immunotoxins were administered at a concentration of 10 nM. Cell viability was determined by an impedance-based real-time cytotoxicity assay and cell indexes were normalized when compounds were added. Curves represent the mean, $n = 1–3$. For better comparison, some samples are equally drawn in more than one panel.

Trastuzumab was non-toxic at a concentration of 10 nM while ST was slightly toxic at the same concentration (NCI = 6.3) (Figure 26a). In the case of NK cells from donor I, the sole addition of

NK cells already caused an effect on BT-474 cells as the cell viability diminished (NCI = 5.06). However, this effect was much more pronounced when NK cells were administered in the presence of Trastuzumab (NCI = 1.33) and ST (NCI = 2.45). In the case of NK cells from donor II, the addition of NK cells also caused an effect on BT-474 cells and the cell viability was reduced to an NCI of 5.37. This effect was again much more pronounced when the NK cells were given in combination with Trastuzumab (NCI = 3.07) and ST (NCI = 4.62).

Cetuximab and SC were also tested at 10 nM and both compounds were non-toxic to cells as the cell viability at the end of the experiment was similar to the untreated control. In the case of NK cells from donor I, cell-mediated cytotoxicity was observed when BT-474 cells were incubated with Cetuximab (NCI = 1.92) and SC (NCI = 0.25) (Figure 26b). In the case of NK cells from donor II, this phenomenon was also observed (NCI = 1.59 for Cetuximab and NCI = 0.21 for SC). The ability to trigger ADCC was confirmed in the case of unconjugated antibodies but most importantly in the case of both ST and SC immunotoxins.

### 3.5.7.    Synergism between immunotoxins and SO1861

The experiment described in the previous section (3.5.6) was continued by addition of 2.5 µg/ml (1.34 µM) SO1861 to monitor the synergistic effect between the immunotoxins and the triterpenoidal saponin (Figure 27). Curves were normalized again at 70.5 h. The impedance signal of the untreated control cells slowly decreased until the end of the experiment (NCI = 0.80). SO1861 was applied at a non-cytotoxic concentration (NCI = 0.87).

The addition of SO1861 caused the death of all BT-474 cells, which were treated with ST or SC (10 nM) in the absence of NK cells. In contrast, no effect was observed in the cells treated with unconjugated Trastuzumab or Cetuximab, indicating that the presence of saporin was necessary to elicit cell death in the presence of saponins. The addition of SO1861 also resulted in cell death of all the remaining BT-474 cells previously treated with NK cells from donor I and either ST (Figure 27a) or SC (Figure 27b). Similarly, the addition of SO1861 resulted in cell death of almost all BT-474 cells previously treated with NK cells from donor II and ST (Figure 27a) and the curve of cells remaining after SC-dependent ADCC (NK cells from donor II) finally accomplished death of all cells after the addition of SO1861 (Figure 27b).
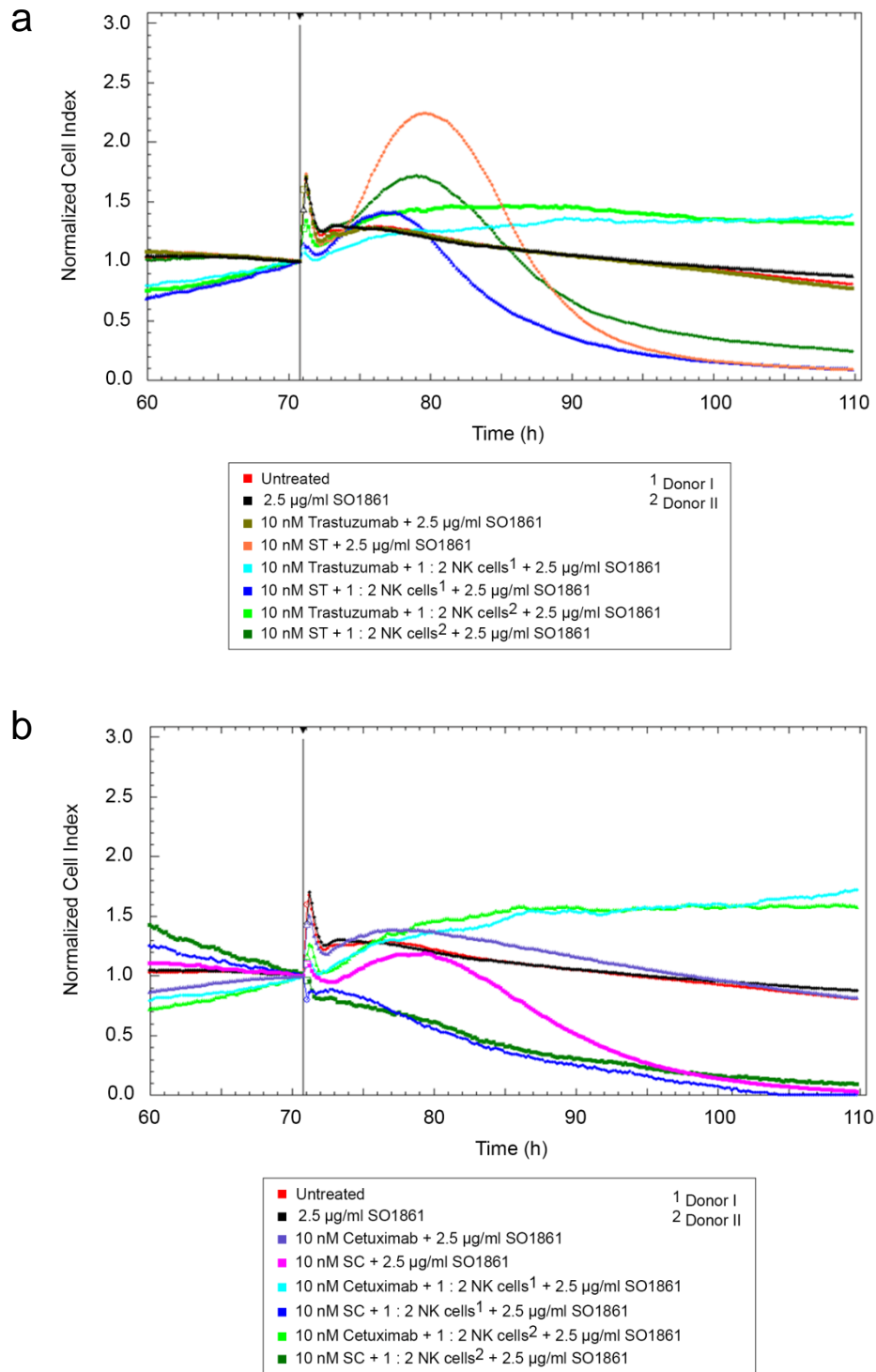
**Figure 27.** Synergistic augmentation of the cytotoxicity of immunotoxins by SO1861. The experiment of section 3.5.6 (see Figure 26) was continued by addition of SO1861 (2.5 µg/ml) to all previously treated cells at 71 h. **(a)** SO1861 was added to BT-474 cells previously incubated with Trastuzumab and ST ± 1:2 NK cells from donor I and II. **(b)** In the same way, SO1861 was added to BT-474 cells previously treated with Cetuximab and SC ± 1:2 NK cells from both donors. All unconjugated antibodies and immunotoxins were administered at a concentration of 10 nM. Cell indexes were normalized again after addition of SO1861. Curves represent the mean, $n = 1–3$. For better comparison, some samples are equally drawn in more than one panel.

Furthermore, these results indicated that the immunotoxins and triterpenoidal saponins can be separately administered to cells. Cells were initially treated with only immunotoxins and no synergistic enhancement of the cytotoxicity was observed. However, 47.5 h after addition of the immunotoxins, SO1861 was added to cells and at that moment cytotoxicity of immunotoxins was tremendously enhanced.

### 3.5.8. Short term stability of ST and SC

Short term stability is a relevant requisite to properly explain the results of the previous experiments. Especially in the case of ADCC mediated by immunotoxins (see section 3.5.6), a combined effect of cell-mediated and toxin-mediated cytotoxicity can only take place when no short term degradation of the cross-linkage between saporin and the monoclonal antibodies occurs in the extracellular medium. If degradation of immunotoxins would happen, then cell-mediated cytotoxicity would be triggered actually by the unconjugated antibodies but not by immunotoxins.

The samples were incubated at 37 °C for 6 and 24 h and thereafter the two bands corresponding to ST and the two bands corresponding to SC were clearly detected (Figure 28), similarly to the results observed in the SDS-PAGE of ST and SC in Figure 22a. Most interestingly, no degradation products were observed as indicated by the absence of a band for free saporin. On the other hand, saporin that served as a positive control was detected at the expected position.
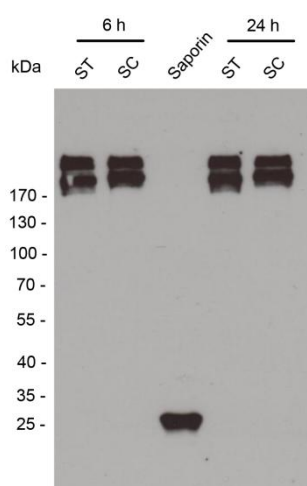


**Figure 28.** Determination of the short term stability of immunotoxins by Western blot. ST and SC were incubated at 37 °C for 6 and 24 h with conditioned medium [Roswell Park Memorial Institute (RPMI)-1640 medium supplemented with 10% fetal bovine serum (FBS) and 1% Penicillin/Streptomycin (PS), which was consumed for one week by BT-474 cells at 37 °C and 5% $CO_2$ and centrifuged at 800$g$ for 5 min before addition to proteins] to determine the stability of the conjugates under these conditions. Note that no degradation products of the conjugates were detected with a primary polyclonal antibody against saporin. Unconjugated saporin was used as positive control.

The observation that ST and SC were totally stable in a short term and were not susceptible to degradation in the extracellular milieu further promotes the development of a platform technology for the enhanced endo/lysosomal escape of immunotoxins. In this platform, immunotoxins differing in their ligand specifically bind to target receptors, interact with the innate immune system, exhibit cell-killing activity, and most importantly, their endo/lysosomal escape and cytotoxicity is dramatically enhanced by triterpenoidal saponins. Further experiments by confocal microscopy were conducted to corroborate these findings.

### 3.5.9. Internalization and colocalization of immunotoxins

To study the specificity of the internalization of immunotoxins by fluorescence microscopy, cells were treated with saporin-Trastuzumab-Alexa Fluor 488 ($^{Alexa}$ST) in the absence and presence of an excess of Trastuzumab. The internalization of $^{Alexa}$ST was visualized 24 h after addition of the immunotoxins to the cells (Figure 29a). The cellular morphology was still intact indicating that the labeled immunotoxin was not toxic at the administered concentration. $^{Alexa}$ST accumulated mostly in organelles surrounding the cell nucleus. However, when cells were competitively treated with $^{Alexa}$ST and an excess of Trastuzumab, the amount of internalized immunotoxin decreased dramatically (Figure 29b), thus pointing to a specific receptor-dependent internalization of ST.

In order to identify the organelles, in which the accumulation of the immunotoxins took place after internalization, colocalization with red dextran was investigated (Figure 29c). The labeled immunotoxin accumulated in the vesicles that surround the nucleus and colocalized with red dextran demonstrating that ST accumulated in acidic vesicles such as late endosomes and lysosomes.

### 3.5.10. Endo/lysosomal escape of immunotoxins

Further cells were treated with $^{Alexa}$ST for 24 h to visualize the endo/lysosomal escape of the immunotoxin by live cell imaging (Figure 30). After the incubation time, $^{Alexa}$ST accumulated, as expected from the previous experiments, again mainly in acidic organelles surrounding the nucleus and no endo/lysosomal release was observed.

Interestingly, a small amount of protein remained bound to the receptors in the cell membrane (Figure 30, see red arrows in the merged picture). During the first 140 s of the experiment, no release of $^{Alexa}$ST from the vesicles was observed. At that moment, SO1861 was added at a non-toxic concentration of 2.5 µg/ml (1.34 µM) and 300 s later the first indications of the endo/lysosomal escape appeared (Figure 30, see red arrows in the pictures with the green fluorescence channel). After the formation of a bubble in the cellular vesicle, toxin diffused to the cytosol. Endo/lysosomal escape of $^{Alexa}$ST was observed in three time intervals (440–460 s, 520–560 s, 640–700 s). In these three cases, a perturbation in the vesicle membrane was formed leading to the release of saporin to the cytosol.
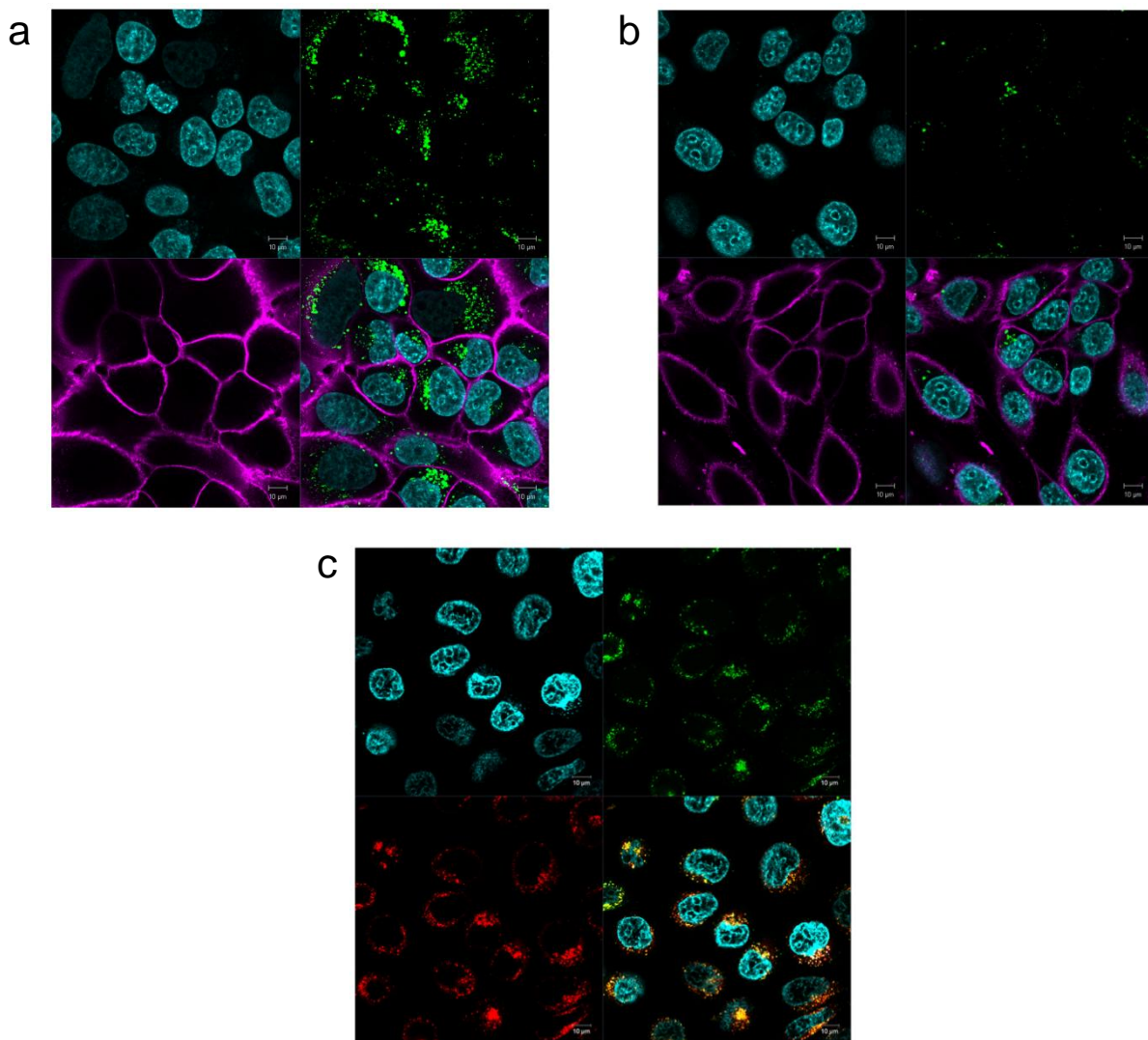


**Figure 29.** Internalization and colocalization studies of immunotoxins. **(a)** BT-474 cells were visualized by live cell imaging (confocal fluorescence microscopy) 24 h after addition of $^{Alexa}$ST. The cell nucleus is visualized in cyan fluorescence (upper left quarter), the cell membrane in magenta (lower left quarter) and immunotoxins in green (upper right quarter). The lower right quarter shows the merger. **(b)** Cells were treated for 24 h with $^{Alexa}$ST and an excess of Trastuzumab. **(c)** Cells were coincubated with red dextran, which accumulates in acidic vesicles. Cells were observed with the LSM780 laser scanning microscope equipped with a Plan-Apochromat 63×/1.40 oil objective.
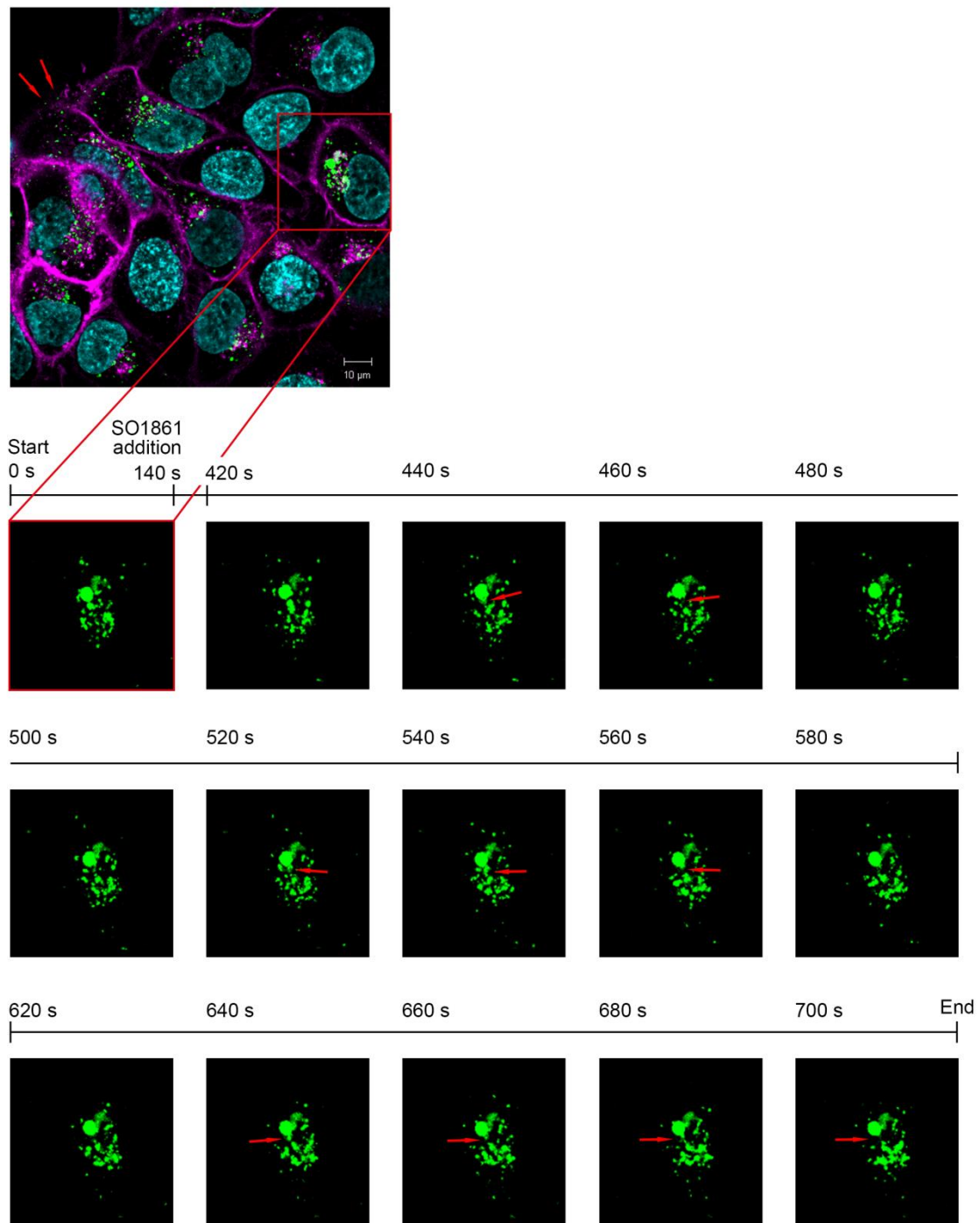
**Figure 30.** Visualization of endo/lysosomal escape of immunotoxins by live cell imaging (confocal fluorescence microscopy). After the incubation of BT-474 cells with $^{Alexa}$ST for 24 h, most of the immunotoxin accumulated in acidic organelles surrounding the nucleus although a minor amount remained bound to the receptors in the cell membrane (red arrows in the merged picture). No endo/lysosomal escape was observed at the beginning of the experiment. However, after addition of 2.5 µg/ml SO1861, release of toxin was detected in three time intervals (440–460 s, 520–560 s, 640–700 s; red arrows in pictures with green fluorescence channel). In this experiment, confocal fluorescence microscopy was performed with the LSM780 laser scanning microscope equipped with a Plan-Apochromat 63×/1.40 oil objective.

## 3.6. Ligand specificity in the enhancement of immunotoxins by triterpenoidal saponins

### 3.6.1. Optimization of cell number for XTT assay

Before the cytotoxicity of saporin-Rituximab (SR), saporin-anti-CD22 and saporin-anti-CD25 was evaluated, the initial cell number for the 2,3-bis-(2-methoxy-4-nitro-5-sulfophenyl)-$2H$-tetrazolium-5-carboxanilide (XTT) assay had to be optimized. The optimal initial number of Ramos cells in the proliferation assay was determined by measuring the viability of different initial amounts of cells (Figure 31). In this case, cell viability cannot be measured by the MTT assay since this method is only appropriate for adherent cells but Ramos cells are cells in suspension.
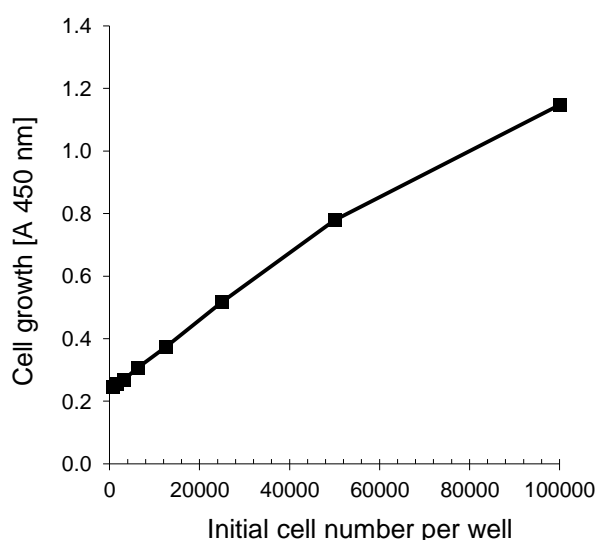


**Figure 31.** Optimization of the initial cell number in a proliferation assay (XTT assay). Ramos cells were initially seeded in different amounts in a 96-well plate and cell viability was directly analyzed by an XTT assay. Data represents the mean ± SD, $n = 3$. Error bars cannot be seen due to their small size.

In the case of Ramos cells, a directly proportional increase of the initial cell number per well and absorbance ($A_{450\ nm}$) was observed from 800 to 50,000 cells. A saturation of the absorbance signal was observed at initial cell numbers higher than 50,000. Consequently, the initial cell number of 20,000 Ramos cells/well was selected as optimal for the evaluation of the cytotoxicity of immunotoxins in further proliferation assays (XTT assay).

### 3.6.2. Cytotoxicity of SR and other immunotoxins in combination with SO1861

In order to investigate the ligand specificity and to validate the intended platform technology for the enhanced endo/lysosomal escape of targeted toxins, the cytotoxicity of SR, saporin-anti-CD22 and saporin-anti-CD25 and of their combinations with SO1861 was studied on Ramos cells (Figure 32). Saporin-anti-CD22 and saporin-anti-CD25 are two commercially available immunotoxins.

The cytotoxicity of SA1641, SA1657 and SO1861 was firstly evaluated in Ramos cells as a control to find the highest non-cytotoxic concentration of the triterpenoidal saponins. In the case of SA1641 (Figure 32a) and SA1657 (Figure 32b), the saponins were non-toxic at all the concentrations tested. Therefore, it was not possible to calculate $GI_{50}$ values on Ramos cells for both triterpenoidal saponins ($GI_{50} > 2$ µg/ml). In the case of SO1861 (Figure 32c), the saponin was slightly toxic at the concentration range of 0.13–1.00 µg/ml. However, SO1861 presented major toxicity at the highest concentration tested (2.00 µg/ml) and cell viability was reduced to a 43%. The $GI_{50}$ value for SO1861 in Ramos cells was calculated to 1.73 µg/ml. Based on these observations, the concentration of 1 µg/ml (0.54 µM) SO1861 was used in the following proliferation assays.

Subsequently, cytotoxicity of immunotoxins was evaluated in combination with triterpenoidal saponins. In the case of SR (Figure 32d), the highest concentration tested reduced cell viability to a 54%. To get a hint of the $GI_{50}$, the last two values of the curve were linearly extrapolated, since the four parameter logistic non-linear regression model was not possible due to the lack of cytotoxicity evaluation at high concentrations and the limited amount of immunotoxins. In this way, $GI_{50}$ value of SR was linearly extrapolated to 10.97 nM. However, SR + 1 µg/ml (0.54 µM) SO1861 resulted in a $GI_{50}$ of 0.075 nM, representing an enhancement factor of 150-fold. In the case of saporin-anti-CD22 (Figure 32e), the highest concentration tested reduced cell viability to a 42% and $GI_{50}$ was calculated to 0.14 nM. Although saporin-anti-CD22 + SO1861 achieved potentiated cytotoxicity ($GI_{50}$ of 0.0073 nM), the phenomenon was not as prominent as before and an enhancement factor of 19-fold was observed. Finally, in the case of saporin-anti-CD25 (Figure 32f), a 32% inhibition of cell growth (68% viability) was observed at the highest concentration tested and therefore it was not possible to calculate the $GI_{50}$ (> 10 nM). However, in combination with SO1861, saporin-anti-CD25 exhibited tremendous augmentation of the cytotoxic effect, reducing the cytotoxicity to 53% viability even at the lowest concentration tested (0.00001 nM). The $GI_{50}$ value of saporin-anti-CD25 + SO1861 was 0.00038 nM and the enhancement factor was > 26,000-fold.
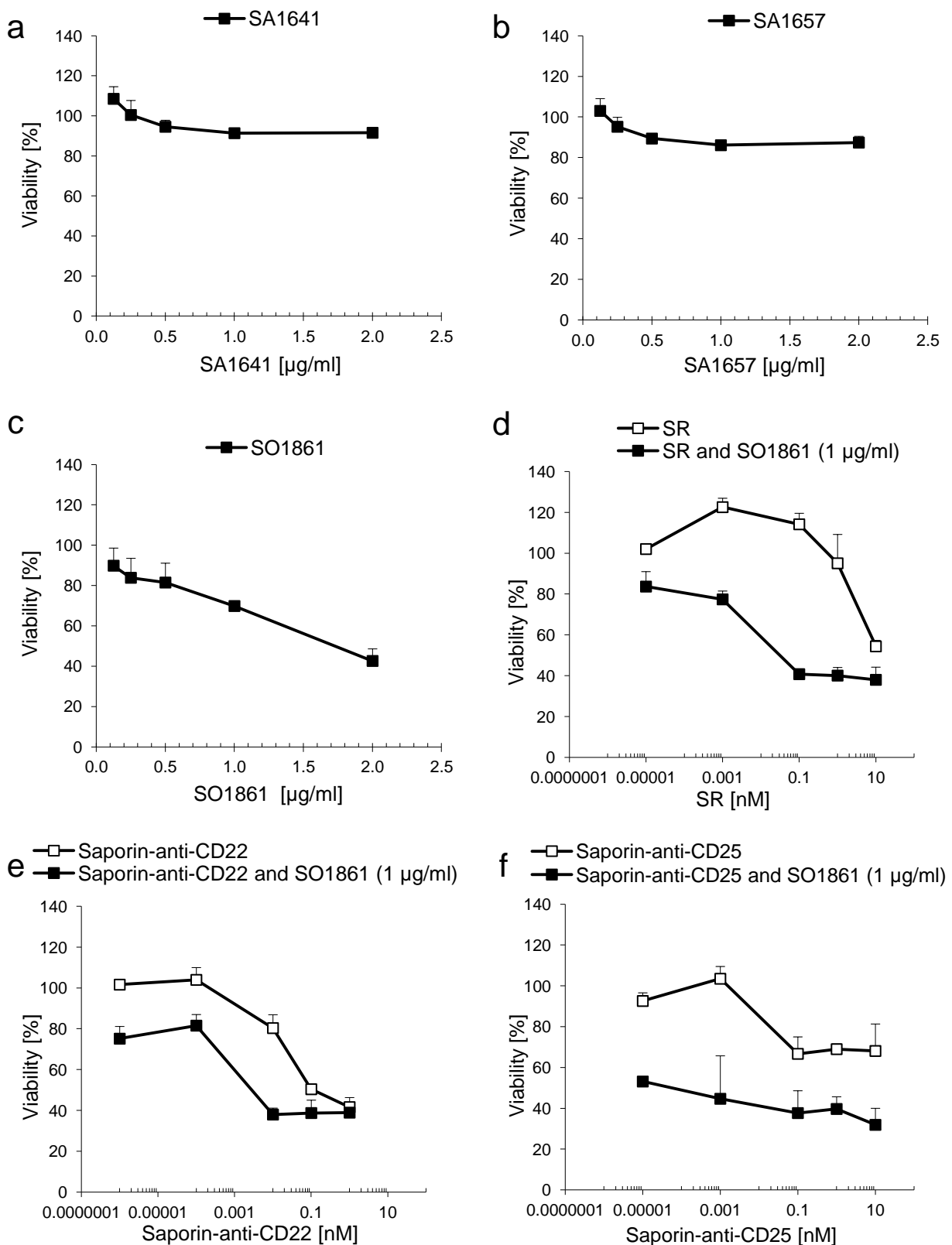
**Figure 32.** Cytotoxicity of SR, saporin-anti-CD22 and saporin-anti-CD25 in combination with SO1861. Ramos cells (20,000 cells/well) were treated with **(a)** SA1641, **(b)** SA1657 or **(c)** SO1861 at the concentrations from 0.13 to 2.00 µg/ml. Furthermore, Ramos cells were treated with **(d)** SR, **(e)** saporin-anti-CD22 or **(f)** saporin-anti-CD25 in a concentration range from 0.000001 to 10 nM ± SO1861 (1 µg/ml). After 72 h, cell viability was measured by an XTT assay and referred to untreated control cells. Each data point represents the mean ± SD, $n = 3$.

The synergistic augmentation of the cytotoxicity by triterpenoidal saponins was described for the two immunotoxins ST and SC in the previous sections 3.5.4 and 3.5.7. In this section, the cytotoxicity of three further immunotoxins (SR, saporin-anti-CD22 and saporin-anti-CD25) was demonstrated to be synergistically potentiated by triterpenoidal saponins. Since the cytotoxicity enhancement was now observed in five saporin-based immunotoxins, the technology for enhanced endo/lysosomal escape of immunotoxins by triterpenoidal saponins was validated to have a substantial potential to serve as a platform for intracellular drug delivery.

## 3.7. Expression of an enzymatically inactive mutant of saporin (saporin-KQ)

### 3.7.1. *N*-glycosidase activity of saporin-KQ

The establishment of an expression system for an enzymatically inactive variant of saporin (saporin-KQ) previously reported in the literature [168] was of great interest to expand the intended platform for enhanced targeted intracellular delivery of drugs in general. In such a platform, saporin-KQ will enhance the endo/lysosomal escape of its cargo but will not cause any associated cytotoxicity.

In order to check that saporin-KQ was enzymatically inactive, the *N*-glycosidase activity of saporin was compared to that of saporin-KQ. Saporin was used as a positive control and BSA as a negative control. In the case of saporin, the release of adenine after incubation with herring sperm DNA was 89.4 pmol adenine/pmol toxin/h. However, in the case of saporin-KQ, no adenine release was observed after incubation of the inactive mutant with the substrate. Furthermore, in the case of the negative control, no adenine release was observed as well. In brief, enzymatic inactivity of saporin-KQ was confirmed.

### 3.7.2. Cytotoxicity of saporin-KQ in combination with SO1861

Cytotoxicity of saporin and its combination with SO1861 was compared to the effect of saporin-KQ on ECV-304 cells (Figure 33) to check that the enzymatically inactive saporin was non-cytotoxic. Saporin presented notable cytotoxic effects at the highest concentration tested (1,000 nM) and reduced cell viability to 49% (Figure 33a). The $GI_{50}$ of saporin was calculated to 976 nM. Furthermore, saporin + 2 µg/ml (1.07 µM) SO1861 resulted in a strong enhancement of the cytotoxicity, achieving a decrease in cell viability to 62% even at the lowest concentration tested

(0.1 nM). The GI$_{50}$ of saporin in combination with SO1861 was 0.43 nM and the enhancement factor was 2,200-fold. Saporin-KQ behaved in a different way (Figure 33b). According to its mutation which turns saporin-KQ into an enzymatically inactive protein, saporin-KQ did not present any cytotoxicity up to 1,000 nM. Therefore, absence of cytotoxicity was confirmed in the case of saporin-KQ. Nevertheless, in the presence of SO1861, saporin-KQ caused inhibition of cell growth at the two highest concentrations tested (presumably due to known mechanisms unrelated to enzymatic activity such as inducing apoptosis through mitochondrial cascade [184]) and cell viability was reduced to 23% (100 nM) and 39% (1,000 nM).

In conclusion, the expression system for the variant of saporin lacking enzymatic activity and cytotoxicity (saporin-KQ) was successfully established. In the future, saporin-KQ may be used for the development of a platform system for enhanced endo/lysosomal escape of non-toxic protein therapeutics.
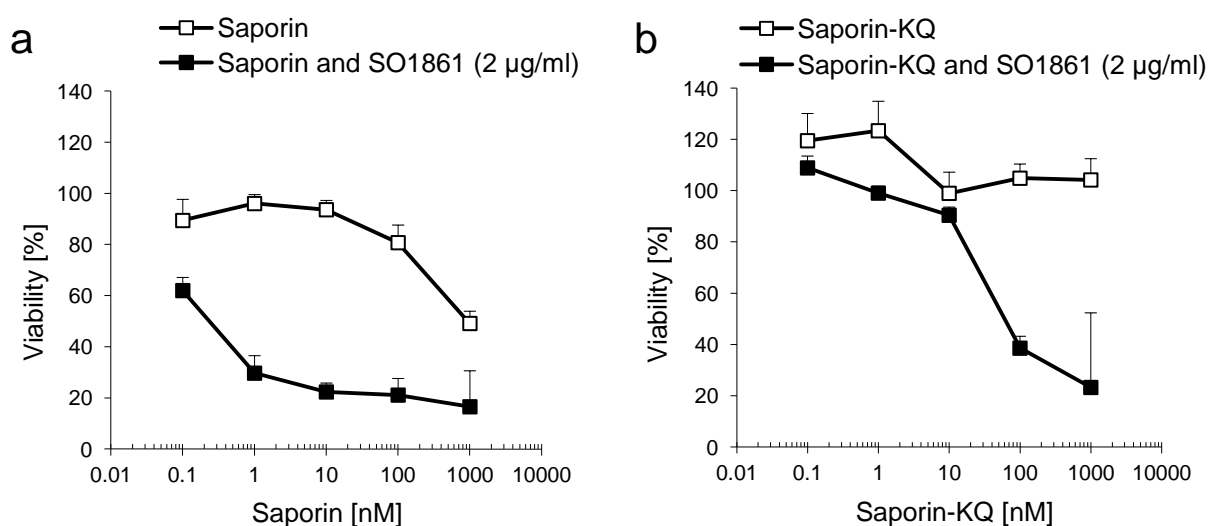


**Figure 33.** Comparison of the cytotoxicity of saporin and its enzymatically inactive mutant saporin-KQ. ECV-304 cells (4,000 cells/well) were treated with **(a)** saporin or **(b)** saporin-KQ in a concentration range from 0.1 to 1,000 nM ± SO1861 (2 µg/ml) for 48 h. Cell viability was determined by an MTT assay and referred to untreated control cells. Data represents the mean ± SD, $n = 4$.

## 3.8. Design of a reporter assay for the endo/lysosomal escape

### 3.8.1. Peroxidase activity of SH

Saporin-horseradish peroxidase (SH) was used to develop a reporter assay for the endo/lysosomal escape of toxins. The development of such a reporter assay will allow the investigation of the intracellular distribution of toxins in the presence of endo/lysosomal escape enhancers such as triterpenoidal saponins.

To determine if the peroxidase activity of HRP had been affected by the chemical conjugation process and to define the sensitivity of the conjugate, peroxidase activity of SH was measured at a series of concentrations ranging from 0.00001 to 100 nM (Figure 34). In the lower concentrations (0.00001 to 0.01 nM), the enzymatic activity of SH was not detectable. The first detectable signals in the presence of SH appeared with concentrations between 0.01 to 0.1 nM of the conjugate. Then, a linear correlation between the absorbance and concentration of the conjugate was observed in the range from 0.1 to 10 nM SH. Finally, for concentrations higher than 10 nM, a saturation of the absorbance signal was detected.
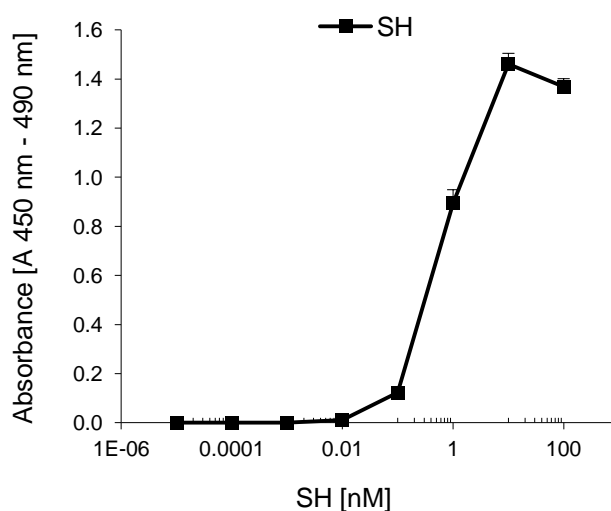


**Figure 34.** Peroxidase activity of SH. Peroxidase activity was evaluated at the concentrations from 0.00001 to 100 nM SH. The conjugate was added to a substrate solution of 0.4 mg/ml 3,3′,5,5′-tetramethylbenzidine (TMB), 0.2 µg/ml $H_2O_2$, 80 mM citric acid, pH 3.95 and the reaction was stopped after 15 min at room temperature by addition of 50 µl $H_2SO_4$ (3.3 M). Each data point is the mean ± SD, $n = 3$.

### 3.8.2. *N*-glycosidase activity of SH

The *N*-glycosidase activity of SH was compared to that of saporin to investigate if the enzymatic activity of the toxin moiety had been influenced by the chemical conjugation process. In this way, saporin was used as a positive control and HRP as a negative control. SH caused a release of adenine of 46.3 pmol adenine/pmol toxin/h after incubation with herring sperm DNA. Since the adenine release of saporin was calculated to 117.6 pmol adenine/pmol toxin/h, the *N*-glycosidase activity of SH was reduced to 39.3%. However, although the *N*-glycosidase activity of the toxin moiety was reduced after the chemical conjugation, SH still presented enzymatic activity and was therefore suitable for further studies. No adenine release was observed in the case of the negative control.

### 3.8.3. Cytotoxicity of SH in combination with SA1641

In order to discover if the endo/lysosomal escape of SH will be enhanced by triterpenoidal saponins in the same way as the unconjugated saporin (toxin without the cargo), cytotoxicity of SH and its combination with SA1641 was compared to the properties of saporin on ECV-304 cells (Figure 35). Similarly to the previous experiments, saporin showed cytotoxic effects and caused a reduction of the viability to 61% of at a concentration of 100 nM (Figure 35a). The $GI_{50}$ of saporin was linearly extrapolated to 146.75 nM (see dotted line in Figure 35a), as mentioned before in the case of SR (see section 3.6.2). In combination with 5 μg/ml (3.05 μM) SA1641, saporin cytotoxicity was drastically enhanced, causing a reduction of cell viability to 54% at a concentration of 0.1 nM. The $GI_{50}$ of saporin in combination with SA1641 was 0.20 nM and the enhancement factor was 750-fold.

In the case of SH (Figure 35b), no cytotoxicity was shown up to a concentration of 100 nM. However, in the presence of SA1641, SH exerted cytotoxicity at the two highest concentrations tested: cell viability was reduced to 51% at 10 nM and to 16% at 100 nM. The $GI_{50}$ of SH in combination with SA1641 was 13.28 nM and the enhancement factor was of at least 8-fold but presumably much higher. The estimated minimum $GI_{50}$ value of > 100 nM for the cytotoxicity of SH alone was used to perform this calculation. It is remarkable that the cytotoxicity enhancement also took place when saporin was chemically coupled to another protein, indicating that the endo/lysosomal escape enhancement of saporin mediated by triterpenoidal saponins can also occur when a cargo or a reporter (HRP) is attached to saporin.
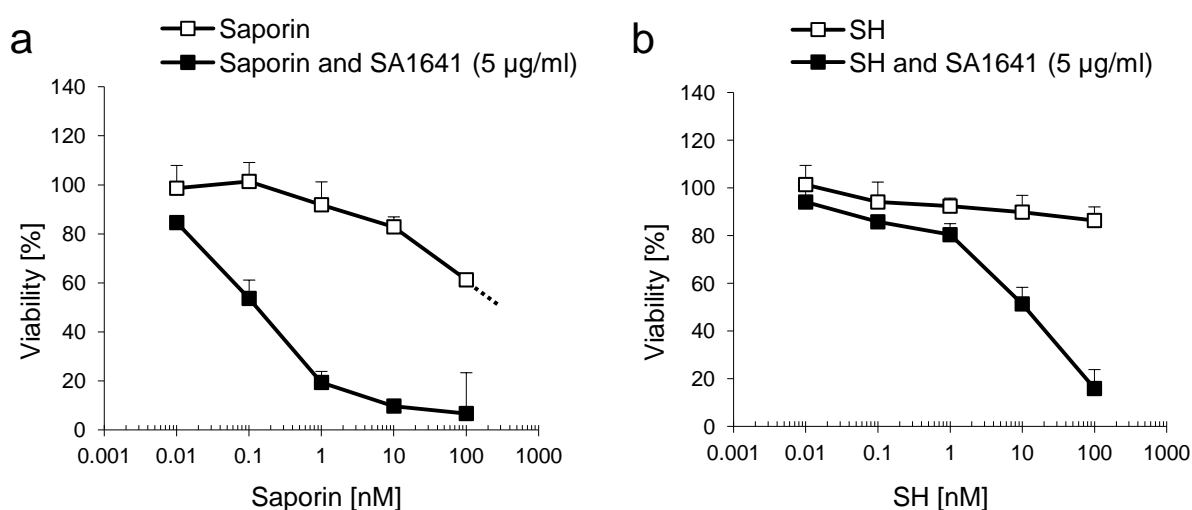


**Figure 35.** Comparison of the cytotoxicity of SH and saporin in combination with SA1641. ECV-304 cells were treated with **(a)** saporin or **(b)** SH in a concentration range from 0.01 to 100 nM ± SA1641 (5 μg/ml). Similarly to the phenomenon observed with saporin, the cytotoxicity of SH was enhanced in the presence of triterpenoidal saponins. Cell viability was measured by an MTT assay and referred to untreated control cells. The dotted line corresponds to a linear extrapolation to determine the $GI_{50}$ of saporin. Data represents the mean ± SD, $n = 4$.

### 3.8.4. Endo/lysosomal release of SH from isolated organelles

For the successful establishment of a reporter assay for the endo/lysosomal escape mediated by endo/lysosomal escape enhancers such as triterpenoidal saponins, it is required to detect differences between the toxin-reporter conjugate entrapped in the endo/lysosomal vesicles and the toxin-reporter conjugate efficiently delivered into the cytosol. For this purpose, endo/lysosomal release of SH in isolated organelles from cells previously treated with the conjugate (100 nM SH for 6 h) was evaluated in the presence of SA1641 by measuring the peroxidase activity of the released conjugate (Figure 36).

Firstly, as a control, short term permeabilizing effects of SA1641 on lysosomal membranes from isolated organelles (without the conjugate) were determined by the lysosomal enzyme β-*N*-acetylglucosaminidase (NAG) release assay to find the highest non-permeabilizing concentration of triterpenoidal saponins (Figure 36a). In the case of digitonin (positive control, highly lytic saponin), slight membrane permeabilizing effects on the lysosomal membrane were first observed at a concentration of 5 µM ($A_{405nm}$ = 0.090). Permeabilizing effects of digitonin progressively increased as concentrations of the saponin were augmented to 10 µM ($A_{405nm}$ = 0.135) and to 50 µM ($A_{405nm}$ = 0.275). Digitonin presented the highest permeabilizing effects within the three saponins tested. In the case of α-hederin (negative control, non-lytic saponin), no membrane permeabilizing effects were observed on the lysosomal membrane. Even at the highest concentration tested, only a very slight release of NAG was measured ($A_{405nm}$ = 0.080 at 50 µM). SA1641 had substantial membrane permeabilizing effects at a concentration of 50 µM ($A_{405nm}$ = 0.132). However, at lower concentrations, SA1641 did not present any permeabilizing effects on lysosomal membranes and the absorbance values were comparable to those of α-hederin.

Then, the endo/lysosomal escape of SH was evaluated alone or in the presence of triterpenoidal saponins in isolated organelles (pre-loaded with SH) (Figure 36b). Endo/lysosomal release of SH in isolated organelles was also investigated in the presence of digitonin (positive control) and α-hederin (negative control). In the case of a specific augmentation of the endo/lysosomal release of SH in the presence of SA1641, higher amounts of the conjugate are expected to be released at low concentrations of SA1641 (< 50 µM, see previous paragraph) that present no or only moderate membrane permeabilizing effects. In such a case, SH would be released from the lysosomes due to a specific interaction with SA1641 and not due to unspecific membrane permeabilizing effects.
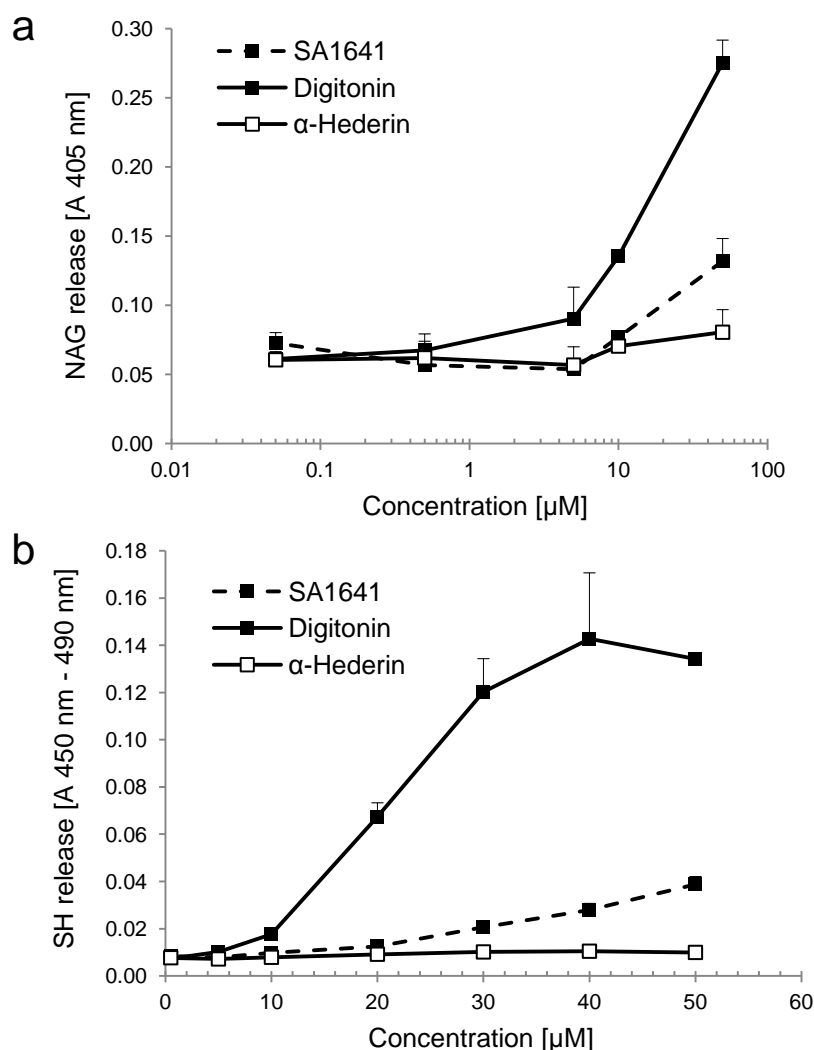
**Figure 36.** Endo/lysosomal release of SH from isolated cellular organelles pre-loaded with the conjugate. **(a)** Evaluation of SA1641 permeabilizing effects on lysosomal membranes from ECV-304 cells by a NAG assay. Lysosomes were isolated by cell homogenization and differential centrifugation. The crude lysosomal fraction was treated with SA1641, digitonin (positive control, highly lytic saponin) and α-hederin (negative control, non-lytic saponin) at 0.05, 0.5, 5, 10 and 50 μM at 37 °C for 1 h. **(b)** Release of SH from cellular vesicles pre-loaded with the conjugate. ECV-304 cells were treated with SH at the concentration of 100 nM for 6 h and subsequently lysosomes loaded with the conjugate were isolated as described before. The resulting crude lysosomal fraction was treated with SA1641, digitonin (positive control) and α-hederin (negative control) at 0.5, 5, 10, 20, 30, 40 and 50 μM at 37 °C for 1 h. After centrifugation, the endo/lysosomal escape of SH was determined by measuring the peroxidase activity of the released conjugate. The supernatant containing the released conjugate was added to a substrate solution of 0.4 mg/ml TMB, 0.2 μg/ml $H_2O_2$, 80 mM citric acid, pH 3.95 and the reaction was stopped after 15 min at room temperature by addition of 50 μl $H_2SO_4$ (3.3 M). Each data point represents the mean ± SD, $n = 3$.

However, no such specific release of SH was observed in the presence of SA1641. Although cytotoxicity enhancement is already observed at 5 μg/ml (3.05 μM) SA1641 (see section 3.8.3), no specific endo/lysosomal release of SH was observed at this concentration ($A_{450 - 490\ nm}$ = 0.008). Endo/lysosomal release of SH increased slightly as the concentration was augmented to 30 μM ($A_{450 - 490\ nm}$ = 0.021), 40 μM ($A_{450 - 490\ nm}$ = 0.028) and 50 μM ($A_{450 - 490\ nm}$ = 0.039), most probably only due to unspecific membrane permeabilizing effects. In the case of digitonin, high

endo/lysosomal release of SH was shown at 30 µM ($A_{450-490\,nm}$ = 0.120), 40 µM ($A_{450-490\,nm}$ = 0.143) and 50 µM ($A_{450-490\,nm}$ = 0.134) due to unspecific disruption of lysosomal membranes. In the case of α-hederin, no endo/lysosomal release of SH was observed at all the concentrations tested.

### 3.8.5. Endo/lysosomal release of SH determined by cell fractionation

Alternatively, in order to measure the specific augmentation of the endo/lysosomal release of SH mediated by triterpenoidal saponins, cells were first treated either with SH (100 nM) or with SH + 5 µg/ml (3.05 µM) SA1641. After the incubation time and cell fractionation, the endo/lysosomal release of the toxin-reporter conjugate was evaluated by measuring peroxidase activity in the cytosolic fraction and in the lysosomal fraction. The quotient of the peroxidase activity in the cytosolic fraction and the peroxidase activity in the lysosomal fraction (CF/LF) is proportional to the relative amount of SH released into the cytosol.

Unfortunately, the CF/LF value mirrored contradictory results in repeated experiments. Peroxidase activity detected in the cytosolic fractions was very close to the detection limit ($A_{450-490\,nm}$ = 0.018–0.030), and therefore, small variations in the absorbance values greatly influenced the CF/LF ratio. In one example, the CF/LF value of the cells treated with SA1641 (0.082) was higher than that of the cells treated without the triterpenoidal saponin (0.072). However, in another example, the CF/LF value of the cells treated with SA1641 (0.107) was lower than that of the cells treated without the triterpenoidal saponin (0.151). In short, the measurements close to the detection limit resulted in a bad reproducibility and prevented the precise calculation of ratios representing the endo/lysosomal escape of SH in the presence or absence of triterpenoidal saponins. Regrettably, the reporter assay for endo/lysosomal escape using HRP is not suitable to quantify the endo/lysosomal release of protein-based therapeutics.

## 3.9. Enhanced expression of targeted toxins

### 3.9.1. Cytotoxicity in real time of SE and DE

Saporin-epidermal growth factor (SE) and dianthin-30-epidermal growth factor (DE) were compared in order to find which of the two targeted toxins is more suitable for further development with respect to their expression yield, cytotoxicity to bacteria and to eukaryotic

cells. Higher expression levels were obtained in the case of DE (see section 3.2.4). However, to consider the higher expression yield as an advantage for the production of targeted toxins, it should not have any influence on their cytotoxicity.

For this reason, the cytotoxicity of SE and DE was evaluated in real time on HER14 cells (Figure 37). Approximately at 28 h, an increase of the impedance signal occurred in case of all the samples, probably due to the disturbances arising from the addition of the compounds. The curve representing the untreated control cells achieved a minimum (NCI = 0.97) at 36 h and started to grow again until the end of the experiment (NCI = 1.45). Doxorubicin, which is a cytotoxic agent used in cancer chemotherapy, served as a toxic control. Doxorubicin was very toxic at the highest concentration tested (1,000 nM) and there was a continuous decrease in the impedance until the end of the experiment (NCI = 0.21). However, doxorubicin at a concentration of 1 nM was non-toxic and cells grew similarly to untreated cells as evidenced by the increasing impedance signal.
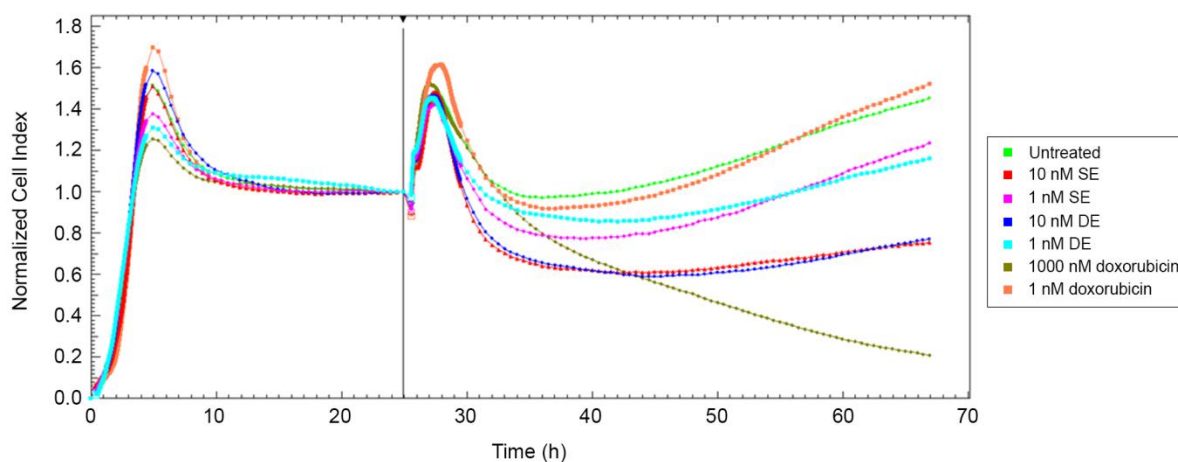


**Figure 37.** Cytotoxicity assay of SE and DE in real time. HER14 cells (8,000 cells/well) were treated with only medium (untreated control) or with targeted toxins at the concentrations of 1 and 10 nM for 42 h. Cells were further treated with doxorubicin at 1 and 1,000 nM (toxic control). Cell viability was analyzed in real time by an impedance-based cytotoxicity assay and cell indexes were normalized at the time of compounds addition. Curves are the mean, $n = 2$–6.

In the case of SE, cells treated with a concentration of 10 nM reached a minimum at 42 h (NCI = 0.61) and increased slowly until the end of the experiment (NCI = 0.76). A lower concentration of 1 nM was less toxic to the cells. Therefore, the minimum of the curve had a higher value (NCI = 0.78 at 39 h) and the end point was also higher (NCI = 1.24). In the case of DE, cells behaved almost in the same way as those treated with SE. In the presence of 10 nM DE the curves achieved a minimum (NCI = 0.59) at 45 h and increased slightly until the end of the experiment (NCI = 0.77). At the lower concentration of DE (1 nM) the curve had a minimum (NCI = 0.86)

at 40 h and finished with an NCI of 1.16. Since cytotoxicity curves of SE and DE had a very similar pattern, the higher expression levels of DE did not affect the cytotoxic activity, indicating correct protein folding.

### 3.9.2. Toxicity of targeted toxins to bacteria

The lower protein yield after expression of SE could be related with a higher toxicity of the targeted toxin to the bacteria during the expression process. To investigate this aspect, the toxicity of SE and DE to *Escherichia coli* was determined during their heterologous expression by monitoring the growth patterns of bacteria transformed with $6\times$ his-tagged-SE-pET11d or $6\times$ his-tagged-DE-pET11d (Figure 38).
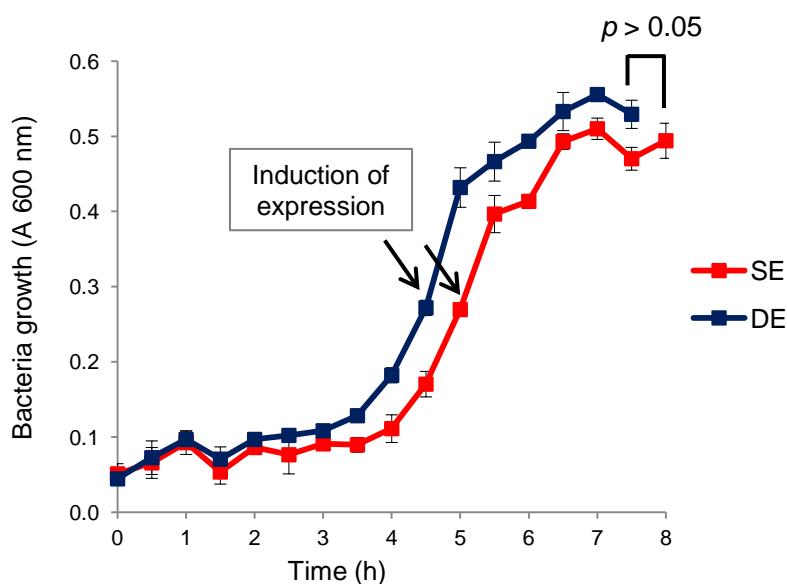


**Figure 38.** Toxicity of SE and DE during heterologous expression in *Escherichia coli*. Bacteria were allowed to grow until an optical density ($A_{600nm}$) of approximately 0.27 was reached. The expression of targeted toxins was then induced by addition of IPTG (see arrows). Bacterial growth was measured every 30 min for a total period of 3 h. The growth patterns of bacteria expressing SE or DE are similar in both cases. Remarkably, the difference between the two growth curves is not significant at the end of the experiment (*t*-test, $p > 0.05$). Each data point represents the mean ± SD, $n = 3$.

After induction of expression by addition of isopropyl β-D-1-thiogalactopyranoside (IPTG) (see arrows in Figure 38), the growth curves of bacteria expressing SE and DE behaved similarly in both cases and the optical density ($A_{600nm}$) at the end of the experiment was not significantly different (*t*-test, $p > 0.05$). Therefore, differences in protein yield between SE and DE were not caused by a different toxicity of the targeted toxins to the bacteria used for recombinant expression.

### 3.9.3.   Structural alignment of the toxin moieties from the fusion proteins

Alignment of the toxins was suggested as an approach to discover if certain structural features of the targeted toxins correlate to the different protein yields after heterologous expression. For this reason, saporin and dianthin-30, the two toxin moieties of SE and DE respectively, were structurally aligned to compare their three-dimensional shape (Figure 39). In contrast to Figure 18, where differences between RTA compared to other type I RIPs have been depicted, Figure 39 shows the differences between saporin and dianthin-30. Firstly, the backbone of both toxins was aligned as traces (Figure 39a). Five main structural differences were identified and highlighted in boxes (differences 1–5, see Figure 39a). Secondly, the alignment was displayed using the secondary structure of the proteins (Figure 39b). The same five main structural differences were highlighted as well (differences 1–5, see Figure 39b). In case of difference 2, both toxins present a β-strand conformation. Differences 3 and 4 show a loop for both proteins where only a spatial position slightly changes, but not the overall conformation. However, in the case of differences 1 and 5, there is a change in the conformation. In both situations, saporin presents a loop but dianthin-30 comprises a β-strand conformation. In general, these five main structural differences could be related with the different expression pattern of the targeted toxins.
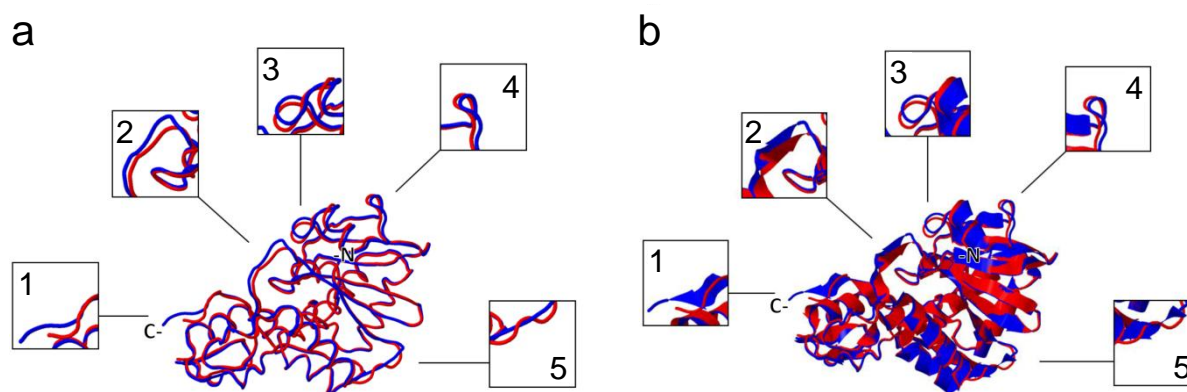


**Figure 39.** Structural alignment of saporin and dianthin-30. **(a)** The backbone of both proteins is shown as traces. Major structural differences between saporin (in red) and dianthin-30 (in blue) are highlighted in boxes and labeled with numbers (1–5). **(b)** The secondary structure is presented with cartoons. The same major structural differences are highlighted in boxes (1–5). The secondary structure is different in 1 and 5, as saporin has a loop structure but dianthin-30 presents a β-strand conformation.

### 3.9.4.   Amino-acid sequence alignment of the fusion proteins

To analyze the relevance of the five main structural differences found in the previous section 3.9.3, an amino-acid sequence alignment was performed for SE and DE. The identity of the two fusion proteins is 84 % (269/321) and their similarity is 92 % (295/321). There is a single one-residue gap in saporin after position 57. Sequence fragments corresponding to the five main

structural differences identified before in the structural alignment of saporin and dianthin-30 were indicated with black squares and the same numeration (1–5, see Figure 19). While differences 5, 2, 3 and 4 (in this order) are close to the N-terminus, difference 1 is near the C-terminus of both toxin moieties. The details of these five main differences are presented in Table 9. There are other differences between the amino-acid sequences of the two fusion proteins, but these do not have relevance for their spatial structure.

It should be considered that the only variable part of both fusion proteins is the toxic moiety. If only the toxin moieties are aligned, the identity between both proteins is 80 % (203/255), their similarity is 90 % (229/255) and there is a gap in saporin after position 48. The N-terminus that comprises the 6× his-tag and the C-terminus that comprises EGF are identical.

**Table 9.** Differences between SE and DE identified after structural (1–5, see Figure 39) and amino-acid sequence (1–5, see Figure 19) alignments of both proteins.

| Difference | Position (in SE) | Amino-acid sequence (in SE) | Structural conformation (in SE) | Position (in DE) | Amino-acid sequence (in DE) | Structural conformation (in DE) |
|---|---|---|---|---|---|---|
| 1 | 259–262 | GKPK | loop | 260–263 | GRPK | β-strand |
| 2 | 53–58 | GPPSK–E | β-strand | 53–59 | GAPSTTD | β-strand |
| 3 | 102–105 | SEIT | loop | 103–106 | NQIT | loop |
| 4 | 116–119 | ATTA | loop | 117–120 | VVVA | loop |
| 5 | 19–24 | VNPTAG | loop | 19–24 | ANPSAS | β-strand |

Presumably, minimal differences such as some of the short sequences (1–5) identified in the structural and amino-acid sequence alignments, may be responsible for a strong variation of protein expression between SE and DE targeted toxins.

## 3.10. Specificity of the toxin moiety in the enhancement of targeted toxins by triterpenoidal saponins

### 3.10.1. Cytotoxicity of DT$_{390}$-EGF in combination with SO1861

Diphtheria toxin$_{390}$-epidermal growth factor (DT$_{390}$-EGF) was needed in order to investigate the endo/lysosomal escape of a bacterial toxin in the presence of triterpenoidal saponins. DT$_{390}$-EGF is composed of the catalytic and translocation domain of diphtheria toxin fused to EGF.

Cytotoxicity of $DT_{390}$-EGF was measured in presence of Saponinum album (SA) (Figure 40). Saporin was tested in combination with 2 µg/ml (1.33 µM) SA as a positive control for the enhancing effects mediated by triterpenoidal saponins (Figure 40a). The highest concentration tested of saporin (1,000 nM) reduced cell viability to 42% and $GI_{50}$ was calculated to 823 nM. The combination of saporin and SA caused potentiated cytotoxicity ($GI_{50}$ of 0.43 nM). Cytotoxicity was observed even at the lowest concentration tested (64% viability at 0.1 nM) and the enhancement factor was 1,900-fold.

In the case of $DT_{390}$-EGF (Figure 40b), cytotoxicity was observed at the three highest concentrations tested (10–1,000 nM). At 10 nM of $DT_{390}$-EGF, cell viability was reduced to 73% and the $GI_{50}$ value was calculated to 61.5 nM. Interestingly, although $DT_{390}$-EGF is a targeted toxin based on a bacterial toxin (and not on a type I RIP), its combination with SA resulted in cytotoxicity enhancement and cytotoxic effects were observed down to a concentration of 0.1 nM (69% viability). The $GI_{50}$ of $DT_{390}$-EGF in the presence of SA was 0.73 nM and this resulted in an enhancement factor of 85-fold.
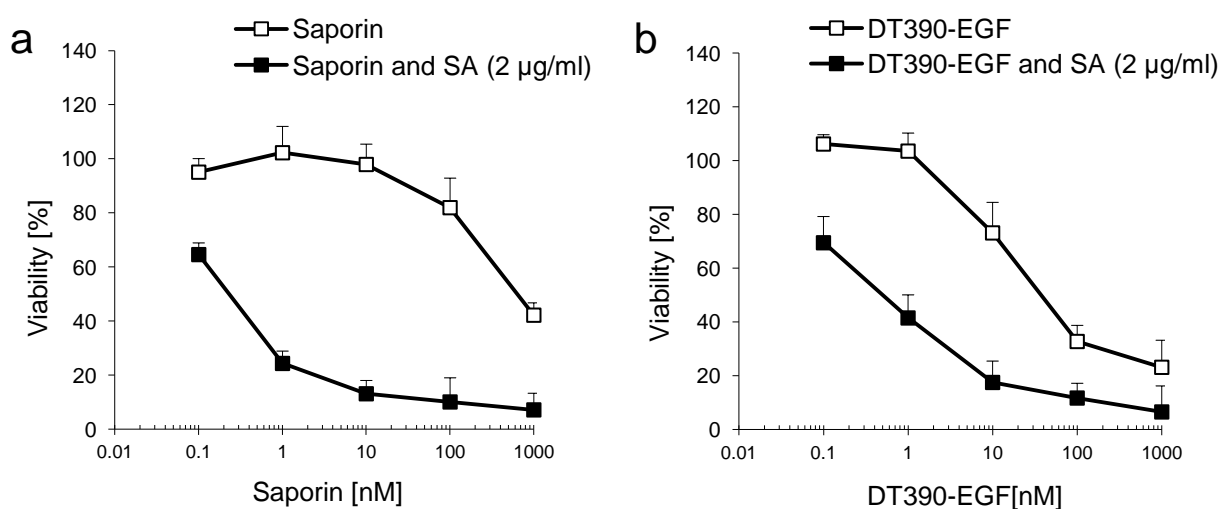


**Figure 40.** Cytotoxicity of saporin and $DT_{390}$-EGF in combination with SA. ECV-304 cells (4,000 cells/well) were treated with either **(a)** saporin or **(b)** $DT_{390}$-EGF in a concentration range from 0.1 to 1,000 nM ± SA (2 µg/ml) for 48 h. Cell viability was measured by an MTT assay and referred to untreated control cells. Data represents the mean ± SD, $n = 4$.

## 3.10.2. Real-time cytotoxicity of targeted toxins in combination with SO1861

The toxin specificity of the cytotoxicity enhancement of targeted toxins by triterpenoidal saponins was studied by measuring the potentiation effects in the case of three targeted toxins bearing the same ligand (SE, DE and $DT_{390}$-EGF) (Figure 41). Cells proliferated well until the time of normalization. In the case of untreated control cells, only fresh medium was added and

the NCI increased continuously until reaching a maximum of 1.35 at 31.0 h. Thereafter, untreated cells stopped to grow and the NCI was slightly reduced until an NCI of 1.11 at the end of the experiment. In the case of cells treated with 2 µg/ml (1.07 µM) SO1861, cells reached a very similar growth to untreated cells 40 h past seeding, although it resulted in slight cytotoxicity during the last 10 h of the experiment (NCI = 0.88 at 49.5 h).
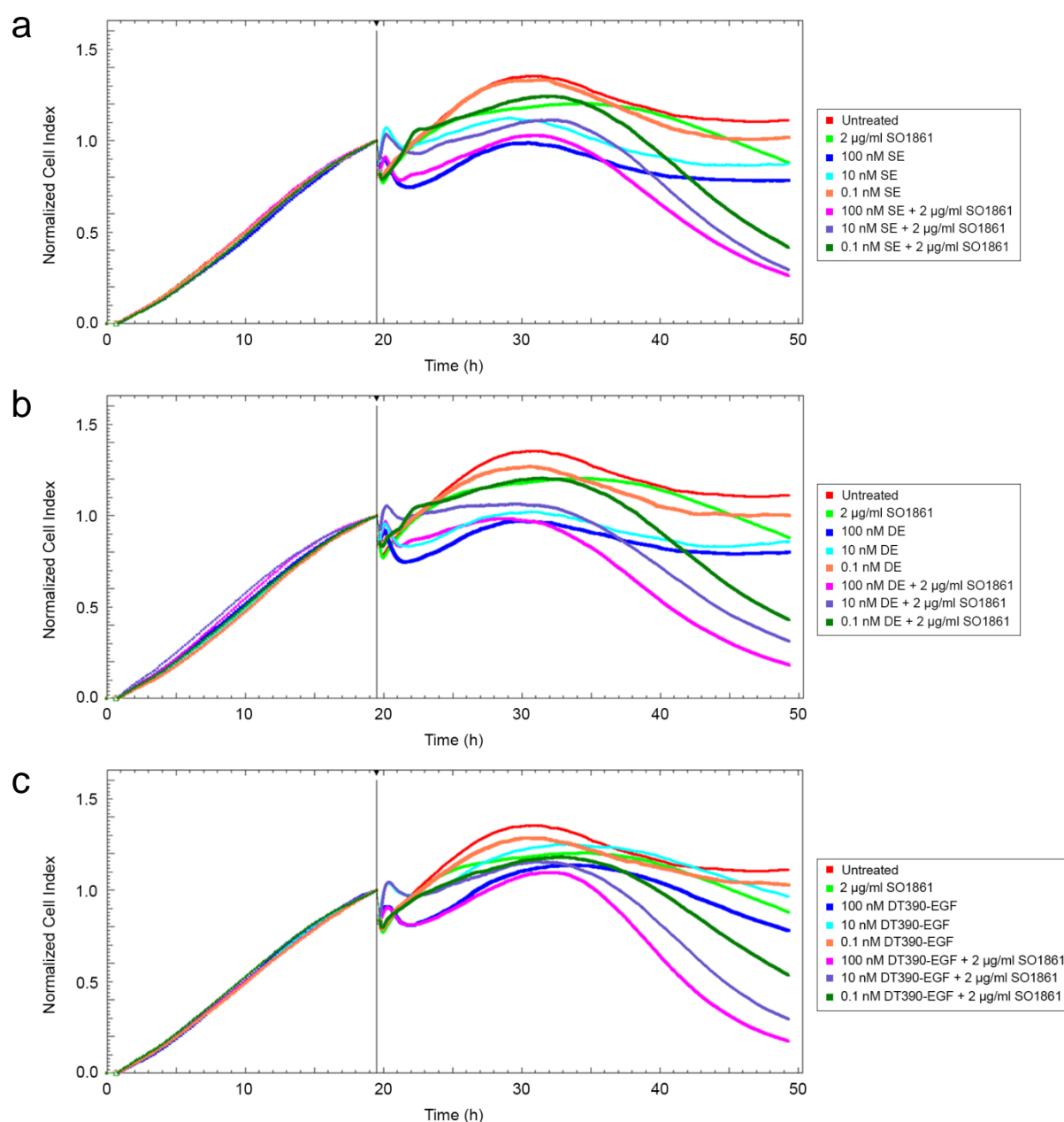


**Figure 41.** Real-time monitoring of the cytotoxicity of targeted toxins in combination with SO1861. ECV-304 cells (2,000 cells/well) were treated with **(a)** SE, **(b)** DE and **(c)** DT$_{390}$-EGF in a concentration range from 0.1 to 100 nM ± SO1861 (2 µg/ml) for 30 h. Cell viability was analyzed in real time by an impedance-based cytotoxicity assay. Cell indexes were normalized when the compounds were added to cells. Curves show the mean, $n = 3$–8. Curves corresponding to untreated control cells and cells treated with only SO1861 are equally represented in each figure for easier comparison.

SE, DE and $DT_{390}$-EGF were cytotoxic in a concentration-dependent manner. NCIs at the end of the experiment for the three targeted toxins ± SO1861 are detailed in Table 10. When the targeted toxins consisting of type I RIPs (SE and DE) were administered in the presence of SO1861, their cytotoxicity was tremendously enhanced. In contrast, the toxin domain of $DT_{390}$-EGF is not based on a type I RIP but has a bacterial origin and was therefore not expected to exert synergistic cytotoxicity enhancement in the presence of triterpenoidal saponins. Nevertheless, although in a minor degree, the cytotoxicity augmentation by SO1861 was also observed in the case of $DT_{390}$-EGF.

**Table 10.** NCIs for SE, DE and $DT_{390}$-EGF at the end of the real-time cytotoxicity assay (see Figure 41). As detailed in the figure legend, ECV-304 cells (2,000 cells/well) were incubated with SE, DE and $DT_{390}$-EGF at the concentrations of 0.1, 10 and 100 nM ± SO1861 (2 µg/ml) for 30 h. Each value represents the mean of NCIs at the end of the experiment, $n = 3$–8.

| | NCIs at the end of the experiment | | | | | |
| --- | --- | --- | --- | --- | --- | --- |
| | − SO1861 | | | + SO1861 (2 µg/ml) | | |
| Concentration of targeted toxin | 0.1 nM | 10 nM | 100 nM | 0.1 nM | 10 nM | 100 nM |
| SE | 1.02 | 0.87 | 0.78 | 0.42 | 0.30 | 0.27 |
| DE | 1.00 | 0.86 | 0.80 | 0.43 | 0.31 | 0.19 |
| $DT_{390}$-EGF | 1.03 | 0.97 | 0.78 | 0.54 | 0.30 | 0.18 |

To sum up the results of this work, membrane permeabilizing effects of oleanane saponins on cellular and lysosomal membranes were observed from 6 µM and hemolysis from 3 µM. Cytotoxicity of saporin and gelonin augmented in combination with oleanane saponins at non-permeabilizing concentrations (> 550- and > 270-fold, respectively) but cytotoxicity of RTA was not potentiated. Saporin was further used to construct two immunotoxins based on Trastuzumab and Cetuximab. Both immunotoxins specifically delivered saporin into target cells, triggered the ADCC and their cytotoxicity was tremendously enhanced by oleanane saponins. The cytotoxicity enhancement was also observed in the case of SR, saporin-anti-CD22 and saporin-anti-CD25 (150-, 19- and 26,000-fold, respectively), thus validating the platform for enhanced endo/lysosomal escape. In addition, the enzymatically inactive variant of saporin (saporin-KQ) was successfully expressed and characterized *in vitro* but the establishment of a reporter assay for the endo/lysosomal escape based on peroxidase activity failed. Finally, DE was found to be more suitable for further development than SE, since its expression yield was significantly higher. Both cytotoxicities of SE and DE were synergistically enhanced in the presence of oleanane saponins, as well as $DT_{390}$-EGF but in a minor degree (85-fold).

# 4. Discussion

## 4.1. Evaluation of membrane permeabilizing effects of oleanane saponins

The investigation of membrane permeabilizing effects facilitates the distinction of unspecific membrane permeabilization by oleanane saponins (a subclass of triterpenoidal saponins) generally at higher concentrations from the specific process of endo/lysosomal escape of certain type I ribosome-inactivating protein (RIPs) by structurally specific oleanane saponins at low concentrations that do not involve unspecific disruption of endo/lysosomal membranes.

Membrane permeabilizing effects of saponins were monitored in real time. Apart from digitonin, which had slight effects on cell membranes at 3 µM, saponins did not show any lytic effects up to 6 µM. In the case of digitonin (steroidal backbone), the normalized cell index (NCI) values increased rapidly after 1 h at low concentrations (6 and 12 µM) but remained linear at a higher concentration (24 µM). At these low concentrations the cell membrane may be able to reverse rapidly the membrane permeabilizing effects of digitonin probably due to membrane repairing mechanisms. Digitonin disturbs cell membranes because it forms a complex with the cholesterol in cell membrane [46, 185]. As cholesterol is transported from the endoplasmic reticulum where it is biosynthesized to the plasma membrane [186], it is hypothesized that cells may quickly reverse the permeabilizing effects of digitonin providing new molecules of cholesterol and degrading the cholesterol-digitonin complexes. However, this repairing mechanism may only work up to a certain concentration. With higher concentrations (24 µM) the cell membrane may be saturated with digitonin and the repairing process may not take place. In the case of oleanane saponins (triterpenoidal backbone), NCI values remained linear or even decreased after addition of saponins. As oleanane saponins have a different kind of aglycone compared to digitonin, the interaction with the membrane may be based on other type of interactions than those with digitonin, and therefore the repairing mechanisms could be different or non-existing.

Another interesting aspect was observed in the cells treated with Saponinum album (SA) at 12 µM. The NCI curve revealed a first and a second minimum indicating a two-step kinetic. The cell membrane may have been partially disrupted in a first phase. Cells were probably unable to reverse this effect and membrane permeabilization further continued in a second phase. Furthermore, although purified from the same plant, *Quillaja* saponin 1 and 2 (crude extracts from different suppliers) revealed a different permeabilizing activity on cell membranes. This

phenomenon could be probably explained due to the variable amount of sapogenin content from each sample, being 20–35% for *Quillaja* saponin 1 but 10–11% for *Quillaja* saponin 2.

Results obtained with the propidium iodide (PI) test were in accordance to those obtained by the real-time monitoring. Membrane permeabilizing effects were likewise not observable up to 6 μM. Nevertheless, the comparison of the two methods used for studying the permeabilizing effects on cell membranes was also a point of interest. First of all, the technical problems of the PI uptake assay due to the total disruption of cells at high saponin concentrations can be avoided in the real-time monitoring assay, as there was always a measurable signal in the second method. In addition, in the real-time monitoring, the immediate lysis of cells (case of Triton X-100 at 5%) can be differentiated from a rapid progressive lysis of the cell membrane (case of SO1861 at 24 μM). This phenomenon was not observed with the PI uptake assay. Finally, the real-time monitoring permitted the analysis of the kinetics of membrane permeabilization and the detection of membrane perturbation with lower saponin concentrations. For example, while an effect on cell membrane was observed with SA and SA1641 at 12 μM, no such effect was observed with the PI uptake assay. For all these reasons, impedance-based real-time monitoring is considered as a better method with higher sensitivity and which provide more valuable information than being obtained from other methods.

The β-*N*-acetylglucosaminidase (NAG) release assay was performed in order to directly characterize membrane permeabilizing effects on lysosomal membranes since previous permeabilization analyses of oleanane saponins were only applied to the cell membrane [82]. The saponins tested did not cause disruption of lysosomal membranes up to 6 μM. In order to avoid accumulation of therapeutics inside endosomal and lysosomal vesicles during intracellular drug delivery, lysogenic properties of several approaches have been studied, for example use of fusogenic lipids [187], membrane-disruptive peptides [188], polymers [189] or lysosomotropic agents [190] and photochemical internalization [117], but the number of systems is still limited and their efficacy is variable. In this context, saponins with high membrane permeabilizing effects on lysosomal membranes such as SO1861 or SA without having effects on plasma membranes appear to be a promising strategy to solve the hurdle of endo/lysosomal entrapment of protein-based therapeutics.

The hemolysis assay was conducted in order to investigate the short term effect of saponins on the cell membrane of red blood cells (RBCs). Hemolytic activity is a crucial aspect, which has to be quantified before starting *in vivo* studies, as a pre-requisite for animal therapy is a non-

hemolytic saponin. Interestingly, all oleanane saponins did not present any hemolytic activity up to 3 μM.

Different permeabilizing effects of the same saponins on the three types of membranes may be caused by the different membrane composition of ECV-304 cell membranes, lysosomal membranes and RBC membranes. Saponins are reported to interact with membrane sterols, in particular with cholesterol, and to form micelle-like aggregations [191]. Furthermore, saponins are known for their ability to bind to the membrane lipids of RBCs and form bridges between the same kind of cell [192]. Slight differences in the membrane composition of cholesterol and lipids can generate changes in membrane sensibility to saponins. For example, *Quillaja* saponin 2 only presented membrane permeabilizing effects on RBCs but not in other membrane types, which may be attributed to a higher cholesterol content in the cell membrane of RBCs [193] making them more susceptible to saponins.

A structure-activity relationship could be established in the case of purified saponins, which present structural differences and different permeabilizing effects, such as digitonin, glycyrrhizinic acid, SA1641 and SO1861. A steroidal skeleton with an attached sugar chain might cause high membrane permeabilizing effects, as observed with digitonin. An oleanane skeleton with only one sugar chain appears to not cause any permeabilizing effects (glycyrrhizinic acid) but the effects can augment when a second sugar chain is attached to the aglycone (SA1641, SO1861). Further, the presence of an hydroxyl group at position 16 in an oleanane skeleton from a bisdesmosidic saponin (SO1861) might increase hemolysis [194] and membrane permeabilizing effects of saponins.

## 4.2. General considerations on the platform technology for endo/lysosomal escape

The development of a platform technology for an endo/lysosomal escape enhancement of targeted toxins by triterpenoidal saponins was the main objective of this work. It has been reported that structurally specific oleanane saponins tremendously enhance the cytotoxicity of certain type I RIPs such as saporin and dianthin-30. However, this effect has been studied only in the case of two targeted toxins consisting of the same ligand, namely saporin-epidermal growth factor (SE) and dianthin-30-epidermal growth factor (DE). The development of a platform system based on this synergistic natural principle is expected to result in an enhanced endo/lysosomal escape and consequently enhanced cytotoxicity of targeted toxins that differ in

their ligand, thus making it possible to target different types of cancer cells with higher specificity and efficacy.

Recombinantly expressed saporin was suitable to be conjugated to different monoclonal antibodies in order to develop the intended platform technology since after heterologous expression, purification and characterization, the toxin was active and its cytotoxicity was enhanced in the presence of triterpenoidal saponins. Mechanistic studies by live cell imaging corroborated that the cytotoxicity enhancement of saporin in the presence of SA1641 is a consequence of a drastic enhancement of the toxin's endo/lysosomal escape. Most probably, SA1641 interacts specifically with saporin in the acidic endo/lysosomal environment and this specifically mediates the endo/lysosomal escape of saporin [6].

The successful conjugation and purification of two immunotoxins based on saporin and different ligands [saporin-Trastuzumab (ST) and saporin-Cetuximab (SC)] facilitated the establishment of the platform system. The synergistic enhancement of the immunotoxins by SO1861 was confirmed after evaluation of the cytotoxicity in real time, thus indicating that the delivery of saporin into targeted cancer cells was specifically enhanced by triterpenoidal saponins.

Several aspects of the immunotoxins were further characterized to validate the enhanced endo/lysosomal escape of targeted toxins by triterpenoidal saponins. Chemical modification of a therapeutic antibody with a toxin may affect solubility, stability, binding affinity, enzymatic activity and effector reactions. To check if there was any effect of the cross-linking reactions, the *N*-glycosidase activity of the saporin-monoclonal antibody conjugates was evidenced by the adenine cleavage from herring sperm DNA.

To exclude any further influences of the chemical cross-linking reactions, the binding of the modified antibodies to the tumor-specific cellular receptors was verified by the interaction of ST to the soluble recombinant epidermal growth factor receptor 2 (HER2) and SC to the soluble extracellular domain of epidermal growth factor receptor (EGFR) in a surface plasmon resonance-based binding assay. Specificity of the binding is another therapeutic aspect that renders the antibodies to be highly successful in clinics. It was confirmed by inhibition of cytotoxic effects in the presence of unconjugated antibodies in excess.

Furthermore, saporin-modified antibodies retained their ability to trigger an ADCC response. ADCC is an important aspect for therapeutic monoclonal antibodies (e.g. Trastuzumab, Cetuximab, Rituximab, Alemtuzumab and Ofatumumab) [195]. Notably, there was a clear ADCC with the immunotoxins, which was comparable to the effect of unconjugated antibodies.

This immunotoxin mediated effect may be summarized as the *immunotoxin-dependent cell-mediated cytotoxicity* (IDCC). A stability assay confirmed that the molecules responsible for triggering IDCC against tumor cells were indeed the immunotoxins and not antibodies released from the modified immunotoxins by proteolytic degradation or cleavage of the disulfide bond.

Despite the fact that some investigations already indicated that there may be a contribution of the ADCC to the therapeutic efficacy of an immunotoxin [56, 57], it is still a common understanding that immunotoxins do not present an immunotherapeutic mechanism of action such as the ability to trigger ADCC [58]. This assumption is expected to hold true for an appreciable number of immunotoxins that were designed with antibody fragments, that lack the Fc portion and therefore the ability to interact with natural killer (NK) cells [196]. Nevertheless, immunotoxins were also constructed with complete monoclonal antibodies that possess the Fc part [49]. In the past, a few immunotoxins consisting of Trastuzumab or Cetuximab as targeting moiety coupled with some plant or bacterial toxins as toxic moiety, such as a truncated version of *Pseudomonas* exotoxin A [197], gelonin [198] or saporin [199, 200], were designed. It can be therefore expected that these immunotoxins retain the reported ability of the integrated monoclonal antibodies to trigger ADCC after chemical conjugation to the toxin.

The immunotoxins ST and SC were only slightly toxic or non-toxic to the tumor cells at a concentration of 10 nM during 37 h (see Figure 26) and the incubation of cells for 24 h with a concentration of 100 nM also resulted in no toxicity (see Figure 29a). Therapeutically established antibodies were used for the construction of immunotoxins. Since the mechanism of action of this kind of antibodies is the engagement with cell surface receptors (to either activate or inhibit signaling), or to interact with the innate immune system, it is generally desirable that the antigen-antibody complex should not be rapidly internalized [50]. Therefore, the use of Trastuzumab and Cetuximab as immunotoxin ligands would cause a long internalization cycle and lower cytotoxicity during the first hours of incubation.

However, it has been shown that a substantially higher efficacy of the immunotoxins based on certain type I RIPs can be achieved by co-administration of triterpenoidal saponins [119, 164]. This effect depends on the presence of saporin or dianthin-30 [82]. Therefore, the saporin-containing immunotoxins were incubated in the presence of the purified saponin SO1861. A synergistic effect between saporin and SO1861 resulted in a tremendous increase of the cytotoxicity of the immunotoxins. This aspect, which is the basis of the platform technology for enhanced endo/lysosomal escape, is very relevant for the perspective of immunotoxin applications, as these augmentation effects allow the decrease of effective doses in patients

resulting in amelioration of side effects. Reduced dosages may concomitantly circumvent an expected immune reaction that can block the immunotoxins.

As mentioned before, an important objective is to combine the functionality of monoclonal antibodies (binding to targeted receptors and triggering of ADCC) with the functionality of immunotoxins (specific toxin delivery). A discussion about how these two functionalities act and how the toxicity of the conjugate is drastically augmented by triterpenoidal saponin is included below. First, immunotoxins are expected to specifically bind to targeted tumor cells. Following the addition of NK cells, the Fc domains can interact with the FcγRIII of these cells, resulting in the initiation of the ADCC [201]. However, part of the immunotoxins will trigger their internalization due to the binding of the antibody units to the cellular receptors (EGFR [183] and HER2 [202]) and therefore the IDCC effect will decrease to the same extent as the amount of internalized immunotoxin increases. After a certain time, internalized immunotoxins will be accumulated in endosomes and finally lysosomes. In these acidic organelles, the disulfide bond introduced during the conjugation of saporin to the monoclonal antibodies will be cleaved and free saporin will be released into the lysosomal environment [203]. Following the addition of SO1861, an interaction between the toxin and SO1861 occurs and this will result in the endo/lysosomal escape of saporin [6] leading to the induction of apoptosis by the enzymatic removal of a specific adenine residue at position 4324 of the 28S rRNA [204]. Therefore, the addition of SO1861 will concomitantly enhance the cytotoxicity of the toxin moiety of the immunotoxin. The specific binding of immunotoxins to tumor-specific cellular receptors, the accumulation of immunotoxins in acidic organelles and the endo/lysosomal escape of delivered toxin mediated by triterpenoidal saponins were further confirmed by live cell imaging using fluorescence labeled ST (saporin-Trastuzumab-Alexa Fluor 488, [Alexa]ST) (see Figure 29 and Figure 30).

These results open a path for applying the intended platform technology for enhanced endo/lysosomal escape to immunotoxins constructed with other therapeutic antibodies directed to cancer-specific cellular receptors that are already in the market such as Rituximab, Panitumumab and Ofatumumab. Animal experiments to evaluate toxicity and antitumoral efficacy, as well as to characterize the immunogenicity of the immunotoxins in mice are of great importance for the future of targeted tumor therapies with modified antibodies described here. The use of a platform system may assist to overcome present limitations by clinical resistance [205] for a number of antibody-based tumor therapies. This can further help to achieve a successful and efficient treatment of solid tumors and hematologic malignancies.

## 4.3. Ligand specificity of enhanced endo/lysosomal escape

The ligand specificity of the enhanced endo/lysosomal escape is an important aspect that should be discussed in order to achieve optimized effects in the platform technology for enhanced cytotoxicity of targeted toxins. Cytotoxicity enhancement by triterpenoidal saponins was observed in the case of five immunotoxins consisting of saporin and different monoclonal antibodies, namely Trastuzumab, Cetuximab, Rituximab, anti-CD22 and anti-CD25 (see sections 3.5.4 and 3.6.2). Furthermore, a targeted toxin consisting of saporin and EGF presented augmentation effects in the presence of triterpenoidal saponins (see section 3.10.2).

In each of these cases, targeted toxins were based on the same toxin (saporin) but contained different ligand moieties. Since targeted toxins showed different enhancement factors in the presence of triterpenoidal saponins and their only difference is the nature of their ligand, ligand specificity plays a determining role in the platform system to predict the magnitude of the cytotoxicity enhancement.

There are various factors related to the ligand moiety of an immunotoxin which may have an influence on its final cytotoxicity. First, the affinity of the targeting moiety to the target receptor, the nature of the target receptor [206] and, in the case of an antibody or antibody fragment as targeting moiety, the specific epitope on the target receptor [207] may affect the efficacy of a targeted toxin. Further parameters having an impact on the cytotoxicity of an immunotoxin may be the level of receptor expression on target cells and the internalization process of the ligand-receptor complex [208]. Both rate of endocytosis and intracellular trafficking after internalization of the complex are relevant for the final efficacy of the targeted toxin [209].

Expression levels of EGFR have been already described to have a direct influence on the cytotoxicity enhancement of SE by triterpenoidal saponins [121]. A similar phenomenon was observed in the case of SC. This immunotoxin was first tested in TSA-EGFR cells (see section 3.5.4) and the cytotoxicity of the combination of SC and triterpenoidal saponins only resulted in total cell death at 100 nM and only slight cytotoxicity at 1 nM of SC. However, the same immunotoxin was applied in combination with triterpenoidal saponins to BT-474 cells (see section 3.5.5) and a total cell death was achieved even at a concentration of 0.001 nM. The different cytotoxic properties of SC on different cell lines can be attributed to the different expression levels of EGFR on the cell surface of each respective cell type.

The analysis of ST (anti-CD20), saporin-anti-CD22 and saporin-anti-CD25 was performed in the same cell line (Ramos cells) but nevertheless the cytotoxicity enhancement factors in the

presence of triterpenoidal saponins were completely different in the case of each immunotoxin. The different affinities of the monoclonal antibodies to the corresponding target receptors or the diverse expression levels of each cellular receptor can explain these observations. For example, receptor over-expression is reported in Ramos cells for CD20 [210] and CD22 [211]. Contrastingly, although expression of CD25 is also described in Ramos cells [212], it is not over-expressed compared to the two other cellular receptors.

In addition, the variability in the cytotoxicity enhancement factors of the three immunotoxins ST, saporin-anti-CD22 and saporin-anti-CD25 can be caused as well by different internalization processes of the immunotoxin-receptor complexes. Specially in the case of saporin-anti-CD25, its highest enhancement factor (> 26,000-fold) may be explained by the lower expression levels of the target receptor (causing a low cytotoxicity by the immunotoxin alone) but the high endocytosis rate of the ligand-receptor complex [213] (quickly achieving high cytotoxicity within the few molecules internalized and released into the cytosol in the presence of triterpenoidal saponins).

Interestingly, the platform technology for an enhanced endo/lysosomal escape has been successfully tested for targeted toxins based on either monoclonal antibodies (Trastuzumab, Cetuximab, Rituximab, anti-CD22 and anti-CD25, see sections 3.5.4 and 3.6.2) or non-antibody ligands (EGF, see section 3.10.2). As advantages and disadvantages exist for each type [208], the fact that the platform system works for both types of targeted toxins (those consisting of monoclonal antibodies and those of non-antibody ligands) provides great flexibility when planning the construction of new conjugates for an enhanced targeted tumor therapy. In general, targeted toxins composed of other monoclonal antibodies and growth factors should be constructed and evaluated in the presence of triterpenoidal saponins to achieve more information about the ligand specificity of the platform technology for enhanced endo/lysosomal escape. Antibody fragments present some other advantages in comparison to monoclonal antibodies such as improved tumor penetration and lower immunogenicity [214]. Therefore, the construction of targeted toxins comprised of saporin and antibody fragments, and their application in combination with triterpenoidal saponins should be investigated in the future.

Finally, since the synergistic cytotoxicity enhancement was observed in already six saporin-based targeted toxins including ST, SC, saporin-Rituximab (SR), saporin-anti-CD22, saporin-anti-CD25 and SE, the platform technology for enhanced endo/lysosomal escape of immunotoxins by triterpenoidal saponins was validated for its application in both solid tumors and hematologic malignances.

## 4.4. Toxin specificity of enhanced endo/lysosomal escape

The toxin specificity of the enhanced endo/lysosomal escape by triterpenoidal saponins is another important aspect that should be discussed in order to achieve optimized effects in the presented platform technology. Tremendous cytotoxicity enhancement was observed in the case of two plant toxins (saporin and gelonin, see section 3.4.1) and two targeted toxins consisting of either saporin or dianthin-30 as toxin moiety and EGF as ligand (see section 3.10.2). In addition, slight enhancement by triterpenoidal saponins was observed in the cytotoxicity of the targeted toxin diphtheria toxin$_{390}$-epidermal growth factor (DT$_{390}$-EGF) (catalytic and translocation domain of diphtheria toxin fused to EGF, see sections 3.10.1 and 3.10.2).

There is one main factor related to the toxins which has a direct influence on their final cytotoxicity. Independently of the route of internalization, toxins must cross at least one lipid barrier from a vesicular compartment to arrive at the cytosol and exhibit their catalytic activity [215]. In fact, triterpenoidal saponins specifically mediate the release of certain toxins from the endo/lysosomes to the cytosol [6]. Therefore, toxins presenting augmentation effects may successfully achieve the endo/lysosomal escape in the presence of triterpenoidal saponins, so that they can cross the lipid barrier and cause cytotoxicity. In contrast, toxins without enhancement properties may remain entrapped in their respective vesicular compartments and finally be degraded in the lysosomes.

Previous studies had been conducted to investigate if the cytotoxicity enhancement of naturally occurring, ligand-free toxins by triterpenoidal saponins is dependent on the nature of the toxin [36]. In these investigations, the cytotoxicity of the type I RIPs saporin and agrostin was identified to be drastically enhanced by triterpenoidal saponins, whereas only a very slight or no enhancement was observed for the type II RIPs nigrin b and ricin A-chain (RTA, catalytic domain of ricin), for the cyanobacterial heptapeptide toxin microcystin-LR and for the bacterial diphtheria toxin A-chain (catalytic domain of diphtheria toxin).

Apparently, only certain type I RIPs are synergistically enhanced in the presence of triterpenoidal saponins. Structural and amino-acid sequence alignments facilitated the identification of 10 amino acids (G35, G60, R86, A97, N185, N190, N199, Q237, K239 and K253 in the amino-acid sequence of saporin) that may be relevant for the cytotoxicity enhancement of type I RIPs by triterpenoidal saponins (see section 3.4.4). Interestingly, besides the small neutral amino acids G and A, all other amino acids are those with an NH$_2$ in the side

chain (i.e. amine group in K, amide group in N and Q, guanidine group in R). The presence of these chemical groups in the surface of the toxins may be relevant for the augmentation effects.

Agrostin, although it has been reported for their enhancing properties [40], was not included in the alignments because no amino-acid sequence and three-dimensional structure has been reported so far. Therefore, it will be of great interest if the amino-acid sequence of agrostin is investigated in the future. The identification of the 10 relevant amino acids in the amino-acid sequence of agrostin would confirm their importance in the cytotoxicity enhancement.

Triterpenoidal saponins specifically mediate the escape of saporin out of the late endosomes and lysosomes, probably due to an interaction between the triterpenoidal saponins and saporin triggered by the acidification of the vesicles [6]. In contrast, RTA follows a different intracellular route from saporin to enter the cytosol [19]. After internalization, RTA does not accumulate in late endosomes and lysosomes but is retrogradely transported to the Golgi-apparatus and subsequently to the endoplasmic reticulum, where it finally reaches the cytosol with the assistance of the endoplasmic reticulum-associated degradation (ERAD) [216].

The differences in cytotoxicity enhancement between RTA and all the other type I RIRs saporin, dianthin-30 and gelonin could be due to the lack of interaction between RTA and triterpenoidal saponins in acidic conditions. Alternatively, taking into consideration the different intracellular trafficking, the differences in cytotoxicity enhancement could be because of the accumulation of RTA and triterpenoidal saponins in different intracellular compartments, thus preventing both compounds to physically interact in the same vesicle. Similarly, the 10 amino acids that may be relevant for the cytotoxicity enhancement could be responsible for the interaction of type I RIPs with triterpenoidal saponins in acidic environments, but could be relevant instead for the accumulation of the toxins in late endosomes and lysosomes.

The cytotoxicity of further type I RIPs and even other kinds of toxins should be later evaluated in combination with triterpenoidal saponins. The identification of more type I RIPs that are synergistically enhanced will lead to the alignment of their amino-acid sequences with the sequences of the already identified toxins (saporin, dianthin-30 and gelonin). These new alignments can provide further information to characterize the amino acids that are responsible for the cytotoxicity enhancement of the toxins.

Alternatively, in order to check the relevance of the 10 identified amino acids, these amino acids could be modified by mutagenesis and the mutated toxins (e.g. saporin with punctual mutations [217]) could be evaluated in the presence of triterpenoidal saponins. A concrete amino acid will

be identified as relevant if after its mutation, the cytotoxicity enhancement properties of the mutated protein are lost.

In the case of targeted toxins, the ability of the toxin moiety to escape from a vesicular compartment into the cytosol is also a crucial factor to anticipate their final cytotoxicity [206]. Targeted toxins evaluated in this study (SE, DE and $DT_{390}$-EGF) were based on the same targeting moiety (EGF) but contained different toxin moieties. Since targeted toxins showed different enhancement levels in the presence of triterpenoidal saponins and their only difference is the nature of their toxin moiety, toxin specificity plays a determining role in the platform system to predict the magnitude of the cytotoxicity enhancement.

In previous studies, the cytotoxicity enhancement was observed for SE and DE, while cytotoxicity of targeted toxins comprised as well of EGF as ligand but of RTA, $DT_{390}$ or ETA' (catalytic and translocation domain of *Pseudomonas* exotoxin A) as toxin moiety showed only slight or no enhancement [82].

One of the hypothesis that has been considered is that the endo/lysosomal escape of targeted toxins mediated by triterpenoidal saponins is dependent on the high isoelectric point (pI) of the toxin moiety. This was the case for saporin (pI = 9.45) and dianthin-30 (pI = 9.48) but not of other proteins lacking synergistic enhancing properties such as RTA (pI = 7.1) or $DT_{390}$ (pI 5.1) and ETA' (pI = 4.8). However, the observation that a targeted toxin comprising of pancreatic RNase I (pI = 9.1) as toxin moiety and EGF as ligand did not result in synergistic cytotoxicity enhancement [82] indicated that the hypothesis was not generally valid. Most probably, as there is a high identity between the amino-acid sequences of saporin and dianthin-30 (80%) that does not exist between saporin and the other toxins, there must be a relationship between the amino-acid sequence of the toxin moieties and the ability of the triterpenoidal saponins to synergistically augment their cytotoxicity. For this reason, the preparation of further targeted toxins comprising of toxin moieties with high identity to either saporin or dianthin-30 and their evaluation in combination with triterpenoidal saponins would shed light on this second hypothesis.

Further advantages have been reported for dianthin-30 in comparison to other type I RIPs such as saporin, namely lower immunogenicity [218] and better recombinant expression yields (see section 3.2.4). For these reasons, the construction of further targeted toxins consisting of dianthin-30 and different ligands will be compatible with the application of the here presented

platform technology and will additionally entail lower immunogenicity and higher expression yields.

Another option to reduce the immunogenicity of the protein moiety is the mutagenesis of the certain responsible amino acids. Some toxins, such as the plant type I RIP bouganin [219] and a truncated version of the bacterial *Pseudomonas* exotoxin A [220], have already been modified to achieve lower immunogenicity. As a result of this process, it is expected that saporin can also be genetically converted into de-immunized saporin. The lower immunogenicity of this mutated saporin should be later proved *in vivo*, for example by immunization of mice with either native saporin or de-immunized saporin, evaluation of the antibody titers in the sera and comparison of the values between the two corresponding toxins. The whole de-immunization process can be further applied to other toxins presenting synergistic cytotoxicity enhancement by triterpenoidal saponins (dianthin-30 and gelonin).

The synergistic endo/lysosomal escape enhancement mediated by triterpenoidal saponins is most prominent in type I RIP-based targeted toxins such as SE and DE. However, despite the fact that DT$_{390}$-EGF is a bacterial toxin-based targeted toxin with a completely different enzymatic mechanism, such synergistic augmentation effects were observed in a minor degree in the case of this targeted toxin. The fact that DT, in contrast to other bacterial toxins, enters the cytosol directly from the endosomes [221] could be a relevant aspect in the case of the observed slight cytotoxicity enhancement of DT$_{390}$-EGF by triterpenoidal saponins. A considerable number of targeted toxins are based on bacterial toxins [222]. However, interaction between bacterial toxins and triterpenoidal saponins is an aspect that has not been intensively studied. Since diphtheria toxin has been used in a number of clinical trials and so far the only approved targeted toxin in the clinics was based on this toxin [223], an enhancement factor of around 85-fold is already a phenomenon to be considered and further investigations in this orientation will be of major interest.

## 4.5. Expression of the enzymatically inactive mutant saporin-KQ

The successful establishment of an expression system for an enzymatically inactive mutant of saporin (saporin-KQ) described in the literature [168] opens the possibility to expand the described platform technology for enhanced non-toxic intracellular drug delivery. Suppressed enzymatic activity of the inactive mutant of saporin was confirmed by an *N*-glycosidase assay. In

addition, saporin-KQ did not present in cell culture any cytotoxic effects in a concentration range from 0.1 to 1,000 nM.

Despite saporin-KQ was neither enzymatically active nor cytotoxic, it revealed cytotoxic effects in combination with SO1861 at the concentrations of 100 and 1,000 nM. As the mutant saporin-KQ cannot kill cells by adenine release from the rRNA, it is hypothesized that it induces caspase-dependent apoptosis *via* the mitochondrial or intrinsic pathway, independently of translation inhibition [184].

Saporin-KQ may be used in the future in combination with triterpenoidal saponins as a shuttle system to achieve an enhanced non-toxic intracellular drug delivery. In this approach, saporin-KQ would act as a carrier and a protein-based drug of interest would be the cargo. Both saporin-KQ and the drug of interest would be conjugated by a non-cleavable cross-linkage (without a disulfide bond) to avoid lysosomal degradation [224]. After administration of the conjugate to cells in the presence of triterpenoidal saponins, an enhanced endo/lysosomal escape of the conjugate containing the desired drug would be achieved. Further research in this direction will be of major importance.

## 4.6. Design of a reporter assay for endo/lysosomal escape

A reporter assay for the endo/lysosomal escape is of great interest because it will facilitate the study of this process. In order to design such a reporter assay, horseradish peroxidase (HRP) was appropriately selected as the reporter since the peroxidase activity of the conjugate (saporin-horseradish peroxidase, SH) had a high sensitivity (see section 3.8.1) and consequently the presence of the conjugate was expected to be detected even at a low concentration of 0.01 nM.

Cytotoxicity of the conjugate was utilized as a first strategy to find out whether intracellular trafficking of SH is influenced in the presence of triterpenoidal saponins. As the cytotoxicity of SH was augmented in combination with SA1641, it was assumed that the cytosolic uptake of the conjugate increases in the presence of triterpenoidal saponins. Therefore, further investigations were performed to discover if it was possible to monitor the endo/lysosomal release of SH by detecting its peroxidase activity.

Firstly, endo/lysosomal release of SH was studied in isolated organelles from cells previously treated with the conjugate. Lysosomes loaded with SH were incubated in the presence of SA1641 at non-permeabilizing concentrations. However, no specific release of SH from the

isolated lysosomes was observed. It is known from other publications that the release of diphtheria toxin's catalytic domain (C domain) from endosomes into the cytosol requires a host cell cytosolic translocation factor complex, which consists of the chaperone heat shock protein 90 (Hsp 90) and thioredoxin reductase [225]. Furthermore, host cell Hsp 90 is also essential for the translocation of *Clostridium botulinum* C2 toxin from endosomes into the cytosol [226] and for the transfer of cholera toxin A1 subunit from the endoplasmic reticulum to the cytosol [227]. Similarly, since a certain amount of SH must definitively escape from the endo/lysosomes in the presence of triterpenoidal saponins because cytotoxicity was observed [see cytotoxicity enhancement at 5 µg/ml (3.05 µM) SA1641 in Figure 35b], a possible explanation for the lack of SH release from the isolated organelles (see SH release at 5 µM SA1641 in Figure 36b) is the necessity of a certain cytosolic machinery to efficiently mediate the specific endo/lysosomal release of saporin (or saporin conjugates such as SH) in the presence of triterpenoidal saponins. An alternative hypothesis is that the amount of SH that escapes from the isolated endo/lysosomes is so low that its measurement remains under the limit of detection but it is high enough to cause cell death.

Secondly, endo/lysosomal release of SH was examined after incubating the cells with the combination of the conjugate and SA1641 and subsequent fractionation. The endo/lysosomal release of SH was evaluated by measuring peroxidase activity in the cytosolic fraction and in the lysosomal fraction. Unfortunately, it was not possible to adequately detect differences in the endo/lysosomal escape of SH in the presence or absence of triterpenoidal saponins, since the peroxidase activity detected in the cytosolic fractions was very close to the detection limit. Therefore, results were not reproducible and the strategy of using HRP as a reporter for endo/lysosomal escape in further experiments was discarded.

A reporter assay for the endo/lysosomal escape process can be employed to identify, which part of the amino-acid sequence of saporin is responsible for the interaction with triterpenoidal saponins and the subsequent endo/lysosomal escape enhancement. After preparation of several deletion fragments by molecular cloning and heterologous expression [228, 229] of the enzymatically inactive saporin (saporin-KQ, see previous section 4.5), these fragments would have been coupled to HRP to identify fragments that induce a potentiated endo/lysosomal release in the presence of triterpenoidal saponins. Since deletion fragments of saporin-KQ lose their cytotoxicity, the readout of this experiment would have been the peroxidase activity of the reporter.

Another possible approach to identify the relevant amino acids of saporin responsible for the interaction with triterpenoidal saponins consists in the fragmentation of saporin-KQ by recombinant techniques and its subsequent conjugation to a second toxin without enhancing properties such as RTA. In this way, the second toxin is the reporter and the readout of the experiment is cytotoxicity. In the case that certain fragments are responsible for an enhanced endo/lysosomal release in the presence of triterpenoidal saponins, the release of the conjugate (deletion fragment coupled to RTA) into the cytosol will be augmented and thus the cytotoxicity of the reporter toxin will be enhanced. Such small amino-acid sequences can be recombinantly attached to other toxins or protein-based therapeutics in order to potentiate their endo/lysosomal escape and thus create a platform for enhanced protein-based intracellular drug delivery.

## 4.7. Enhanced expression of targeted toxins

A significant difference in the protein yield between the two fusion proteins SE and DE was observed after heterologous expression in an *Escherichia coli* system and purification under identical conditions. The study of the reasons why these two highly homologous targeted toxins resulted in significantly different expression levels can result in a new approach to achieve optimized production of targeted toxins.

In general, the total yield of a protein after heterologous expression is influenced by several factors. One of the reasons can be attributed to preferences in codon usage [230]. When proteins are synthesized by ribosomes, a deficiency of loaded tRNAs for rare codons can result in termination of the translation process [231]. However, this phenomenon does not explain the differences in SE and DE expression levels, since SE that is expressed in a lower amount contains only 3 rare codons (R [AGG] at position 175, 191 and 246) while DE that is expressed in a higher amount contains 5 rare codons (R [AGG] at position 38, 78, 176, 192 and 247) with respect to the applied host organism (Rare Codon Search, http://www.bioline.com/calculator/ 01_11.html). In addition, the host *Escherichia coli* Rosetta 2(DE3) pLysS supplies additional tRNAs for the arginine codons AGG and AGA. Further factors that influence the heterologous expression are the presence of mimics of the Shine-Dalgarno sequence [232] and the secondary structure of the mRNA. However, factors mentioned above cannot explain the different yield of SE and DE because no Shine-Dalgarno-like sequences have been identified and the secondary structures of the mRNA, determined by Mfold [167], do not present any conformation responsible for translational pausing.

Another critical factor is the potential degradation of the expressed protein by bacterial proteases [233]. These proteases often recognize recombinant proteins as foreign entities and thus degrade them faster than most bulk proteins [234]. After expression and purification of SE and DE, a main difference is observed by gel electrophoresis (see Figure 9g and h, respectively). Bands of SE are diffuse while bands of DE are more discrete. The diffuse pattern of the SE bands is a typical feature of the degradation by bacterial proteases after prokaryotic protein expression. Although SE and DE are not reported to contain specific recognition sites for bacterial proteases, the amino-acid sequence and three-dimensional structure of both proteins was aligned and compared in order to further investigate this phenomenon.

The structural alignment revealed five major differences, two of which were of main interest as the secondary structure changes from loop (in saporin) to β-strand (in dianthin-30). The five major structural differences were then assigned to the amino-acid sequence alignment. Firstly, one difference of the secondary structure was found at the N-terminus and the second at the C-terminus of the toxins. The difference at the N-terminus consisted in a change from V, T and G (positions 19, 22 and 24 in SE) to A, S and S (same positions in DE, see section 3.9.4). If this short sequence of SE is degraded directly after protein expression in bacteria, the 6× his-tag will be cleaved from the fusion protein and therefore it will not be possible to purify the fragment by Ni-NTA affinity chromatography, resulting in a lower amount of SE than DE after expression and purification under the same conditions. The difference at the C-terminus was a change from K (position 260 in SE) to R (position 261 in DE). Although these two amino acids are structurally similar, degradation at the C-terminus region appears to specifically occur in the case of SE, resulting in the purification of a truncated protein (observed in the diffuse band of SE). Secondly, the amino-acid sequence alignment pointed to a third relevant difference between the two targeted toxins, which was also detected as one of the major structural differences (but without change of secondary structure). The presence of a gap in SE (after position 57) that is replaced by an extra amino acid in DE (T in position 58) may also be a reason why DE is better expressed than SE.

In conclusion, small structural differences between SE and DE, most probably the change of three amino acids at the N-terminus, the change of one amino acid at the C-terminus and an extra amino acid in position 58 of DE, result in a strong variation of protein expression. Presumably, these minimal differences may be responsible for the better protection of DE against bacterial proteases which leads to a higher protein yield. Construction of dianthin-30-based targeted toxins may represent an advantage due to the more effective heterologous expression. In future, the

responsible sequences of dianthin-30 may be used to replace corresponding sequences in other RIPs in order to improve the expression of targeted anti-tumor toxins.

The basics for the platform technology developed in this work open up the possibility of constructing new immunotoxins bearing further tumor targeted therapeuctic antibodies that are already in use in the clinics and enhance their efficacy by structurally specific oleanane saponins. The platform system suggests promising results in forthcoming *in vivo* studies where the toxicity and efficacy of the enhanced immunotoxins will be evaluated. Furthermore, the presented platform for endo/lysosomal escape enhancement of targeted toxins may allow in the future the achievement of treatments with higher success for a number of diseases, including solid tumors and hematologic malignances.

# 5. Summary

Targeted toxins are protein-based therapeutics under investigation for their usage in targeted tumor therapies. They are composed of a toxic enzyme, such as the ribosome-inactivating protein (RIP) saporin, and a targeting ligand, such as growth factors or monoclonal antibodies. After specific binding to target cells and subsequent internalization, their efficacy is dramatically reduced by their accumulation and degradation in the lysosomes. Certain structurally specific oleanane saponins (a subclass of triterpenoidal saponins) that specifically augment the endo/lysosomal escape of particular RIPs may be of great help to circumvent this limiting step.

The main objective of this work was the establishment of a platform technology for the enhanced endo/lysosomal escape of targeted toxins, in order to increase their efficacy and concomitantly reduce dosages, side effects and adverse immune reactions in patients. The platform technology was developed by constructing targeted toxins consisting of saporin and different therapeutic monoclonal antibodies. In this system, the ligand of the saporin-based targeted toxins can be exchanged depending on the target cell type, and the synergistic principle between saporin and oleanane saponins can be simultaneously exploited to achieve tremendous cytotoxicity augmentation effects.

As a first step, the membrane permeabilizing effects of oleanane saponins were studied on different biological membranes. Oleanane saponins showed permeabilizing effects on cellular and lysosomal membranes at concentrations of 6 μM and higher and hemolysis at 3 μM and higher. The specific endo/lysosomal escape of targeted toxins is not based on these unspecific membrane permeabilizing effects of triterpenoidal saponins and occurs at lower concentrations.

To develop the platform technology, two immunotoxins were created by cross-linking the therapeutic antibodies Trastuzumab and Cetuximab to saporin. It was demonstrated that the immunotoxins deliver their toxic payload into the target cells and trigger the antibody-dependent cell-mediated cytotoxicity (ADCC). Immunotoxins preserved the advantages of the naked monoclonal antibodies while, most importantly, their direct cytotoxicity was drastically augmented in combination with triterpenoidal saponins achieving death of all cells down to concentrations of 0.001 nM. The platform was validated by the analysis of three further immunotoxins consisting of saporin and the monoclonal antibodies Rituximab, anti-CD22 and anti-CD25. The cytotoxicity of the three immunotoxins was also augmented in the presence of triterpenoidal saponins (150-, 19- and 26,000-fold, respectively).

In addition, targeted toxins consisting of saporin-epidermal growth factor (SE) and dianthin-30-epidermal growth factor (DE) were investigated in the present work. Although both targeted toxins were recombinantly expressed and purified under identical conditions, a significantly higher expression yield was observed in the case of DE. Since cytotoxicity of SE and DE was comparable on bacteria and HER14 cells, dianthin-30 may be a more suitable toxin for further development of targeted toxins.

When SE, DE and diphtheria $toxin_{390}$-epidermal growth factor ($DT_{390}$-EGF) were applied in the presence of oleanane saponins, the cytotoxicity of SE and DE was drastically enhanced. Despite the fact that $DT_{390}$-EGF is a bacterial toxin-based targeted toxin, enhancement of cytotoxicity was also observed (85-fold). Further investigations should be conducted to better understand the effects of the toxin in the platform system.

The present work opens up numerous vistas for exploiting the presented platform technology. This approach holds promise in *in vitro* experiments as well as in *in vivo* studies where the endo/lysosomal pathways are exploited. The presented platform for the enhanced endo/lysosomal escape of targeted toxins may serve as a basis for the treatment of a variety of diseases and may help to achieve more efficient and successful treatments of solid tumors and hematologic malignances.

# 6. Zusammenfassung

Zielgerichtete Toxine sind proteinbasierte Therapeutika, die im Hinblick auf ihre Anwendung in der zielgerichteten Tumortherapie erforscht werden. Sie bestehen aus einem toxischen Enzym, zum Beispiel einem Ribosomen inaktivierenden Protein (RIP) wie Saporin, und einem Liganden, wie einem Wachstumsfaktor oder einem monoklonalen Antikörper. Nach spezifischer Bindung an die Zielzellen und anschließender Internalisierung wird ihre Effektivität aufgrund ihrer Akkumulation und Degradation in den Lysosomen dramatisch verringert. Bestimmte strukturspezifische oleanane Saponine (eine Subklasse von triterpenoiden Saponinen), welche spezifisch die endo/lysosomale Freisetzung von gewissen RIPs verstärken, können dabei helfen, diese limitierenden Schritte zu umgehen.

Das Hauptziel dieser Arbeit war die Etablierung einer Plattformtechnologie für die verstärkte endo/lysosomale Freisetzung von zielgerichteten Toxinen, um deren Effektivität zu erhöhen und gleichzeitig Dosis, Nebeneffekte und nachteilige Immunreaktionen am Patienten zu verringern. Die Plattformtechnologie wurde durch die Herstellung von zielgerichteten Toxinen, basierend auf Saporin und unterschiedlichen therapeutischen Antikörpern, entwickelt. In diesem System kann der Ligand der Saporin basierten, zielgerichteten Toxine je nach Zielzelltyp ausgetauscht werden. Das synergistische Prinzip zwischen Saporin und den oleananen Saponinen kann simultan genutzt werden, um eine deutliche Verstärkung der Zytotoxizität zu erreichen.

Zunächst wurde der membranpermeabilisierende Effekt von oleananen Saponinen auf unterschiedlichen biologischen Membranen evaluiert. Die oleananen Saponine zeigten bei Konzentrationen ab 6 µM einen permeabilisierenden Effekt auf zelluläre und lysosomale Membranen. Bei einer Konzentration von 3 µM konnten hämolytische Effekte nachgewiesen werden. Die spezifische endo/lysosomale Freisetzung von zielgerichteten Toxinen basiert nicht auf diesem unspezifischen, membranpermeabilisierende Effekt von triterpenoiden Saponinen, sondern geschieht bereits bei niedrigeren, nicht lytischen Konzentrationen.

Um die Plattformtechnologie zu entwickeln, wurden zwei Immunotoxine durch chemische Kopplung von Saporin mit den therapeutischen Antikörpern Trastuzumab bzw. Cetuximab konstruiert. Es konnte gezeigt werden, dass die Immuntoxine ihren toxischen Gehalt in die Zielzellen einbringen und die antikörperabhängige, zellvermittelte Zytotoxizität (ADCC) auslösen. Die Immuntoxine behielten die Vorteile des reinen monoklonalen Antikörpers bei, während die Zytotoxizität in Kombination mit triterpenoiden Saponinen drastisch erhöht werden

konnte und der Tod aller Zellen schon bei Konzentrationen von 0.001 nM eintrat. Die Plattformtechnologie wurde durch die Analyse von drei weiteren Immuntoxinen bestehend aus Saporin und den monoklonalen Antikörpern Rituximab, anti-CD22 und anti-CD25 validiert. Es konnte zusätzlich eine Erhöhung (150-, 19- bzw. 26,000-fach) der Zytotoxizität der drei Immuntoxine in Anwesenheit der triterpenoiden Saponine erreicht werden.

Darüber hinaus wurden in dieser Arbeit zielgerichtete Toxine untersucht, bei denen jeweils der epidermale Wachstumsfaktor an den C-Terminus von entweder Saporin (SE) oder Dianthin-30 (DE) fusioniert wurde. Obwohl beide zielgerichteten Toxine rekombinant exprimiert und unter identischen Bedingungen gereinigt wurden, konnte eine signifikant höhere Ausbeute der Expression im Fall von DE beobachtet werden. Da die Zytotoxizität von SE und DE auf Bakterien und HER14-Zellen vergleichbar war, könnte Dianthin-30 die geeignetere Wahl für die weitere Entwicklung von zielgerichteten Toxinen sein.

Wurden ECV-304-Zellen mit SE, DE oder mit dem Fusionsprodukt aus Diphtheriatoxin$_{390}$ und dem epidermalen Wachstumsfaktor (DT$_{390}$-EGF) in Anwesenheit von oleananen Saponinen behandelt, konnte eine drastisch erhöhte Zytotoxizität von SE und DE beobachtet werden. Trotz des Umstandes, dass DT$_{390}$-EGF ein bakteriell basiertes, zielgerichtetes Toxin ist, wurde auch hierbei eine Zytotoxizitätsverstärkung beobachtet (85-fach). Weitere Untersuchungen sollten an dieser Stelle durchgeführt werden, um die Aufgaben des Toxins im Plattformsystem besser zu verstehen.

Die vorliegende Arbeit eröffnet eine Vielzahl neuer Perspektiven, um die hier präsentierte Plattformtechnologie nutzen zu können. Dieser Ansatz ist sowohl für *in vitro* Experimente als auch für *in vivo* Studien, bei denen der endo/lysosomale Weg genutzt wird, vielversprechend. Die Plattformtechnologie für eine verstärkte endo/lysosomale Freisetzung von zielgerichteten Toxinen könnte als Grundlage für die Behandlung von unterschiedlichen Erkrankungen dienen. Sie könnte darüber hinaus helfen, solide Tumorformen und leukämische Krebsformen effizienter und erfolgreicher zu behandeln.

# 7. References

[1]     Peumans WJ, Hao Q, Van Damme EJ. Ribosome-inactivating proteins from plants: more than RNA N-glycosidases? FASEB J, 2001; 15(9): 1493-506.

[2]     Sokolowska I, Walchli S, Wegrzyn G, Sandvig K, Slominska-Wojewodzka M. A single point mutation in ricin A-chain increases toxin degradation and inhibits EDEM1-dependent ER retrotranslocation. Biochem J, 2011; 436(2): 371-85.

[3]     Pastan I, Hassan R, Fitzgerald DJ, Kreitman RJ. Immunotoxin therapy of cancer. Nat Rev Cancer, 2006; 6(7): 559-65.

[4]     Puri M, Kaur I, Perugini MA, Gupta RC. Ribosome-inactivating proteins: current status and biomedical applications. Drug Discov Today, 2012; 17(13-14): 774-83.

[5]     Chambery A, Di Maro A, Monti MM, Stirpe F, Parente A. Volkensin from Adenia volkensii Harms (kilyambiti plant), a type 2 ribosome-inactivating protein. Eur J Biochem, 2004; 271(1): 108-17.

[6]     Weng A, Thakur M, von Mallinckrodt B, Beceren-Braun F, Gilabert-Oriol R, Wiesner B, Eichhorst J, Bottger S, Melzig MF, Fuchs H. Saponins modulate the intracellular trafficking of protein toxins. J Control Release, 2012; 164(1): 74-86.

[7]     Kreitman RJ. Immunotoxins for targeted cancer therapy. AAPS J, 2006; 8(3): E532-51.

[8]     Spooner RA, Watson PD, Marsden CJ, Smith DC, Moore KA, Cook JP, Lord JM, Roberts LM. Protein disulphide-isomerase reduces ricin to its A and B chains in the endoplasmic reticulum. Biochem J, 2004; 383(Pt 2): 285-93.

[9]     Bellisola G, Fracasso G, Ippoliti R, Menestrina G, Rosen A, Solda S, Udali S, Tomazzolli R, Tridente G, Colombatti M. Reductive activation of ricin and ricin A-chain immunotoxins by protein disulfide isomerase and thioredoxin reductase. Biochem Pharmacol, 2004; 67(9): 1721-31.

[10]    Spooner RA, Lord JM. How ricin and Shiga toxin reach the cytosol of target cells: retrotranslocation from the endoplasmic reticulum. Curr Top Microbiol Immunol, 2012; 357: 19-40.

[11]    Wesche J, Rapak A, Olsnes S. Dependence of ricin toxicity on translocation of the toxin A-chain from the endoplasmic reticulum to the cytosol. J Biol Chem, 1999; 274(48): 34443-9.

[12]    Slominska-Wojewodzka M, Gregers TF, Walchli S, Sandvig K. EDEM is involved in retrotranslocation of ricin from the endoplasmic reticulum to the cytosol. Mol Biol Cell, 2006; 17(4): 1664-75.

[13]    Spooner RA, Hart PJ, Cook JP, Pietroni P, Rogon C, Hohfeld J, Roberts LM, Lord JM. Cytosolic chaperones influence the fate of a toxin dislocated from the endoplasmic reticulum. Proc Natl Acad Sci U S A, 2008; 105(45): 17408-13.

[14]    Fabbrini MS, Rappocciolo E, Carpani D, Solinas M, Valsasina B, Breme U, Cavallaro U, Nykjaer A, Rovida E, Legname G, Soria MR. Characterization of a saporin isoform with lower ribosome-inhibiting activity. Biochem J, 1997; 322 (Pt 3): 719-27.

[15]    Rajagopal V, Kreitman RJ. Recombinant toxins that bind to the urokinase receptor are cytotoxic without requiring binding to the alpha(2)-macroglobulin receptor. J Biol Chem, 2000; 275(11): 7566-73.

[16]    Ippoliti R, Lendaro E, Benedetti PA, Torrisi MR, Belleudi F, Carpani D, Soria MR, Fabbrini MS. Endocytosis of a chimera between human pro-urokinase and the plant toxin saporin: an unusual internalization mechanism. FASEB J, 2000; 14(10): 1335-44.

[17]    Chan WL, Shaw PC, Tam SC, Jacobsen C, Gliemann J, Nielsen MS. Trichosanthin interacts with and enters cells via LDL receptor family members. Biochem Biophys Res Commun, 2000; 270(2): 453-7.

[18]    Bolognesi A, Polito L, Scicchitano V, Orrico C, Pasquinelli G, Musiani S, Santi S, Riccio M, Bortolotti M, Battelli MG. Endocytosis and intracellular localisation of type 1 ribosome-inactivating protein saporin-s6. J Biol Regul Homeost Agents, 2012; 26(1): 97-109.

[19]    Vago R, Marsden CJ, Lord JM, Ippoliti R, Flavell DJ, Flavell SU, Ceriotti A, Fabbrini MS. Saporin and ricin A chain follow different intracellular routes to enter the cytosol of intoxicated cells. FEBS J, 2005; 272(19): 4983-95.

[20]    Barbieri L, Battelli MG, Stirpe F. Ribosome-inactivating proteins from plants. Biochim Biophys Acta, 1993; 1154(3-4): 237-82.

[21]    Vincken JP, Heng L, de Groot A, Gruppen H. Saponins, classification and occurrence in the plant kingdom. Phytochemistry, 2007; 68(3): 275-97.

[22]    Hostettmann K, Marston A. Saponins. Cambridge University Press: Cambridge 1995.

[23]    Thakur M, Melzig MF, Fuchs H, Weng A. Chemistry and pharmacology of saponins: special focus on cytotoxic properties. Botanics: Targets and Therapy, 2011; 1: 19-29.

[24]    el Izzi A, Benie T, Thieulant ML, Le Men-Olivier L, Duval J. Stimulation of LH release from cultured pituitary cells by saponins of Petersianthus macrocarpus: a permeabilizing effect. Planta Med, 1992; 58(3): 229-33.

[25]    Glauert AM, Dingle JT, Lucy JA. Action of Saponin on Biological Cell Membranes. Nature, 1962; 196(4858): 953-955.

[26]    Francis G, Kerem Z, Makkar HP, Becker K. The biological action of saponins in animal systems: a review. Br J Nutr, 2002; 88(6): 587-605.

[27]    Fuchs H, Bachran D, Panjideh H, Schellmann N, Weng A, Melzig MF, Sutherland M, Bachran C. Saponins as tool for improved targeted tumor therapies. Curr Drug Targets, 2009; 10(2): 140-51.

[28]    Gaidi G, Correia M, Chauffert B, Beltramo JL, Wagner H, Lacaille-Dubois MA. Saponins-mediated potentiation of cisplatin accumulation and cytotoxicity in human colon cancer cells. Planta Med, 2002; 68(1): 70-2.

[29]    Jia WW, Bu X, Philips D, Yan H, Liu G, Chen X, Bush JA, Li G. Rh2, a compound extracted from ginseng, hypersensitizes multidrug-resistant tumor cells to chemotherapy. Can J Physiol Pharmacol, 2004; 82(7): 431-7.

[30]    Sun HX, Xie Y, Ye YP. Advances in saponin-based adjuvants. Vaccine, 2009; 27(12): 1787-96.

[31]    Skene CD, Sutton P. Saponin-adjuvanted particulate vaccines for clinical use. Methods, 2006; 40(1): 53-9.

[32]    Gauthier C, Legault J, Girard-Lalancette K, Mshvildadze V, Pichette A. Haemolytic activity, cytotoxicity and membrane cell permeabilization of semi-synthetic and natural lupane- and oleanane-type saponins. Bioorg Med Chem, 2009; 17(5): 2002-8.

[33]    Segal R, Shatkovsky P, Milo-Goldzweig I. On the mechanism of saponin hemolysis–I. Hydrolysis of the glycosidic bond. Biochem Pharmacol, 1974; 23(5): 973-81.

[34]    Woldemichael GM, Wink M. Identification and biological activities of triterpenoid saponins from Chenopodium quinoa. J Agric Food Chem, 2001; 49(5): 2327-32.

[35]    Bachran D, Schneider S, Bachran C, Weng A, Melzig MF, Fuchs H. The endocytic uptake pathways of targeted toxins are influenced by synergistically acting Gypsophila saponins. Mol Pharm, 2011; 8(6): 2262-72.

[36]    Hebestreit P, Weng A, Bachran C, Fuchs H, Melzig MF. Enhancement of cytotoxicity of lectins by Saponinum album. Toxicon, 2006; 47(3): 330-5.

[37]    Böttger S, Melzig MF. Triterpenoid saponins of the Caryophyllaceae and Illecebraceae family. Phytochem Lett, 2011; 4(2): 59-68.

[38]    Böttger S, Hofmann K, Melzig MF. Saponins can perturb biologic membranes and reduce the surface tension of aqueous solutions: A correlation? Bioorg Med Chem, 2012; 20(9): 2822-8.

[39]    Böttger S, Westhof E, Siems K, Melzig MF. Structure-activity relationships of saponins enhancing the cytotoxicity of ribosome-inactivating proteins type I (RIP-I). Toxicon, 2013; 73: 144-50.

[40]    Hebestreit P, Melzig MF. Cytotoxic activity of the seeds from Agrostemma githago var. githago. Planta Med, 2003; 69(10): 921-5.

## 7. References

[41] Weng A, Bachran D, Gorick C, Bachran C, Fuchs H, Melzig MF. A simple method for isolation of Gypsophila saponins for the combined application of targeted toxins and saponins in tumor therapy. Planta Med, 2009; 75(13): 1421-2.

[42] Thakur M, Weng A, Pieper A, Mergel K, von Mallinckrodt B, Gilabert-Oriol R, Gorick C, Wiesner B, Eichhorst J, Melzig MF, Fuchs H. Macromolecular interactions of triterpenoids and targeted toxins: Role of saponins charge. Int J Biol Macromol, 2013; 61C: 285-294.

[43] Bachran C, Sutherland M, Heisler I, Hebestreit P, Melzig MF, Fuchs H. The saponin-mediated enhanced uptake of targeted saporin-based drugs is strongly dependent on the saponin structure. Exp Biol Med (Maywood), 2006; 231(4): 412-20.

[44] Melzig MF, Hebestreit P, Gaidi G, Lacaille-Dubois MA. Structure-activity-relationship of saponins to enhance toxic effects of agrostin. Planta Med, 2005; 71(11): 1088-90.

[45] Weng A, Melzig MF, Bachran C, Fuchs H. Enhancement of saporin toxicity against U937 cells by Gypsophila saponins. J Immunotoxicol, 2008; 5(3): 287-92.

[46] Weng A, Jenett-Siems K, Görick C, Melzig MF. Enhancement of cytotoxicity of ribosome-inactivating-protein type I by saponinum album is not based on stimulation of phagocytosis. J Pharm Pharmacol, 2008; 60(7): 925-930.

[47] Weng A, Bachran C, Fuchs H, Krause E, Stephanowitz H, Melzig MF. Enhancement of saporin cytotoxicity by Gypsophila saponins–more than stimulation of endocytosis. Chem Biol Interact, 2009; 181(3): 424-9.

[48] Frankel AE, Kreitman RJ, Sausville EA. Targeted toxins. Clin Cancer Res, 2000; 6(2): 326-34.

[49] Fuchs H, Bachran C. Targeted tumor therapies at a glance. Curr Drug Targets, 2009; 10(2): 89-93.

[50] Scott AM, Allison JP, Wolchok JD. Monoclonal antibodies in cancer therapy. Cancer Immun, 2012; 12(14): 1-8.

[51] Chames P, Van Regenmortel M, Weiss E, Baty D. Therapeutic antibodies: successes, limitations and hopes for the future. Br J Pharmacol, 2009; 157(2): 220-33.

[52] Abes R, Teillaud JL. Modulation of tumor immunity by therapeutic monoclonal antibodies. Cancer Metastasis Rev, 2011; 30(1): 111-24.

[53] Nahta R. Molecular Mechanisms of Trastuzumab-Based Treatment in HER2-Overexpressing Breast Cancer. ISRN Oncol, 2012; 2012: 428062.

[54] Vlacich G, Coffey RJ. Resistance to EGFR-targeted therapy: a family affair. Cancer Cell, 2011; 20(4): 423-5.

[55] Wong AL, Lee SC. Mechanisms of Resistance to Trastuzumab and Novel Therapeutic Strategies in HER2-Positive Breast Cancer. Int J Breast Cancer, 2012; 2012: 415170.

[56] Flavell DJ, Warnes S, Noss A, Flavell SU. Host-mediated antibody-dependent cellular cytotoxicity contributes to the in vivo therapeutic efficacy of an anti-CD7-saporin immunotoxin in a severe combined immunodeficient mouse model of human T-cell acute lymphoblastic leukemia. Cancer Res, 1998; 58(24): 5787-94.

[57] Flavell DJ, Warnes SL, Noss AL, Flavell SU. Anti-CD7 antibody and immunotoxin treatment of human CD7(+)T-cell leukaemia is significantly less effective in NOD/LtSz-scid mice than in CB.17 scid mice. Br J Cancer, 2000; 83(12): 1755-61.

[58] Dillman RO. Cancer immunotherapy. Cancer Biother Radiopharm, 2011; 26(1): 1-64.

[59] Frankel AE. Reducing the immune response to immunotoxin. Clin Cancer Res, 2004; 10(1 Pt 1): 13-5.

[60] Bostad M, Berg K, Hogset A, Skarpen E, Stenmark H, Selbo PK. Photochemical internalization (PCI) of immunotoxins targeting CD133 is specific and highly potent at femtomolar levels in cells with cancer stem cell properties. J Control Release, 2013; 168(3): 317-26.

[61] Madhumathi J, Verma RS. Therapeutic targets and recent advances in protein immunotoxins. Curr Opin Microbiol, 2012; 15(3): 300-9.

[62] Kioi M, Seetharam S, Puri RK. Targeting IL-13Ralpha2-positive cancer with a novel recombinant immunotoxin composed of a single-chain antibody and mutated Pseudomonas exotoxin. Mol Cancer Ther, 2008; 7(6): 1579-87.

# 7. References

[63]    Pirie CM, Liu DV, Wittrup KD. Targeted cytolysins synergistically potentiate cytoplasmic delivery of gelonin immunotoxin. Mol Cancer Ther, 2013; 12(9): 1774-82.

[64]    Goncalves A, Tredan O, Villanueva C, Dumontet C. [Antibody-drug conjugates in oncology: from the concept to trastuzumab emtansine (T-DM1)]. Bull Cancer, 2012; 99(12): 1183-91.

[65]    Kreitman RJ. Hairy cell leukemia-new genes, new targets. Curr Hematol Malig Rep, 2013; 8(3): 184-95.

[66]    Kreitman RJ. Immunoconjugates and new molecular targets in hairy cell leukemia. Hematology Am Soc Hematol Educ Program, 2012; 2012: 660-6.

[67]    Foyil KV, Bartlett NL. Brentuximab vedotin and crizotinib in anaplastic large-cell lymphoma. Cancer J, 2012; 18(5): 450-6.

[68]    Sheff DR, Daro EA, Hull M, Mellman I. The receptor recycling pathway contains two distinct populations of early endosomes with different sorting functions. J Cell Biol, 1999; 145(1): 123-39.

[69]    Sonnichsen B, De Renzis S, Nielsen E, Rietdorf J, Zerial M. Distinct membrane domains on endosomes in the recycling pathway visualized by multicolor imaging of Rab4, Rab5, and Rab11. J Cell Biol, 2000; 149(4): 901-14.

[70]    Ren J, Kachel K, Kim H, Malenbaum SE, Collier RJ, London E. Interaction of diphtheria toxin T domain with molten globule-like proteins and its implications for translocation. Science, 1999; 284(5416): 955-7.

[71]    Zhan H, Choe S, Huynh PD, Finkelstein A, Eisenberg D, Collier RJ. Dynamic transitions of the transmembrane domain of diphtheria toxin: disulfide trapping and fluorescence proximity studies. Biochemistry, 1994; 33(37): 11254-63.

[72]    Antignani A, Fitzgerald D. Immunotoxins: the role of the toxin. Toxins, 2013; 5(8): 1486-502.

[73]    Chaudhary VK, Jinno Y, FitzGerald D, Pastan I. Pseudomonas exotoxin contains a specific sequence at the carboxyl terminus that is required for cytotoxicity. Proc Natl Acad Sci U S A, 1990; 87(1): 308-12.

[74]    Fitzgerald D. Why toxins! Semin Cancer Biol, 1996; 7(2): 87-95.

[75]    Weldon JE, Xiang L, Chertov O, Margulies I, Kreitman RJ, FitzGerald DJ, Pastan I. A protease-resistant immunotoxin against CD22 with greatly increased activity against CLL and diminished animal toxicity. Blood, 2009; 113(16): 3792-800.

[76]    Leonard JE, Taetle R, To D, Rhyner K. Preclinical studies on the use of selective antibody-ricin conjugates in autologous bone marrow transplantation. Blood, 1985; 65(5): 1149-57.

[77]    Lambert JM, McIntyre G, Gauthier MN, Zullo D, Rao V, Steeves RM, Goldmacher VS, Blattler WA. The galactose-binding sites of the cytotoxic lectin ricin can be chemically blocked in high yield with reactive ligands prepared by chemical modification of glycopeptides containing triantennary N-linked oligosaccharides. Biochemistry, 1991; 30(13): 3234-47.

[78]    Spooner RA, Lord MJ. Immunotoxins: status and prospects. Trends Biotechnol, 1990; 8(7): 189-193.

[79]    Barta SK, Zou Y, Schindler J, Shenoy N, Bhagat TD, Steidl U, Verma A. Synergy of sequential administration of a deglycosylated ricin A chain-containing combined anti-CD19 and anti-CD22 immunotoxin (Combotox) and cytarabine in a murine model of advanced acute lymphoblastic leukemia. Leuk Lymphoma, 2012; 53(10): 1999-2003.

[80]    Wang JL, Zheng YL, Wang BL, Guo AG, Ma R, Jiang YQ. [Construction and activity analysis of a recombinant immunotoxin composed of PE38 and a disulfide stable single-chain antibody]. Chinese Journal of Cellular and Molecular Immunology, 2006; 22(1): 74-7.

[81]    FitzGerald DJ, Kreitman R, Wilson W, Squires D, Pastan I. Recombinant immunotoxins for treating cancer. Int J Med Microbiol, 2004; 293(7-8): 577-82.

[82]    Weng A, Thakur M, Beceren-Braun F, Bachran D, Bachran C, Riese SB, Jenett-Siems K, Gilabert-Oriol R, Melzig MF, Fuchs H. The toxin component of targeted anti-tumor toxins determines their efficacy increase by saponins. Mol Oncol, 2012; 6(3): 323-32.

[83]    Thakur M, Mergel K, Weng A, von Mallinckrodt B, Gilabert-Oriol R, Durkop H, Melzig MF, Fuchs H. Targeted tumor therapy by epidermal growth factor appended toxin and purified

saponin: An evaluation of toxicity and therapeutic potential in syngeneic tumor bearing mice. Mol Oncol, 2013; 7(3): 475-83.

[84] Lappi DA, Ying W, Barthelemy I, Martineau D, Prieto I, Benatti L, Soria M, Baird A. Expression and activities of a recombinant basic fibroblast growth factor-saporin fusion protein. J Biol Chem, 1994; 269(17): 12552-8.

[85] Chiaramonte R, Polizzi D, Bartolini E, Petroni D, Comi P. P1GF-saporin fusion protein: a potential anti-angiogenic agent. Anticancer Drug Des, 1997; 12(8): 649-57.

[86] Lombardi A, Bursomanno S, Lopardo T, Traini R, Colombatti M, Ippoliti R, Flavell DJ, Flavell SU, Ceriotti A, Fabbrini MS. Pichia pastoris as a host for secretion of toxic saporin chimeras. FASEB J, 2010; 24(1): 253-65.

[87] Godal A, Fodstad Ø, Pihl A. Studies on the Mechanism of Action of Abrin-9.2.27 Immunotoxin in Human Melanoma Cell Lines. Cancer Res, 1987; 47(23): 6243-6247.

[88] Entwistle J, Kowalski M, Brown J, Cizeau J, MacDonald G. The Preclinical and Clinical Evaluation of VB6-845: An Immunotoxin with a De-Immunized Payload for the Systemic Treatment of Solid Tumors. Antibody-Drug Conjugates and Immunotoxins. Springer New York, 2013; pp. 349-367.

[89] Francisco JA, Gawlak SL, Miller M, Bathe J, Russell D, Chace D, Mixan B, Zhao L, Fell HP, Siegall CB. Expression and Characterization of Bryodin 1 and a Bryodin 1-Based Single-Chain Immunotoxin from Tobacco Cell Culture. Bioconjug Chem, 1997; 8(5): 708-713.

[90] Frankel AE, Neville DM, Bugge TA, Kreitman RJ, Leppla SH. Immunotoxin therapy of hematologic malignances. Semin Oncol, 2003; 30(4): 545-557.

[91] Dosio F, Brusa P, Crosasso P, Fruttero C, Cattel L, Bolognesi A. Synthesis of different immunotoxins composed by ribosome inactivating proteins non-covalently bound to monoclonal antibody. Il Farmaco, 1996; 51(7): 477-482.

[92] Xia HC, Li F, Zhen L, Zhang ZC. Purification and characterization of Moschatin, a novel type I ribosome-inactivating protein from the mature seeds of pumpkin (Cucurbita moschata), and preparation of its immunotoxin against human melanoma cells. Cell Res, 2003; 13(5): 369-374.

[93] Lorenzetti I, Meneguzzi A, Fracasso G, Potrich C, Costantini L, Chiesa E, Legname G, Menestrina G, Tridente G, Colombatti M. Genetic grafting of membrane-acting peptides to the cytotoxin dianthin augments its ability to de-stabilize lipid bilayers and enhances its cytotoxic potential as the component of transferrin-toxin conjugates. Int J Cancer, 2000; 86(4): 582-589.

[94] Bolognesi A, Tazzari PL, Tassi C, Gromo G, Gobbi M, Stirpe F. A comparison of anti-lymphocyte immunotoxins containing different ribosome-inactivating proteins and antibodies. Clin Exp Immunol, 1992; 89(3): 341-346.

[95] Borthakur G, Rosenblum MG, Talpaz M, Daver N, Ravandi F, Faderl S, Freireich EJ, Kadia T, Garcia-Manero G, Kantarjian H, Cortes JE. Phase 1 study of an anti-CD33 immunotoxin, humanized monoclonal antibody M195 conjugated to recombinant gelonin (HUM-195/rGEL), in patients with advanced myeloid malignancies. Haematologica, 2013; 98(2): 217-221.

[96] Bernhard SL, Better M, Fishwild DM, Lane JA, Orme AE, Garrison DA, Birr CA, Lei SP, Carroll SF. Cysteine Analogs of Recombinant Barley Ribosome Inactivating Protein Form Antibody Conjugates with Enhanced Stability and Potency in vitro. Bioconjug Chem, 1994; 5(2): 126-132.

[97] Ebert RF, Spryn LA. Immunotoxin construction with a ribosome-inactivating protein from barley. Bioconjug Chem, 1990; 1(5): 331-336.

[98] Zheng Q, Xiong YL, Su ZJ, Zhang QH, Dai XY, Li LY, Xiao X, Huang YD. Expression of curcin–transferrin receptor binding peptide fusion protein and its anti-tumor activity. Protein Expr Purif, 2013; 89(2): 181-188.

[99] Ramakrishnan S, Enghlid JJ, Bryant Jr HL, Xu FJ. Characterization of a translation inhibitory protein from Luffa aegyptiaca. Biochem Biophys Res Commun, 1989; 160(2): 509-516.

[100] Gao WD, Zhang RP, Cao HT, Ji RH, Zhang ZC. Construction of Luffin A Immunotoxin and Its in vitro Inhibition Against Human Melanoma Cell M_(21). Chin Sci Bull, 1994; 39(11): 950.

[101]  Xiang Y, Li QY, Wang JH, Wang L, Huang DH, Tang XJ, Zhang M, Zhang WJ, Yang T, Xiao CY. The construction and expression of Luffin-β-targeted fusion immunotoxin as well as its inhibitory effect on non-small cell lung cancer cells. Tumor, 2013; 33(4): 314-320.

[102]  Wang R, Gan C, Gao W, He W, Wang X, Peng Y, Zhuo J, Tan J, Peng X, Wu J, Luo G. A novel recombinant immunotoxin with the smallest ribosome-inactivating protein Luffin P1: T-cell cytotoxicity and prolongation of allograft survival. J Cell Mol Med, 2010; 14(3): 578-586.

[103]  Zhang CL, Yu LZ, Zhao C, Xie SS, Wang RF. Characteristics in Biodistribution and Metabolism of ~(131) I Labeled Immunotoxin Against Human Bladder Carcinoma in Tumor-Bearing Nude Mice. Chinese Journal of Cancer Biotherapy, 2005; 2: 008.

[104]  Uckun FM, Bellomy K, O'Neill K, Messinger Y, Johnson T, Chen CL. Toxicity, Biological Activity, and Pharmacokinetics of TXU (Anti-CD7)-Pokeweed Antiviral Protein in Chimpanzees and Adult Patients Infected with Human Immunodeficiency Virus. J Pharmacol Exp Ther, 1999; 291(3): 1301-1307.

[105]  Lambert JM, Senter PD, Yau-Young A, Blättler WA, Goldmacher VS. Purified immunotoxins that are reactive with human lymphoid cells. Monoclonal antibodies conjugated to the ribosome-inactivating proteins gelonin and the pokeweed antiviral proteins. J Biol Chem, 1985; 260(22): 12035-41.

[106]  Barbieri L, Bolognesi A, Valbonesi P, Polito L, Olivieri F, Stirpe F. Polynucleotide: Adenosine Glycosidase Activity of Immunotoxins Containing Ribosome-Inactivating Proteins. J Drug Target, 2000; 8(5): 281-288.

[107]  O'Toolei JE, Esseltine D, Lynch TJ, Lambert JM, Grossbard ML. Clinical Trials with Blocked Ricin Immunotoxins. Clinical Applications of Immunotoxins. Springer Berlin Heidelberg, 1998; pp. 35-56.

[108]  Benítez J, Ferreras JM, Muñoz R, Arias Y, Iglesias R, Córdoba-Díaz M, del Villar R, Girbés T. Cytotoxicity of an ebulin l-anti-human CD105 immunotoxin on mouse fibroblasts (L929) and rat myoblasts (L6E9) cells expressing human CD105. Med Chem, 2005; 1(1): 65-70.

[109]  Munoz R, Arias Y, Miguel Ferreras J, Jimenez P, Angeles Rojo M, Bernabeu C, Cordoba-Diaz D, Girbes T. Transient Injury-Dependent Up-Regulation of CD105 and its Specific Targeting with an Anti-Vascular Anti-Mouse Endoglin-Nigrin b Immunotoxin. Med Chem, 2012; 8(6): 996-1002.

[110]  Di Massimo AM, Di Loreto M, Pacilli A, Raucci G, D'Alatri L, Mele A, Bolognesi A, Polito L, Stirpe F, De Santis R. Immunoconjugates made of an anti-EGF receptor monoclonal antibody and type 1 ribosome-inactivating proteins from Saponaria ocymoides or Vaccaria pyramidata. Br J Cancer, 1997; 75(6): 822-8.

[111]  French RR, Bell AJ, Hamblin TJ, Tutt AL, Glennie MJ. Response of B-cell lymphoma to a combination of bispecific antibodies and saporin. Leuk Res, 1996; 20(7): 607-617.

[112]  Li YM, Huo YH, Yang MH. Antitumor Effect of Recombinant Immunotoxin EGF-TCSredlk on Tumor-bearing Mouse Model. Journal of Changchun University of Traditional Chinese Medicine, 2011; 5: 9.

[113]  Casellas P, Dussossoy D, Falasca AI, Barbieri L, Guillemot JC, Ferrara P, Bolognesi A, Cenini P, Stirpe F. Trichokirin, a ribosome-inactivating protein from the seeds of Trichosanthes kirilowii Maximowicz. Eur J Biochem, 1988; 176(3): 581-588.

[114]  Shumakov VI, Maisjuk IG, Agapov, II, Shamshiev AT, Muromtceva IB, Maluchenko NV, Pfueller U, Palmer RA, Lentzen H, Tonevitsky AG. In vitro efficacy of conjugates of anti-CD45 monoclonal antibodies with plant toxin A-chains. Transplant Proc, 1998; 30(4): 971-3.

[115]  Lizzi AR, D'Alessandro AM, Zeolla N, Brisdelli F, D'Andrea G, Pitari G, Oratore A, Bozzi A, Ippoliti R. The effect of AZT and chloroquine on the activities of ricin and a saporin-transferrin chimeric toxin. Biochem Pharmacol, 2005; 70(4): 560-9.

[116]  Pirker R, FitzGerald DJ, Raschack M, Frank Z, Willingham MC, Pastan I. Enhancement of the activity of immunotoxins by analogues of verapamil. Cancer Res, 1989; 49(17): 4791-5.

[117]  Weyergang A, Selbo PK, Berstad ME, Bostad M, Berg K. Photochemical internalization of tumor-targeted protein toxins. Lasers Surg Med, 2011; 43(7): 721-33.

[118]   Fuchs H, Bachran C, Li T, Heisler I, Durkop H, Sutherland M. A cleavable molecular adapter reduces side effects and concomitantly enhances efficacy in tumor treatment by targeted toxins in mice. J Control Release, 2007; 117(3): 342-50.

[119]   Heisler I, Sutherland M, Bachran C, Hebestreit P, Schnitger A, Melzig MF, Fuchs H. Combined application of saponin and chimeric toxins drastically enhances the targeted cytotoxicity on tumor cells. J Control Release, 2005; 106(1-2): 123-37.

[120]   Bachran C, Heisler I, Bachran D, Dassler K, Ervens J, Melzig MF, Fuchs H. Chimeric toxins inhibit growth of primary oral squamous cell carcinoma cells. Cancer Biol Ther, 2008; 7(2): 237-42.

[121]   Bachran D, Schneider S, Bachran C, Urban R, Weng A, Melzig MF, Hoffmann C, Kaufmann AM, Fuchs H. Epidermal growth factor receptor expression affects the efficacy of the combined application of saponin and a targeted toxin on human cervical carcinoma cells. Int J Cancer, 2010; 127(6): 1453-61.

[122]   Casellas P, Bourrie BJ, Gros P, Jansen FK. Kinetics of cytotoxicity induced by immunotoxins. Enhancement by lysosomotropic amines and carboxylic ionophores. J Biol Chem, 1984; 259(15): 9359-64.

[123]   Casellas P, Ravel S, Bourrie B, Derocq J, Jansen F, Laurent G, Gros P. T-lymphocyte killing by T101-ricin A-chain immunotoxin: pH-dependent potentiation with lysosomotropic amines. Blood, 1988; 72(4): 1197-1202.

[124]   Siena S, Villa S, Bregni M, Bonnadonna G, Gianni A. Amantadine potentiates T lymphocyte killing by an anti-pan-T cell (CD5) ricin A-chain immunotoxin. Blood, 1987; 69(1): 345-348.

[125]   Marcil J, Ravindranath N, Sairam MR. Cytotoxic activity of lutropin-gelonin conjugate in mouse Leydig tumor cells: Potentiation of the hormonotoxin activity by different drugs. Mol Cell Endocrinol, 1993; 92(1): 83-90.

[126]   Geden SE, Gardner RA, Fabbrini MS, Ohashi M, Phanstiel Iv O, Teter K. Lipopolyamine treatment increases the efficacy of intoxication with saporin and an anticancer saporin conjugate. FEBS J, 2007; 274(18): 4825-4836.

[127]   Akiyama SI, Seth P, Pirker R, FitzGerald D, Gottesman MM, Pastan I. Potentiation of Cytotoxic Activity of Immunotoxins on Cultured Human Cells. Cancer Res, 1985; 45(3): 1005-1007.

[128]   Singh M, Griffin T, Salimi A, Micetich RG, Atwal H. Potentiation of ricin A immunotoxin by monoclonal antibody targeted monensin containing small unilamellar vesicles. Cancer Lett, 1994; 84(1): 15-21.

[129]   Jaffrézou JP, Levade T, Kuhlein E, Thurneyssen O, Chiron M, Grandjean H, Carrière D, Laurent G. Enhancement of Ricin A Chain Immunotoxin Activity by Perhexiline on Established and Fresh Leukemic Cells. Cancer Res, 1990; 50(17): 5558-5566.

[130]   Jaffrézou JP, Levade T, Thurneyssen O, Chiron M, Bordier C, Attal M, Chatelain P, Laurent G. In Vitro and in Vivo Enhancement of Ricin-A Chain Immunotoxin Activity by Novel Indolizine Calcium Channel Blockers: Delayed Intracellular Degradation Linked to Lipidosis Induction. Cancer Res, 1992; 52(5): 1352-1359.

[131]   Pattrick NG, Richardson SCW, Casolaro M, Ferruti P, Duncan R. Poly(amidoamine)-mediated intracytoplasmic delivery of ricin A-chain and gelonin. J Control Release, 2001; 77(3): 225-232.

[132]   Lai PS, Pai CL, Peng CL, Shieh MJ, Berg K, Lou PJ. Enhanced cytotoxicity of saporin by polyamidoamine dendrimer conjugation and photochemical internalization. J Biomed Mater Res A, 2008; 87(1): 147-55.

[133]   Wu YN, Gadina M, Tao-Cheng JH, Youle RJ. Retinoic acid disrupts the Golgi apparatus and increases the cytosolic routing of specific protein toxins. J Cell Biol, 1994; 125(4): 743-753.

[134]   Jaffrézou JP, Sikic BI, Laurent G. Cyclosporin A and cyclosporin SDZ PSC 833 enhance anti-CD5 ricin A-chain immunotoxins in human leukemic T cells. Blood, 1994; 83(2): 482-9.

[135]   Yefenof E, Abboud G, Epszteyn S, Vitetta ES. Treatment of premalignancy: prevention of lymphoma in radiation leukemia virus-inoculated mice by cyclosporin A and immunotoxin. Proc Natl Acad Sci U S A, 1992; 89(2): 728-32.

[136] Hudson TH, Grillo FG. Brefeldin-A enhancement of ricin A-chain immunotoxins and blockade of intact ricin, modeccin, and abrin. J Biol Chem, 1991; 266(28): 18586-18592.

[137] Biberacher V, Decker T, Oelsner M, Wagner M, Bogner C, Schmidt B, Kreitman RJ, Peschel C, Pastan I, Meyer zum Büschenfelde C, Ringshausen I. The cytotoxicity of anti-CD22 immunotoxin is enhanced by bryostatin 1 in B-cell lymphomas through CD22 upregulation and PKC-βII depletion. Haematologica, 2012; 97(5): 771-779.

[138] Davol PA, Bizuneh A, Frackelton AR, Jr. Wortmannin, a phosphoinositide 3-kinase inhibitor, selectively enhances cytotoxicity of receptor-directed-toxin chimeras in vitro and in vivo. Anticancer Res, 1999; 19(3A): 1705-13.

[139] Fitzgerald DJP, Padmanabhan R, Pastan I, Willingham MC. Adenovirus-induced release of epidermal growth factor and pseudomonas toxin into the cytosol of KB cells during receptor-mediated endocytosis. Cell, 1983; 32(2): 607-617.

[140] Griffin TW, Childs LR, FitzGerald DJP, Levin LV. Enhancement of the Cytotoxic Effect of Anti-Carcinoembryonic Antigen Immunotoxins by Adenovirus and Carboxylic Ionophores. J Natl Cancer Inst, 1987; 79(4): 679-685.

[141] Seth P, Fitzgerald D, Ginsberg H, Willingham M, Pastan I. Evidence that the penton base of adenovirus is involved in potentiation of toxicity of Pseudomonas exotoxin conjugated to epidermal growth factor. Mol Cell Biol, 1984; 4(8): 1528-1533.

[142] Goldmacher VS, Blättler WA, Lambert JM, McIntyre G, Stewart J. Cytotoxicity of gelonin conjugated to targeting molecules: effects of weak amines, monensin, adenovirus, and adenoviral capsid proteins penton, hexon, and fiber. Mol Pharm, 1989; 36(5): 818-822.

[143] Chignola R, Anselmi C, Serra MD, Franceschi A, Fracasso G, Pasti M, Chiesa E, Lord JM, Tridente G, Colombatti M. Self-potentiation of Ligand-Toxin Conjugates Containing Ricin A Chain Fused with Viral Structures. J Biol Chem, 1995; 270(40): 23345-23351.

[144] Fuchs H, Bachran C, Flavell D. Diving through Membranes: Molecular Cunning to Enforce the Endosomal Escape of Antibody-Targeted Anti-Tumor Toxins. Antibodies, 2013; 2(2): 209-235.

[145] Elliott G, O'Hare P. Intercellular Trafficking and Protein Delivery by a Herpesvirus Structural Protein. Cell, 1997; 88(2): 223-233.

[146] Oess S, Hildt E. Novel cell permeable motif derived from the PreS2-domain of hepatitis-B virus surface antigens. Gene Ther, 2000; 7(9): 750-758.

[147] Hetzel C, Bachran C, Fischer R, Fuchs H, Barth S, Stöcker M. Small cleavable adapters enhance the specific cytotoxicity of a humanized immunotoxin directed against CD64-positive cells. J Immunother, 2008; 31(4): 370-376.

[148] Kullberg M, Owens JL, Mann K. Listeriolysin O enhances cytoplasmic delivery by Her-2 targeting liposomes. J Drug Target, 2010; 18(4): 313-320.

[149] Browne KA, Blink E, Sutton VR, Froelich CJ, Jans DA, Trapani JA. Cytosolic Delivery of Granzyme B by Bacterial Toxins: Evidence that Endosomal Disruption, in Addition to Transmembrane Pore Formation, Is an Important Function of Perforin. Mol Cell Biol, 1999; 19(12): 8604-8615.

[150] Potala S, Sahoo SK, Verma RS. Targeted therapy of cancer using diphtheria toxin-derived immunotoxins. Drug Discov Today, 2008; 13(17–18): 807-815.

[151] Weldon JE, Pastan I. A guide to taming a toxin – recombinant immunotoxins constructed from Pseudomonas exotoxin A for the treatment of cancer. FEBS J, 2011; 278(23): 4683-4700.

[152] Chaudhary VK, Jinno Y, FitzGerald D, Pastan I. Pseudomonas exotoxin contains a specific sequence at the carboxyl terminus that is required for cytotoxicity. Proc Natl Acad Sci U S A, 1990; 87(1): 308-312.

[153] Wales R, Roberts LM, Lord JM. Addition of an endoplasmic reticulum retrieval sequence to ricin A chain significantly increases its cytotoxicity to mammalian cells. J Biol Chem, 1993; 268(32): 23986-23990.

[154] Seetharam S, Chaudhary VK, FitzGerald D, Pastan I. Increased cytotoxic activity of Pseudomonas exotoxin and two chimeric toxins ending in KDEL. J Biol Chem, 1991; 266(26): 17376-17381.

# 7. References

[155] Yokota S, Hara H, Luo Y, Seon BK. Synergistic Potentiation of In vivo Antitumor Activity of Anti-Human T-Leukemia Immunotoxins by Recombinant α-Interferon and Daunorubicin. Cancer Res, 1990; 50(1): 32-37.

[156] Thiery J, Keefe D, Boulant S, Boucrot E, Walch M, Martinvalet D, Goping IS, Bleackley RC, Kirchhausen T, Lieberman J. Perforin pores in the endosomal membrane trigger the release of endocytosed granzyme B into the cytosol of target cells. Nat Immunol, 2011; 12(8): 770-777.

[157] Flavell DJ, Warnes SL, Bryson CJ, Field SA, Noss AL, Packham G, Flavell SU. The anti-CD20 antibody rituximab augments the immunospecific therapeutic effectiveness of an anti-CD19 immunotoxin directed against human B-cell lymphoma. Br J Haematol, 2006; 134(2): 157-170.

[158] McIntosh DP, Edwards DC, Cumber AJ, Parnell GD, Dean CJ, Ross WCJ, Forrester JA. Ricin B chain converts a non-cytotoxic antibody-ricin A chain conjugate into a potent and specific cytotoxic agent. FEBS Lett, 1983; 164(1): 17-20.

[159] Vitetta ES, Cushley W, Uhr JW. Synergy of ricin A chain-containing immunotoxins and ricin B chain-containing immunotoxins in in vitro killing of neoplastic human B cells. Proc Natl Acad Sci U S A, 1983; 80(20): 6332-6335.

[160] Vitetta ES, Fulton RJ, Uhr JW. Cytotoxicity of a cell-reactive immunotoxin containing ricin A chain is potentiated by an anti-immunotoxin containing ricin B chain. J Exp Med, 1984; 160(1): 341-346.

[161] Weyergang A, Selbo PK, Berg K. Photochemically stimulated drug delivery increases the cytotoxicity and specificity of EGF-saporin. J Control Release, 2006; 111(1-2): 165-73.

[162] Gargouri M, Sapin A, Arıca-Yegin B, Merlin JL, Becuwe P, Maincent P. Photochemical internalization for pDNA transfection: Evaluation of poly(d,l-lactide-co-glycolide) and poly(ethylenimine) nanoparticles. Int J Pharm, 2011; 403(1–2): 276-284.

[163] Thakur M, Mergel K, Weng A, Frech S, Gilabert-Oriol R, Bachran D, Melzig MF, Fuchs H. Real time monitoring of the cell viability during treatment with tumor-targeted toxins and saponins using impedance measurement. Biosens Bioelectron, 2012; 35(1): 503-6.

[164] Bachran C, Durkop H, Sutherland M, Bachran D, Muller C, Weng A, Melzig MF, Fuchs H. Inhibition of tumor growth by targeted toxins in mice is dramatically improved by saponinum album in a synergistic way. J Immunother, 2009; 32(7): 713-25.

[165] Bachran C, Heisler I, Fuchs H, Sutherland M. Influence of protein transduction domains on target-specific chimeric proteins. Biochem Biophys Res Commun, 2005; 337(2): 602-9.

[166] Heisler I, Keller J, Tauber R, Sutherland M, Fuchs H. A cleavable adapter to reduce nonspecific cytotoxicity of recombinant immunotoxins. Int J Cancer, 2003; 103(2): 277-82.

[167] Zuker M. Mfold web server for nucleic acid folding and hybridization prediction. Nucleic Acids Res, 2003; 31(13): 3406-15.

[168] Zarovni N, Vago R, Solda T, Monaco L, Fabbrini MS. Saporin as a novel suicide gene in anticancer gene therapy. Cancer Gene Ther, 2007; 14(2): 165-73.

[169] Dulbecco R, Vogt M. Plaque formation and isolation of pure lines with poliomyelitis viruses. J Exp Med, 1954; 99(2): 167-82.

[170] Barbieri L, Brigotti M, Perocco P, Carnicelli D, Ciani M, Mercatali L, Stirpe F. Ribosome-inactivating proteins depurinate poly(ADP-ribosyl)ated poly(ADP-ribose) polymerase and have transforming activity for 3T3 fibroblasts. FEBS Lett, 2003; 538(1-3): 178-82.

[171] Shevchenko A, Wilm M, Vorm O, Mann M. Mass spectrometric sequencing of proteins silver-stained polyacrylamide gels. Anal Chem, 1996; 68(5): 850-8.

[172] Suckau D, Resemann A, Schuerenberg M, Hufnagel P, Franzen J, Holle A. A novel MALDI LIFT-TOF/TOF mass spectrometer for proteomics. Anal Bioanal Chem, 2003; 376(7): 952-65.

[173] Micheletti C, Orland H. MISTRAL: a tool for energy-based multiple structural alignment of proteins. Bioinformatics, 2009; 25(20): 2663-9.

[174] Savino C, Federici L, Ippoliti R, Lendaro E, Tsernoglou D. The crystal structure of saporin SO6 from Saponaria officinalis and its interaction with the ribosome. FEBS Lett, 2000; 470(3): 239-43.

[175] Fermani S, Falini G, Ripamonti A, Polito L, Stirpe F, Bolognesi A. The 1.4 anstroms structure of dianthin 30 indicates a role of surface potential at the active site of type 1 ribosome inactivating proteins. J Struct Biol, 2005; 149(2): 204-12.

[176] Li HG, Huang PL, Zhang D, Sun Y, Chen HC, Zhang J, Kong XP, Lee-Huang S. A new activity of anti-HIV and anti-tumor protein GAP31: DNA adenosine glycosidase–structural and modeling insight into its functions. Biochem Biophys Res Commun, 2010; 391(1): 340-5.

[177] Weston SA, Tucker AD, Thatcher DR, Derbyshire DJ, Pauptit RA. X-ray structure of recombinant ricin A-chain at 1.8 A resolution. J Mol Biol, 1994; 244(4): 410-22.

[178] Tong L. Combined molecular replacement. Acta Crystallogr A, 1996; A52: 782-784.

[179] Monzingo AF, Collins EJ, Ernst SR, Irvin JD, Robertus JD. The 2.5 A structure of pokeweed antiviral protein. J Mol Biol, 1993; 233(4): 705-15.

[180] Navaza J. AMoRe: an Automated Package for Molecular Replacement. Acta Crystallogr A, 1994; A50: 157-163.

[181] Yan X, Hollis T, Svinth M, Day P, Monzingo AF, Milne GW, Robertus JD. Structure-based identification of a ricin inhibitor. J Mol Biol, 1997; 266(5): 1043-9.

[182] Troise F, Cafaro V, Giancola C, D'Alessio G, De Lorenzo C. Differential binding of human immunoagents and Herceptin to the ErbB2 receptor. FEBS J, 2008; 275(20): 4967-79.

[183] Patel D, Lahiji A, Patel S, Franklin M, Jimenez X, Hicklin DJ, Kang X. Monoclonal antibody cetuximab binds to and down-regulates constitutively activated epidermal growth factor receptor vIII on the cell surface. Anticancer Res, 2007; 27(5A): 3355-66.

[184] Sikriwal D, Ghosh P, Batra JK. Ribosome inactivating protein saporin induces apoptosis through mitochondrial cascade, independent of translation inhibition. Int J Biochem Cell Biol, 2008; 40(12): 2880-8.

[185] Nishikawa M, Nojima S, Akiyama T, Sankawa U, Inoue K. Interaction of Digitonin and Its Analogs with Membrane Cholesterol. J Biochem, 1984; 96(4): 1231-1239.

[186] Kaplan MR, Simoni RD. Transport of cholesterol from the endoplasmic reticulum to the plasma membrane. J Cell Biol, 1985; 101(2): 446-53.

[187] Farhood H, Serbina N, Huang L. The role of dioleoyl phosphatidylethanolamine in cationic liposome mediated gene transfer. Biochim Biophys Acta, 1995; 1235(2): 289-95.

[188] Wadia JS, Stan RV, Dowdy SF. Transducible TAT-HA fusogenic peptide enhances escape of TAT-fusion proteins after lipid raft macropinocytosis. Nat Med, 2004; 10(3): 310-5.

[189] Pack DW, Hoffman AS, Pun S, Stayton PS. Design and development of polymers for gene delivery. Nat Rev Drug Discov, 2005; 4(7): 581-93.

[190] El-Sayed A, Futaki S, Harashima H. Delivery of macromolecules using arginine-rich cell-penetrating peptides: ways to overcome endosomal entrapment. AAPS J, 2009; 11(1): 13-22.

[191] Seeman P. Ultrastructure of membrane lesions in immune lysis, osmotic lysis and drug-induced lysis. Fed Proc, 1974; 33(10): 2116-24.

[192] Gogelein H, Huby A. Interaction of saponin and digitonin with black lipid membranes and lipid monolayers. Biochim Biophys Acta, 1984; 773(1): 32-8.

[193] Ashworth LA, Green C. Plasma membranes: phospholipid and sterol content. Science, 1966; 151(3707): 210-1.

[194] Voutquenne L, Lavaud C, Massiot G, Men-Olivier LL. Structure-Activity Relationships of Haemolytic Saponins. Pharm Biol, 2002; 40(4): 253-262.

[195] Seidel UJ, Schlegel P, Lang P. Natural killer cell mediated antibody-dependent cellular cytotoxicity in tumor immunotherapy with therapeutic antibodies. Front Immunol, 2013; 4(76): 1-8.

[196] Pastan I, Hassan R, FitzGerald DJ, Kreitman RJ. Immunotoxin treatment of cancer. Annu Rev Med, 2007; 58: 221-37.

[197] Barnea I, Ben-Yosef R, Karaush V, Benhar I, Vexler A. Targeting EGFR-positive cancer cells with cetuximab-ZZ-PE38: Results of in vitro and in vivo studies. Head Neck, 2012; 35(8): 1171-7.

[198]  Cao Y, Marks JW, Liu Z, Cheung LH, Hittelman WN, Rosenblum MG. Design optimization and characterization of Her2/neu-targeted immunotoxins: comparative in vitro and in vivo efficacy studies. Oncogene, 2013; 33(4): 429-39.

[199]  Yip WL, Weyergang A, Berg K, Tonnesen HH, Selbo PK. Targeted delivery and enhanced cytotoxicity of cetuximab-saporin by photochemical internalization in EGFR-positive cancer cells. Mol Pharm, 2007; 4(2): 241-51.

[200]  Berstad MB, Weyergang A, Berg K. Photochemical internalization (PCI) of HER2-targeted toxins: synergy is dependent on the treatment sequence. Biochim Biophys Acta, 2012; 1820(12): 1849-58.

[201]  Jefferis R, Lund J. Interaction sites on human IgG-Fc for FcgammaR: current models. Immunol Lett, 2002; 82(1-2): 57-65.

[202]  Vu T, Claret FX. Trastuzumab: updated mechanisms of action and resistance in breast cancer. Front Oncol, 2012; 2(62): 1-6.

[203]  Saito G, Swanson JA, Lee KD. Drug delivery strategy utilizing conjugation via reversible disulfide linkages: role and site of cellular reducing activities. Adv Drug Deliv Rev, 2003; 55(2): 199-215.

[204]  Stirpe F, Bailey S, Miller SP, Bodley JW. Modification of ribosomal RNA by ribosome-inactivating proteins from plants. Nucleic Acids Res, 1988; 16(4): 1349-57.

[205]  Garrett JT, Arteaga CL. Resistance to HER2-directed antibodies and tyrosine kinase inhibitors: mechanisms and clinical implications. Cancer Biol Ther, 2011; 11(9): 793-800.

[206]  Rihova B. Receptor-mediated targeted drug or toxin delivery. Adv Drug Deliv Rev, 1998; 29(3): 273-289.

[207]  Press OW, Martin PJ, Thorpe PE, Vitetta ES. Ricin A-chain containing immunotoxins directed against different epitopes on the CD2 molecule differ in their ability to kill normal and malignant T cells. J Immunol, 1988; 141(12): 4410-7.

[208]  Allen TM. Ligand-targeted therapeutics in anticancer therapy. Nat Rev Cancer, 2002; 2(10): 750-63.

[209]  Kato Y, Seita T, Kuwabara T, Sugiyama Y. Kinetic analysis of receptor-mediated endocytosis (RME) of proteins and peptides: use of RME as a drug delivery system. J Control Release, 1996; 39(2-3): 191-200.

[210]  Walshe CA, Beers SA, French RR, Chan CH, Johnson PW, Packham GK, Glennie MJ, Cragg MS. Induction of cytosolic calcium flux by CD20 is dependent upon B Cell antigen receptor signaling. J Biol Chem, 2008; 283(25): 16971-84.

[211]  Tuscano JM, Kato J, Pearson D, Xiong C, Newell L, Ma Y, Gandara DR, O'Donnell RT. CD22 antigen is broadly expressed on lung cancer cells and is a target for antibody-based therapy. Cancer Res, 2012; 72(21): 5556-65.

[212]  Drexler HG. Guide to Leukemia-Lymphoma Cells Lines, 2nd Edition. Braunschweig, 2010.

[213]  Subtil A, Hemar A, Dautry-Varsat A. Rapid endocytosis of interleukin 2 receptors when clathrin-coated pit endocytosis is inhibited. J Cell Sci, 1994; 107 (Pt 12): 3461-8.

[214]  Reiter Y, Pastan I. Recombinant Fv immunotoxins and Fv fragments as novel agents for cancer therapy and diagnosis. Trends Biotechnol, 1998; 16(12): 513-20.

[215]  Watson P, Spooner RA. Toxin entry and trafficking in mammalian cells. Adv Drug Deliv Rev, 2006; 58(15): 1581-96.

[216]  Lord MJ, Jolliffe NA, Marsden CJ, Pateman CS, Smith DC, Spooner RA, Watson PD, Roberts LM. Ricin. Mechanisms of cytotoxicity. Toxicol Rev, 2003; 22(1): 53-64.

[217]  Bagga S, Seth D, Batra JK. The cytotoxic activity of ribosome-inactivating protein saporin-6 is attributed to its rRNA N-glycosidase and internucleosomal DNA fragmentation activities. J Biol Chem, 2003; 278(7): 4813-20.

[218]  Strocchi P, Barbieri L, Stirpe F. Immunological properties of ribosome-inactivating proteins and a saporin immunotoxin. J Immunol Methods, 1992; 155(1): 57-63.

[219] Cizeau J, Grenkow DM, Brown JG, Entwistle J, MacDonald GC. Engineering and biological characterization of VB6-845, an anti-EpCAM immunotoxin containing a T-cell epitope-depleted variant of the plant toxin bouganin. J Immunother, 2009; 32(6): 574-84.

[220] Onda M, Beers R, Xiang L, Nagata S, Wang QC, Pastan I. An immunotoxin with greatly reduced immunogenicity by identification and removal of B cell epitopes. Proc Natl Acad Sci U S A, 2008; 105(32): 11311-6.

[221] Murphy JR. Mechanism of diphtheria toxin catalytic domain delivery to the eukaryotic cell cytosol and the cellular factors that directly participate in the process. Toxins, 2011; 3(3): 294-308.

[222] Frankel AE, Woo JH, Neville DM. Immunotoxins. Principles of cancer biotherapy. Springer, 2009; pp. 407-449.

[223] Kreitman RJ. Recombinant immunotoxins containing truncated bacterial toxins for the treatment of hematologic malignancies. BioDrugs, 2009; 23(1): 1-13.

[224] Arunachalam B, Phan UT, Geuze HJ, Cresswell P. Enzymatic reduction of disulfide bonds in lysosomes: characterization of a gamma-interferon-inducible lysosomal thiol reductase (GILT). Proc Natl Acad Sci U S A, 2000; 97(2): 745-50.

[225] Ratts R, Zeng H, Berg EA, Blue C, McComb ME, Costello CE, vanderSpek JC, Murphy JR. The cytosolic entry of diphtheria toxin catalytic domain requires a host cell cytosolic translocation factor complex. J Cell Biol, 2003; 160(7): 1139-50.

[226] Haug G, Leemhuis J, Tiemann D, Meyer DK, Aktories K, Barth H. The host cell chaperone Hsp90 is essential for translocation of the binary Clostridium botulinum C2 toxin into the cytosol. J Biol Chem, 2003; 278(34): 32266-74.

[227] Taylor M, Navarro-Garcia F, Huerta J, Burress H, Massey S, Ireton K, Teter K. Hsp90 is required for transfer of the cholera toxin A1 subunit from the endoplasmic reticulum to the cytosol. J Biol Chem, 2010; 285(41): 31261-7.

[228] Pittaluga E, Poma A, Tucci A, Spano L. Expression and characterisation in E. coli of mutant forms of saporin. J Biotechnol, 2005; 117(3): 263-6.

[229] Bonini F, Traini R, Comper F, Fracasso G, Tomazzolli R, Dalla Serra M, Colombatti M. N-terminal deletion affects catalytic activity of saporin toxin. J Cell Biochem, 2006; 98(5): 1130-9.

[230] Gustafsson C, Govindarajan S, Minshull J. Codon bias and heterologous protein expression. Trends Biotechnol, 2004; 22(7): 346-53.

[231] Kane JF. Effects of rare codon clusters on high-level expression of heterologous proteins in Escherichia coli. Curr Opin Biotechnol, 1995; 6(5): 494-500.

[232] Li GW, Oh E, Weissman JS. The anti-Shine-Dalgarno sequence drives translational pausing and codon choice in bacteria. Nature, 2012; 484(7395): 538-41.

[233] Maurizi MR. Proteases and protein degradation in Escherichia coli. Experientia, 1992; 48(2): 178-201.

[234] Rozkov A, Schweder T, Veide A, Enfors S. Dynamics of proteolysis and its influence on the accumulation of intracellular recombinant proteins. Enzyme Microb Technol, 2000; 27(10): 743-748.

# 8. List of publications

## 8.1. Original research articles in peer reviewed journals

[1] M. Thakur, A. Weng, **R. Gilabert-Oriol**, P. Schrade, S. Bachman, B. von Mallinckrodt, C. Bhargava, B. Wiesner, J. Eichhorst, M. F. Melzig, H. Fuchs. Nanosaps: Synergistic carriers for delivery and enhanced endosomal release of tumor targeted toxins. Journal of Controlled Release (2014). Manuscript under revision.

[2] B. von Mallinckrodt, M. Thakur, A. Weng, **R. Gilabert-Oriol**, H. Dürkop, W. Brenner, M. Lukas, N. Beindorff, M. F. Melzig, H. Fuchs. Dianthin-EGF is a highly effective tumor targeted toxin in combination with saponins in a xenograft model for colon carcinoma. Future Oncology (2014). Manuscript under revision.

[3] **R. Gilabert-Oriol**, M. Thakur, B. von Mallinckrodt, C. Bhargava, B. Wiesner, J. Eichhorst, M. F. Melzig, H. Fuchs, A. Weng. Reporter assay for endo/lysosomal escape of toxin-based therapeutics. Toxins (2014) 6:1644-1666.

[4] M. Thakur, G. Jerz, D. Tuwalska, **R. Gilabert-Oriol**, S. Wybraniec, P. Winterhalter, H. Fuchs, A. Weng. High-speed countercurrent chromatographic recovery and off-line electrospray ionization mass spectrometry profiling of bisdesmodic saponins from *Saponaria officinalis* possessing synergistic toxicity enhancing properties on targeted antitumor toxins. Journal of Chromatography B (2014) 955-956:1-9.

[5] **R. Gilabert-Oriol**, M. Thakur, B. von Mallinckrodt, T. Hug, B. Wiesner, J. Eichhorst, M. F. Melzig, H. Fuchs, A. Weng. Modified trastuzumab and cetuximab mediate efficient toxin delivery while retaining antibody-dependent cell-mediated cytotoxicity in target cells. Molecular Pharmaceutics (2013) 10(11):4347-57.

[6] M. Thakur, A. Weng, A. Pieper, K. Mergel, B. von Mallinckrodt, **R. Gilabert-Oriol**, C. Görick, B. Wiesner, J. Eichhorst, M. F. Melzig, H. Fuchs. Macromolecular interactions of triterpenoids and targeted toxins: Role of saponins charge. International Journal of Biological Macromolecules (2013) 61C:285-294.

[7] **R. Gilabert-Oriol**, M. Thakur, C. Weise, J. Dernedde, B. von Mallinckrodt, H. Fuchs, A. Weng. Small structural differences of targeted anti-tumor toxins result in strong variation of protein expression. Protein Expression and Purification (2013) 91(1):54-60.

[8] **R. Gilabert-Oriol**, K. Mergel, M. Thakur, B. von Mallinckrodt, M. F. Melzig, H. Fuchs, A. Weng. Real-time analysis of membrane permeabilizing effects of oleanane saponins. Bioorganic & Medicinal Chemistry (2013) 21(8):2387-95.

[9] M. Thakur, K. Mergel, A. Weng, B. von Mallinckrodt, **R. Gilabert-Oriol**, H. Dürkop, M. F. Melzig, H. Fuchs. Targeted tumor therapy by epidermal growth factor appended toxin and purified saponin: An evaluation of toxicity and therapeutic potential in syngeneic tumor bearing mice. Molecular Oncology (2013) 7(3):475-83.

[10] A. Weng, M. Thakur, B. von Mallinckrodt, F. Beceren-Braun, **R. Gilabert-Oriol**, B. Wiesner, J. Eichhorst, S. Böttger, M. F. Melzig, H. Fuchs. Saponins modulate the intracellular trafficking of protein toxins. Journal of Controlled Release (2012) 164(1):74-86.

[11] M. Thakur, K. Mergel, A. Weng, S. Frech, **R. Gilabert-Oriol**, D. Bachran, M. F. Melzig, H. Fuchs. Real time monitoring of the cell viability during treatment with tumor-targeted toxins and saponins using impedance measurement. Biosensors and Bioelectronics (2012) 35(1):503-6.

[12] A. Weng, M. Thakur, F. Beceren-Braun, D. Bachran, C. Bachran, S. B. Riese, K. Jenett-Siems, **R. Gilabert-Oriol**, M. F. Melzig, H. Fuchs. The toxin component of targeted anti-tumor toxins determines their efficacy increase by saponins. Molecular Oncology (2012) 6(3):323-32.

## 8.2. Review articles in peer reviewed journals

[1] **R. Gilabert-Oriol**, A. Weng, B. von Mallinckrodt, M. F. Melzig, H. Fuchs, M. Thakur. Immunotoxins constructed with ribosome-inactivating proteins and their enhancers: a lethal cocktail with tumor specific efficacy. Current Pharmaceutical Design (2014). Accepted manuscript.

## 8.3. Proceedings in peer reviewed journals

[1] **R. Gilabert-Oriol**, M. Thakur, B. von Mallinckrodt, T. Hug, B. Wiesner, J. Eichhorst, M. F. Melzig, H. Fuchs, A. Weng. Combinatorial approach to drastically enhance the monoclonal antibody efficacy in targeted tumor therapy. AACR-NCI-EORTC International Conference on Molecular Targets and Cancer Therapeutics. Boston, MA, USA: October 19 – 23, 2013 (Poster). Molecular Cancer Therapeutics 2013; 12(11 Suppl):A83

[2] M. Thakur, A. Weng, **R. Gilabert-Oriol**, B. von Mallinckrodt, H. Fuchs, M. F. Melzig. Electromigration pattern of Saponaria saponins determine their synergistic toxicity enhancement ability of Saporin based targeted immunotoxins in vitro and in vivo. 61st Internation Congress and Annual Meeting of the Society for Medicinal Plant and Natural Product Research (GA). Münster, Germany: September 1 – 5, 2013 (Presentation). Planta Medica 2013; 79 - SL32.

[3] A. Weng, M. Thakur, F. Beceren-Braun, **R. Gilabert-Oriol**, S. Boettger, M. F. Melzig, H. Fuchs. Synergistic interaction of triterpenoid saponins and plant protein toxins. International Congress on Natural Products Research. New York City, United States of America: July 28 – August 1, 2012 (Presentation). Planta Medica 2012; 78 - CL36.

[4] A. Weng, M. Thakur, F. Beceren-Braun, K. Mergel, **R. Gilabert-Oriol**, M. F. Melzig, H. Fuchs. Anti-tumor toxins and their efficacy in combination with triterpenoid saponins. Natural Anticancer Drugs. Olomouc, Czech Republic: June 30 – July 4, 2012 (Presentation). Biomedical Papers of the Faculty of Medicine and Dentistry of Palacký University. Volume 156, Supplement 1, 2012.

[5]     M. Thakur, A. Weng, K. Mergel, B. von Mallinckrodt, **R. Gilabert-Oriol**, M. F. Melzig, H. Fuchs. Electrophoretically mobile Saponaria officinalis saponin as a highly synergistic enhancer of tumor specific toxicity for saporin-EGF: in vitro and in vivo evaluation. Natural Anticancer Drugs. Olomouc, Czech Republic: June 30 – July 4, 2012 (Poster). Biomedical Papers of the Faculty of Medicine and Dentistry of Palacký University. Volume 156, Supplement 1, 2012.

## 8.4.  Invited lectures in international conferences

[1]     **R. Gilabert-Oriol**, A. Weng, B. von Mallinckrodt, M. F. Melzig, H. Fuchs, M. Thakur. Immune adjuvant activity of saponins from *Quillaja saponaria* Mol. correlates with their electrophoretic mobility. 17th Annual National Convention and International Symposium on Frontiers in Herbal Cosmetics and Nutraceuticals. Indian Society of Pharmacognosy. Dehradun, India: February 23 – 24, 2013.

[2]     **R. Gilabert-Oriol**, M. Thakur, B. von Mallinckrodt, M. F. Melzig, H. Fuchs, A. Weng. Enhanced targeted tumor therapy by Herceptin® and Erbitux® based immunotoxins in combination with triterpenoidal saponin. Targeting of Bioactives Concepts & Application. Advance Group of Pharmacy Colleges. Kanpur, India: February 10, 2013.

## 8.5.  Presentations in academic conferences

[1]     M. Thakur, A. Weng, B. von Mallinckrodt, **R. Gilabert-Oriol**, M. F. Melzig, H. Fuchs. Saponin-protein interactions role in endosomal transport and drug delivery. 17th Annual National Convention and International Symposium on Frontiers in Herbal Cosmetics and Nutraceuticals. Indian Society of Pharmacognosy. Dehradun, India: February 23 – 24, 2013.

[2]     M. Thakur, A. Weng, B. von Mallinckrodt, **R. Gilabert-Oriol**, M. F. Melzig, H. Fuchs. Targeting therapy at a glance: Role of target efficacy enhancement. Targeting of Bioactives Concepts & Application. Advance Group of Pharmacy Colleges. Kanpur, India: February 10, 2013.

[3]     M. Thakur, K. Mergel, A. Weng, A. Pieper, B. von Mallinckrodt, **R. Gilabert-Oriol**, M. F. Melzig, H. Fuchs. Isolation Techniques of Saponins and their In Vivo Evaluation as Enhancers in Targeted Tumor Therapy. 8th Fabisch-Symposium for Cancer Research and Molecular Cell Biology. 3rd Targeted Tumor Therapies. Berlin, Germany: March 21 – 23, 2012.

[4]     A. Weng, M. Thakur, F. Beceren-Braun, **R. Gilabert-Oriol**, D. Bachran, M. F. Melzig, H. Fuchs. Therapeutic Potential of a Combinatorial Anti-tumor Therapy: Role of the Toxin Moiety. 8th Fabisch-Symposium for Cancer Research and Molecular Cell Biology. 3rd Targeted Tumor Therapies. Berlin, Germany: March 21 – 23, 2012.

## 8.6. Posters in academic conferences

[1] **R. Gilabert-Oriol**, M. Thakur, B. von Mallinckrodt, C. Bhargava, B. Wiesner, J. Eichhorst, M. F. Melzig, H. Fuchs, A. Weng. Monitoring of the endo/lysosomal escape of targeted toxin-based therapeutics: development of a reporter assay. International Conference on From Omics to Novel Therapies in Cancer. Berlin, Germany: May 23 – 24, 2014.

[2] B. von Mallinckrodt, M. Thakur, **R. Gilabert-Oriol**, A. Weng, M. F. Melzig, H. Fuchs. Establishment of a xenograft model for colon carcinoma and testing of a combinatorial therapeutic approach using targeted toxins. International Conference on From Omics to Novel Therapies in Cancer. Berlin, Germany: May 23 – 24, 2014.

[3] **R. Gilabert-Oriol**, M. Thakur, B. von Mallinckrodt, T. Hug, B. Wiesner, J. Eichhorst, M. F. Melzig, H. Fuchs, A. Weng. Bio-betters for Herceptin® and Erbitux®, a new combinatorial approach with structurally specific triterpenoidal saponins in targeted tumor therapy. 13th European Symposium on Controlled Drug Delivery. Egmond aan Zee, The Netherlands: April 16 – 18, 2014.

[4] M. Thakur, A. Weng, **R. Gilabert-Oriol**, B. von Mallinckrodt, M. F. Melzig, H. Fuchs. Nanosaps as delivery agents and endosomal escape enhancers for tumor targeted toxins. 13th European Symposium on Controlled Drug Delivery. Egmond aan Zee, The Netherlands: April 16 –18, 2014.

[5] B. von Mallinckrodt, M. Thakur, **R. Gilabert-Oriol**, A. Weng, M. F. Melzig, H. Fuchs. Dianthin-EGF effectiveness and synergism with triterpenes: target efficacy in a xenograft model. 13th European Symposium on Controlled Drug Delivery. Egmond aan Zee, The Netherlands: April 16 – 18, 2014.

[6] **R. Gilabert-Oriol**, M. Thakur, B. von Mallinckrodt, T. Hug, B. Wiesner, J. Eichhorst, M. F. Melzig, H. Fuchs, A. Weng. Modified Herceptin® and Erbitux® mediate an enhanced toxin delivery and retain antibody-dependent cellular cytotoxicity. International Bioanalytical Congress. Berlin, Germany: September 11 – 12, 2013.

[7] M. Thakur, A. Weng, B. von Mallinckrodt, **R. Gilabert-Oriol**, M. F. Melzig, H. Fuchs. Dual therapeutic approach enhances the efficacy of tumor targeted toxins: in vivo assessment in syngeneic and xenograft models. International Bioanalytical Congress. Berlin, Germany: September 11 – 12, 2013.

[8] **R. Gilabert-Oriol**, K. Mergel, A. Weng, M. Thakur, B. von Mallinckrodt, M. F. Melzig, H. Fuchs. Endo/lysosomal translocation of saporin: characteristics of saponins as innovative tools for enhancement of targeted toxin-based tumor therapies. Emerging Concepts in Cancer. Berlin, Germany: June 15 – 16, 2012.

[9] A. Weng, M. Thakur, F. Beceren-Braun, **R. Gilabert-Oriol**, M. F. Melzig, H. Fuchs. Efficacy of anti-tumor toxins targeting the epidermal growth factor receptor. Emerging Concepts in Cancer. Berlin, Germany: June 15 – 16, 2012.

[10] M. Thakur, K. Mergel, A. Weng, B. von Mallinckrodt, **R. Gilabert-Oriol**, H. Dürkop, M. F. Melzig, H. Fuchs. Synergistic enhancement of tumor targeted toxin Sap3-EGF using purified saponin from Saponaria roots: toxicity and anti-tumor efficacy evaluation in a syngeneic mouse model. Emerging Concepts in Cancer. Berlin, Germany: June 15 – 16, 2012.

[11] **R. Gilabert-Oriol**, A. Weng, M. Thakur, K. Mergel, B. von Mallinckrodt, D. Bachran, M. F. Melzig, H. Fuchs. Saporin-HRP Endo/Lysosomal Escape Enhancement in Isolated Organelles. 8th Fabisch-Symposium for Cancer Research and Molecular Cell Biology. 3rd Targeted Tumor Therapies. Berlin, Germany: March 21 – 23, 2012.

## 8.7. Published research project

[1] **Gilabert Oriol, Roger** (2007). L'smog fotoquímic al Camp de Tarragona, 295 p. En: Gavaldà, Jordi ed. Premis Consell Social URV als millors treballs de recerca de secundària 2006 – 2007, Tarragona, Spain: Consell Social de la URV. ISBN: 978-84-8424-106-5. Published in the CD included in the book of the same title which contains the awarded project abstracts. D.L.: T-1971-07.

# 9. Curriculum vitae

For reasons of data protection,

the curriculum vitae is not included in the online version

For reasons of data protection,

the curriculum vitae is not included in the online version

# 10. Acknowledgments

# 11.   Declaration

I, Roger Gilabert-Oriol, declare that the doctoral thesis entitled "*Development of a platform technology for enhanced endo/lysosomal escape of targeted toxins by structurally specific oleanane saponins*" contains no material that has been submitted previously, in whole or in part, for the award of any other academic degree or diploma. I would hereby like to confirm that there is no conflict of interest in the present study of any kind. Except where otherwise indicated, this thesis is my own original work.


Roger Gilabert-Oriol

Berlin, May 2014